Electronic Supplementary Material (ESI) for Dalton Transactions.

Self-assembly of dinuclear Pd(II)/Pt(II) metallacyclic receptors incorporating *N*-heterocyclic carbene complexes as corners.

Ismael Marcos,[a,†] Olaya Domarco,[a,†] Carlos Peinador,[a] Alberto Fenández, Jesús J. Fernández, Digna Vázquez-García[a,*] and Marcos D. García[a,*]

SUPPORTING INFORMATION

INDEX

1. NMR spectra

1.1. Carbene **6(Pd)**·$2NO_3$.

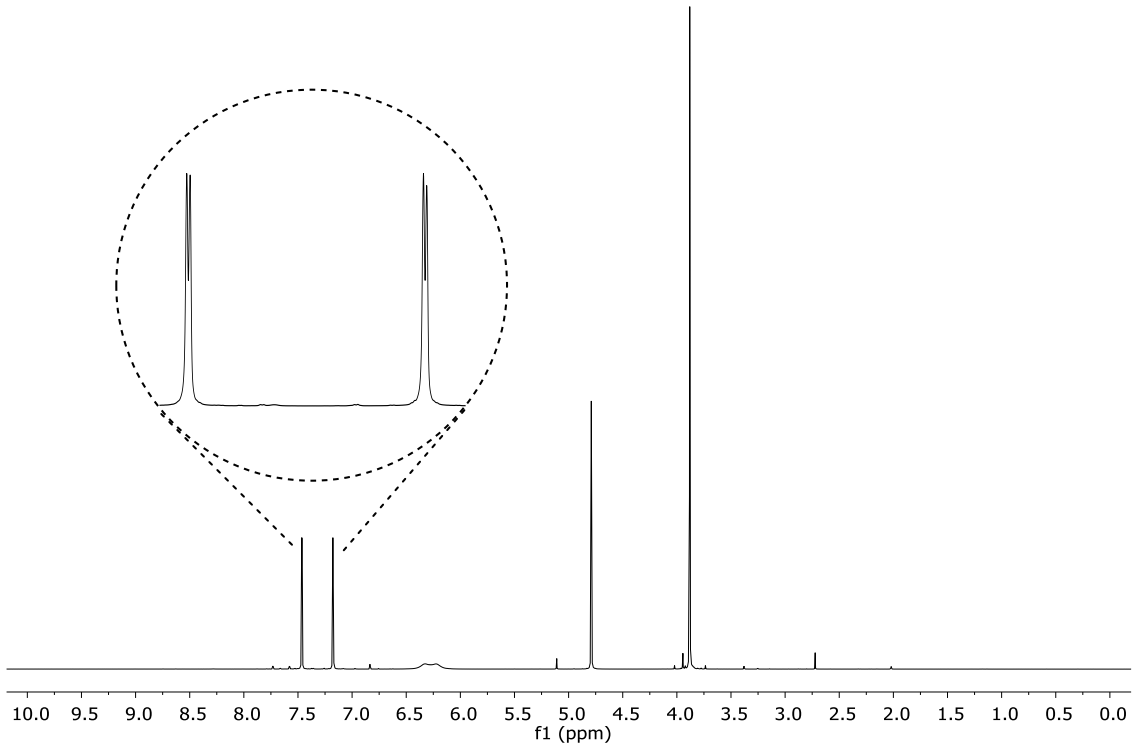

^{1}H NMR (500 MHz, D_2O) full spectra of **6(Pd)**·$2NO_3$.

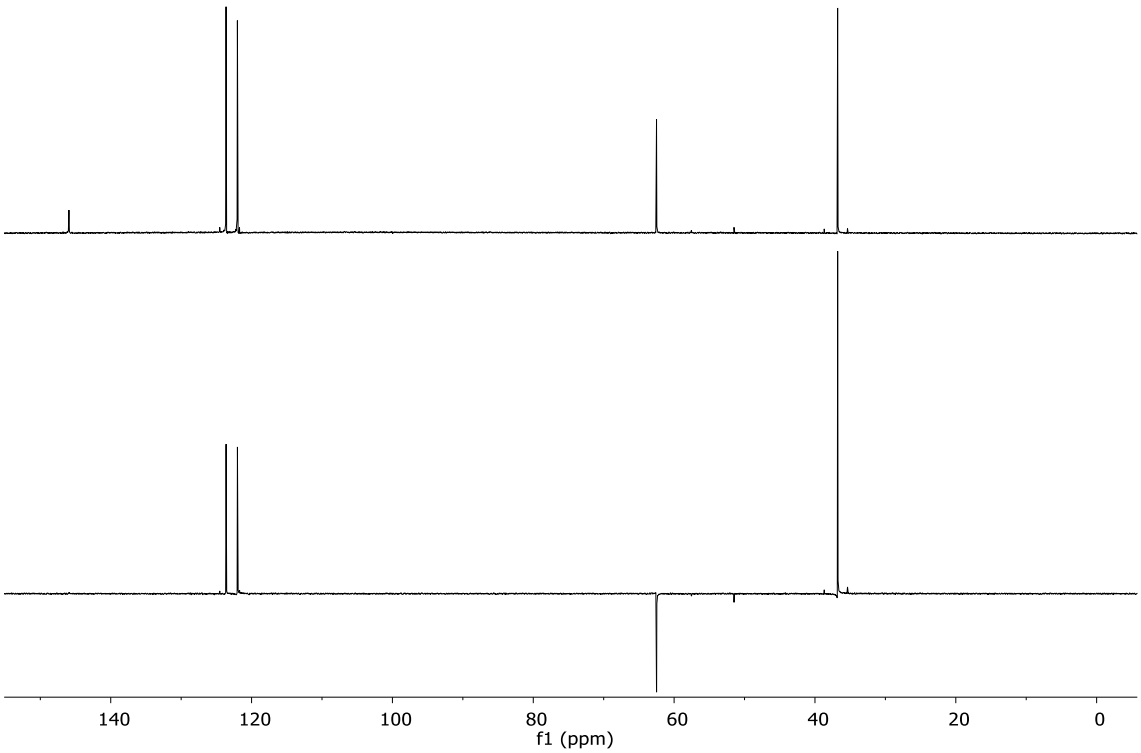

^{13}C NMR and DEPT (125 MHz, D_2O) full spectra of **6(Pd)**·$2NO_3$.

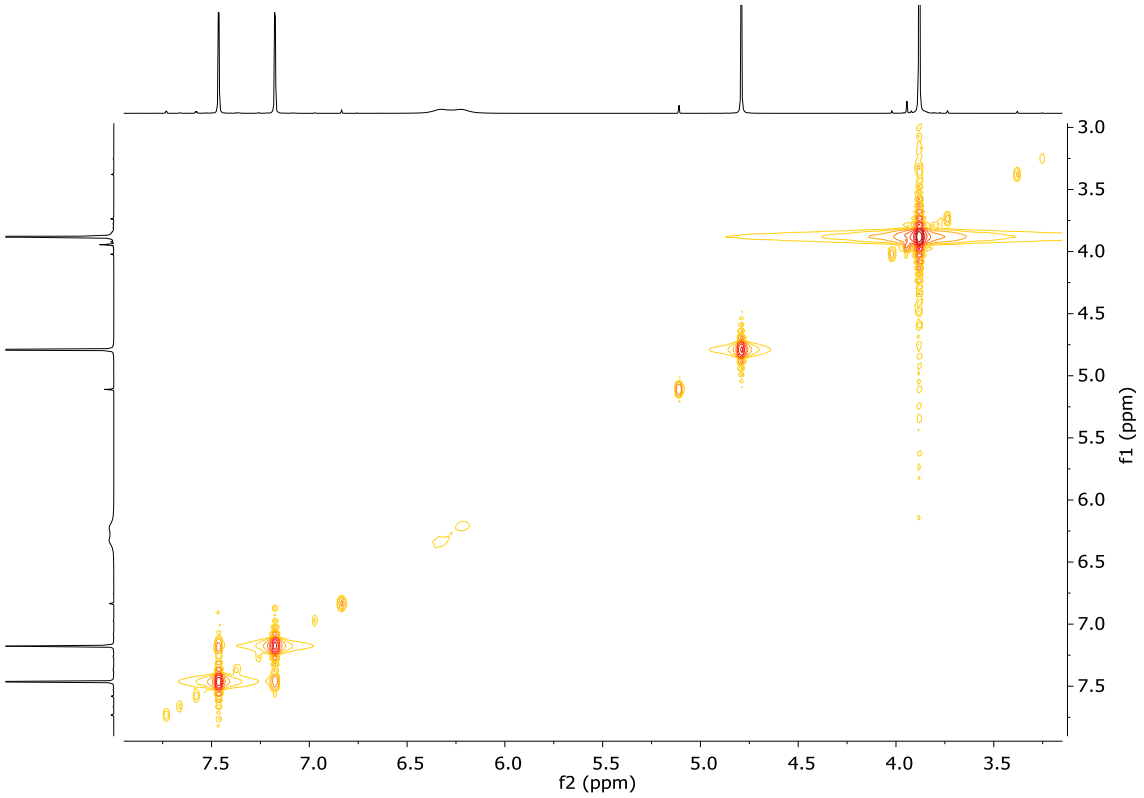

COSY (500 MHz, D_2O) partial spectra of **6(Pd)**·$2NO_3$.

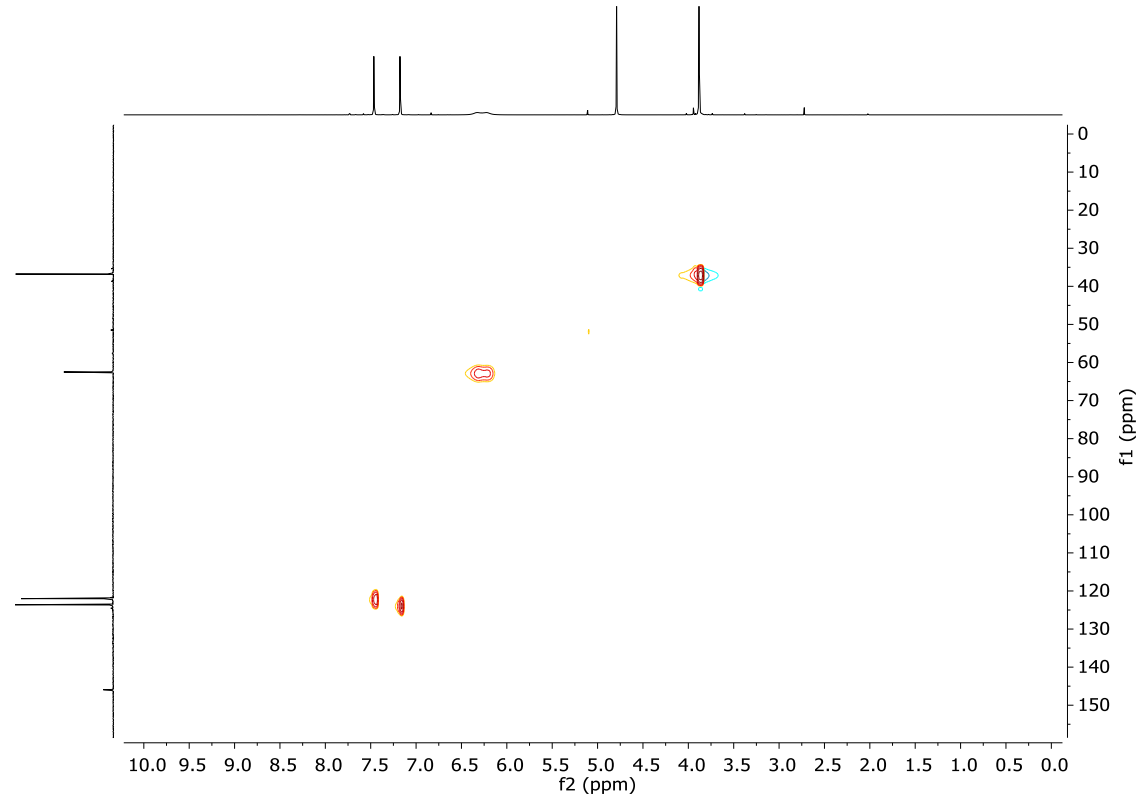

HSQC (125 and 500 MHz, D_2O) full spectra of **6(Pd)**·$2NO_3$.

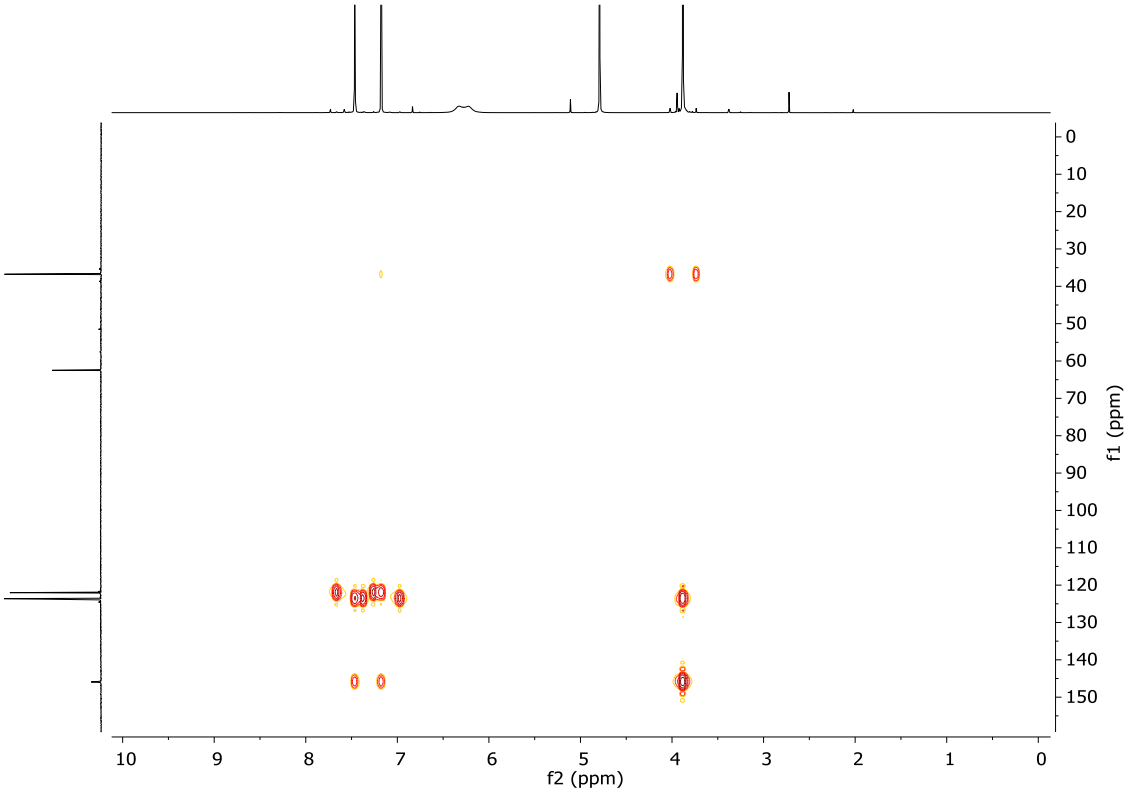

HMBC (125 and 500 MHz, D_2O) full spectra of **6(Pd)**·$2NO_3$.

1.2. Carbene **6(Pt)**·$2NO_3$.

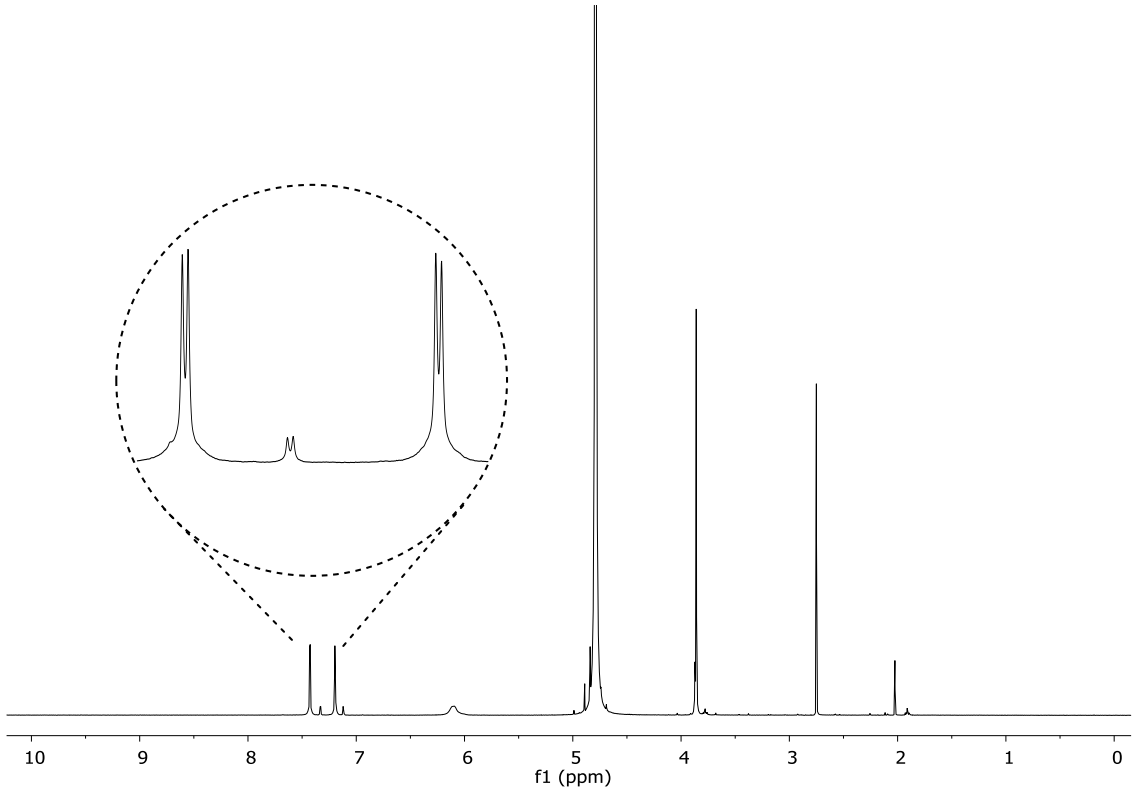

^{1}H NMR (500 MHz, D_2O) full spectra of **6(Pt)**·$2NO_3$.

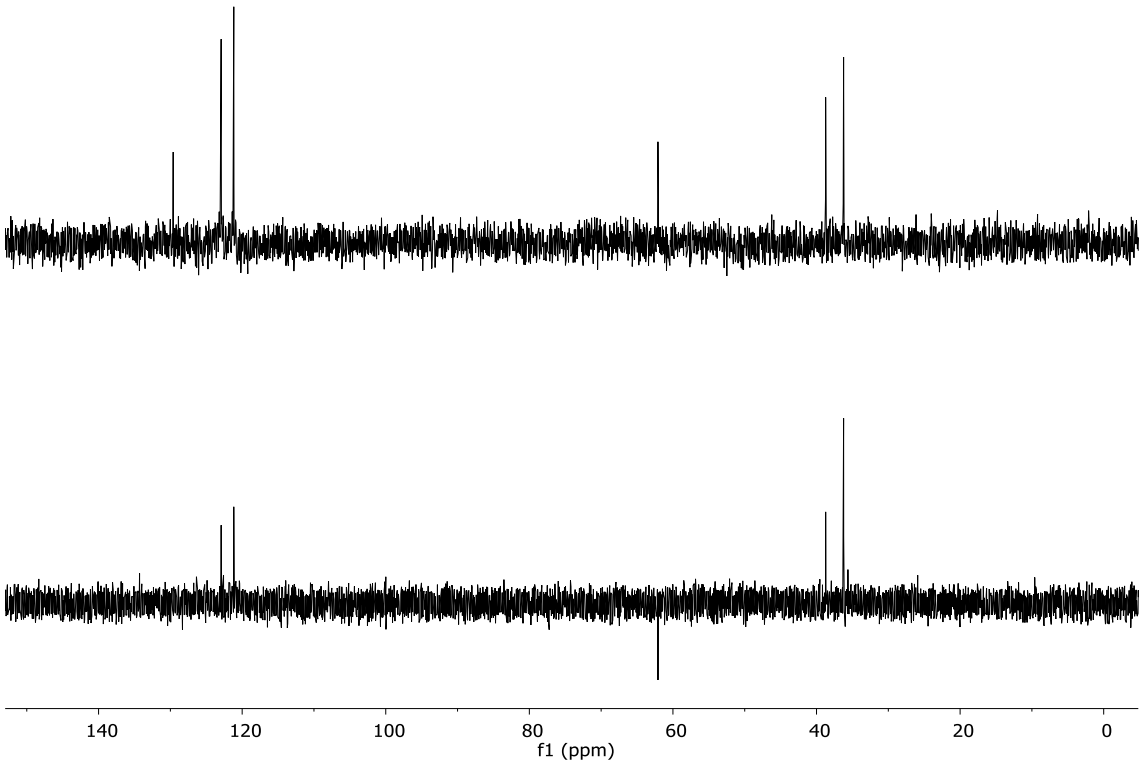

^{13}C NMR and DEPT (125 MHz, D_2O) full spectra of **6(Pt)**·$2NO_3$.

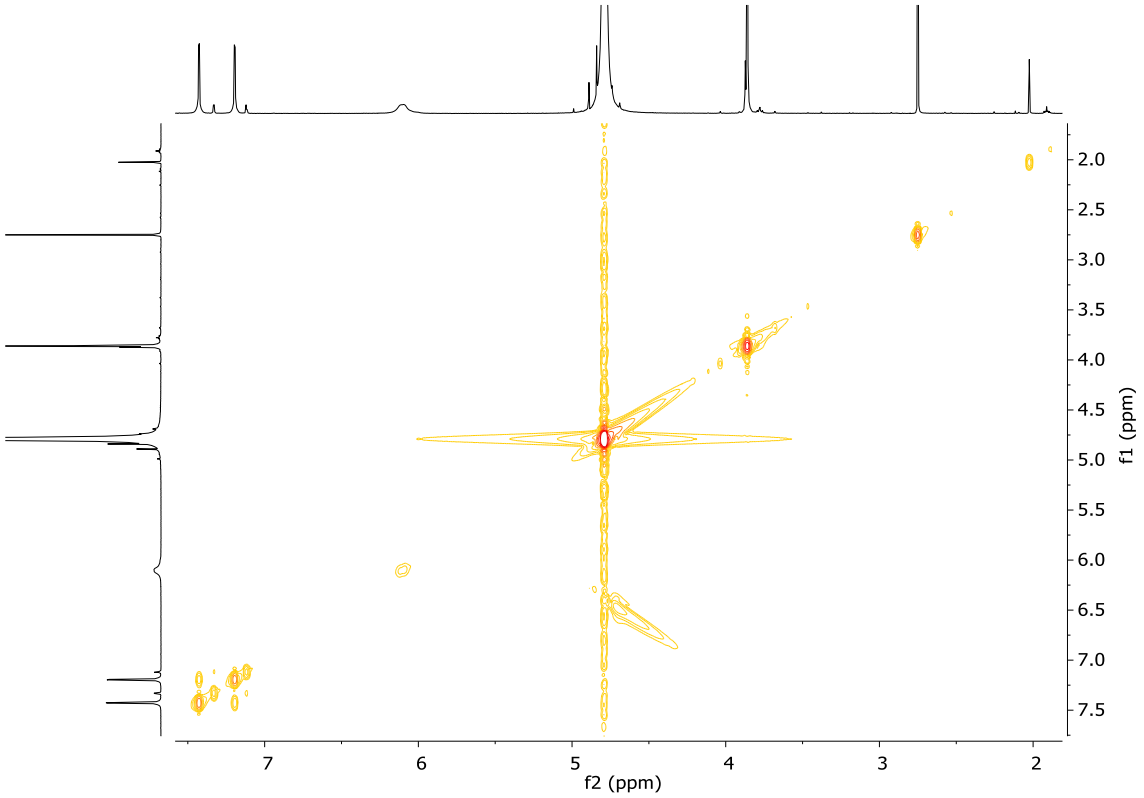

COSY (500 MHz, D_2O) partial spectra of **6(Pt)**·$2NO_3$.

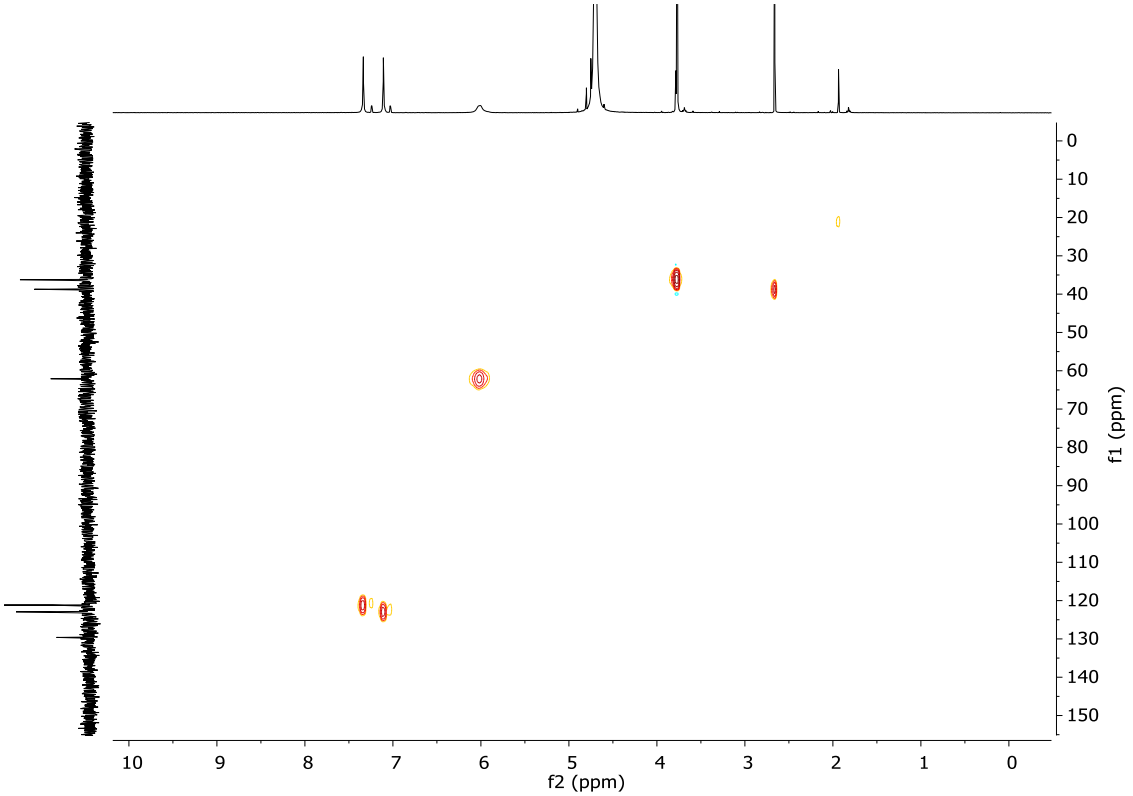

HSQC (125 and 500 MHz, D_2O) full spectra of **6(Pt)**·$2NO_3$.

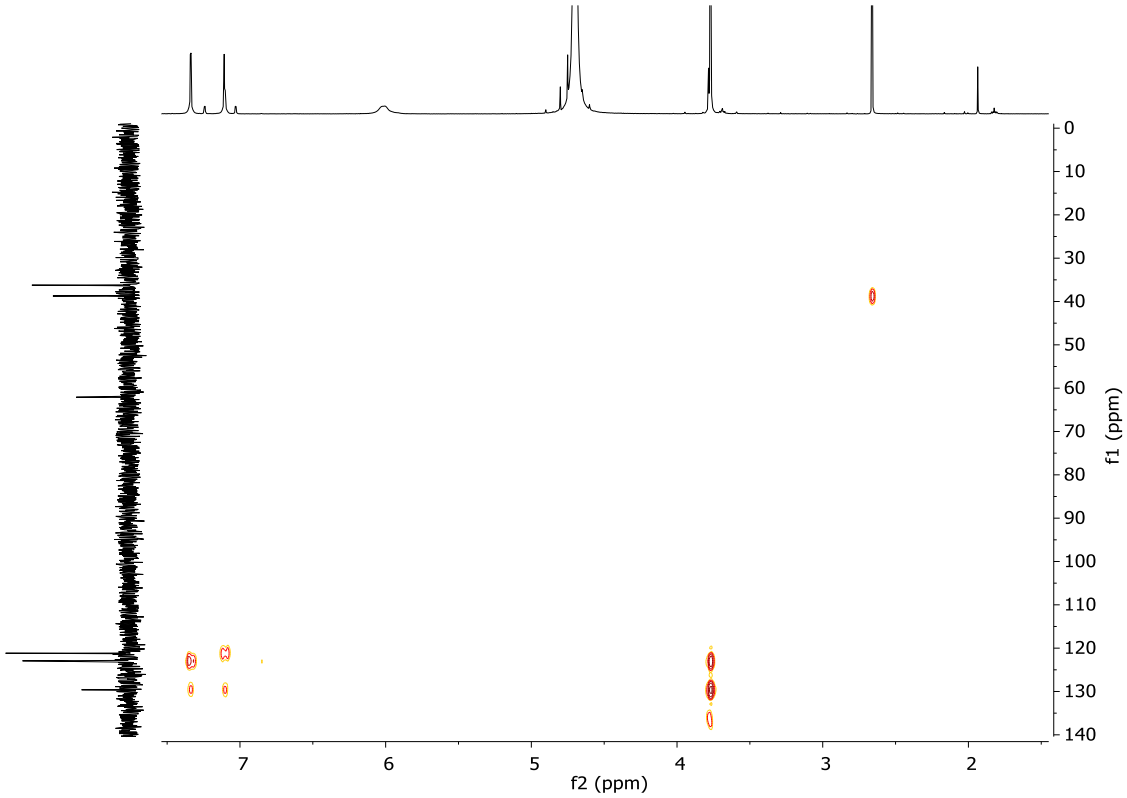

HMBC (125 and 500 MHz, D_2O) partial spectra of **6(Pt)**·$2NO_3$.

1.3. Metallacycle **R1**·6NO_3.

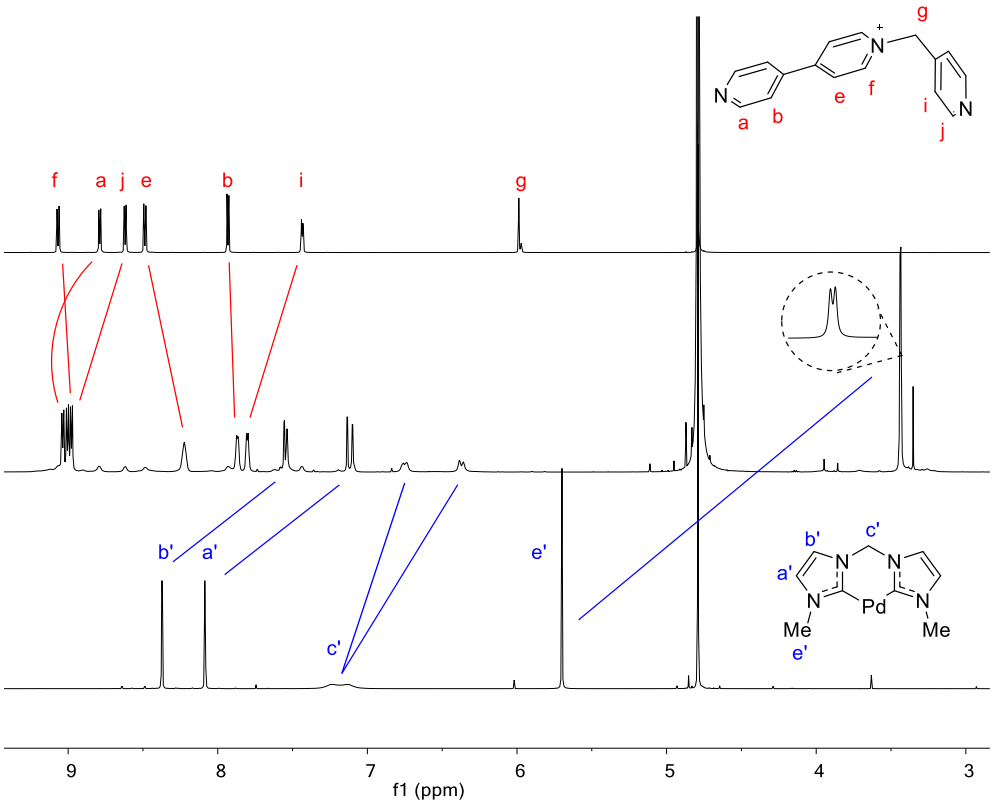

^{1}H NMR (500 MHz, D_2O) spectra of **1** (top), **R1**·6NO_3 (middle) and **6(Pd)**·2NO_3 (bottom).

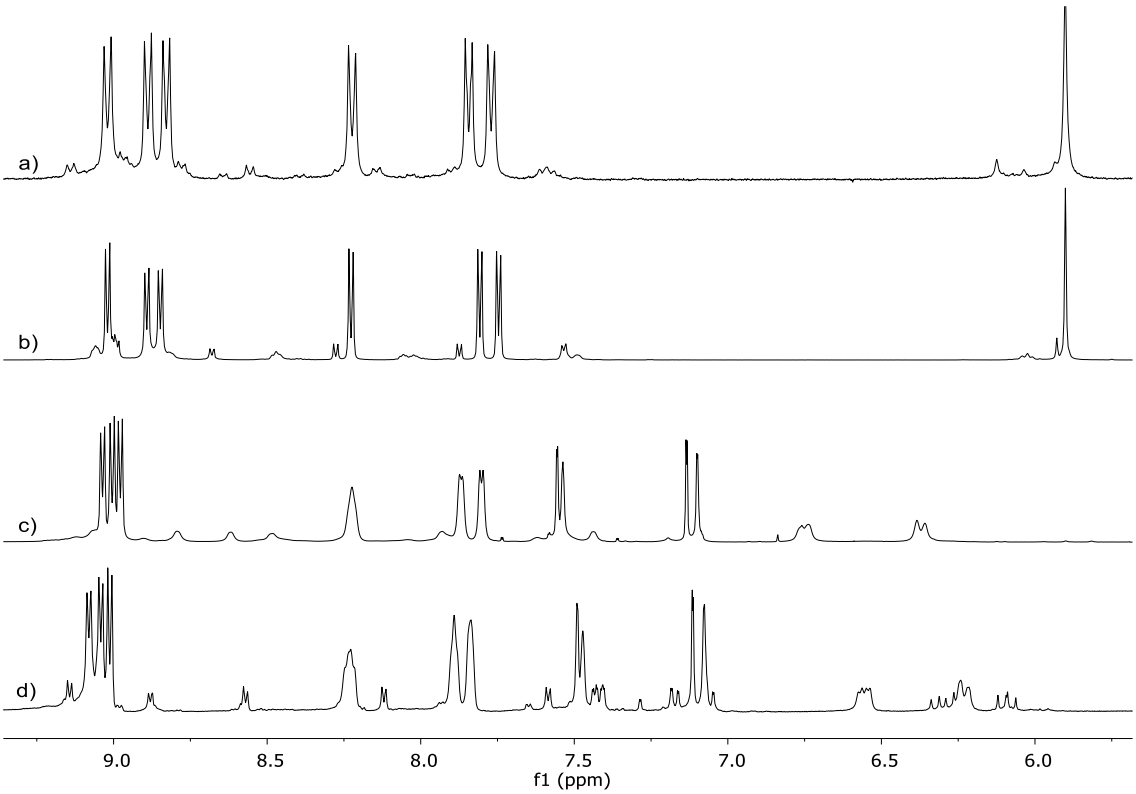

^{1}H NMR (500 MHz, D_2O) partial spectra of metallacycle derived of the ligand **1** with different metal squares: a) **5(Pd)**·2NO_3 ,b) **5(Pt)**·2NO_3,c) **6(Pd)**·2NO_3 and d) **6(Pt)**·2NO_3.

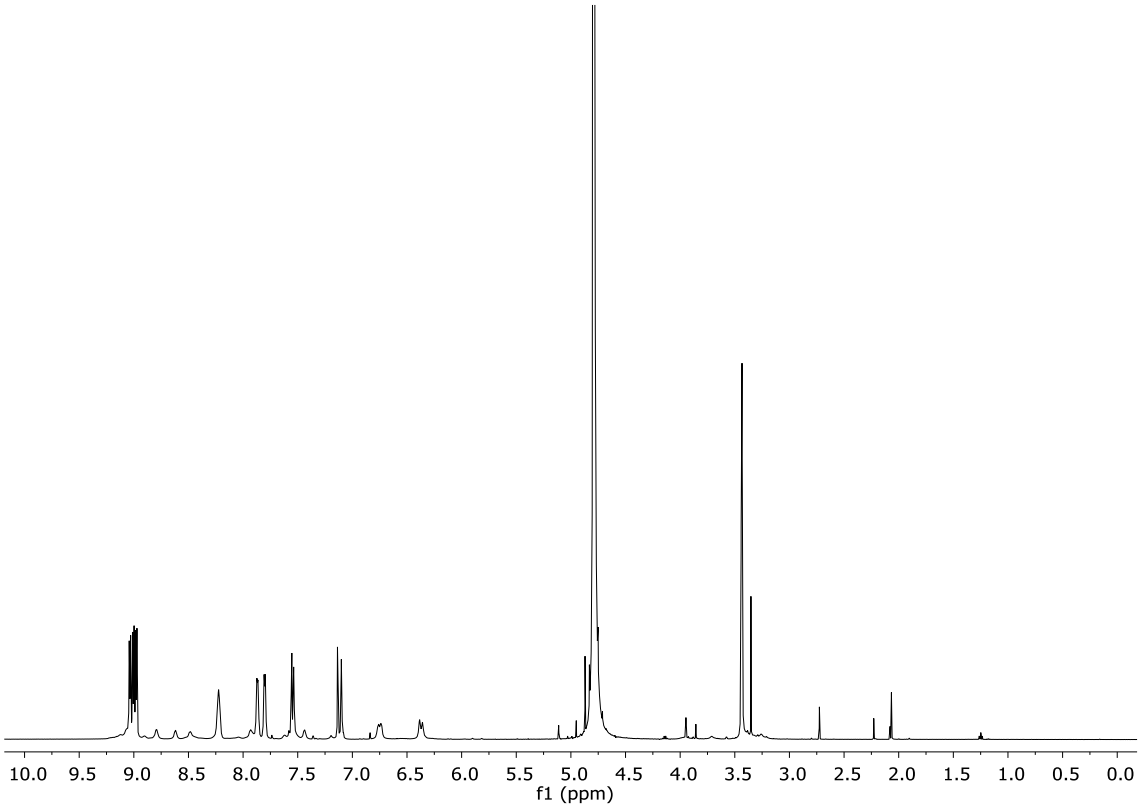

^{1}H NMR (500 MHz, D_2O) full spectra of **R1**·6NO_3.

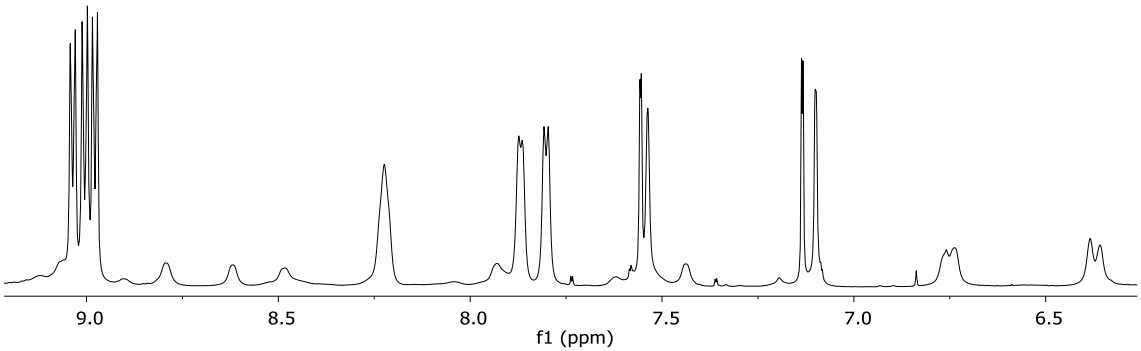

^{1}H NMR (500 MHz, D_2O) partial spectra of **R1**·6NO_3.

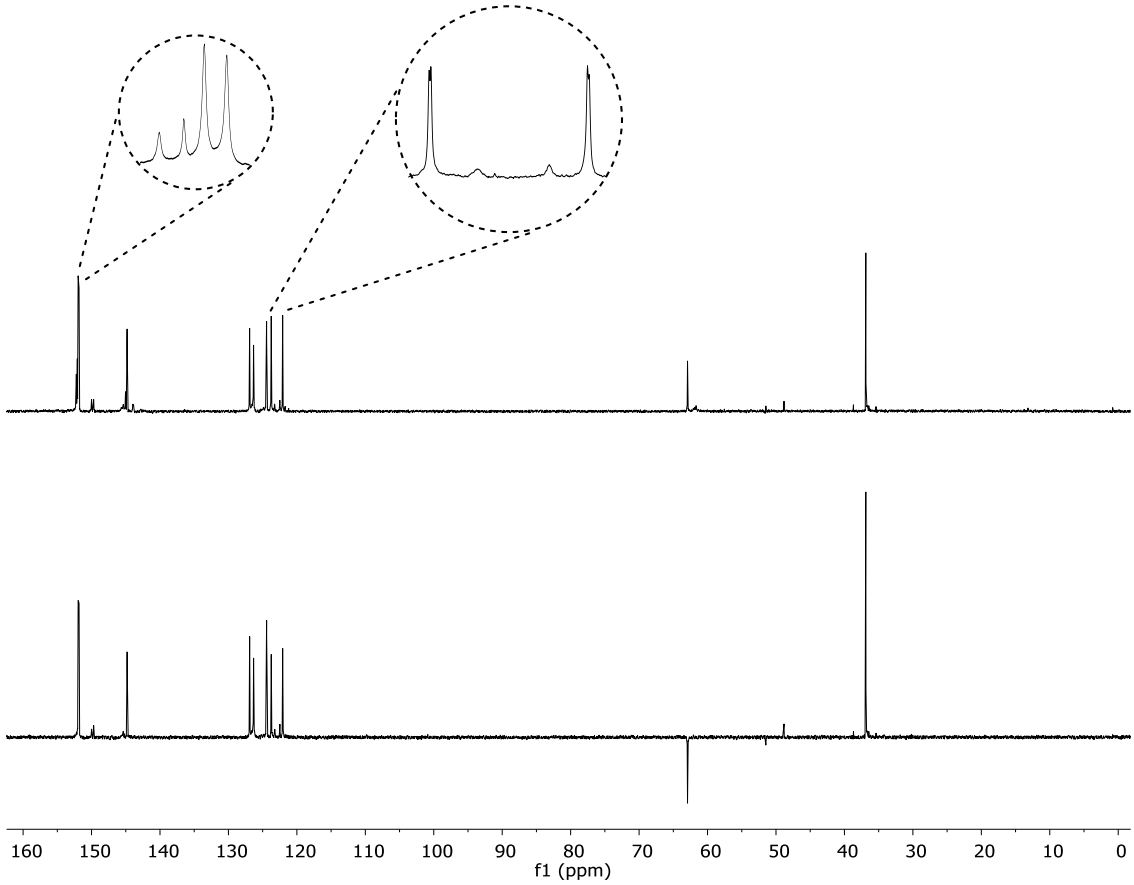

^{13}C NMR and DEPT (125 MHz, D_2O) full spectra of **R1**·6NO_3.

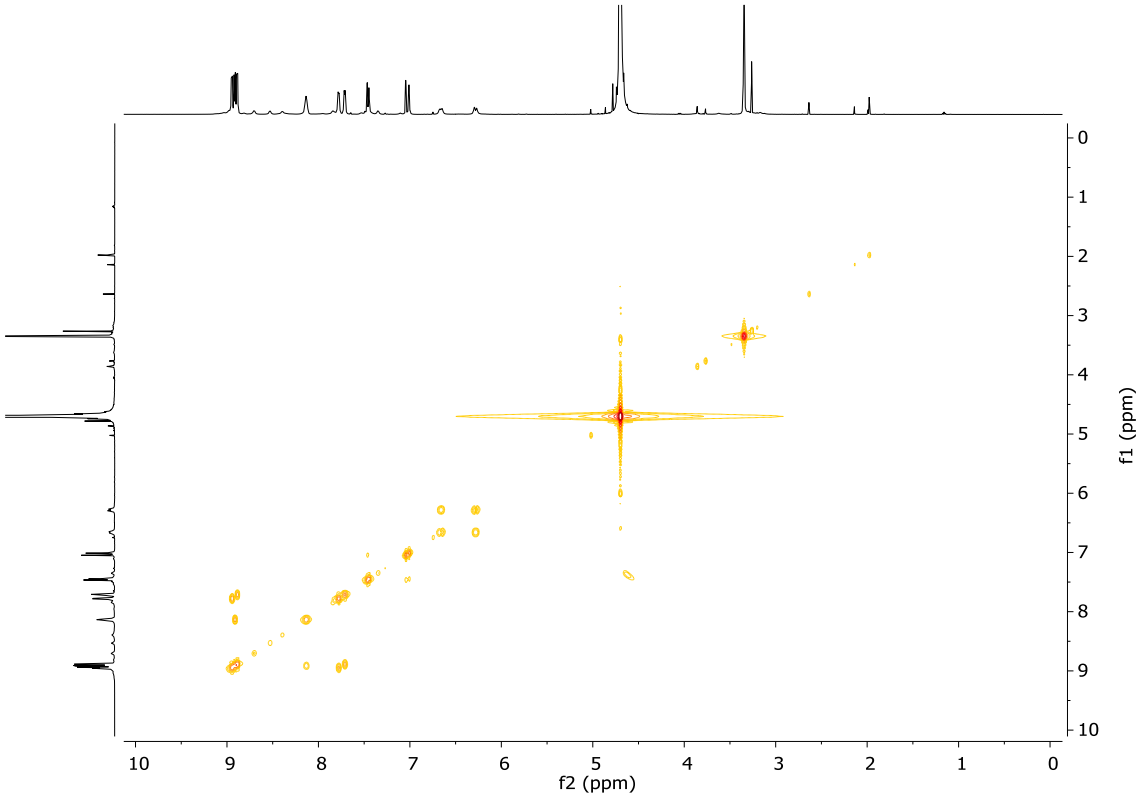

COSY (500 MHz, D_2O) full spectra of **R1**·6NO_3.

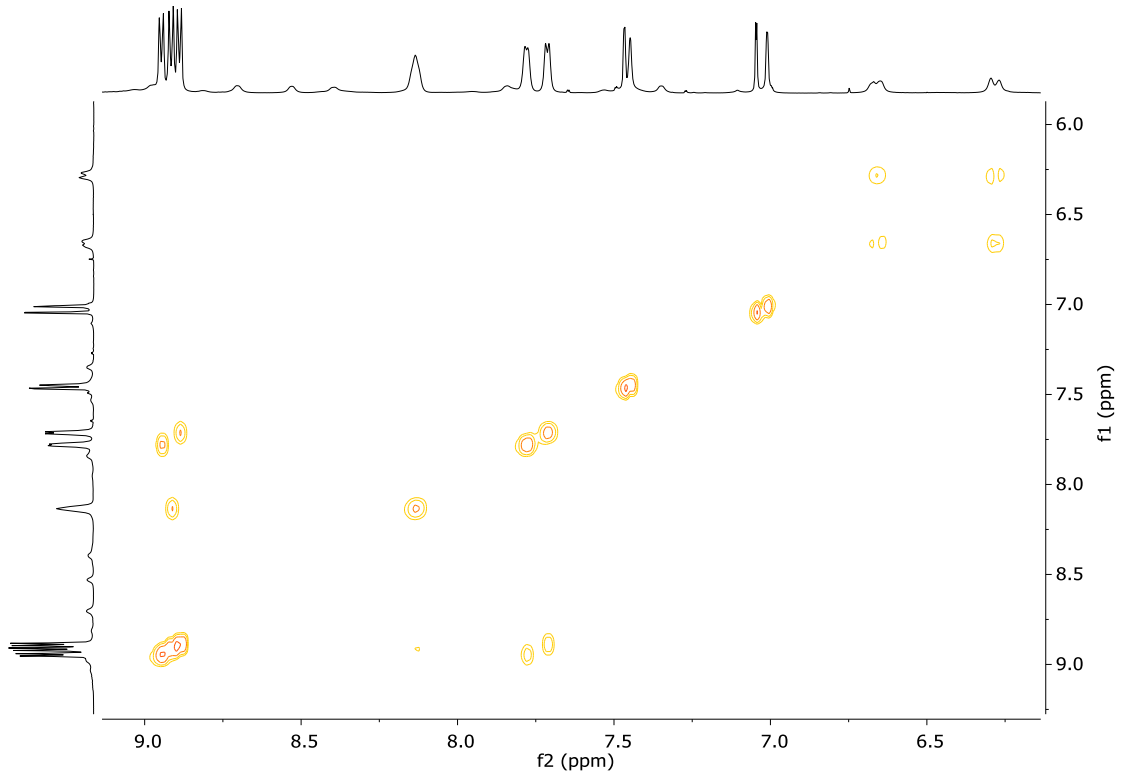

COSY (500 MHz, D_2O) partial spectra of **R1**·$6NO_3$.

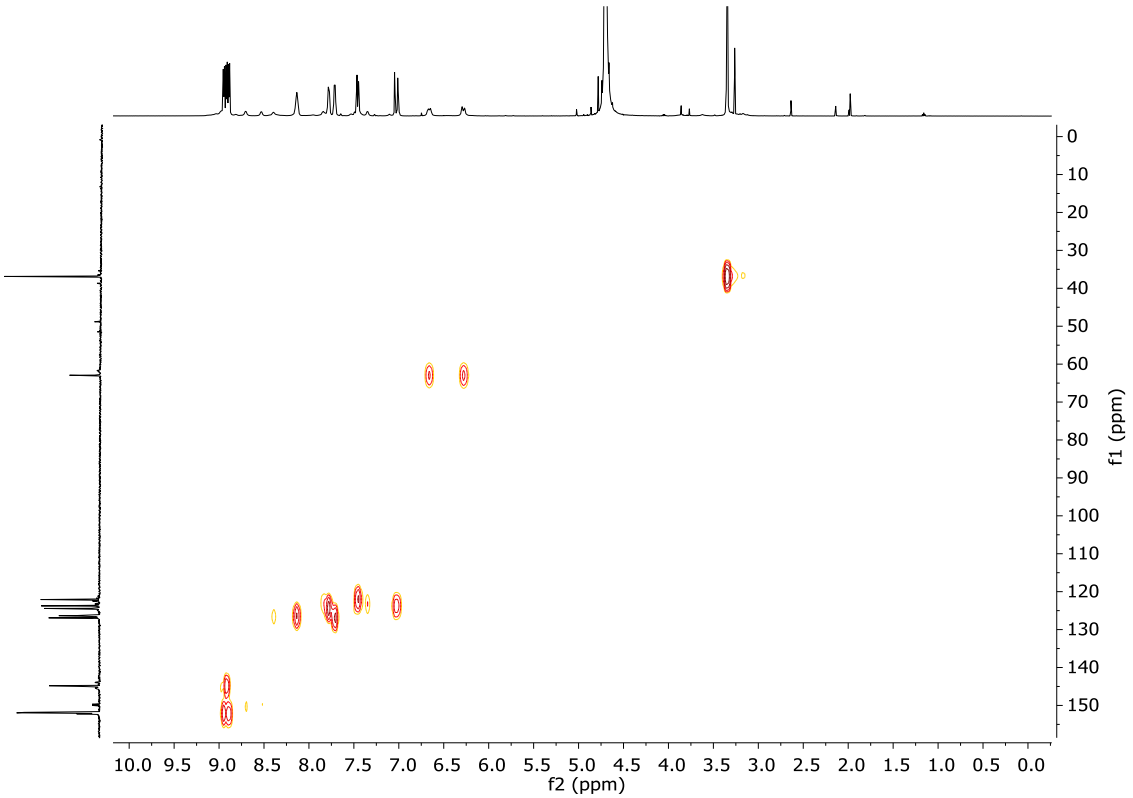

HSQC (125 and 500 MHz, D_2O) full spectra of **R1**·$6NO_3$.

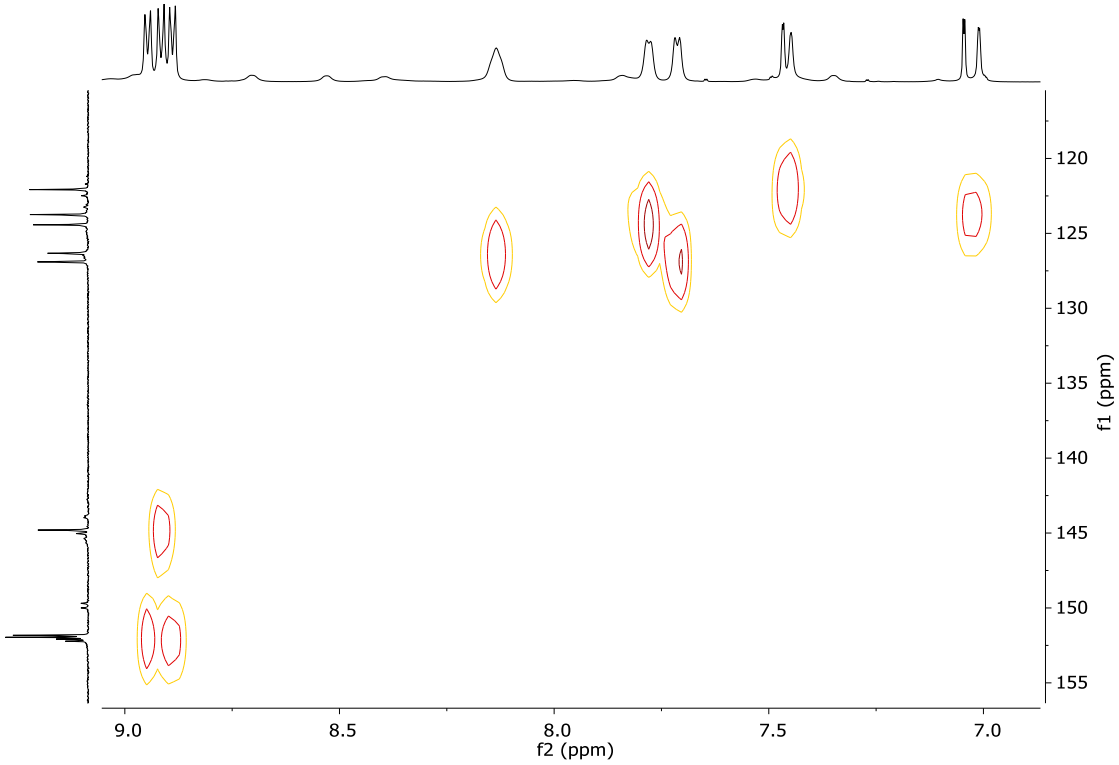

HSQC (125 and 500 MHz, D_2O) detail spectra of **R1**·6NO_3.

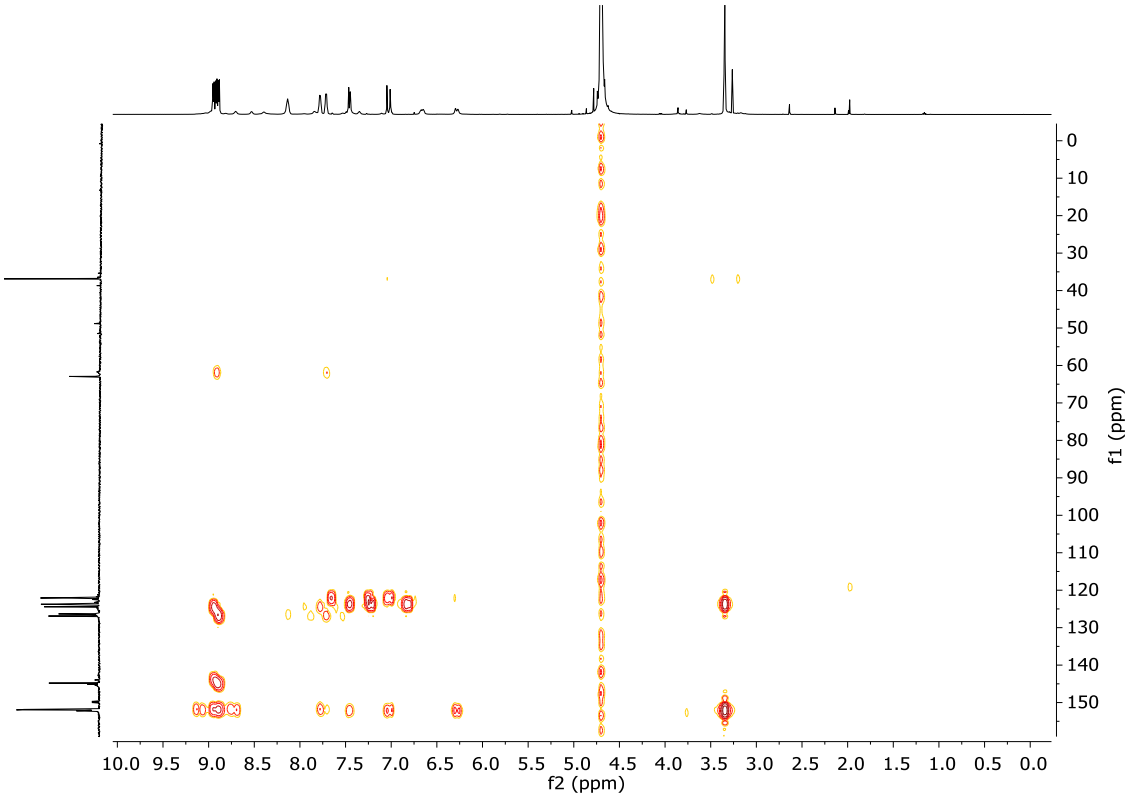

HMBC (125 and 500 MHz, D_2O) full spectra of **R1**·6NO_3.

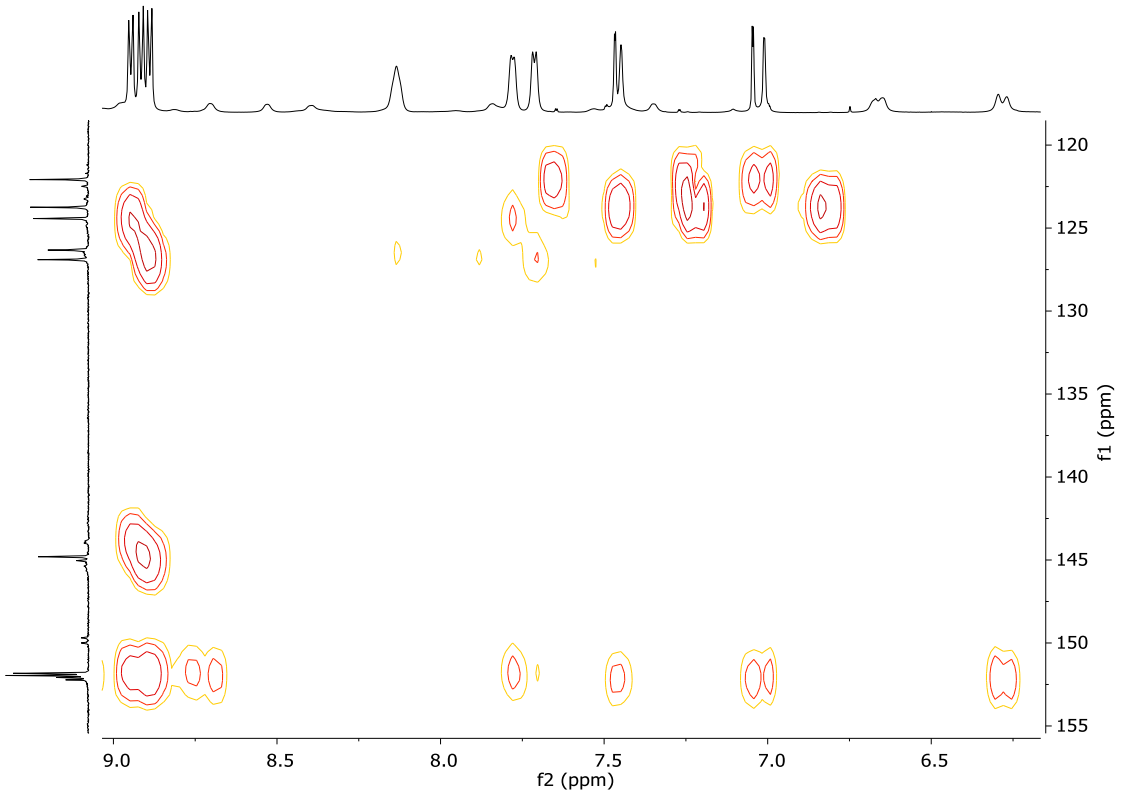

HMBC (125 and 500 MHz, D_2O) detail spectra of **R1**·6NO_3.

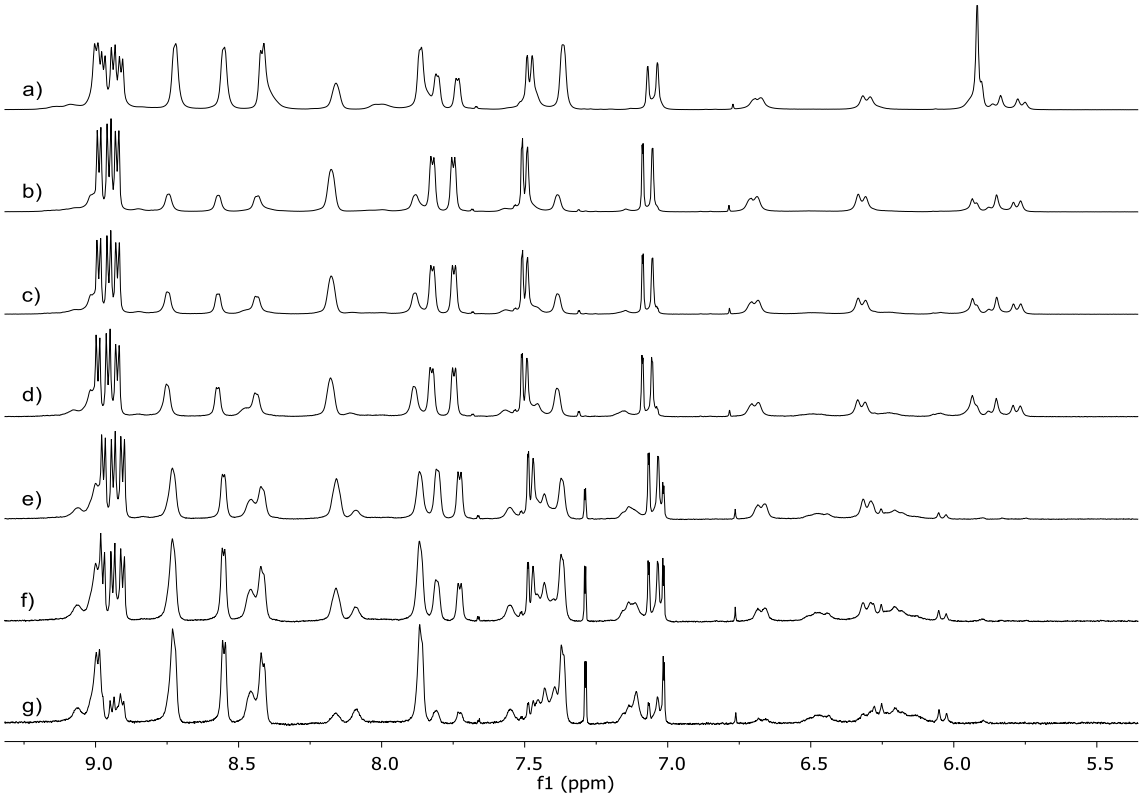

^{1}H NMR (500 MHz, D_2O) partial spectra of **R1**·6NO_3 dilution effect at a) 20 mM, b) 10 mM, c) 5 mM, d) 2.5 mM, e) 1.25 mM, f) 0.75 mM, g) 0.375 mM.

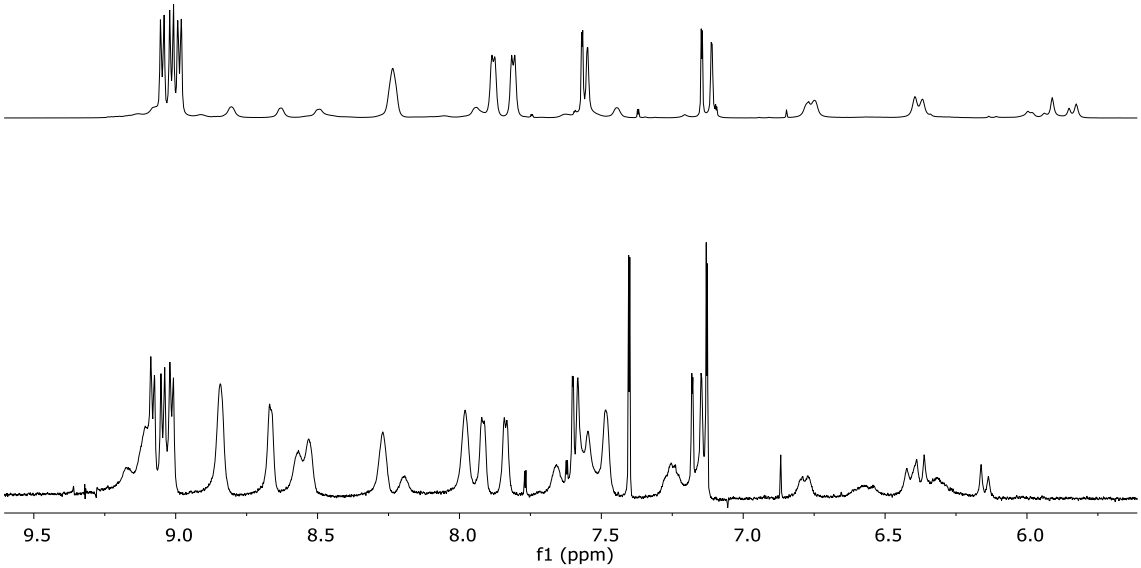

^{1}H NMR (500 MHz, D_2O) partial spectra of **R1**·6NO_3 5mM (top) and **R1**·6NO_3 (bottom) in the presence of 1.6 % of CD_3CN in media.

1.4. Metallacycle **R2**·6NO_3

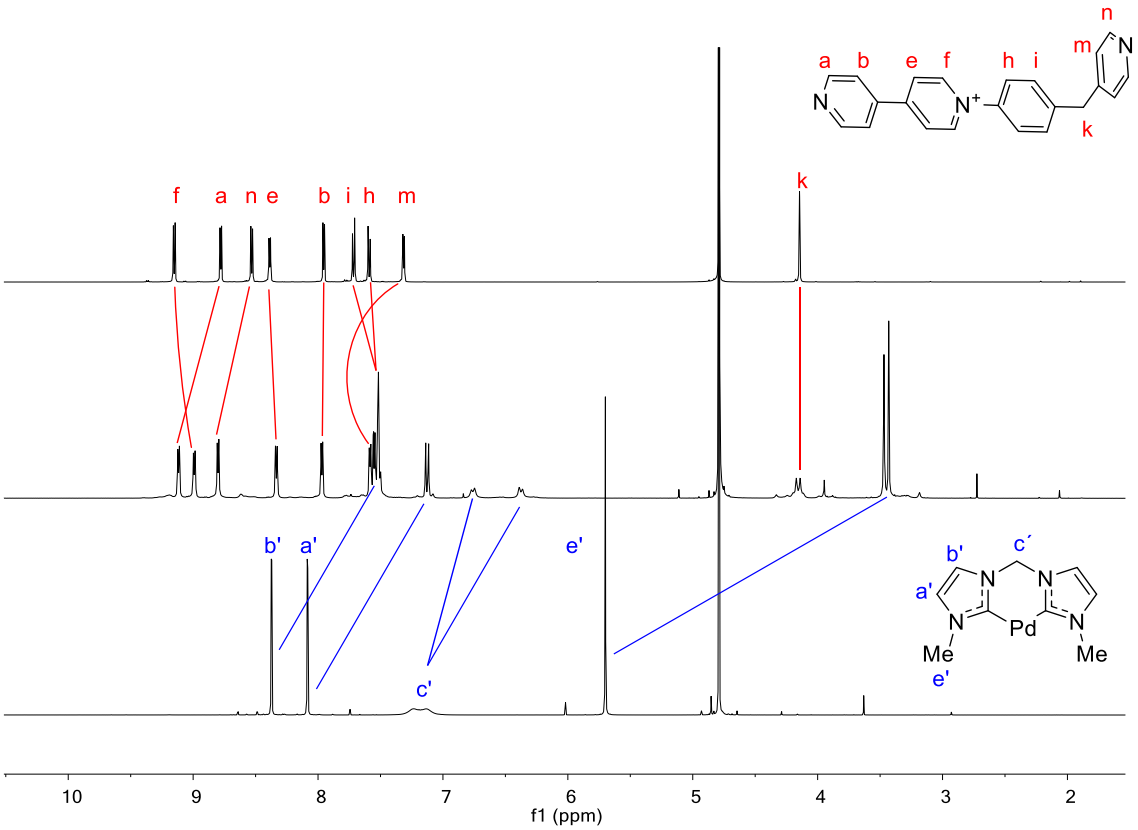

^{1}H NMR (500 MHz, D_2O) spectra of **2** (top), **R2**·6NO_3 (middle), and **6(Pd)**·2NO_3 (bottom).

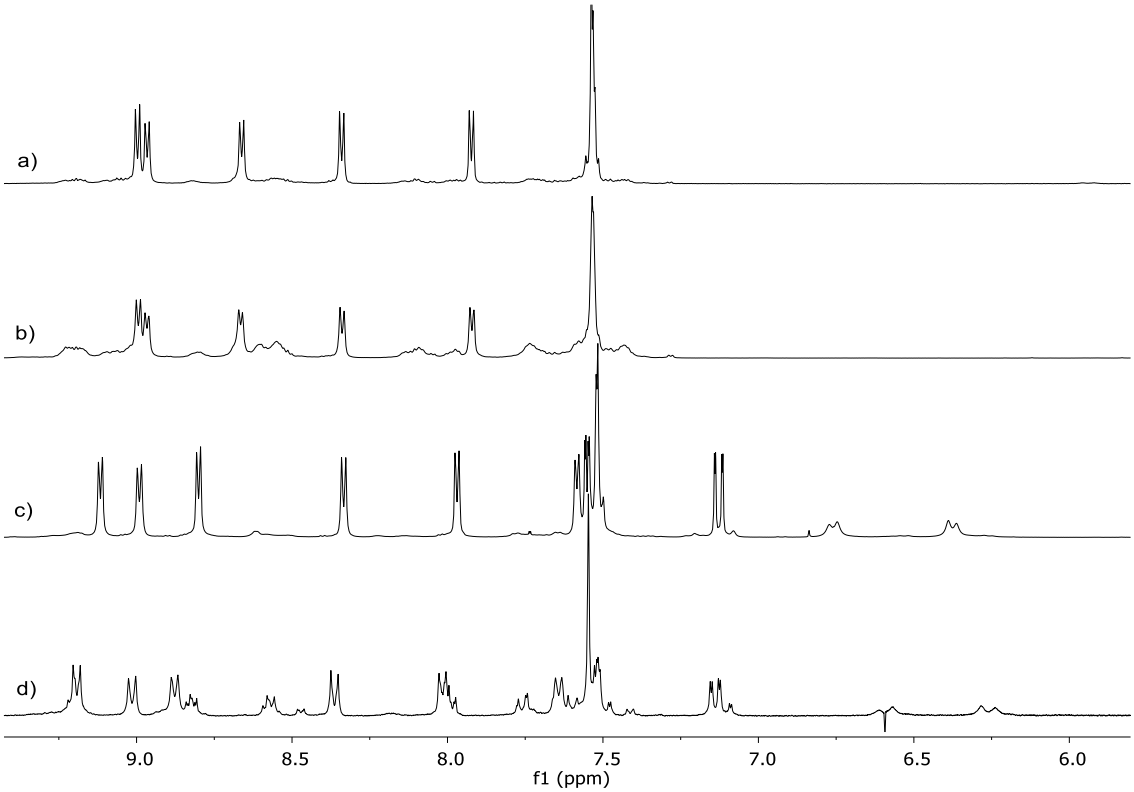

^{1}H NMR (500 MHz, D_2O) partial spectra of metallacycle derived of the ligand **2** with different metal squares: **5(Pd)**·2NO_3**,** b) **5(Pt)**·2NO_3, c) **6(Pd)**·2NO_3 and d) **6(Pt)**·2NO_3.

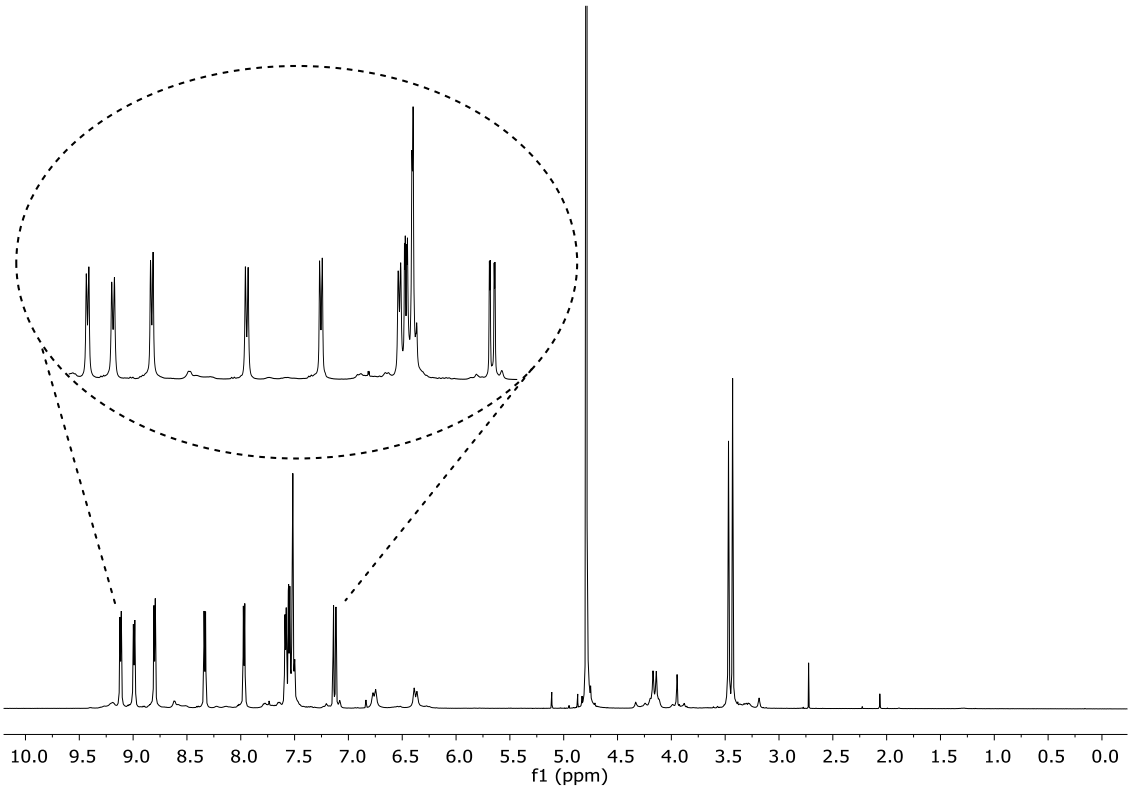

^{1}H NMR (500 MHz, D_2O) full spectra of **R2**·6NO_3

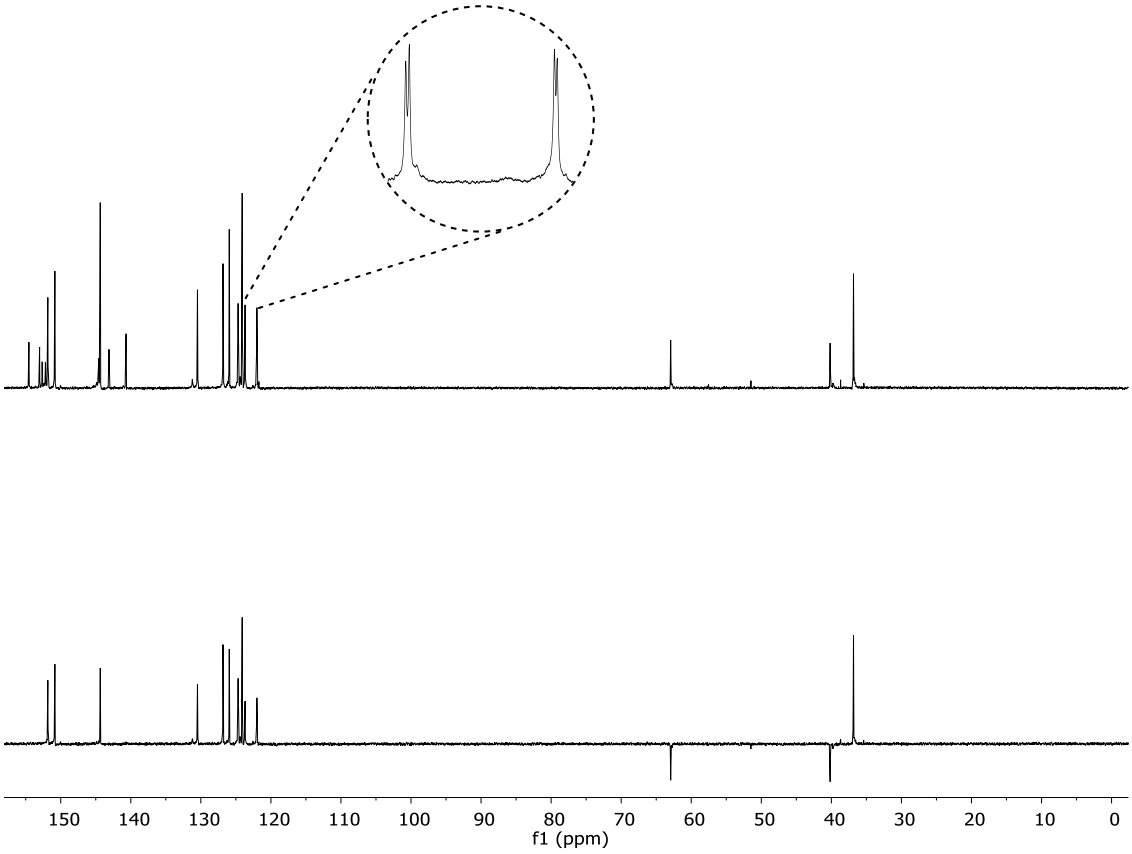

^{13}C NMR and DEPT (125 MHz, D_2O) full spectra of **R2**·6NO_3.

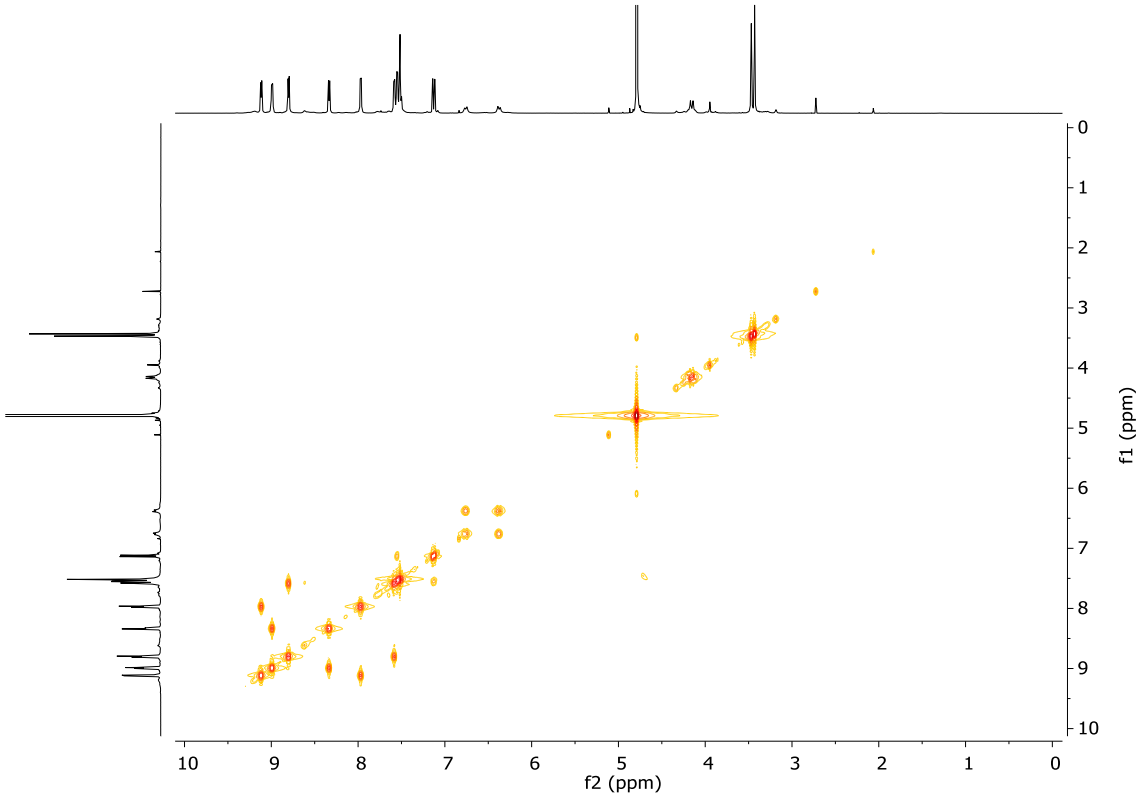

COSY (500 MHz, D_2O) full spectra of **R2**·6NO_3.

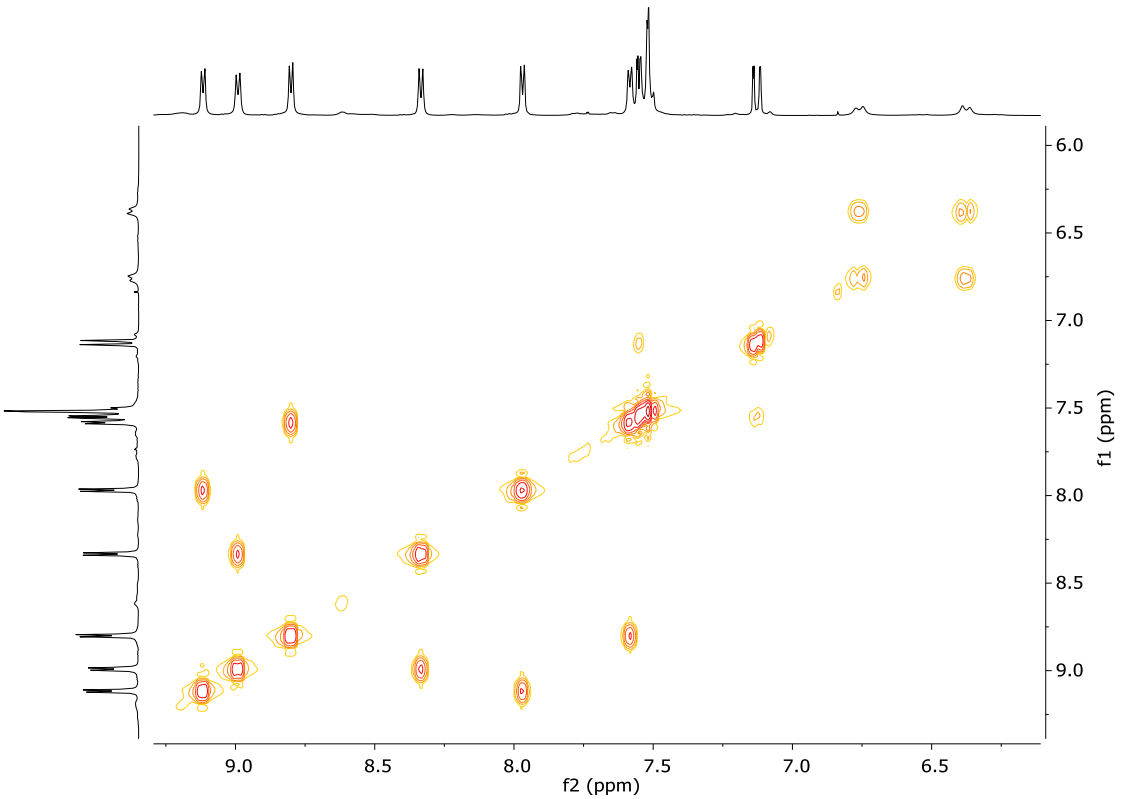

COSY (500 MHz, D_2O) partial espectra of **R2**·6NO_3.

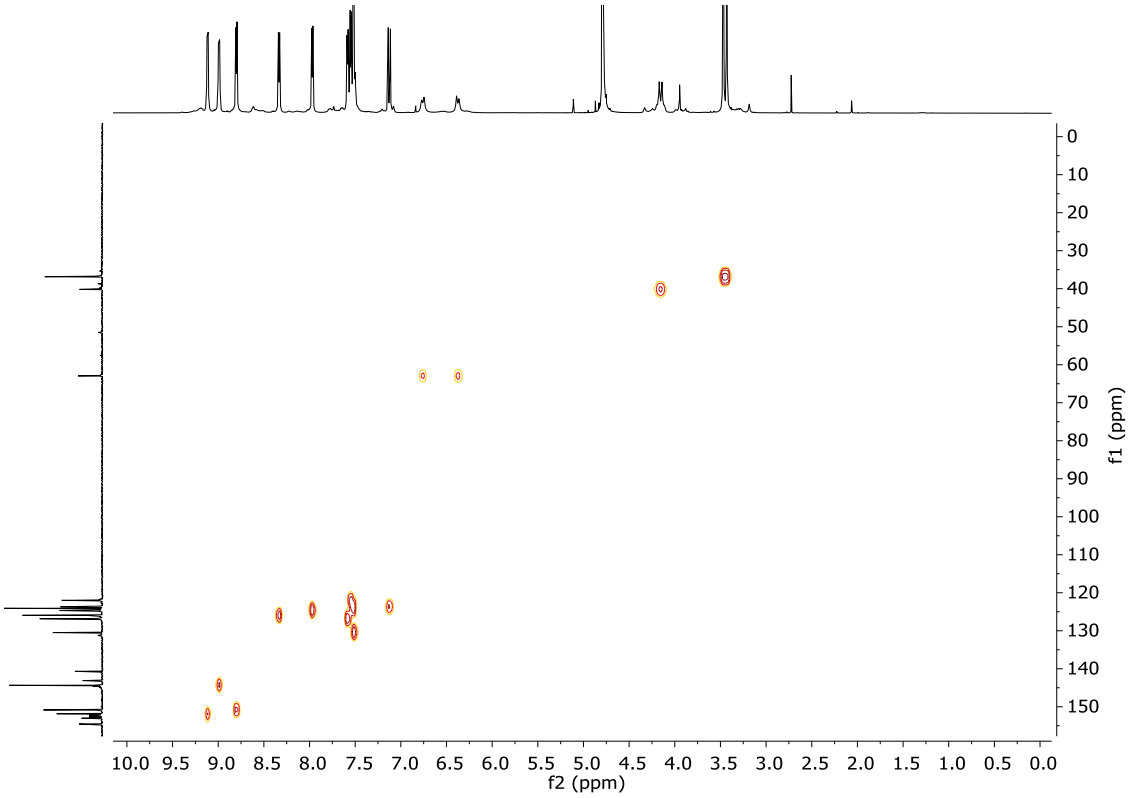

HSQC (125 and 500 MHz, D_2O) full spectra of **R2**·$6NO_3$.

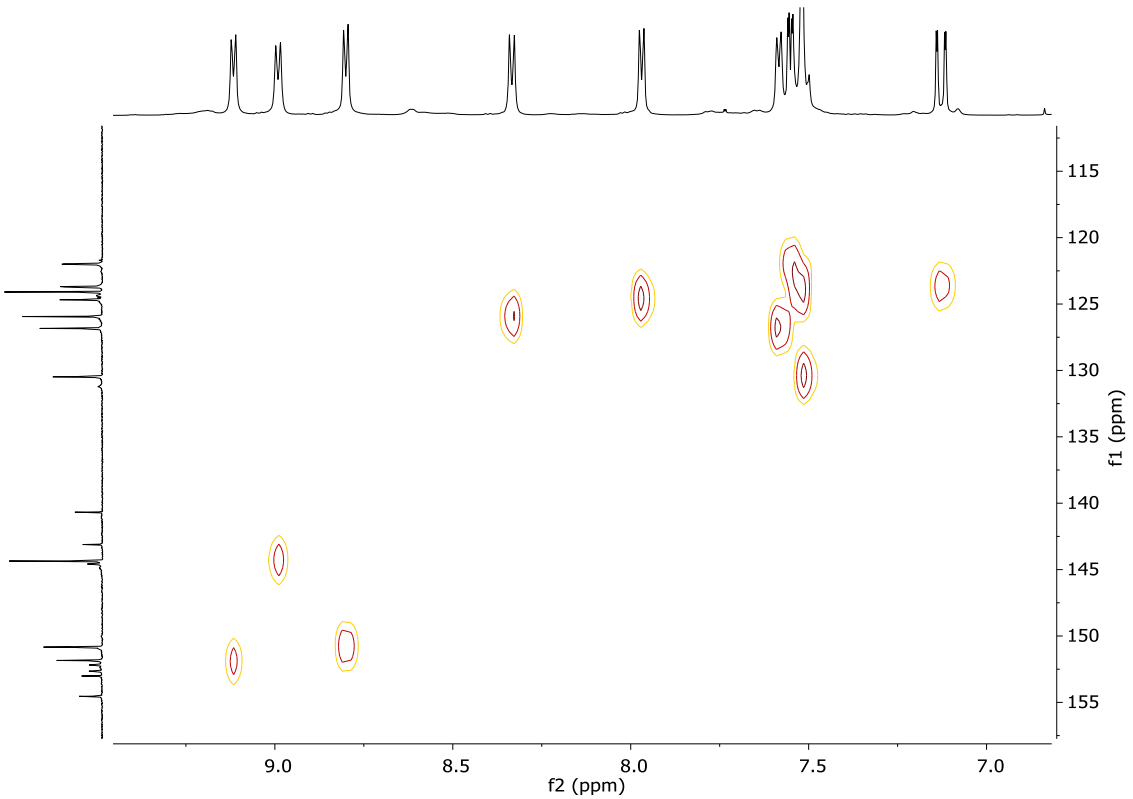

HSQC (125 and 500 MHz, D_2O) partial spectra of **R2**·$6NO_3$.

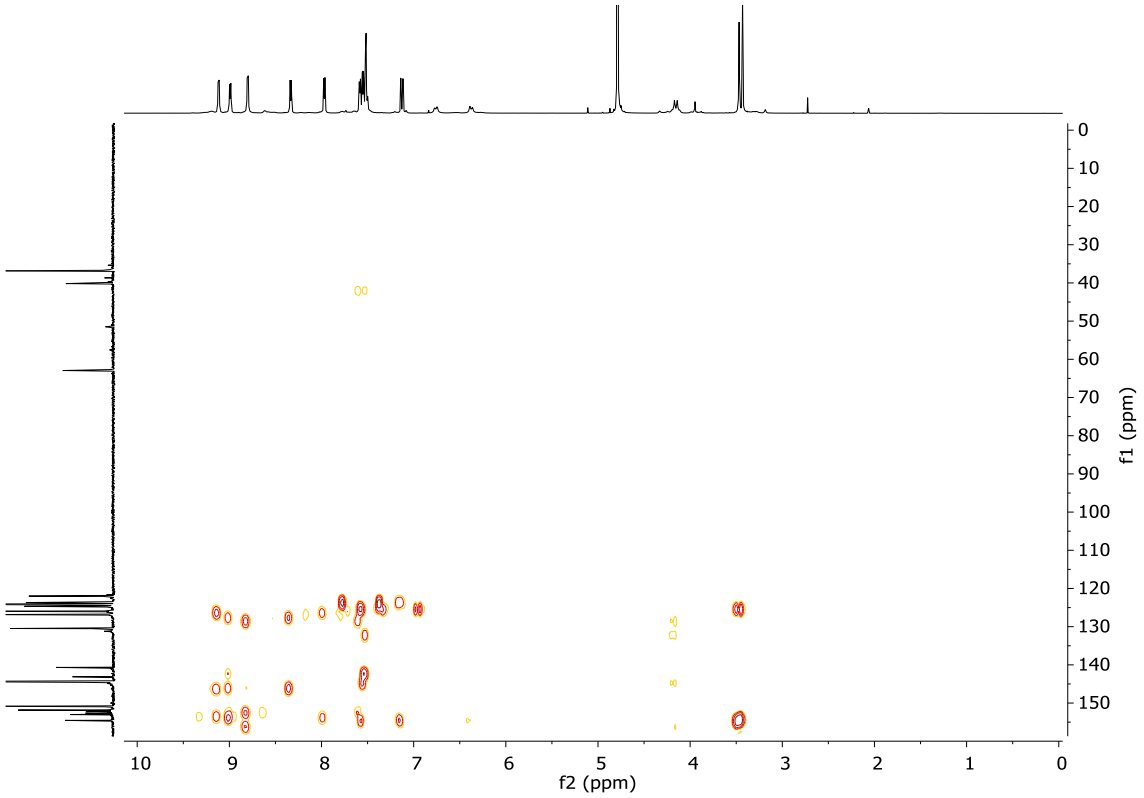

HMBC (125 and 500 MHz, D_2O) full spectra of **R2**·6NO_3.

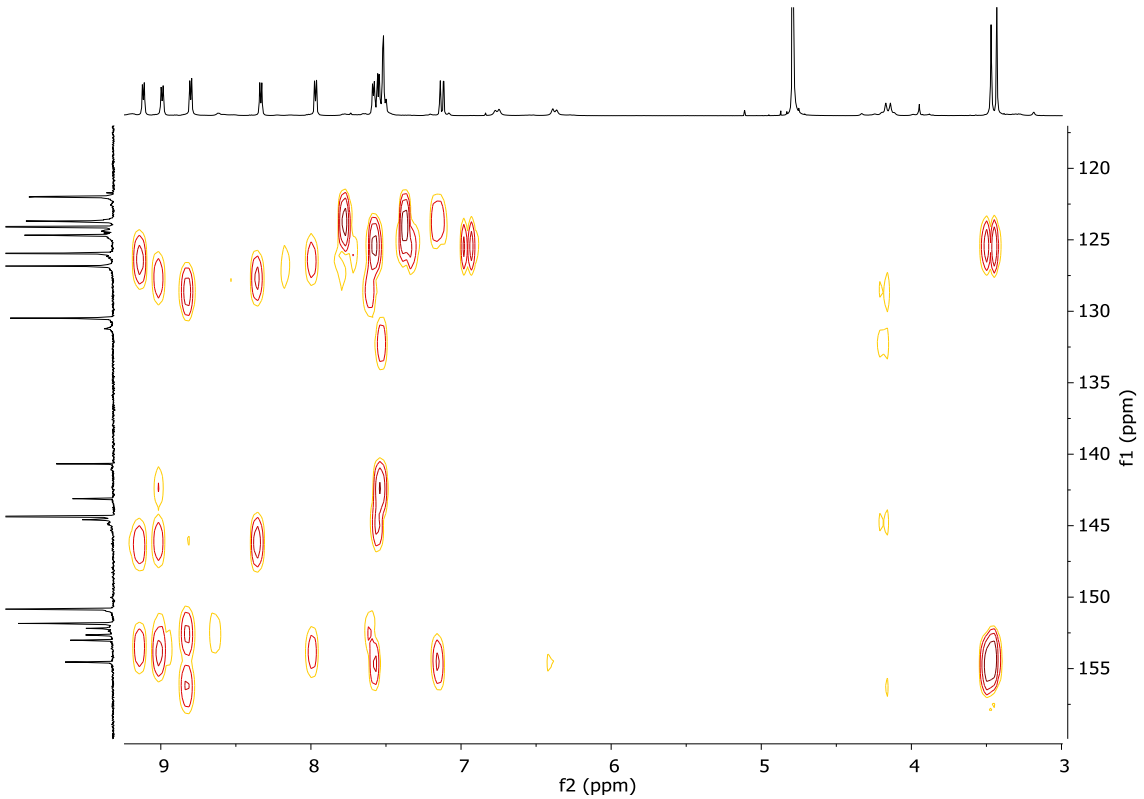

HMBC (125 and 500 MHz, D_2O) partial spectra of **R2**·6NO_3.

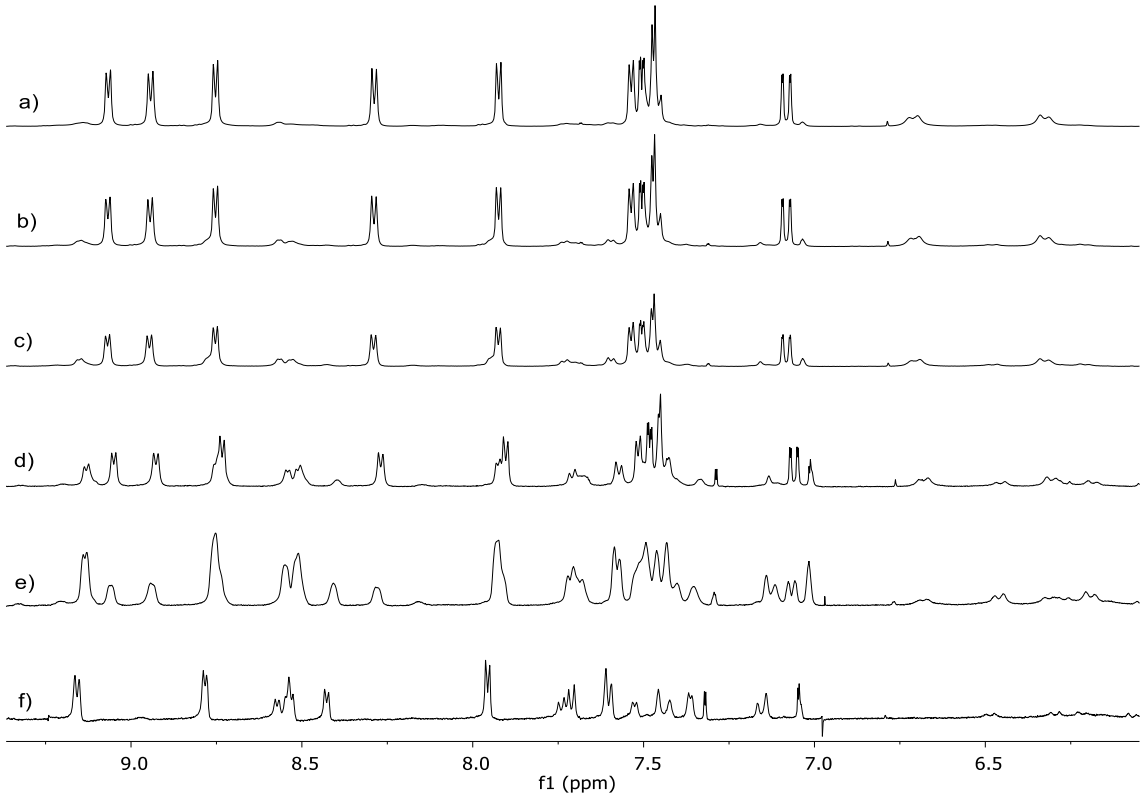

^{1}H NMR (500 MHz, D_2O) full spectra of **R2**·6NO_3 dilution effect at a) 10mM, b) 5mM, c) 2.5mM, d) 1.25 mM, e) 0.75mM and f) 0.1 mM.

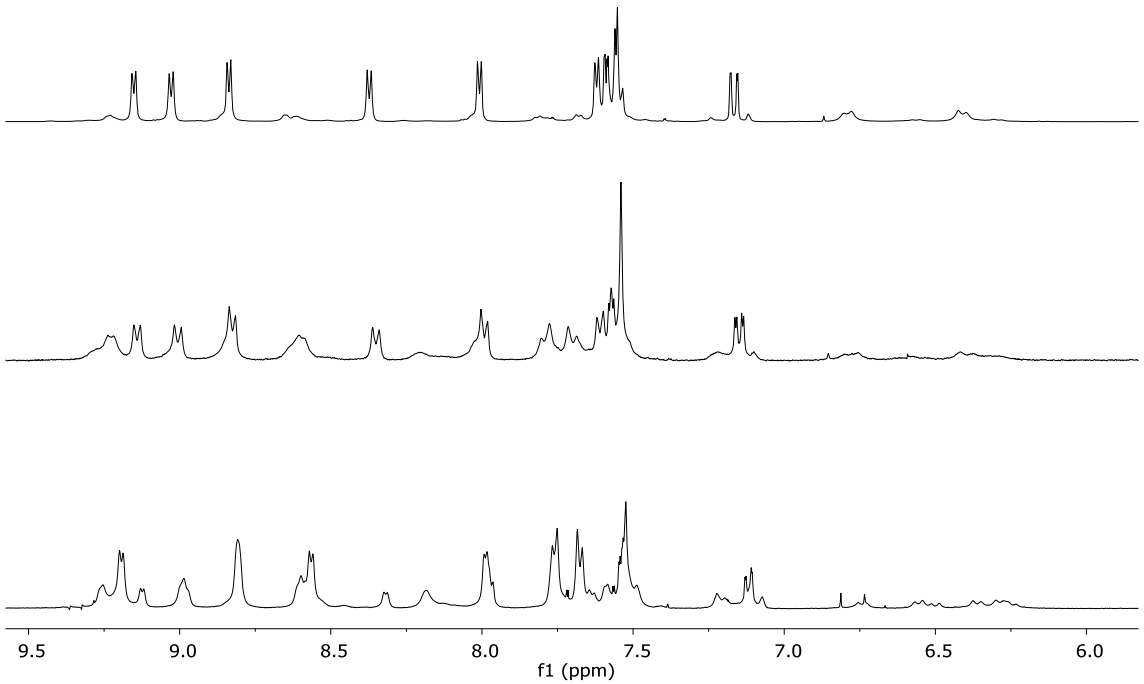

^{1}H NMR (500 MHz, D_2O) partial spectra of **R2**·6NO_3 (5mM, top) and **R2**·6NO_3 in the presence of 1.6 % (middle) and 3.2% (bottom) of CD_3CN in media, respectively.

1.5. Metallacycle **R3**·8NO_3

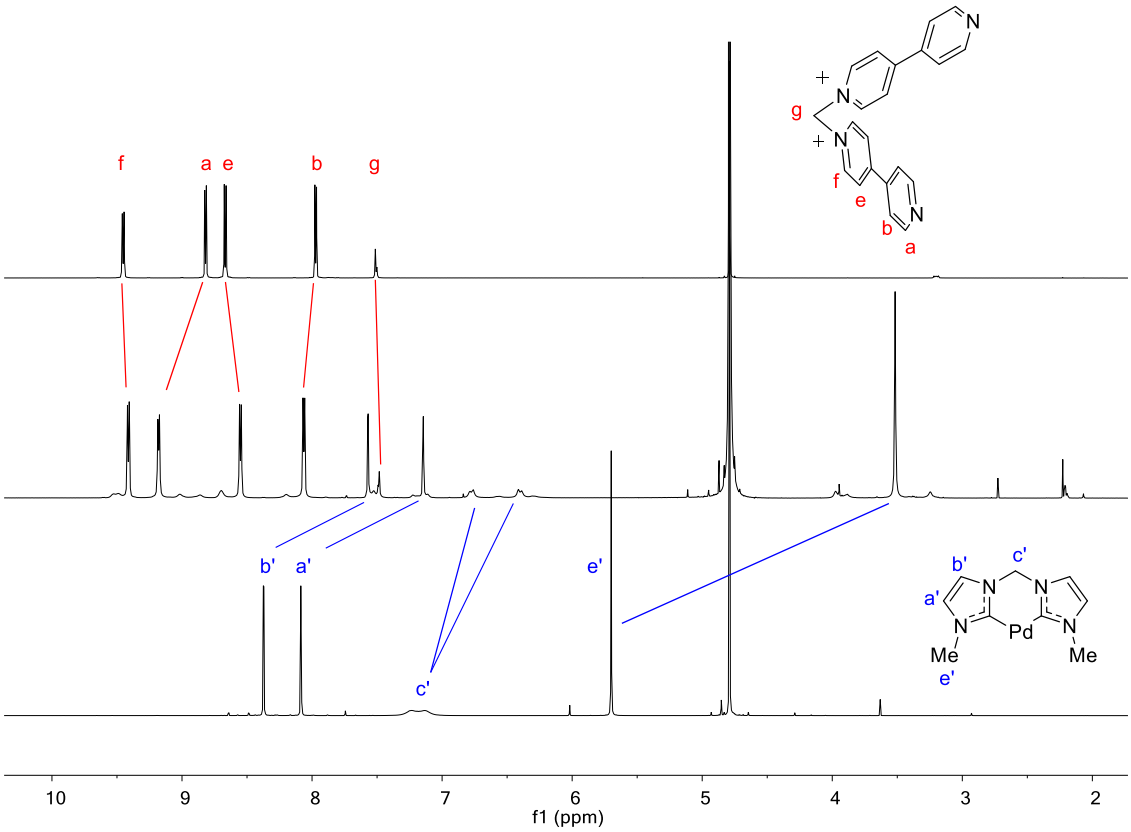

^{1}H NMR (500 MHz, D_2O) espectra of **3** (top), **R3**·8NO_3 (middle) and **6(Pd)**·2NO_3 (bottom).

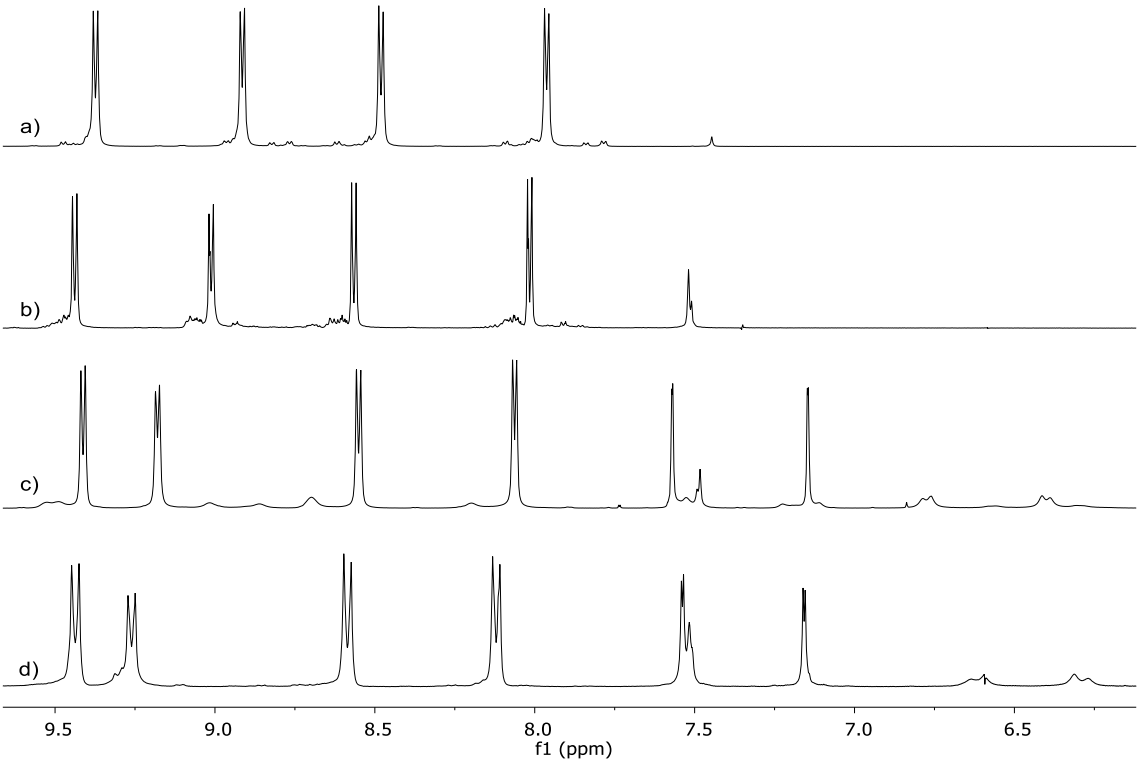

^{1}H NMR (500 MHz, D_2O) partial spectra of metallacycle derived of the ligand **3** with diferent metal squares: a) **5(Pd)**·2NO_3, b) **5(Pt)**·2NO_3, c) **6(Pd)**·2NO_3 and d) **6(Pt)**·2NO_3.

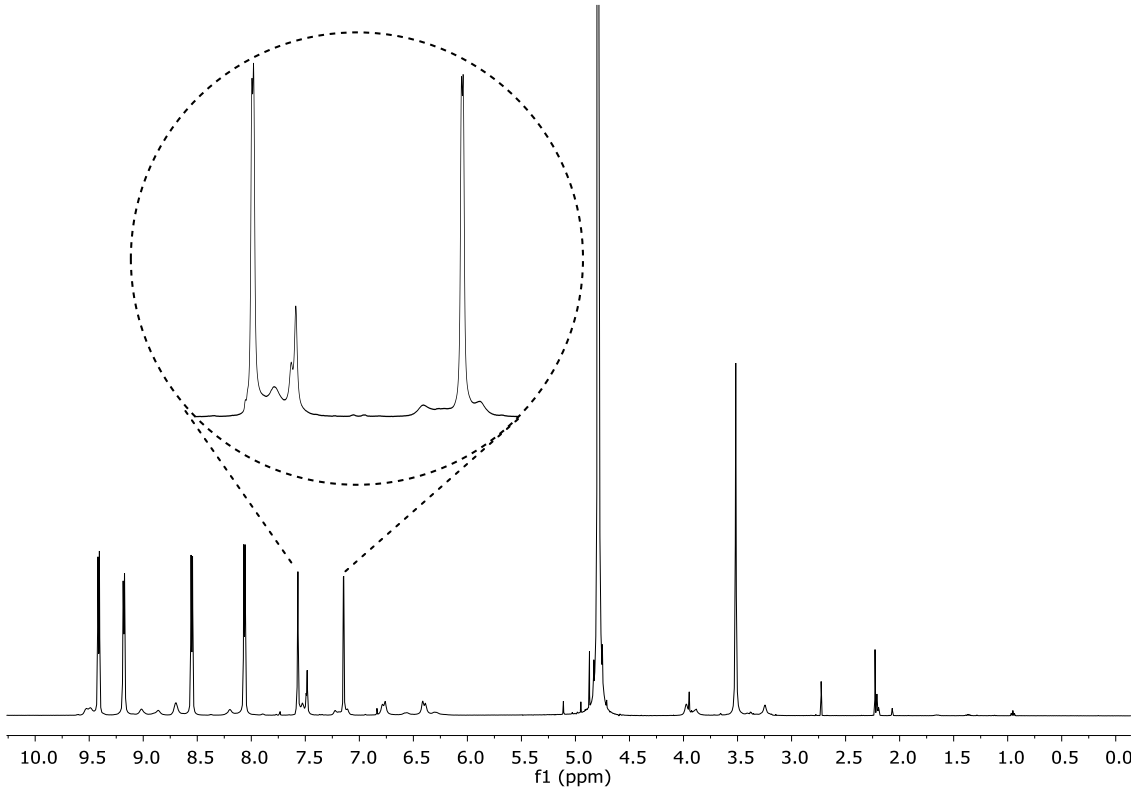

^{1}H NMR (500 MHz, D_2O) full spectra of **R3**·8NO_3.

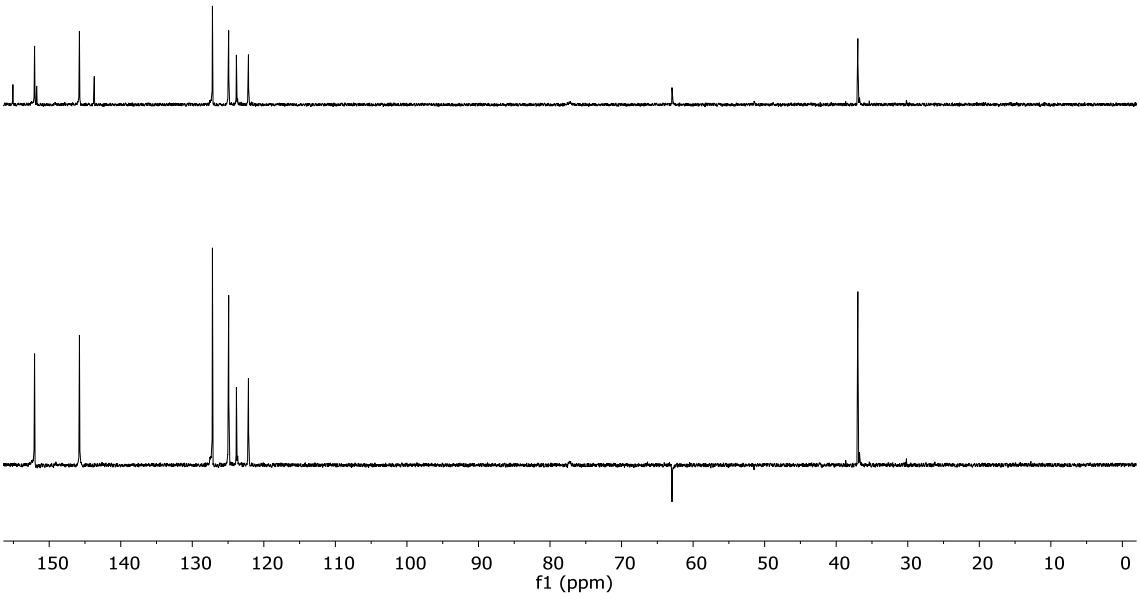

^{13}C NMR and DEPT (125 MHz, D_2O) full spectra of **R3**·8NO_3.

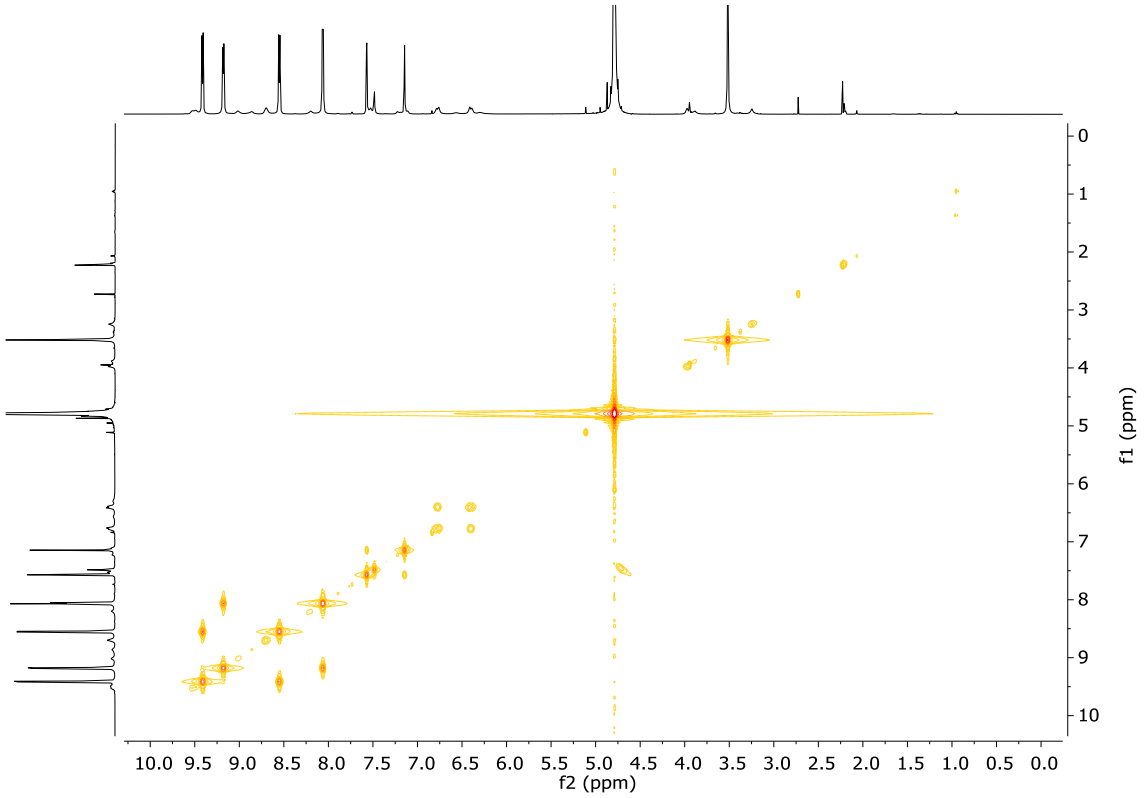

COSY (500 MHz, D_2O) full spectra of **R3**·8NO_3.

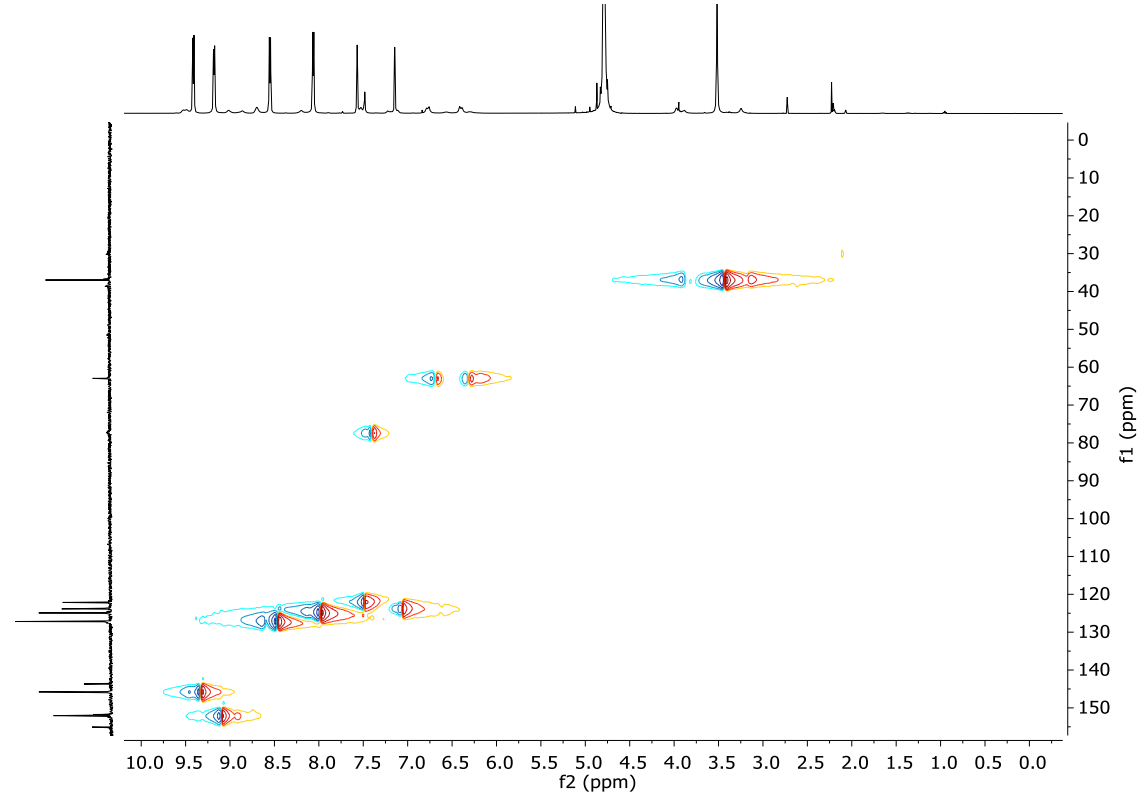

HSQC (125 and 500 MHz, D_2O) full spectra of **R3**·8NO_3.

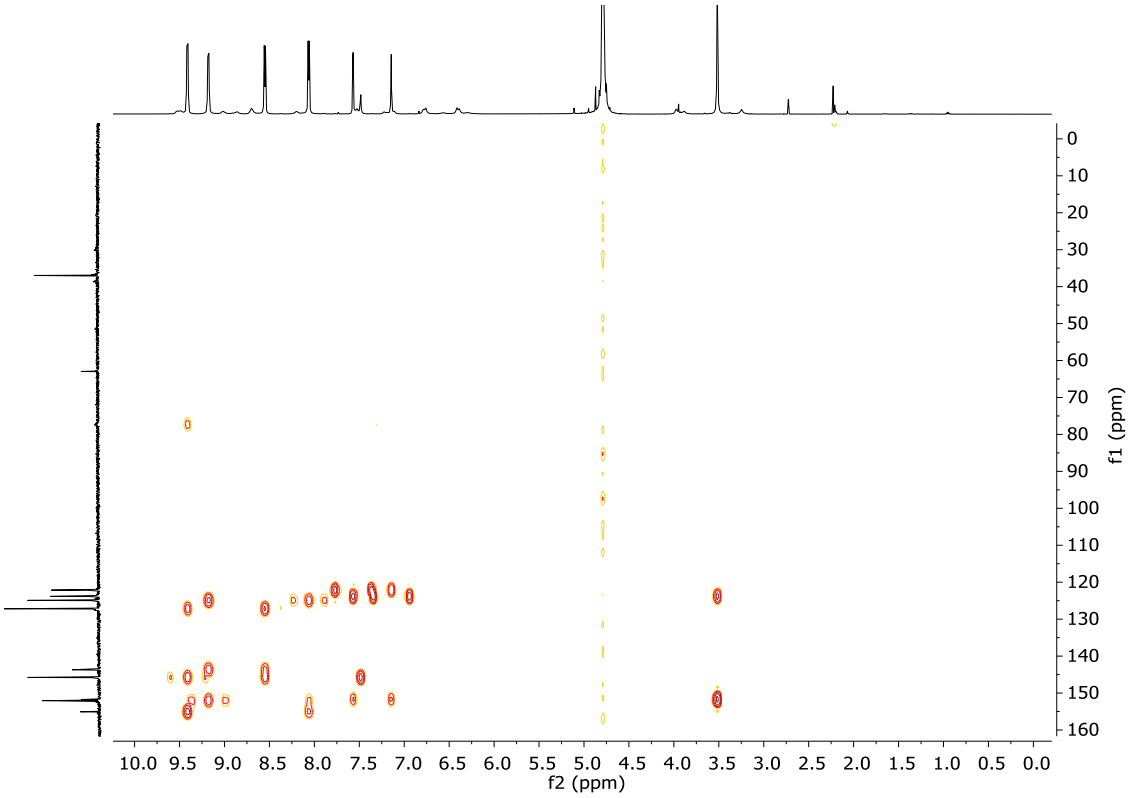

HMBC (125 and 500 MHz, D_2O) partial spectra of **R3**·8NO_3.

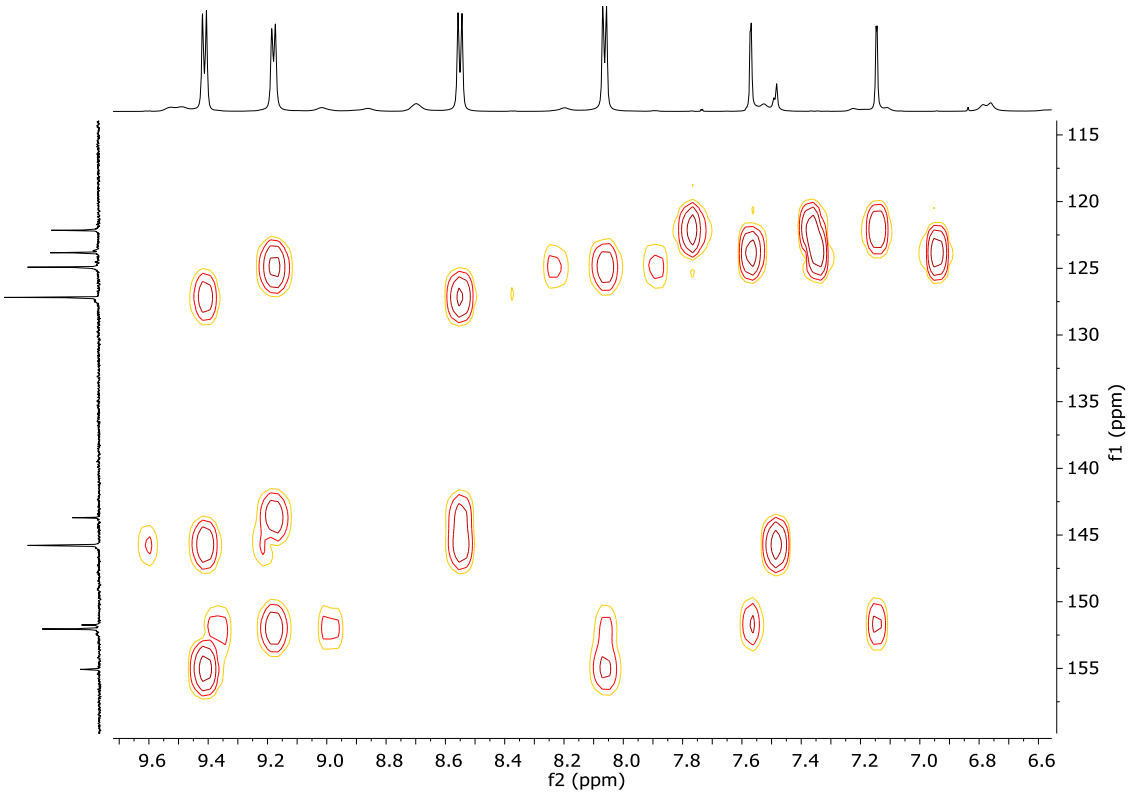

HMBC (125 and 500 MHz, D_2O) partial spectra of **R3**·8NO_3.

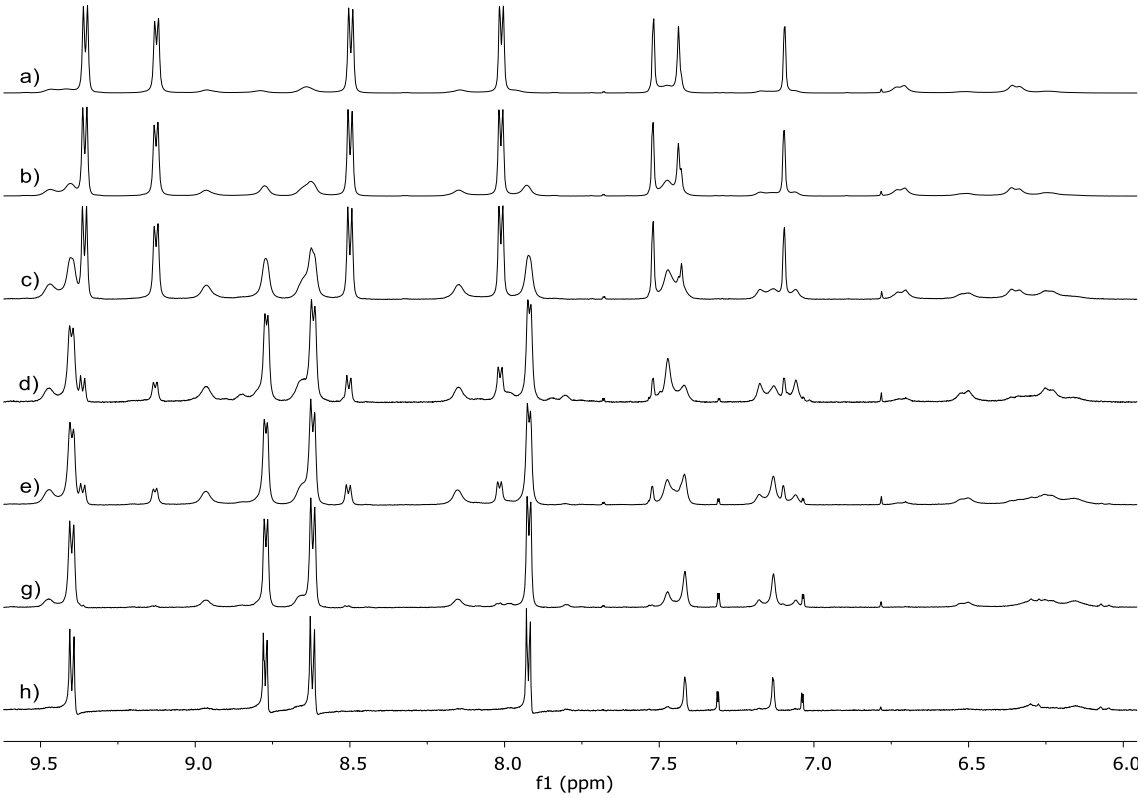

^{1}H NMR (500 MHz, D_2O) partial spectra of **R3**·8NO_3 dilution effect at a) 10 mM. b) 5mM, c) 2.5 mM, d) 1.25 mM, e) 0.75 mM, f) 0.375 mM and g) 0.1 mM.

1.6. Metallacycle **R4**·8NO_3

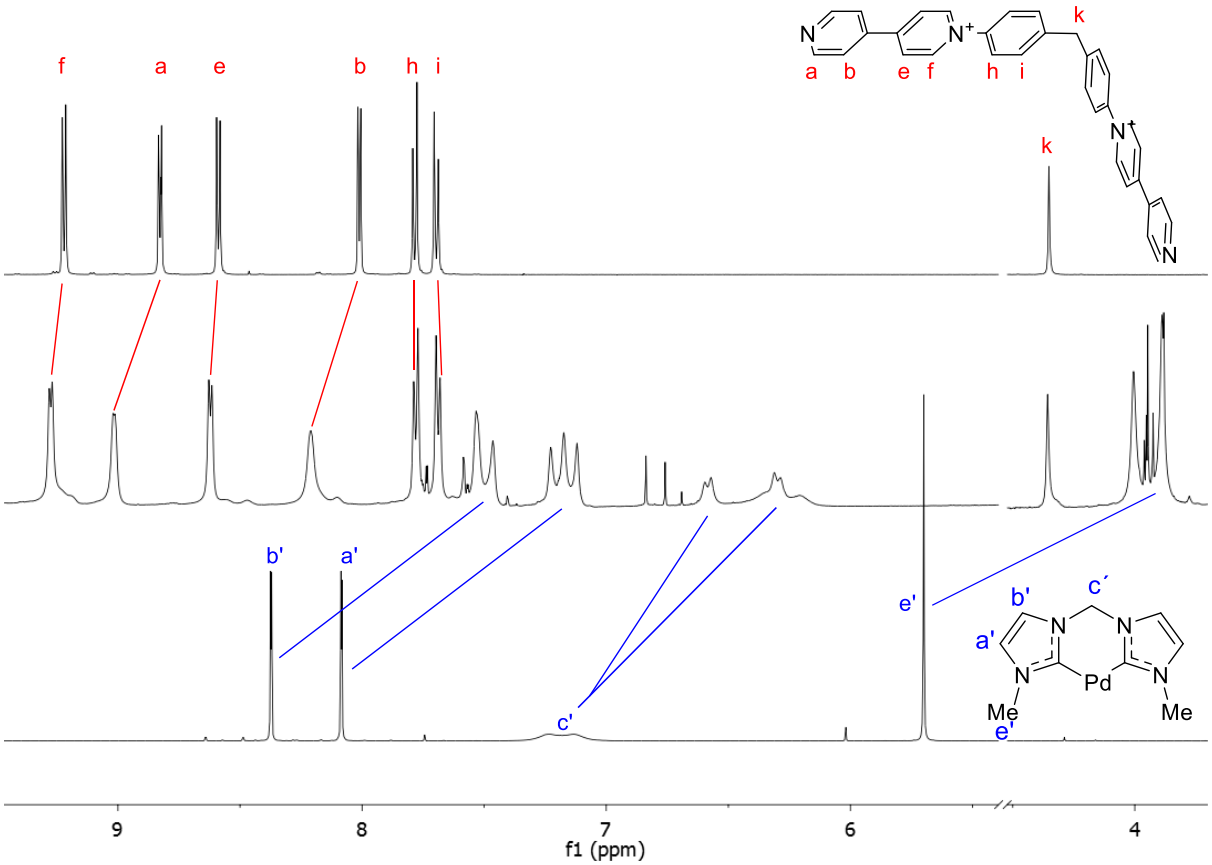

^{1}H NMR (500 MHz, D_2O) partial spectra of **4** (top), **R4**·8NO_3 (middle) and **6(Pd)**·2NO_3 (bottom).

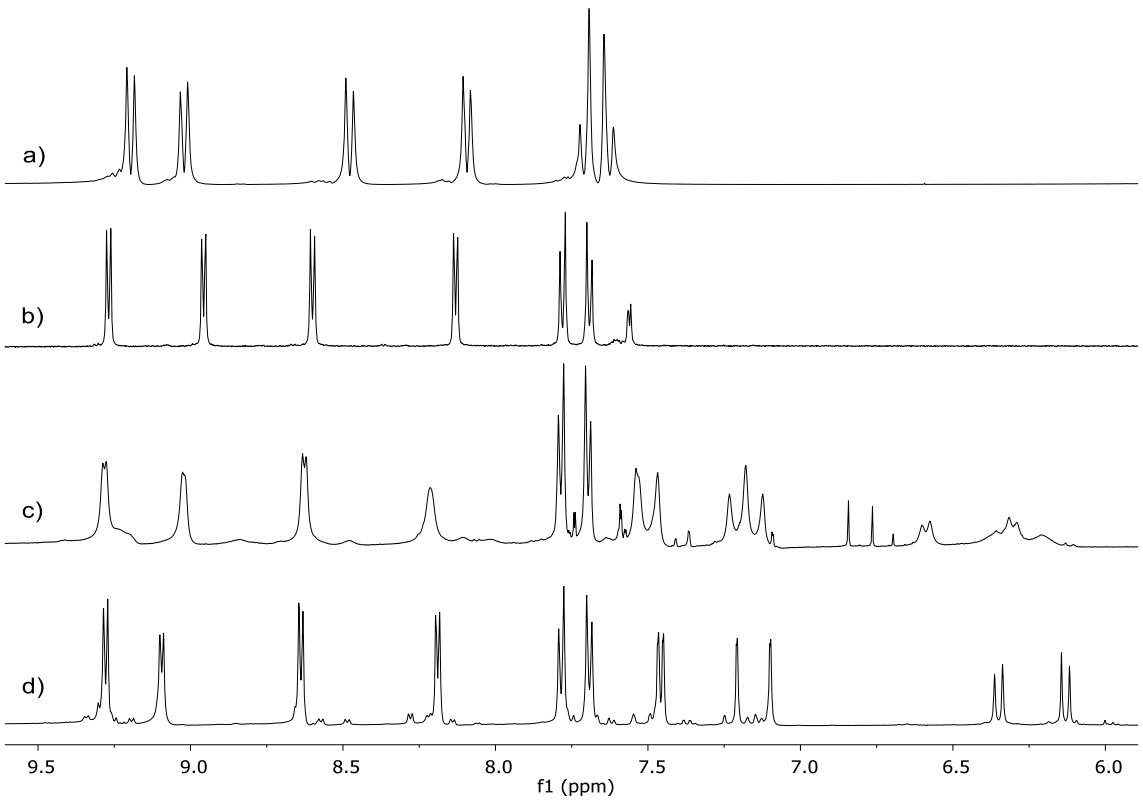

^{1}H NMR (500 MHz, D_2O) full spectra of metallacycle derived of the ligand **4** with diferent metal squares: a) **5(Pd)**·2NO_3, b) **5(Pt)**·2NO_3, c) **6(Pd)**·2NO_3 and d) **6(Pt)**·2NO_3.

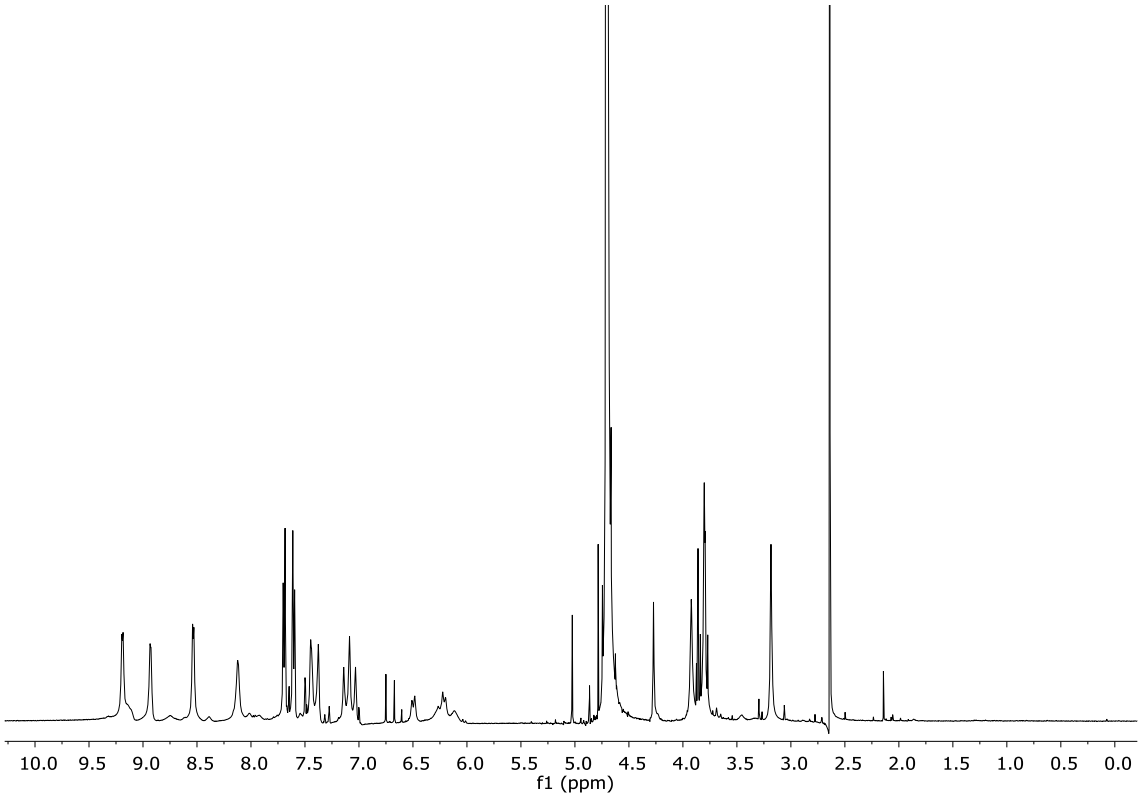

^{1}H NMR (500 MHz, D_2O) full spectra of **R4**·8NO_3.

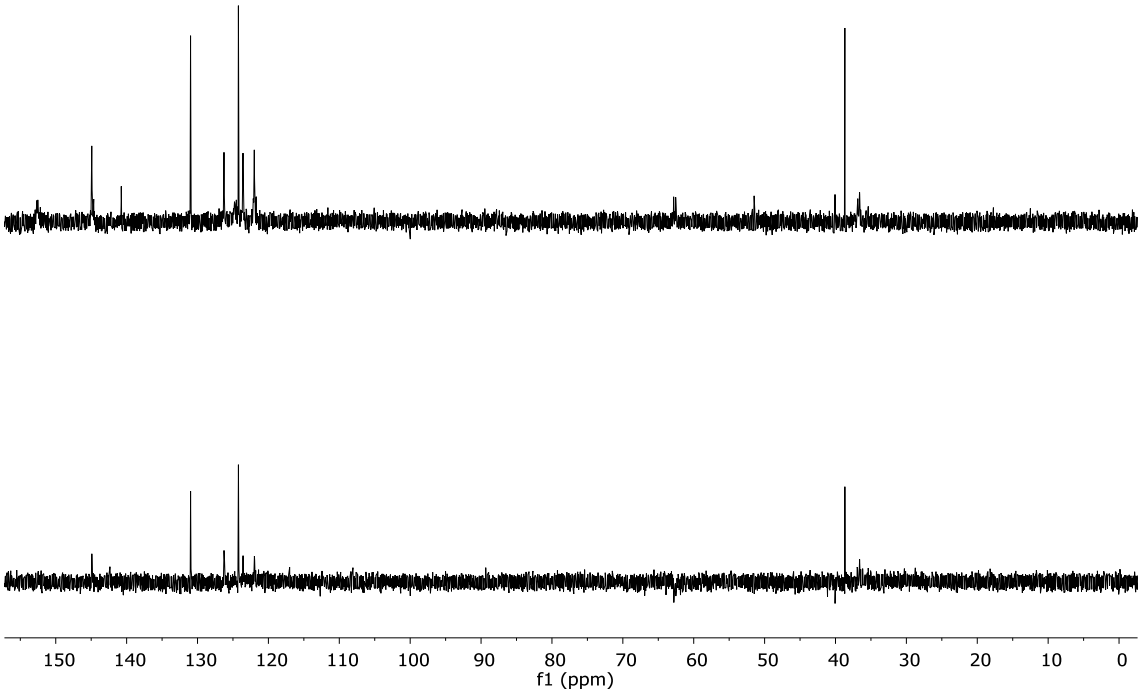

^{13}C NMR and DEPT (125 MHz, D_2O) full spectra of **R4**·8NO_3.

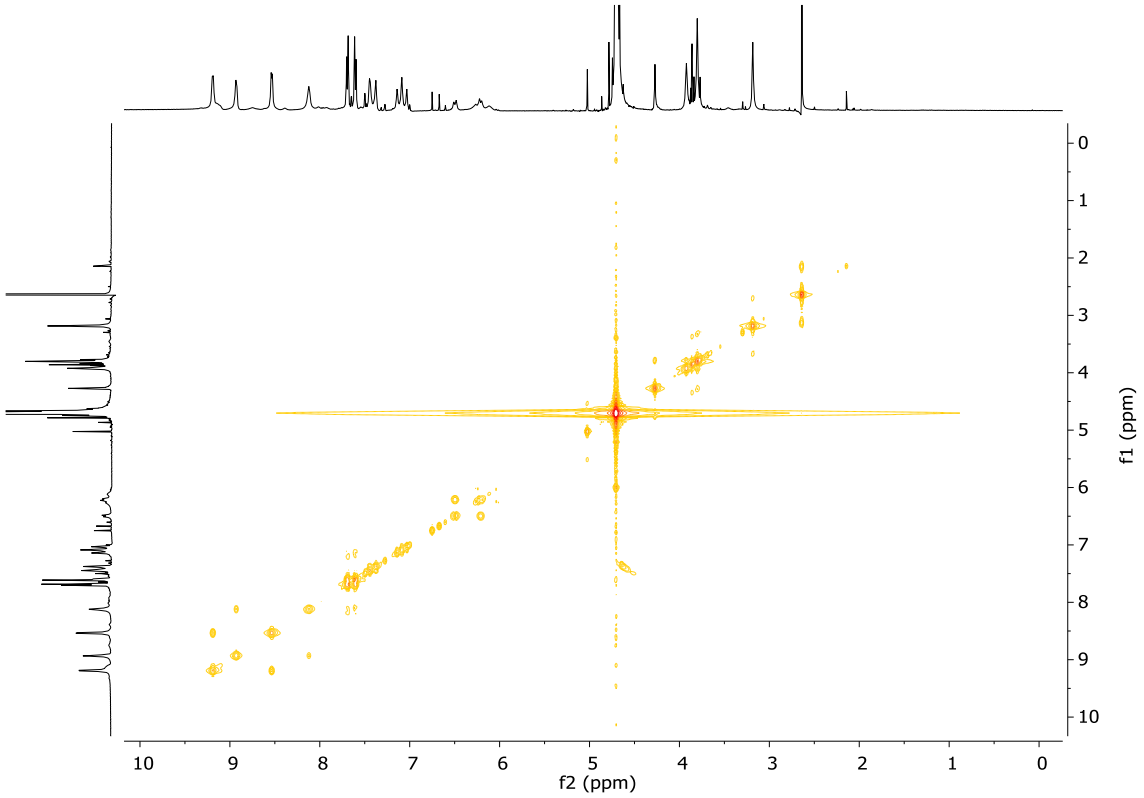

COSY (500 MHz, D_2O) full spectra of **R4**·8NO_3.

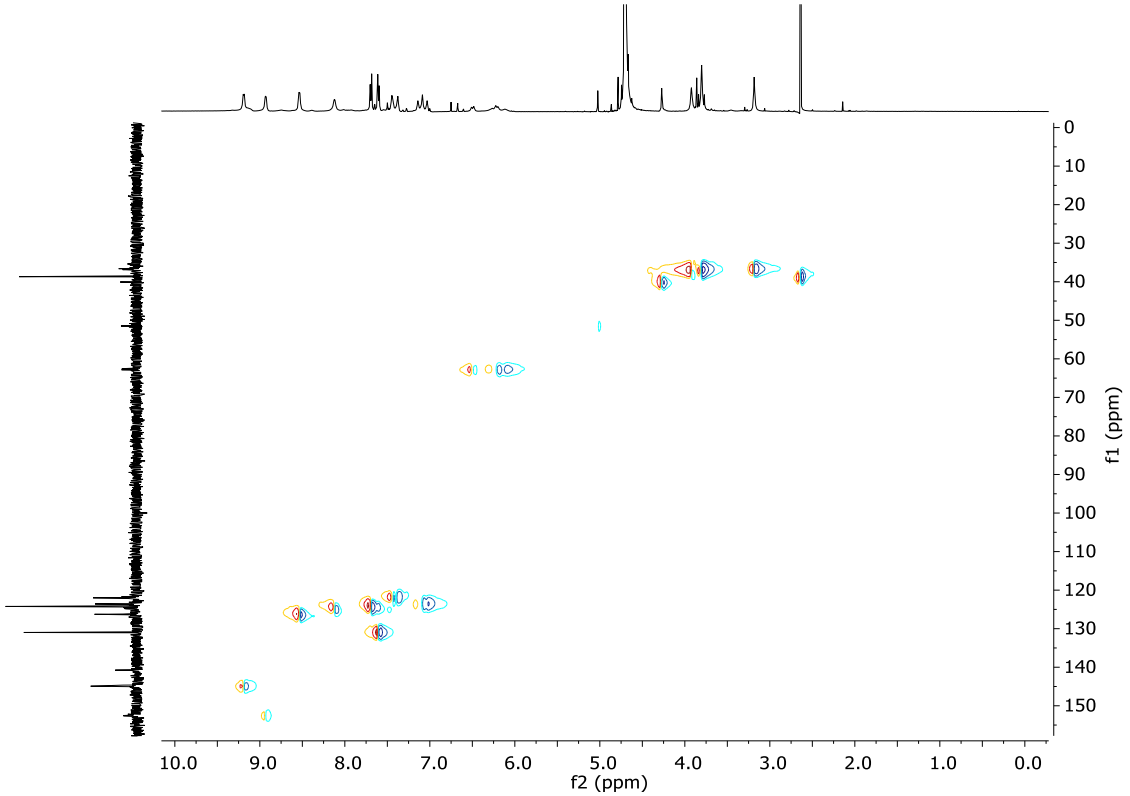

HSQC (125 and 500 MHz, D_2O) full spectra of **R4**·8NO_3.

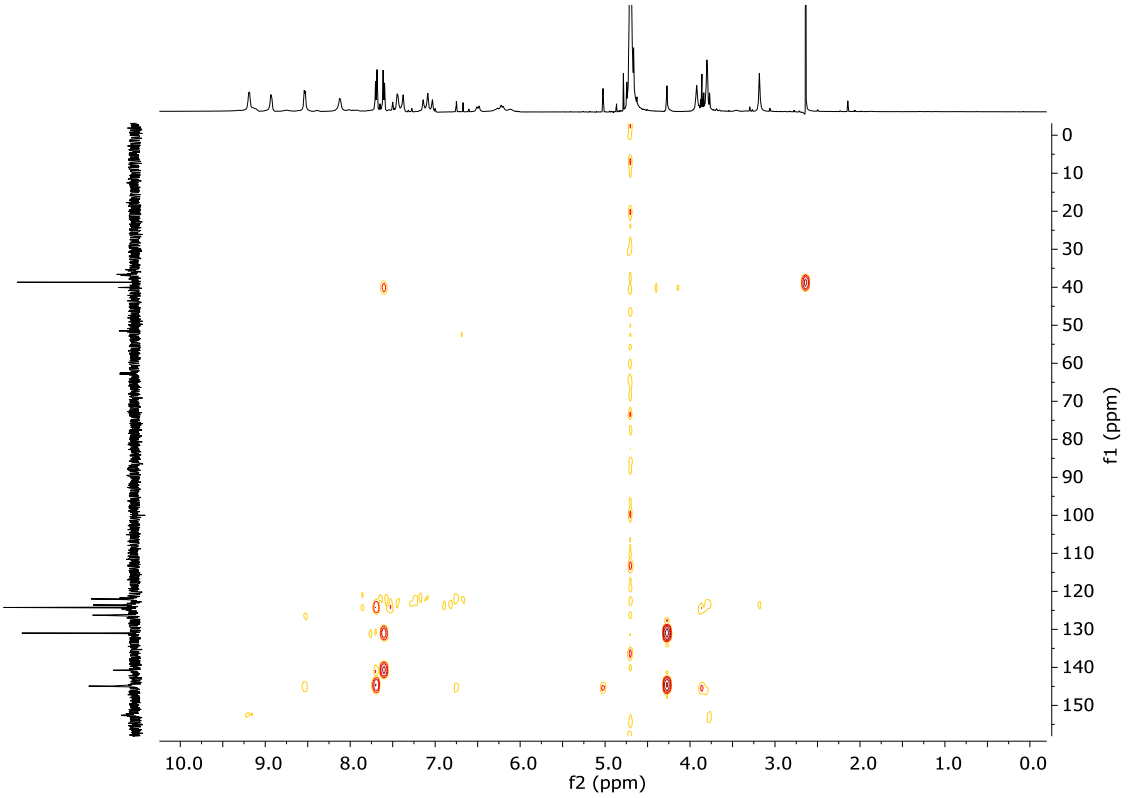

HMBC (125 and 500 MHz, D_2O) partial spectra of **R4**·8NO_3.

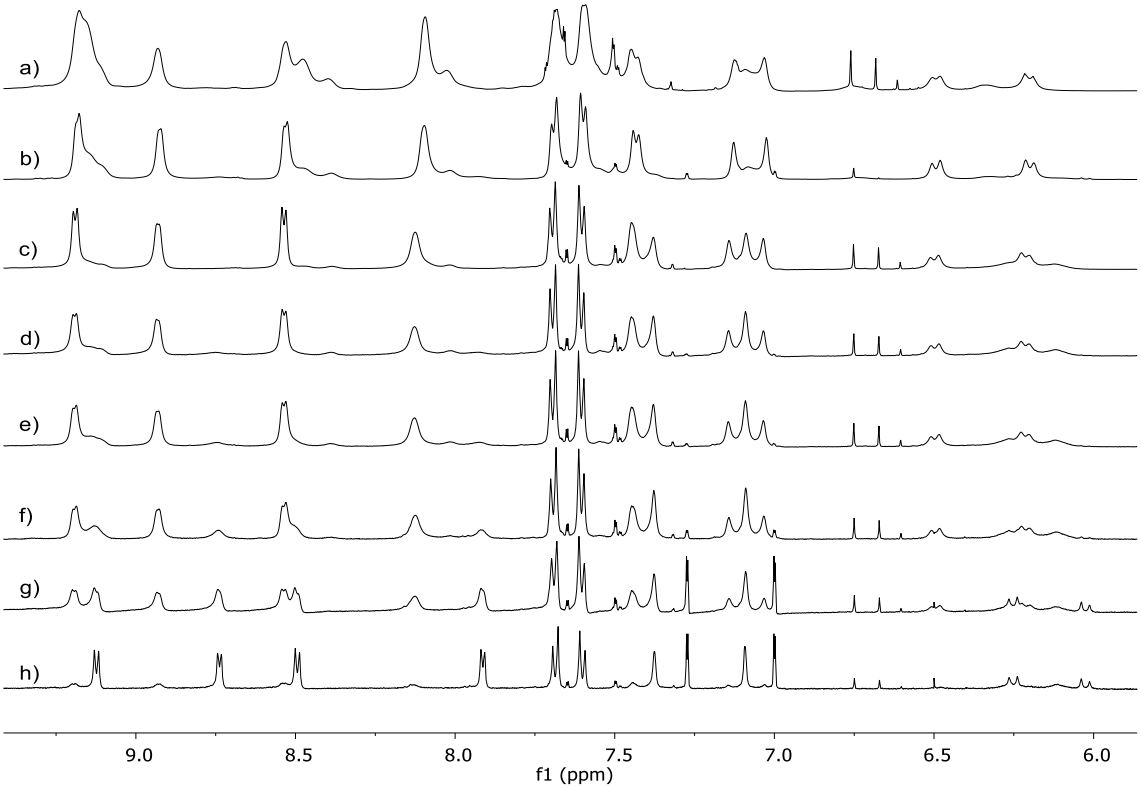

^{1}H NMR (500 MHz, D_2O) partial espectra of **R4**·8NO_3 dilution effect at a) 15 mM, b) 10 mM, c) 5 mM, d) 2.5 mM, e) 1.25 mM, f) 0.75 mM, g) 0.375 mM and h) 0.1 mM.

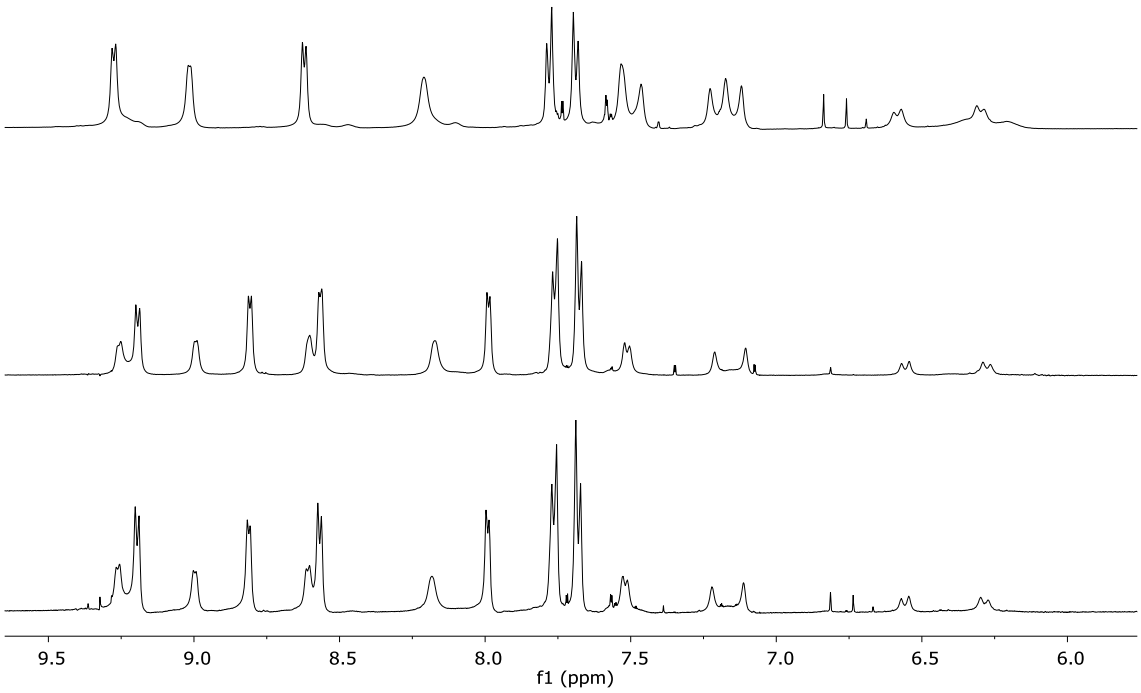

^{1}H NMR (500 MHz, D_2O) partial espectra, from top to bottom, of **R4**·8NO_3 (5mM) and **R4**·8NO_3 in the presence of 1.6 % and 3.2% of CD_3CN in media, respectively.

1.7. Metallacycle **R5**·6NO_3.

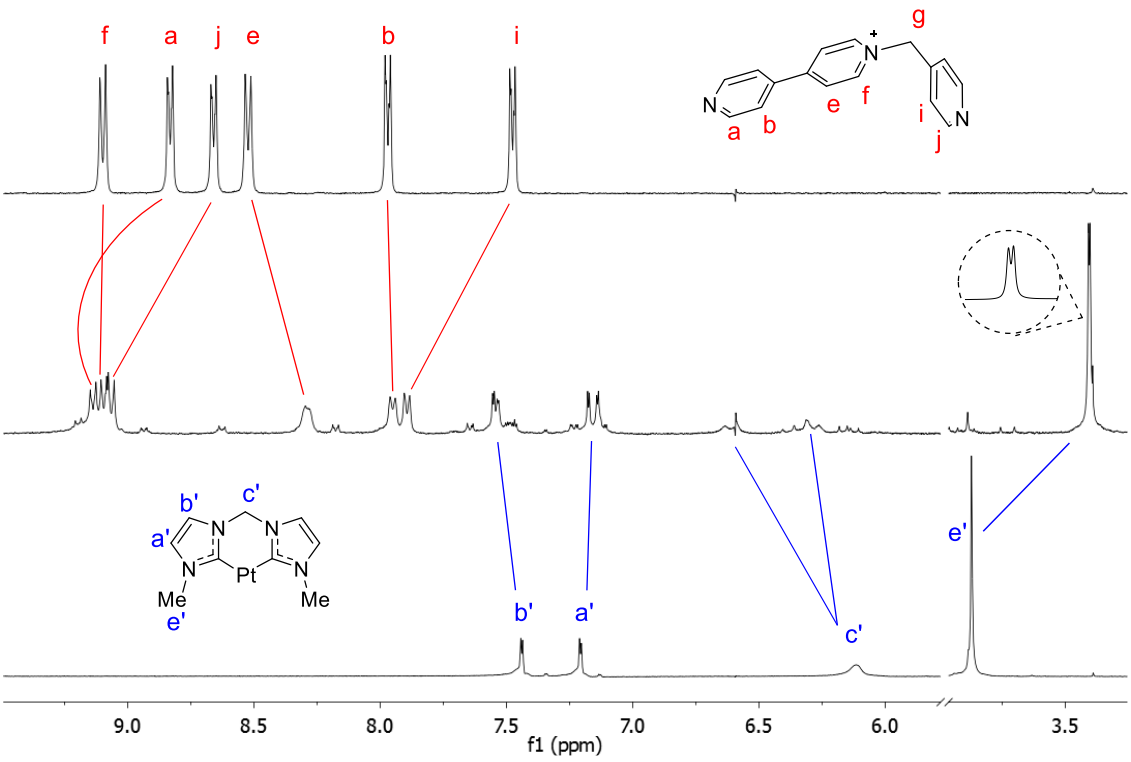

^{1}H NMR (500 MHz, D_2O) spectra of **1** (top), **R5**·6NO_3 (middle) and **6(Pt)**·2NO_3 (bottom).

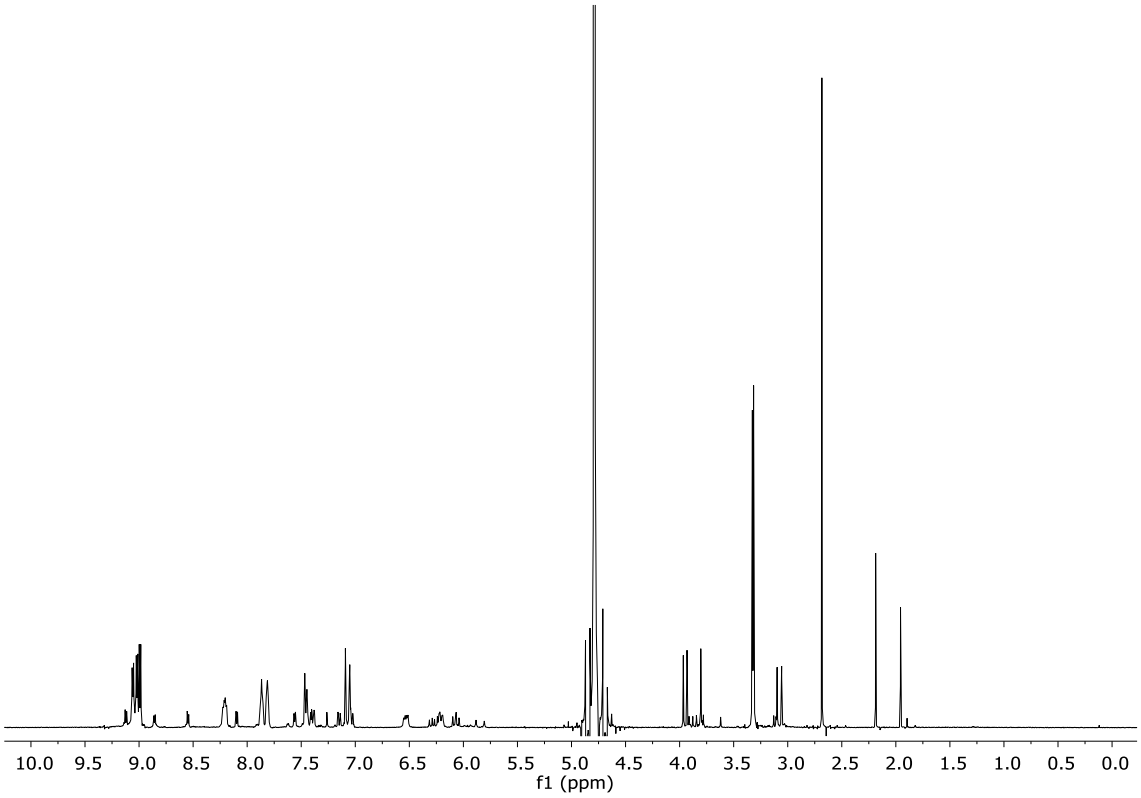

^{1}H NMR (500 MHz, D_2O) full spectra of **R5**·6NO_3.

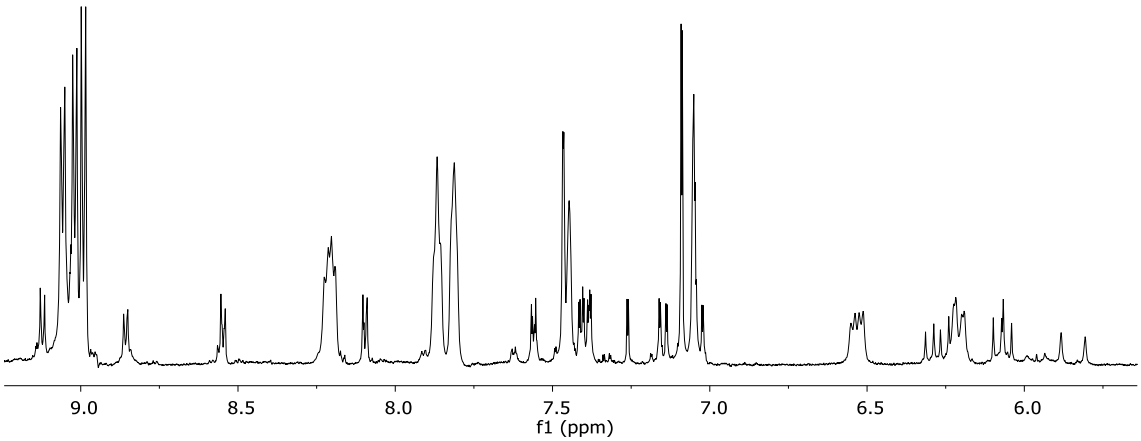

^{1}H NMR (500 MHz, D_2O) partial spectra of **R5**·6NO_3.

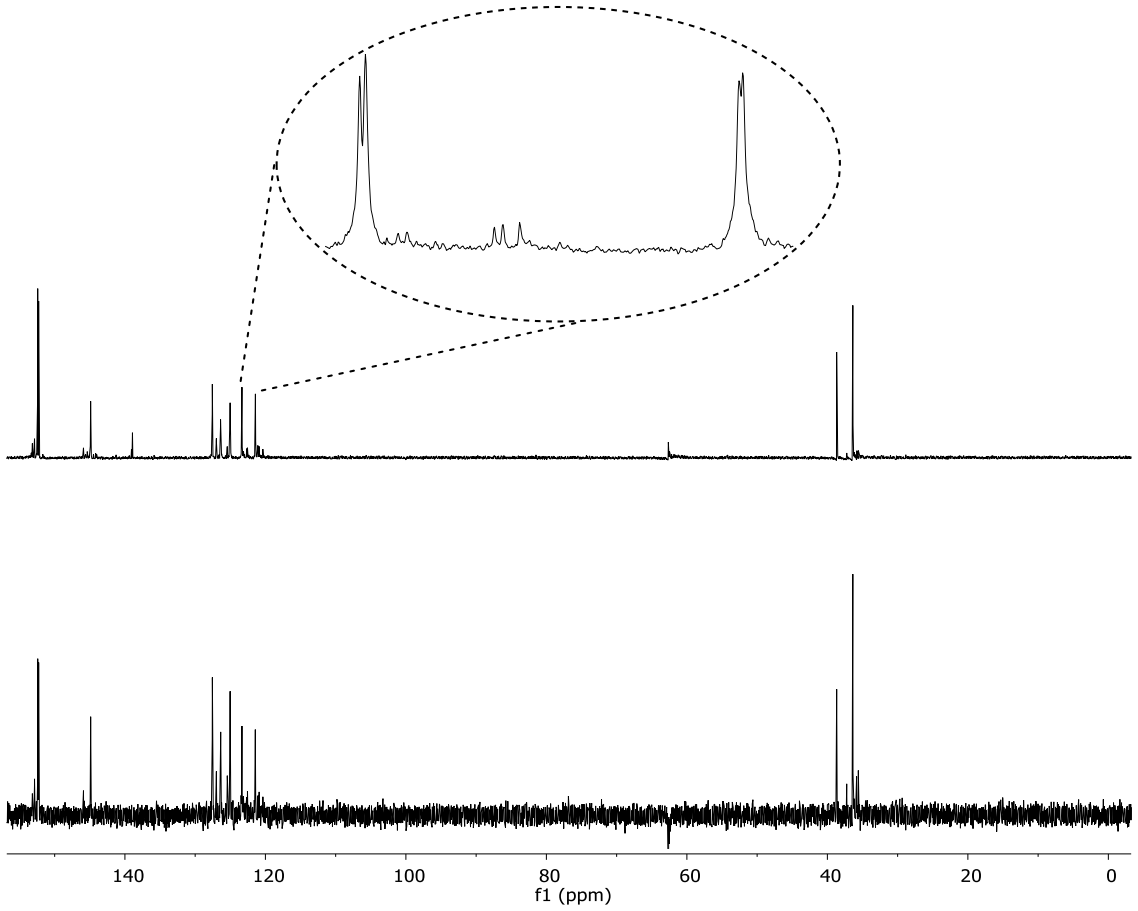

^{13}C NMR and DEPT (125 MHz, D_2O) full spectra of **R5**·6NO_3.

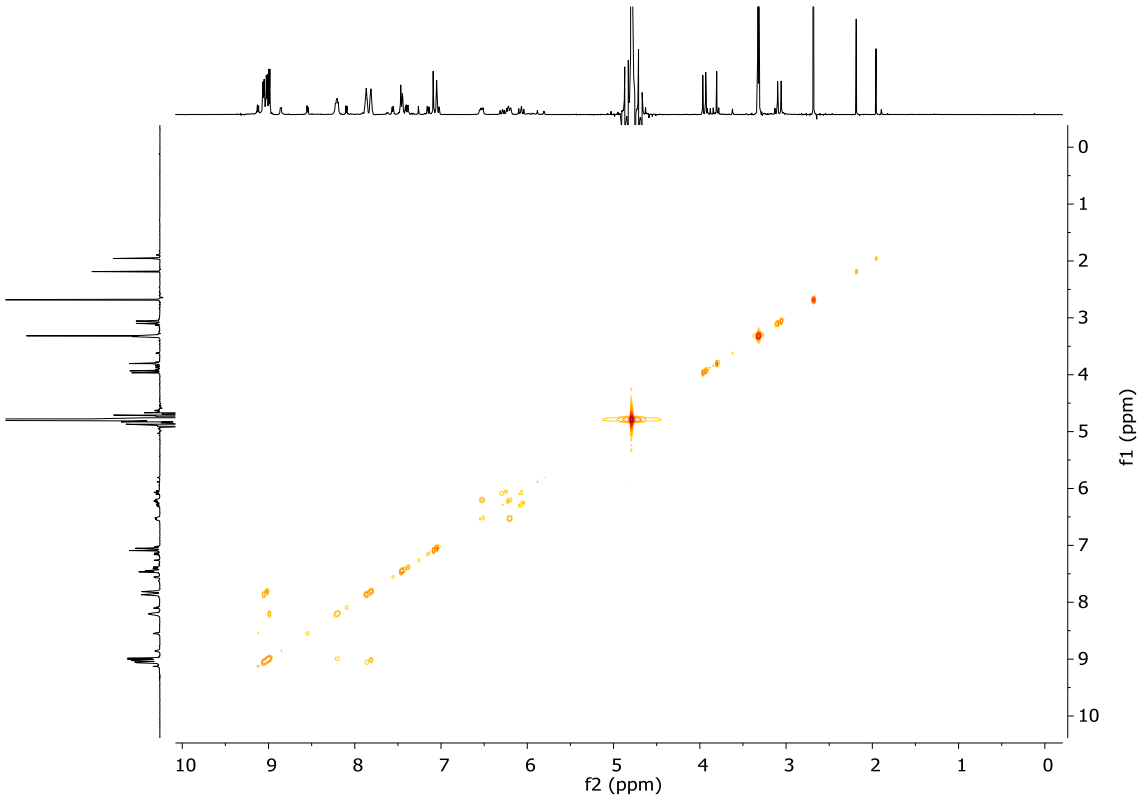

COSY (500 MHz, D_2O) full spectra of **R5**·6NO_3.

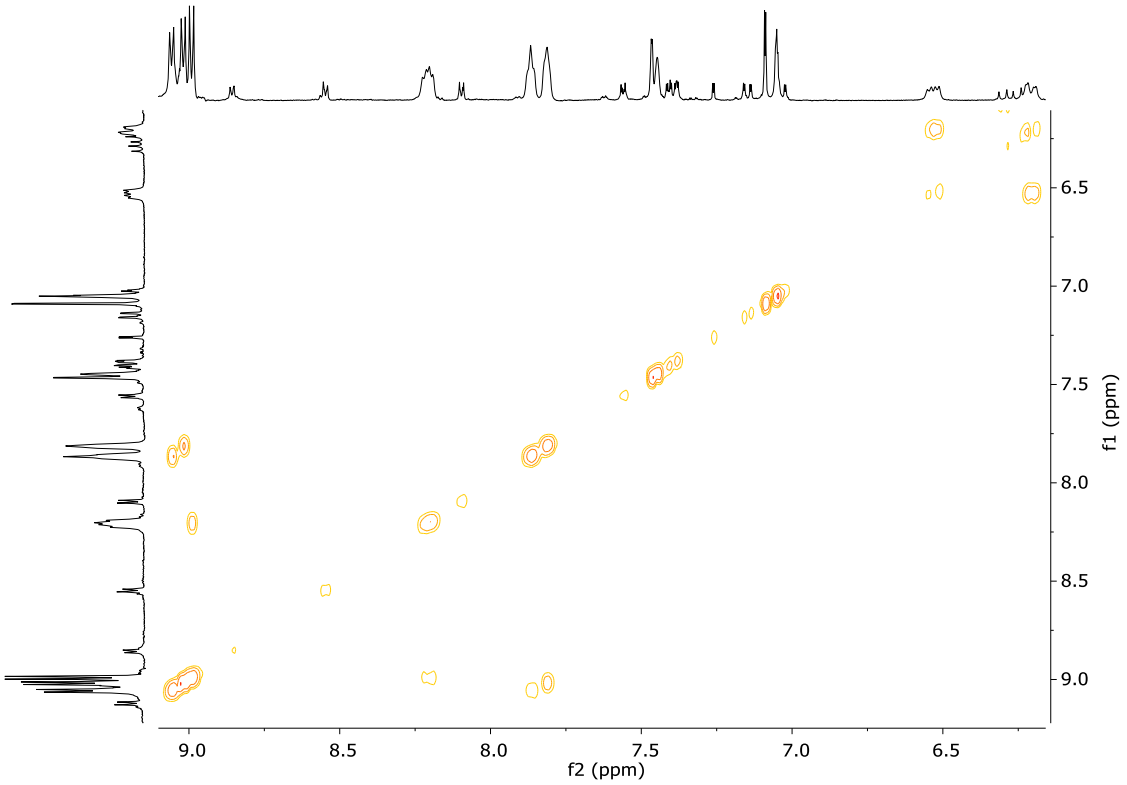

COSY (500 MHz, D_2O) partial spectra of **R5**·6NO_3.

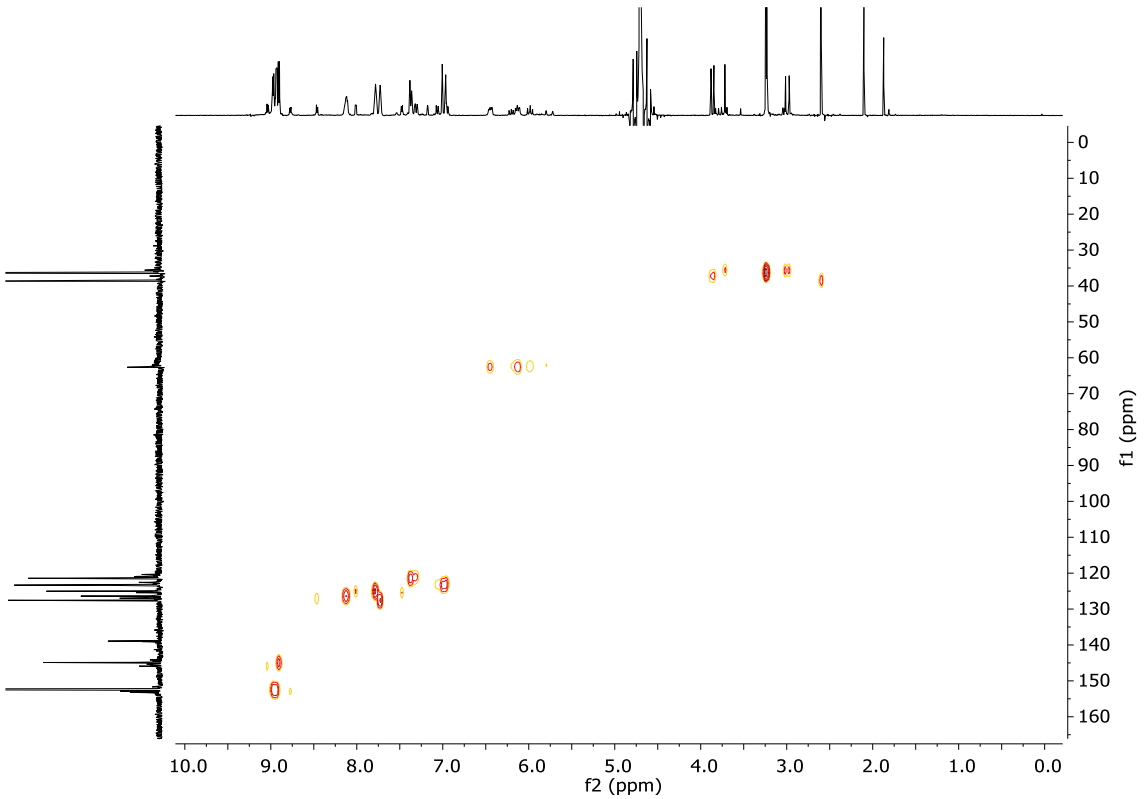

HSQC (125 and 500 MHz, D_2O) full spectra of **R5**·6NO_3.

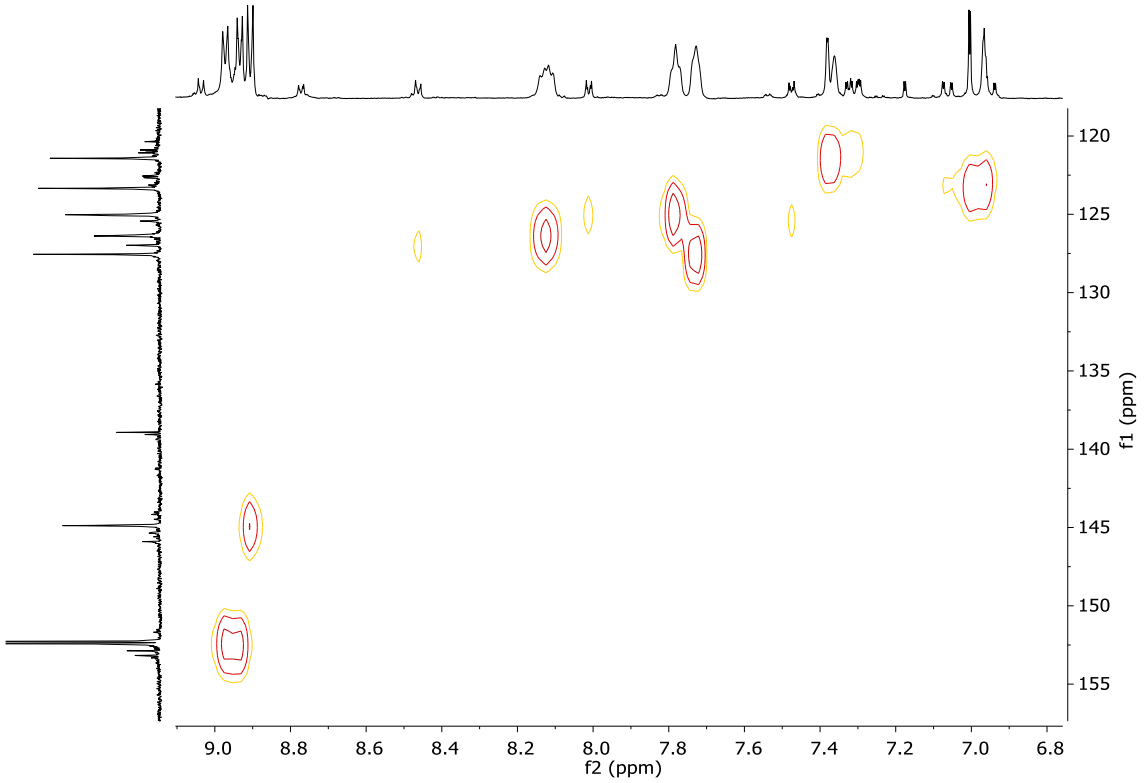

HSQC (125 and 500 MHz, D_2O) partial spectra of **R5**·$6NO_3$.

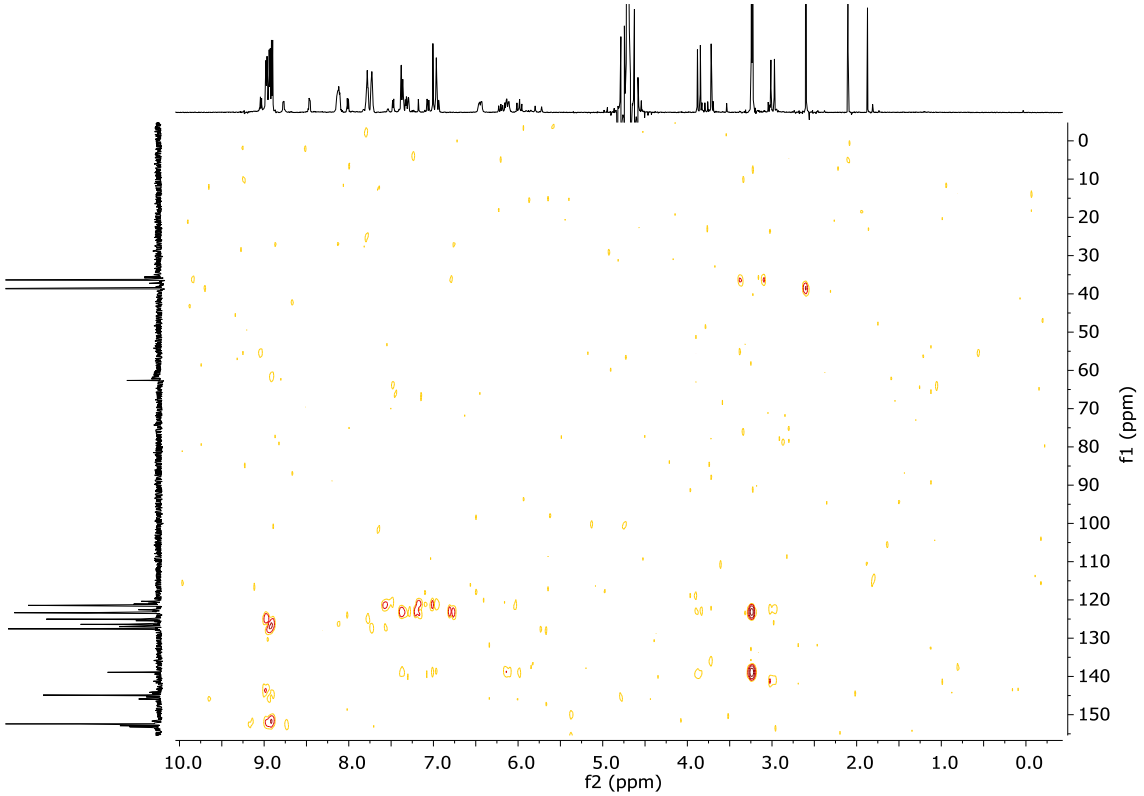

HMBC (1235 and 500 MHz, D_2O) full spectra of **R5**·$6NO_3$.

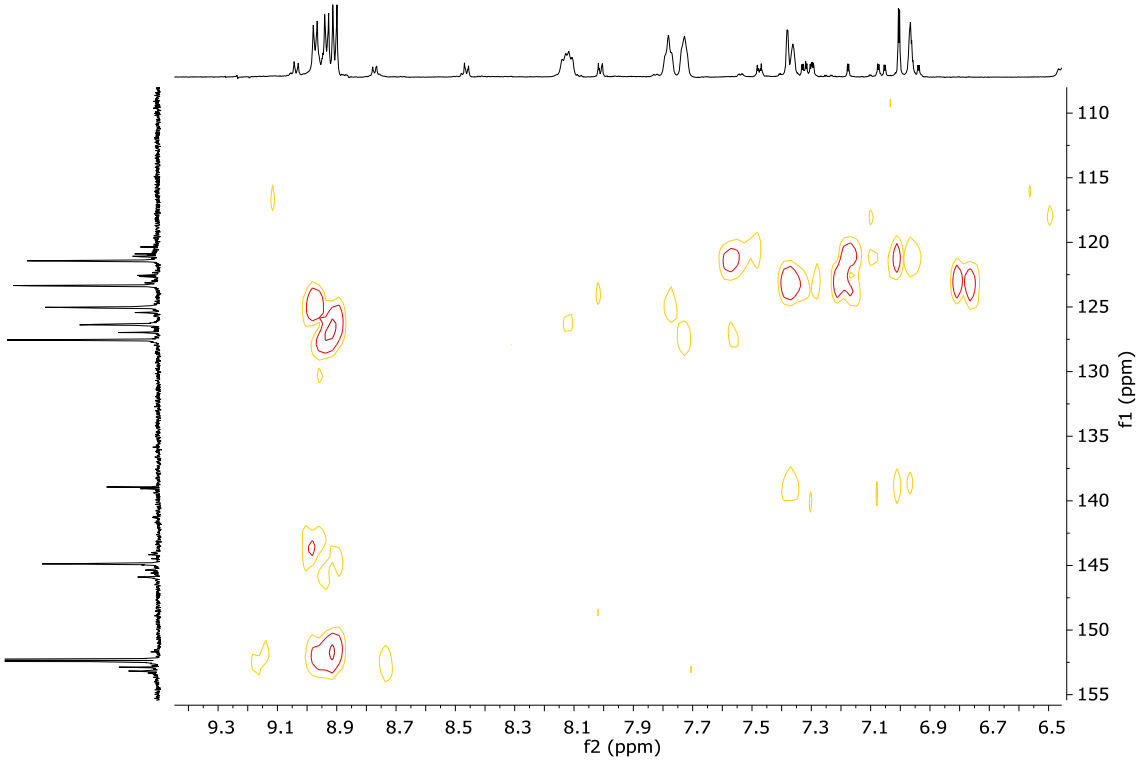

HMBC (125 and 500 MHz, D_2O) partial spectra of **R5**·$6NO_3$.

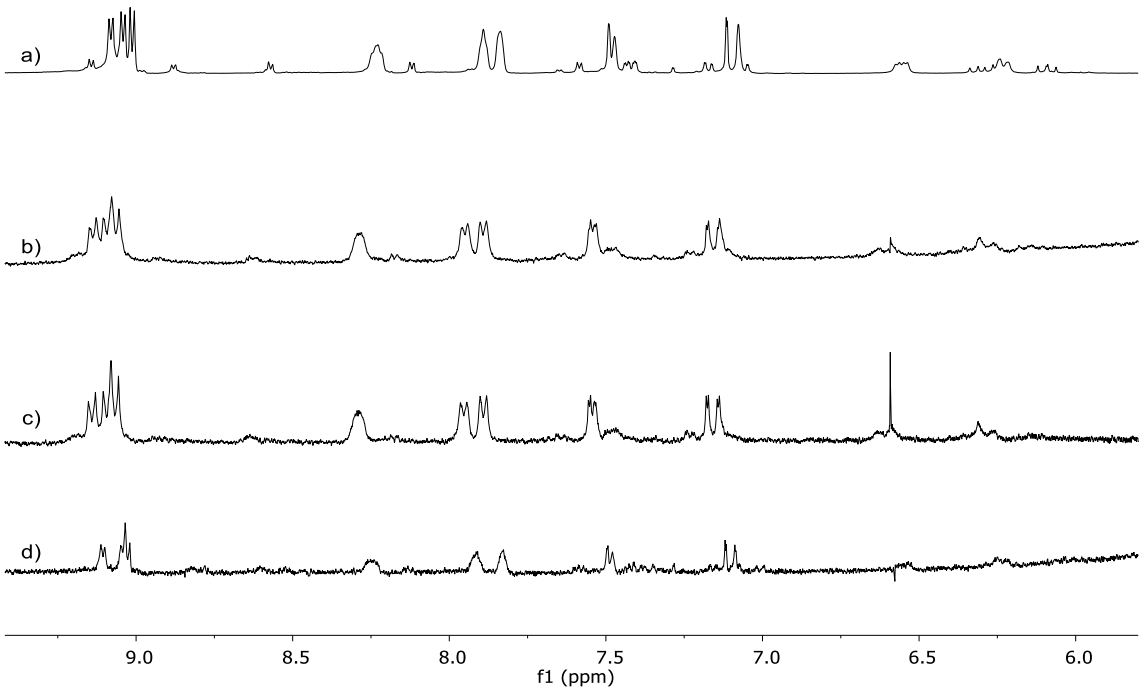

^{1}H NMR (300 MHz, D_2O) partial spectra of **R5**·$6NO_3$ at

a) 5mM; b) 2.5 mM, c) 1.25 mM and d) 0.1 mM.

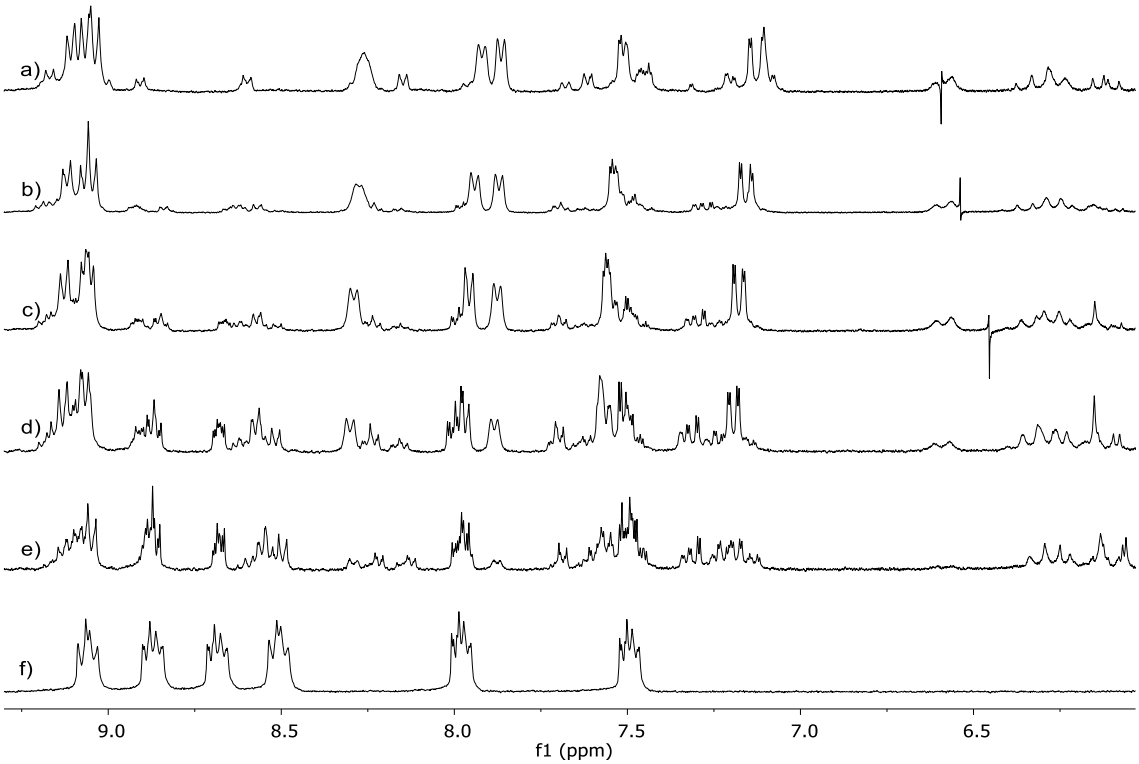

^{1}H NMR (500 MHz, D_2O) partial spectra of a) **R5**·$6NO_3$ (5mM), **R5**·$8NO_3$ in the presence of b) 10 %, c) 20%, d) 30%, and e) 50% of CD_3CN in media, and f) ligand **1** (5 mM, D_2O/CD_3CN 1:1).

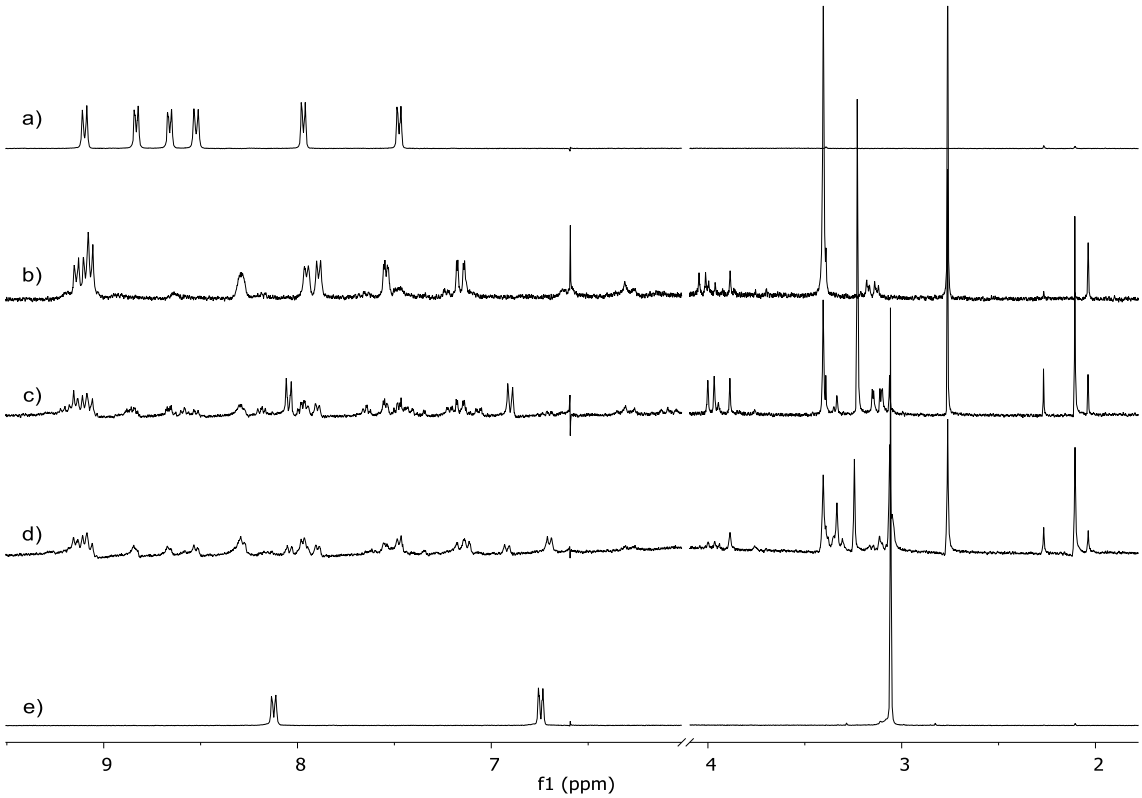

^{1}H NMR (300 MHz, D_2O) partial spectra of a) **1**, b) **R5**·$6NO_3$ (1.25mM), **R5**·$8NO_3$ in the presence of 2 equiv. of dimethylaminopyridine at c) t=0 h and d) t=48h and e) dimethylaminopyridine.

1.8. Metallacycle **R6**·6NO_3.

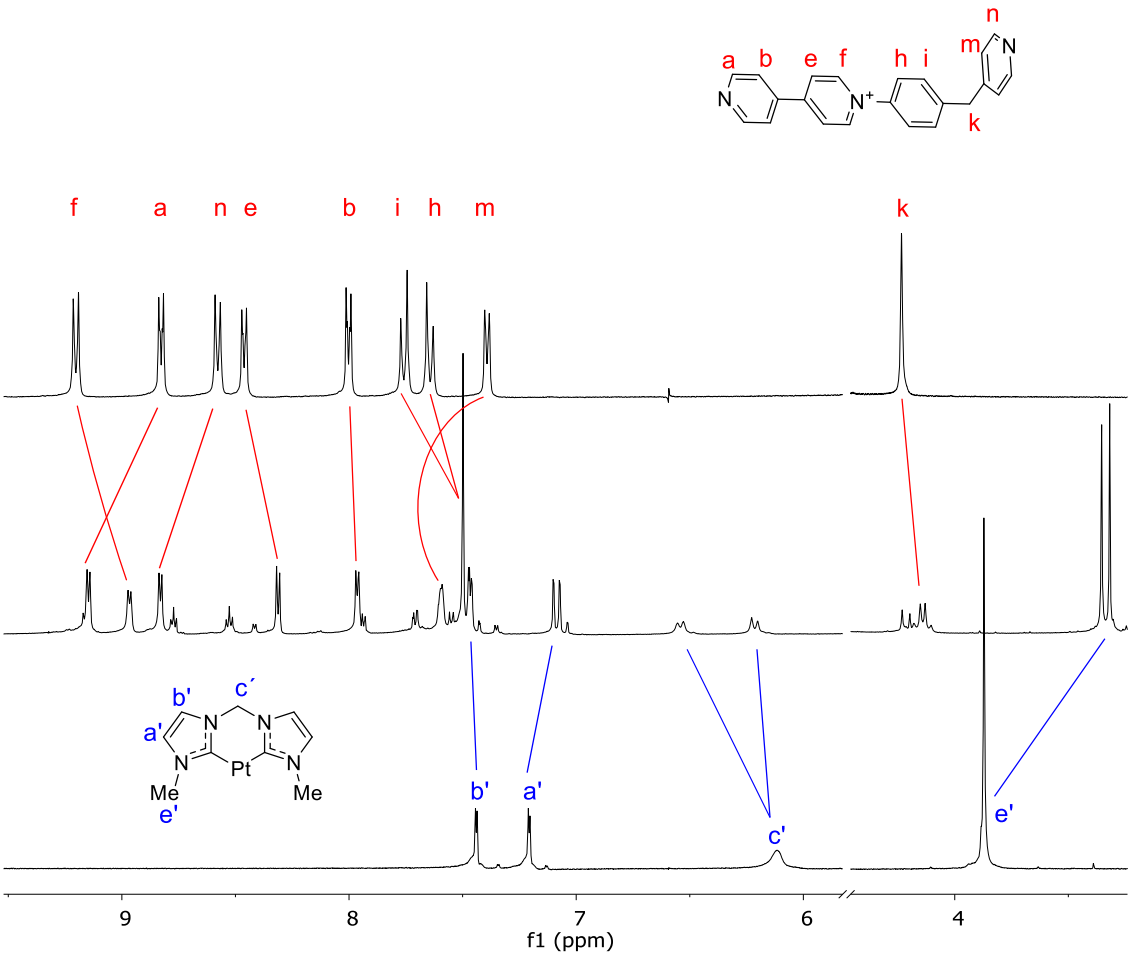

^{1}H NMR (500 MHz, D_2O) partial spectra of **2** (top), **R6**·6NO_3 (middle) and **6(Pt)**·2NO_3 (bottom).

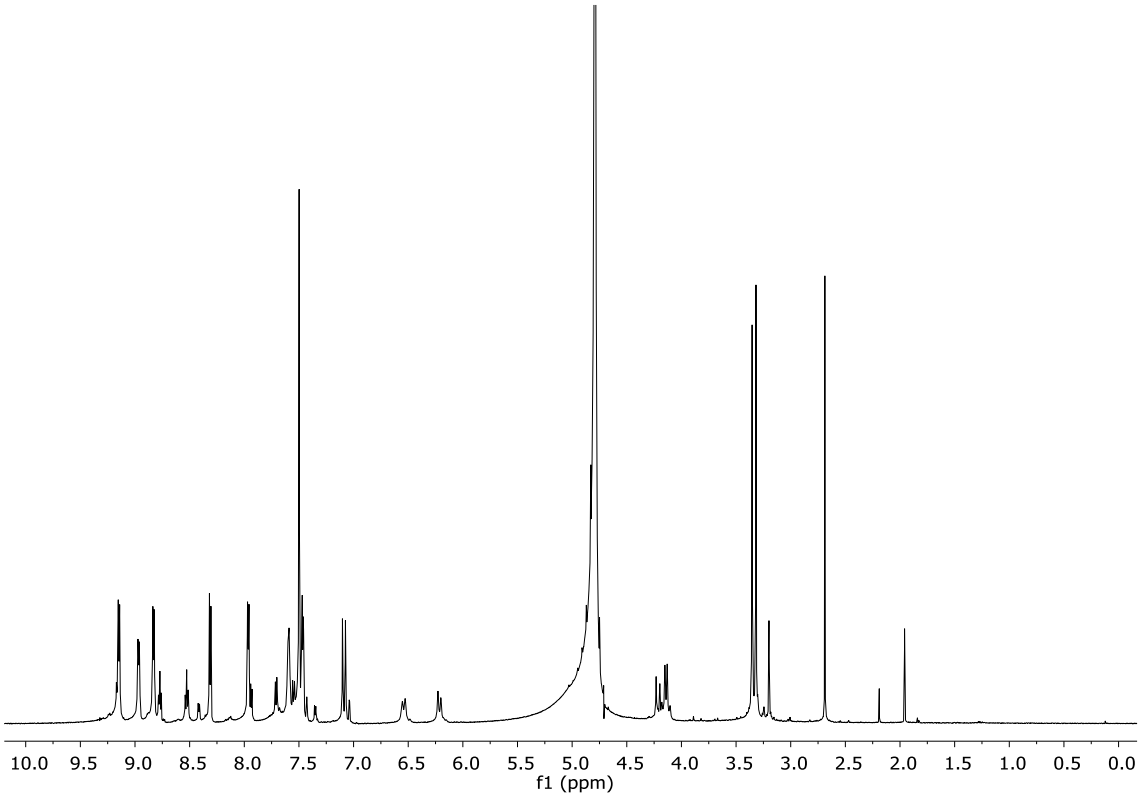

^{1}H NMR (500 MHz, D_2O) full spectra of **R6**·6NO_3.

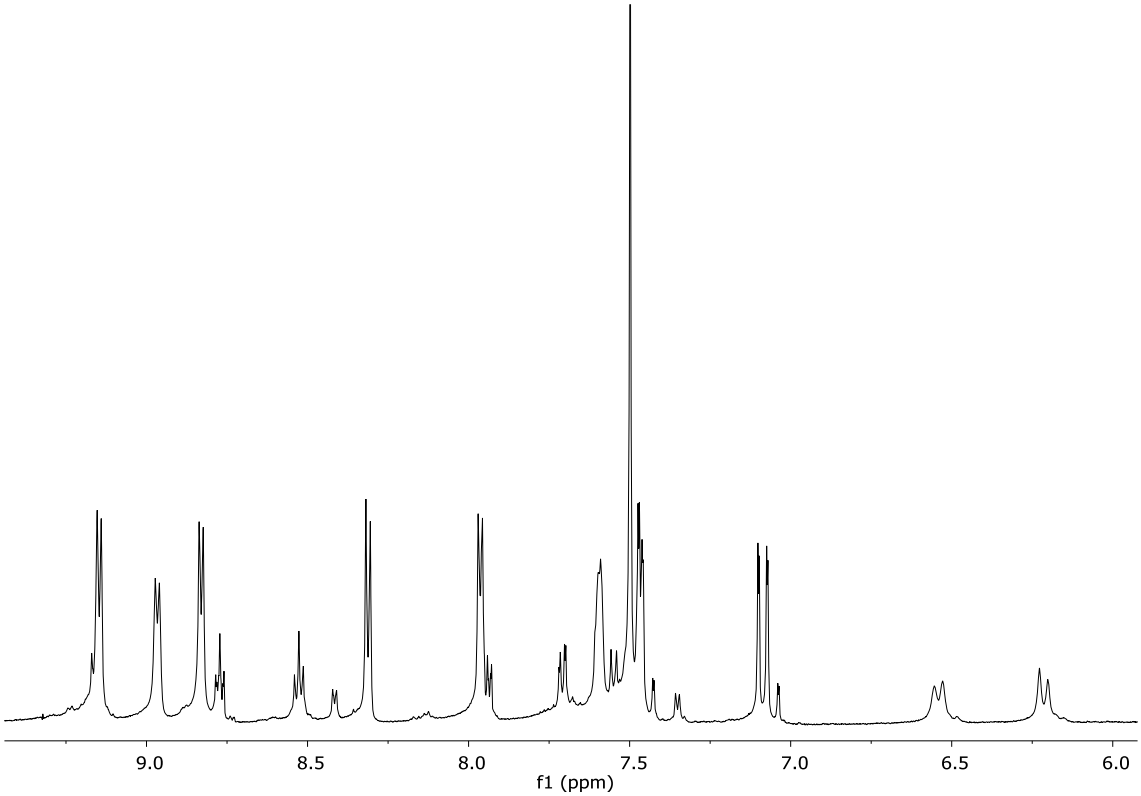

^{1}H NMR (500 MHz, D_2O) partial spectra of **R6**·6NO_3.

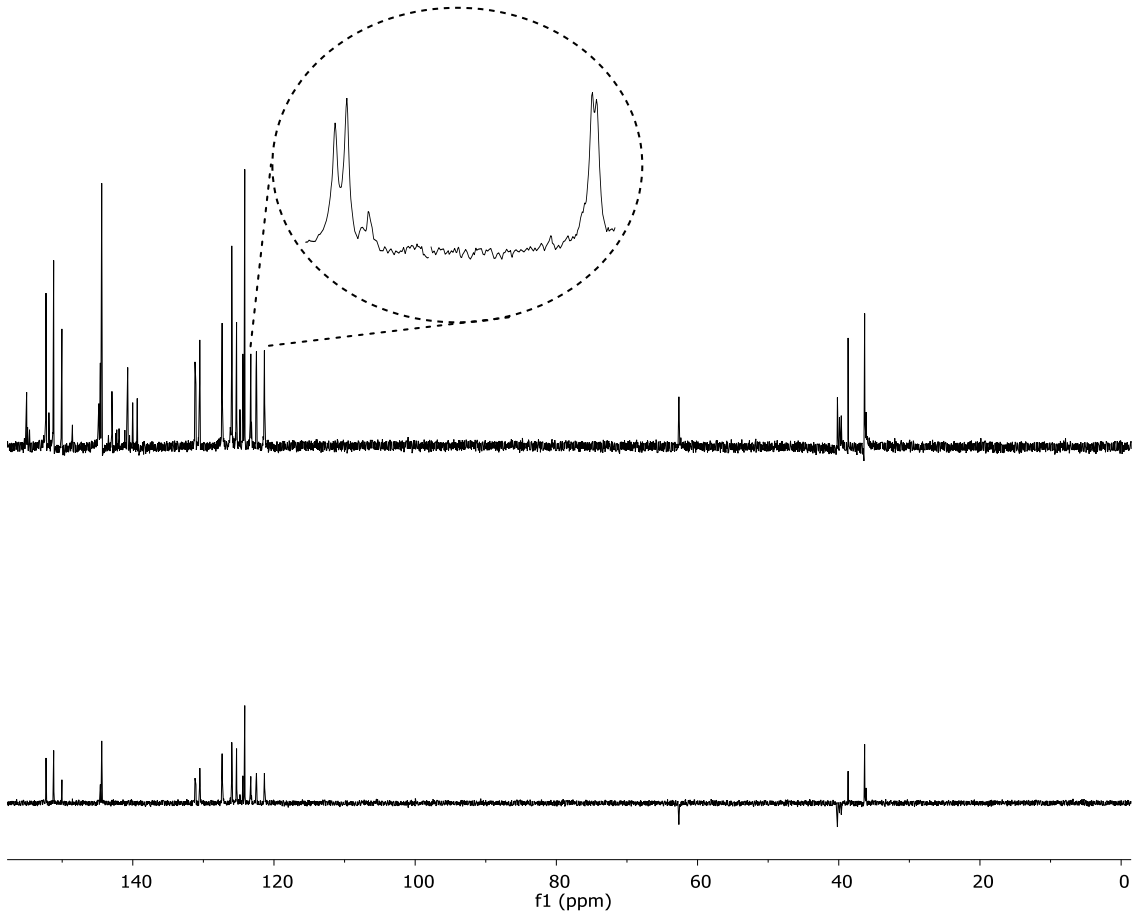

^{13}C NMR (125 MHz, D_2O) full spectra of **R6**·6NO_3.

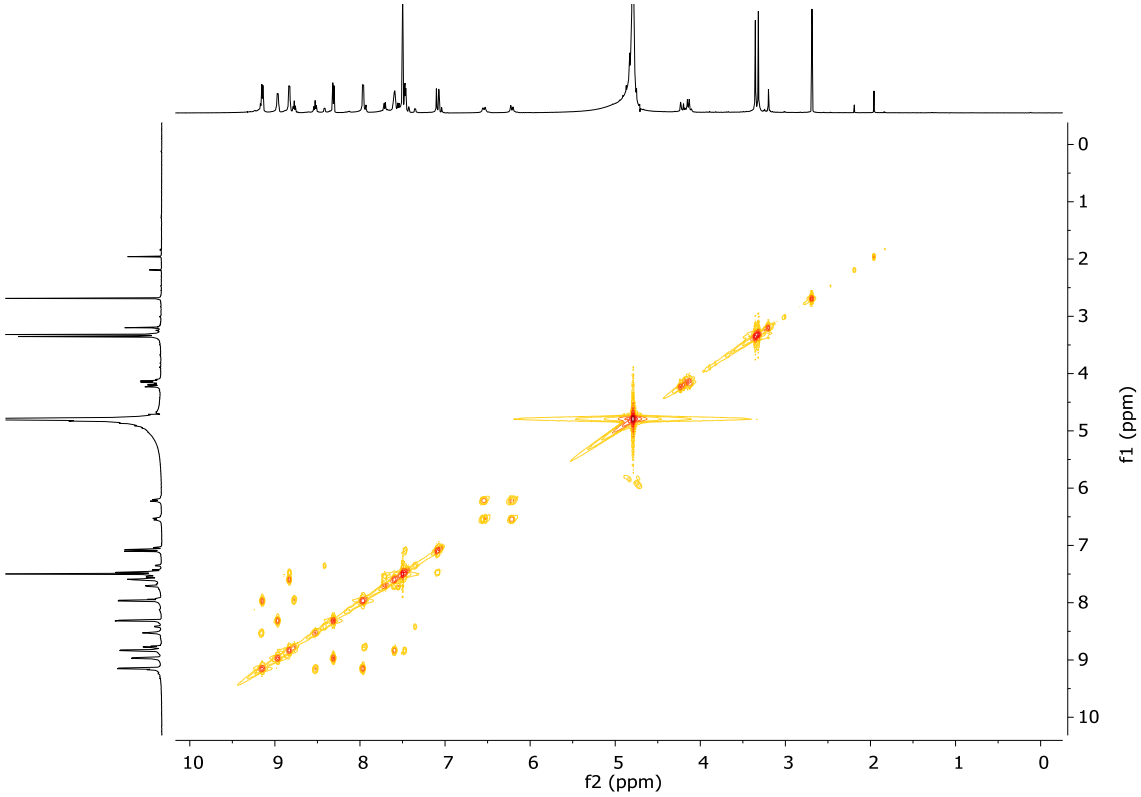

COSY (500 MHz, D_2O) full spectra of **R6**·6NO_3.

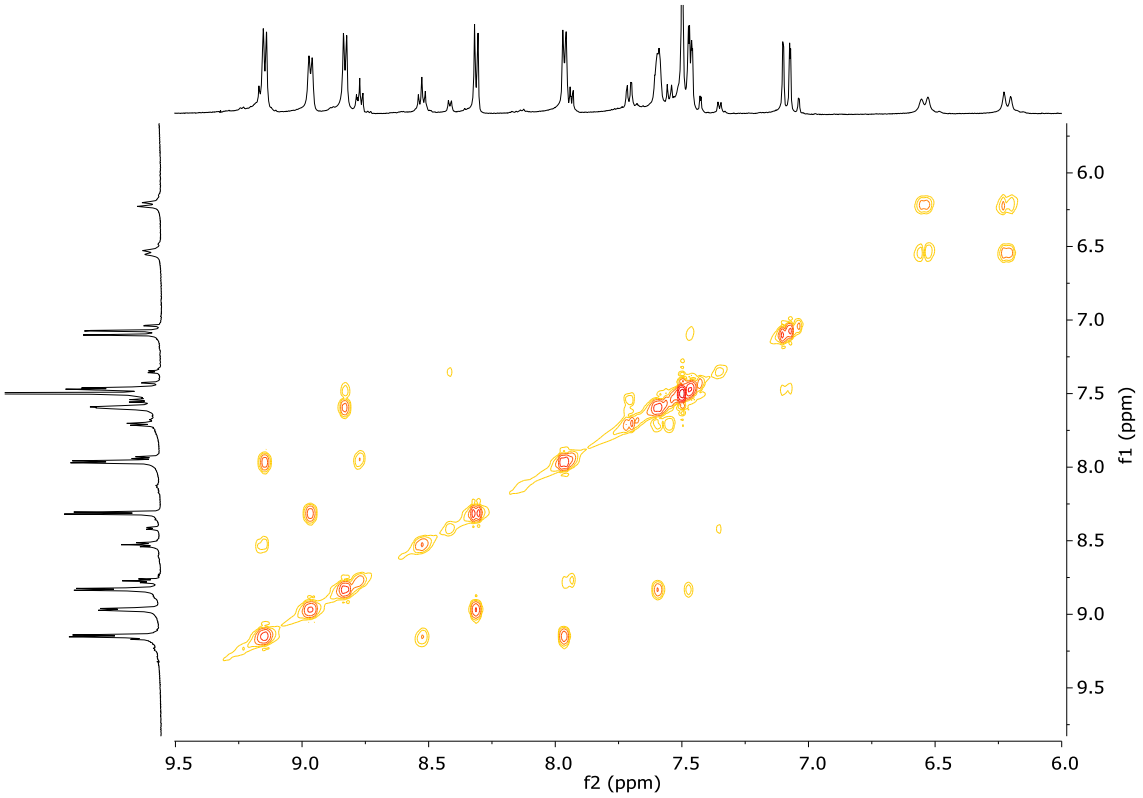

COSY (500 MHz, D_2O) partial spectra of **R6**·6NO_3.

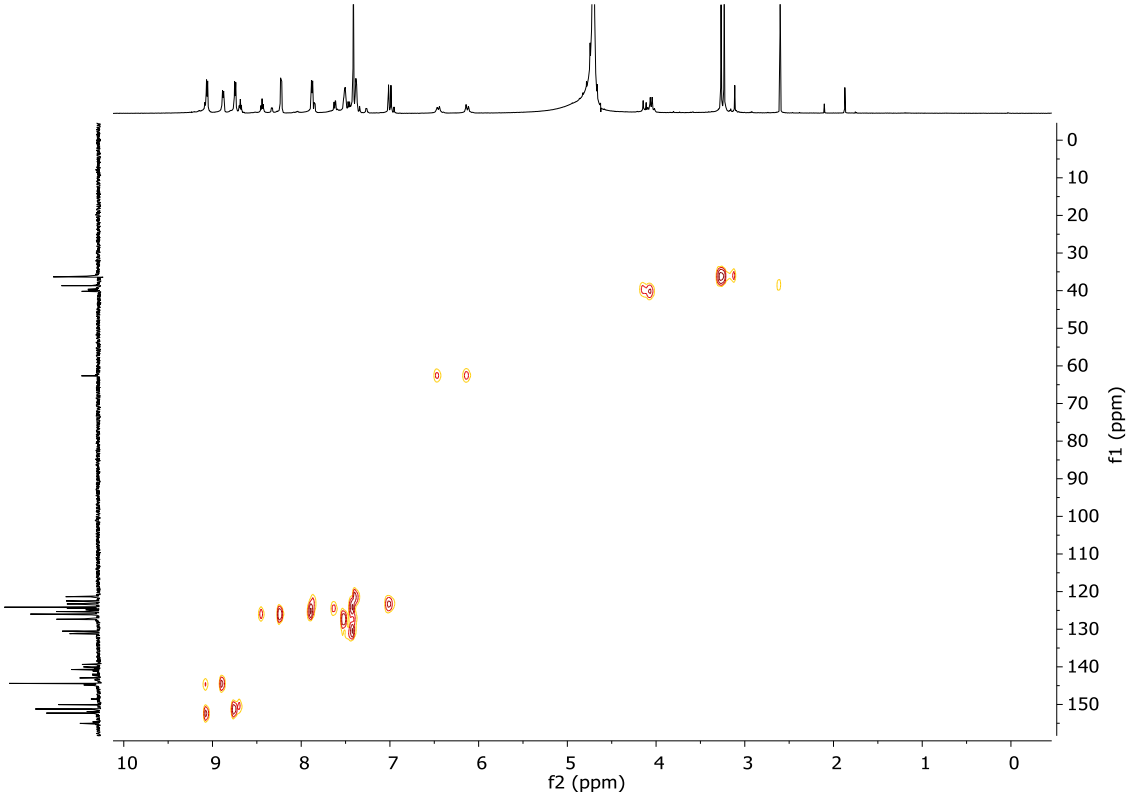

HSQC (125 and 500 MHz, D_2O) full spectra of **R6**·6NO_3.

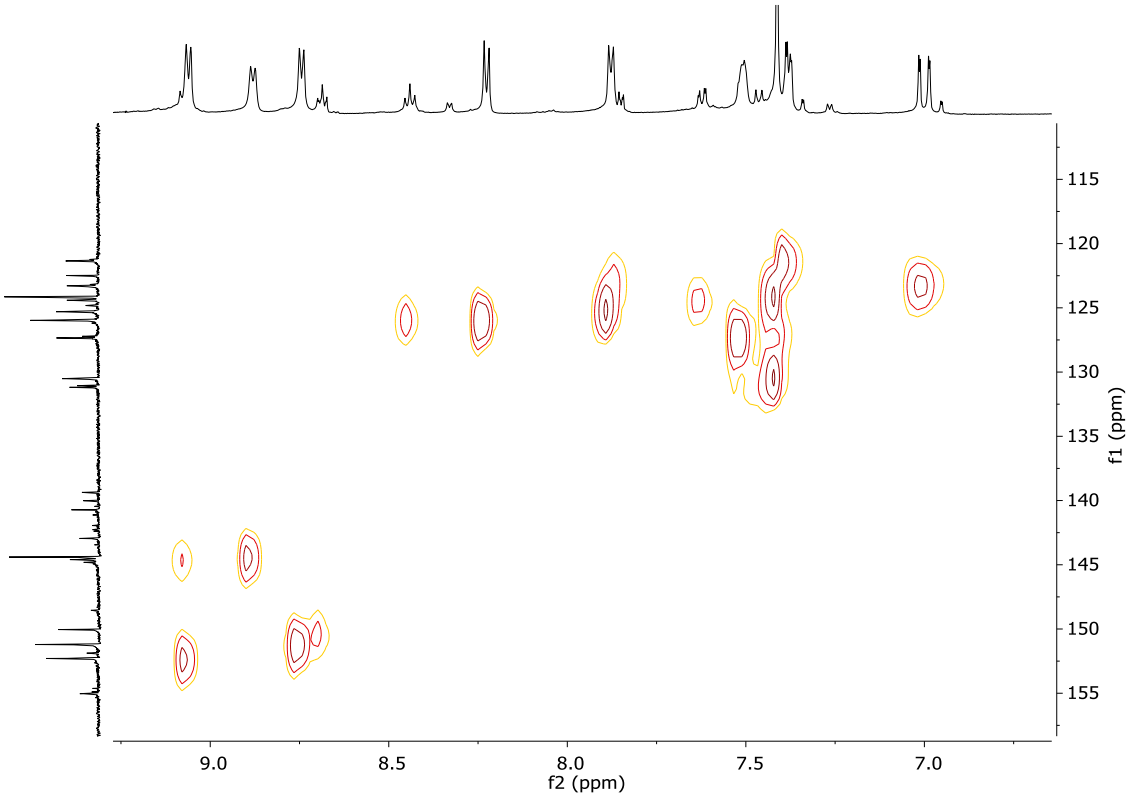

HSQC (125 and 500 MHz, D_2O) partial spectra of **R6**·6NO_3.

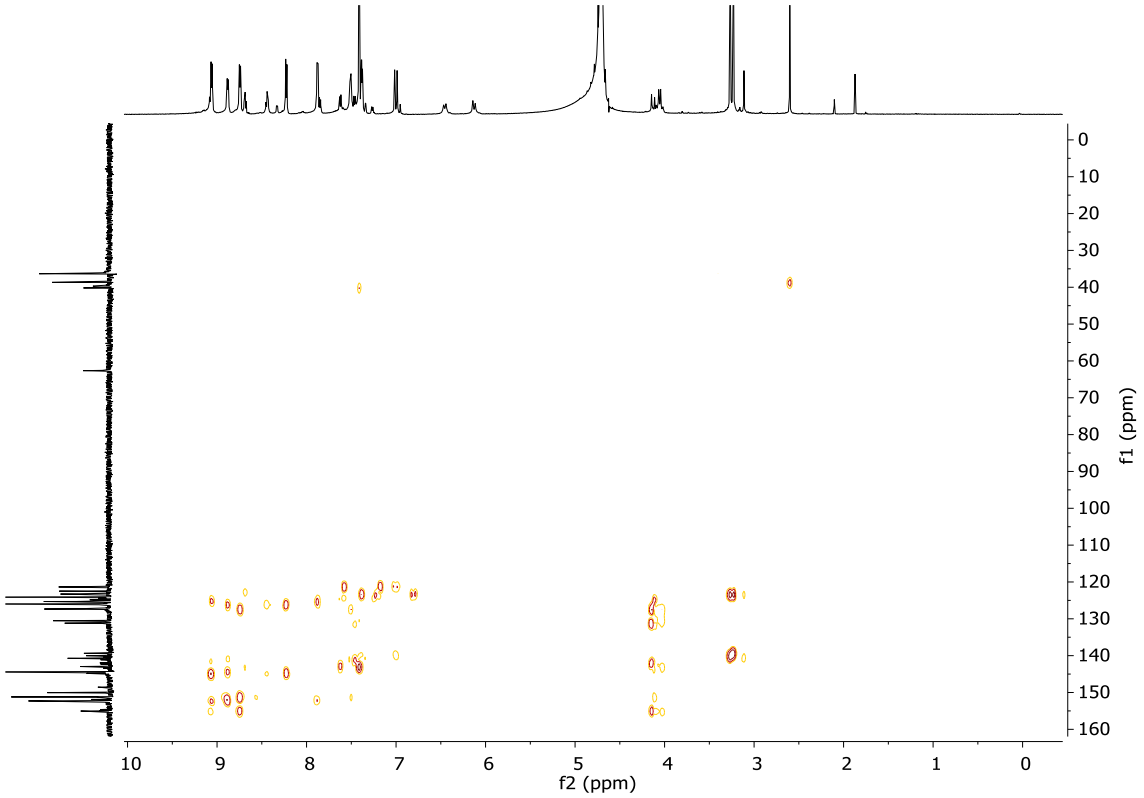

HMBC (125 and 500 MHz, D_2O) full spectra of **R6**·6NO_3.

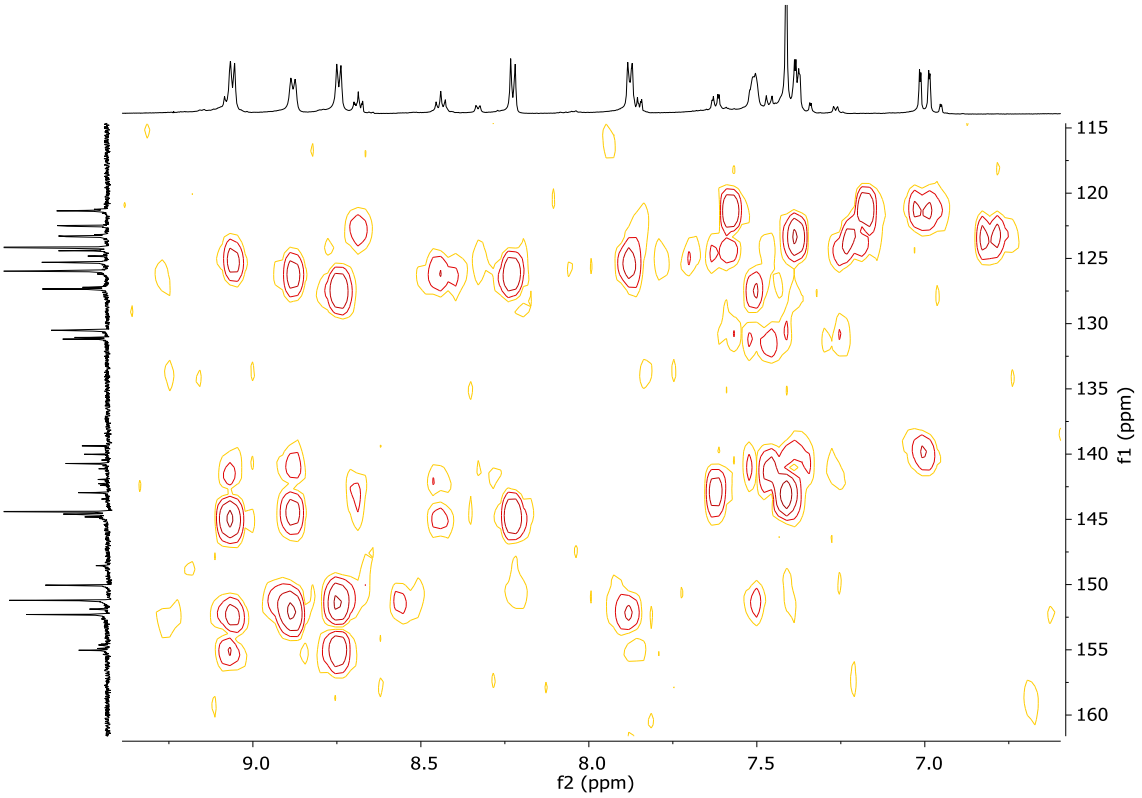

HMBC (125 and 500 MHz, D_2O) full spectra of **R6**·$6NO_3$.

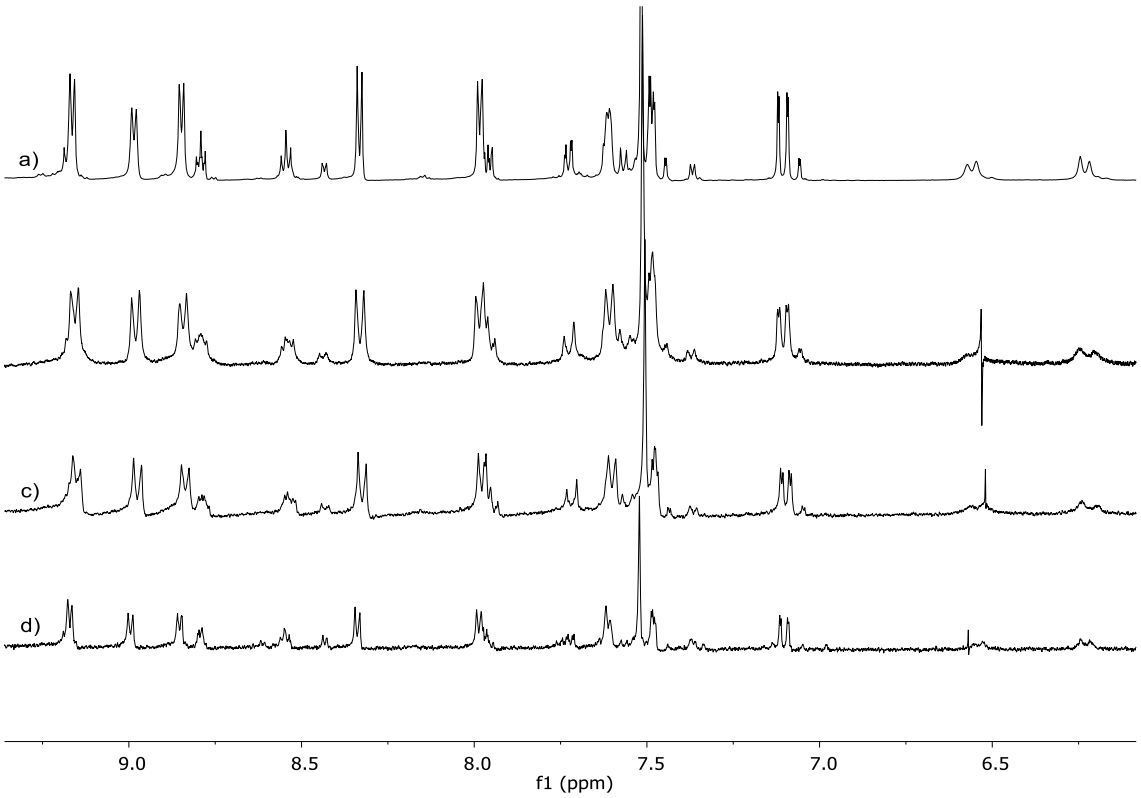

^{1}H NMR (300 MHz, D_2O) partial spectra of **R6**·$6NO_3$ at a) 5mM; b) 2.5 mM, c) 1.25 mM and d) 0.1 mM.

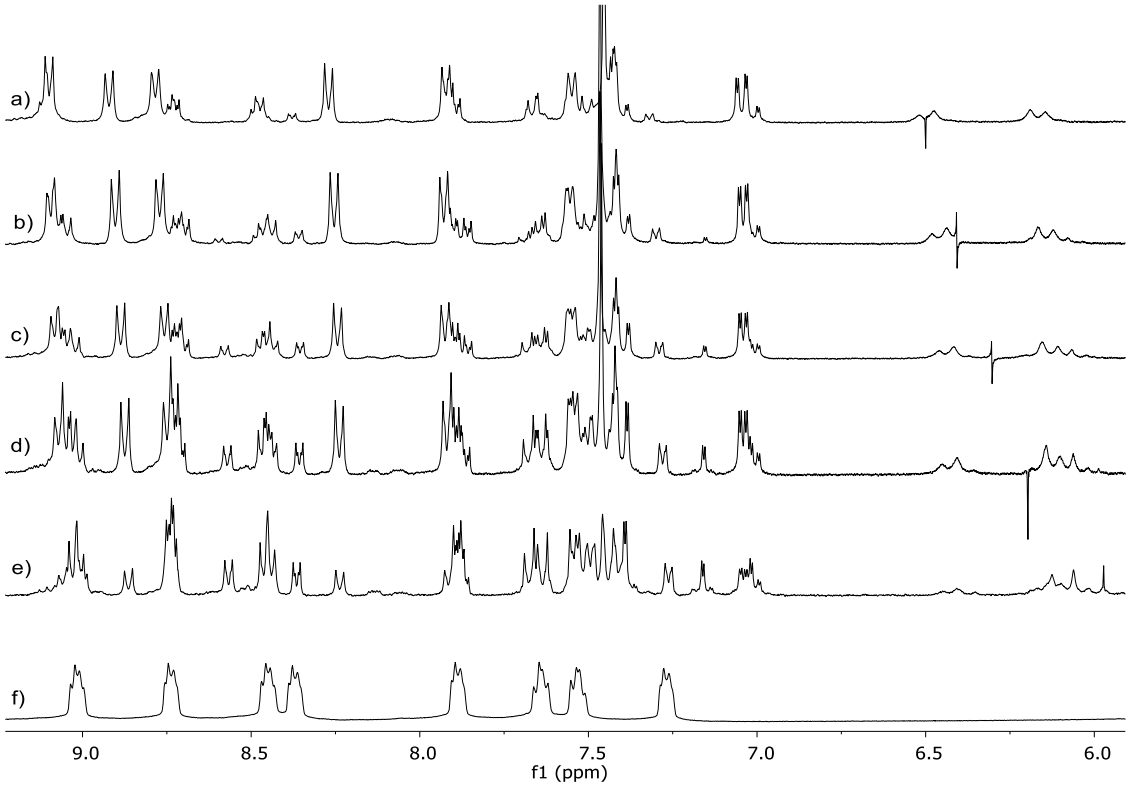

^{1}H NMR (300 MHz, D_2O) comparation spectra of a) **R6**·$6NO_3$ (5mM), **R6**·$6NO_3$ in the presence of b) 10 %, c) 20%, d) 30% and e) 50% of CD_3CN in media, and f) ligand **2** (5 mM, D_2O/CD_3CN 1:1).

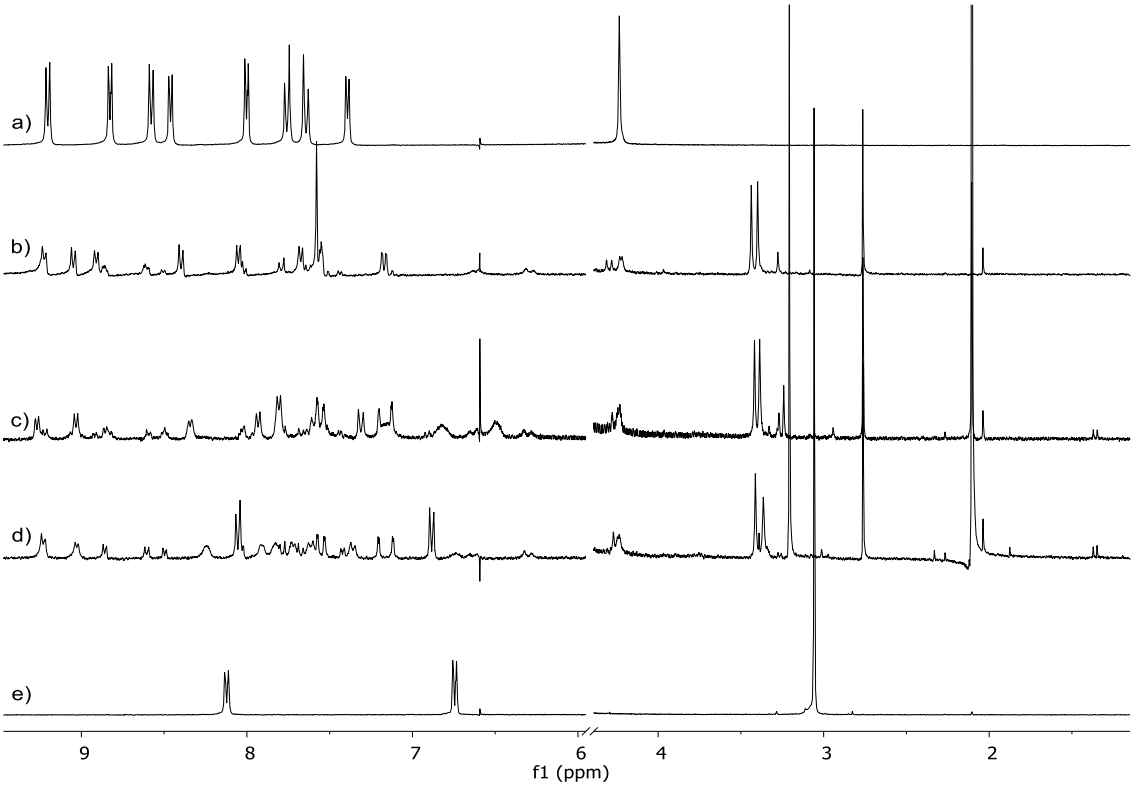

^{1}H NMR (300 MHz, D_2O) partial spectra of a) **2** b) **R6**·$6NO_3$ (1.25mM), **R6**·$6NO_3$ in the presence of 2 equiv. of dimethylaminopyridine 48h, c) **R6**·$6NO_3$ in the presence of 4 equiv. of dimethylaminopyridine and d) t=48h and e) dimethylaminopyridine.

1.9. Metallacycle **R7**·8NO_3.

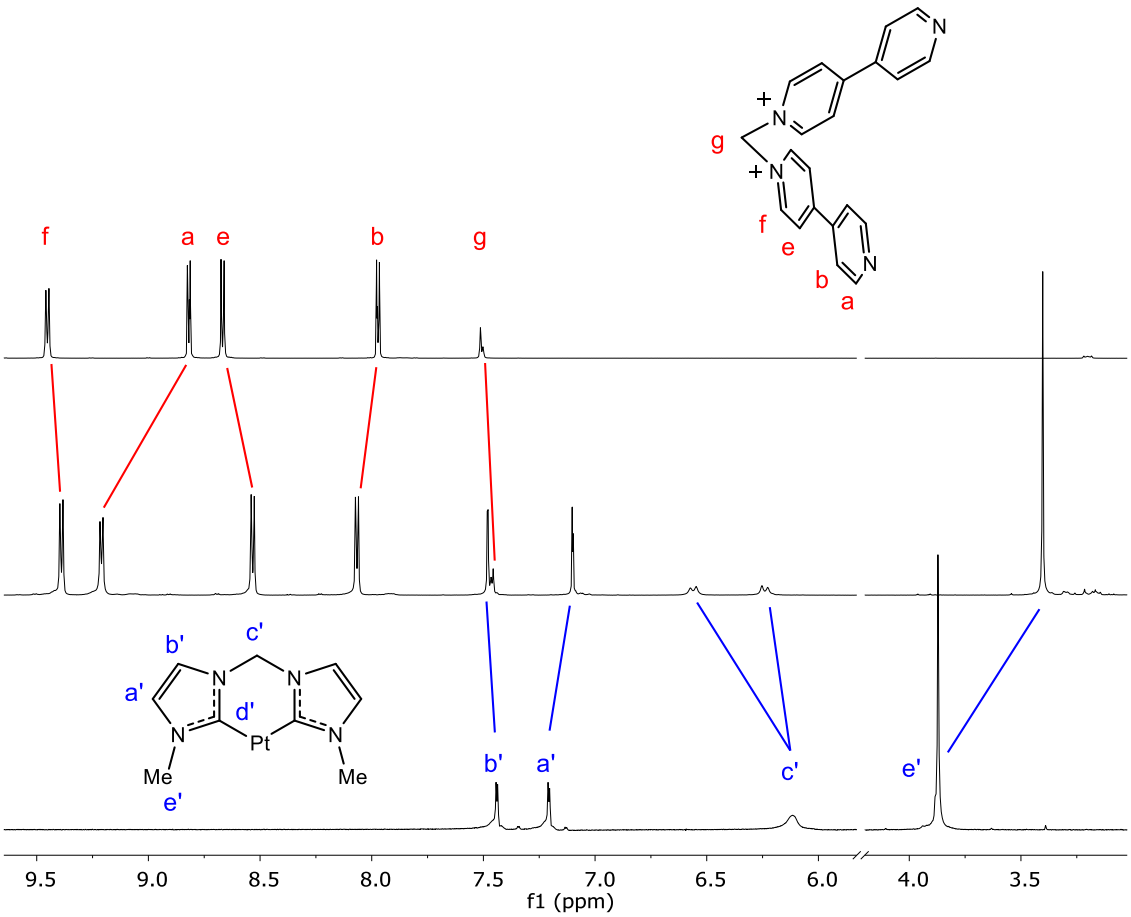

^{1}H NMR (500 MHz, D_2O) spectra of **3** (top), **R7**·8NO_3 (middle) and **6(Pt)**·2NO_3 (bottom).

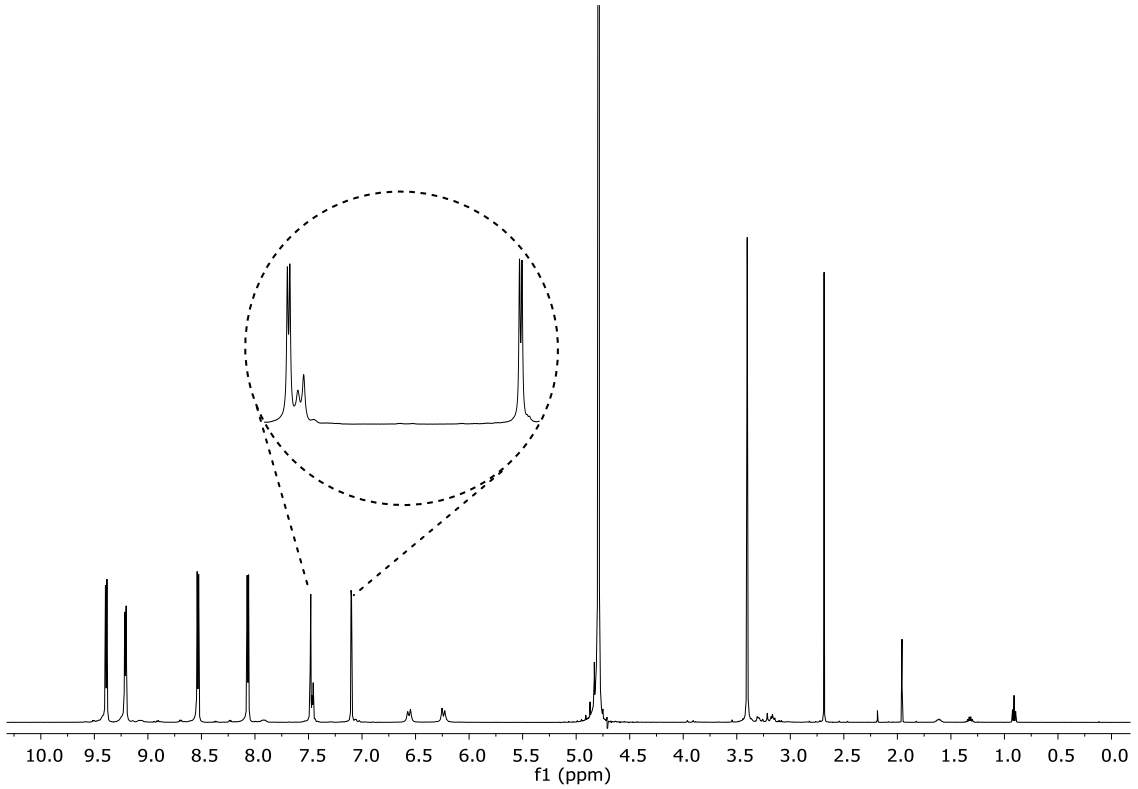

^{1}H NMR (500 MHz, D_2O) full spectra of **R7**·8NO_3.

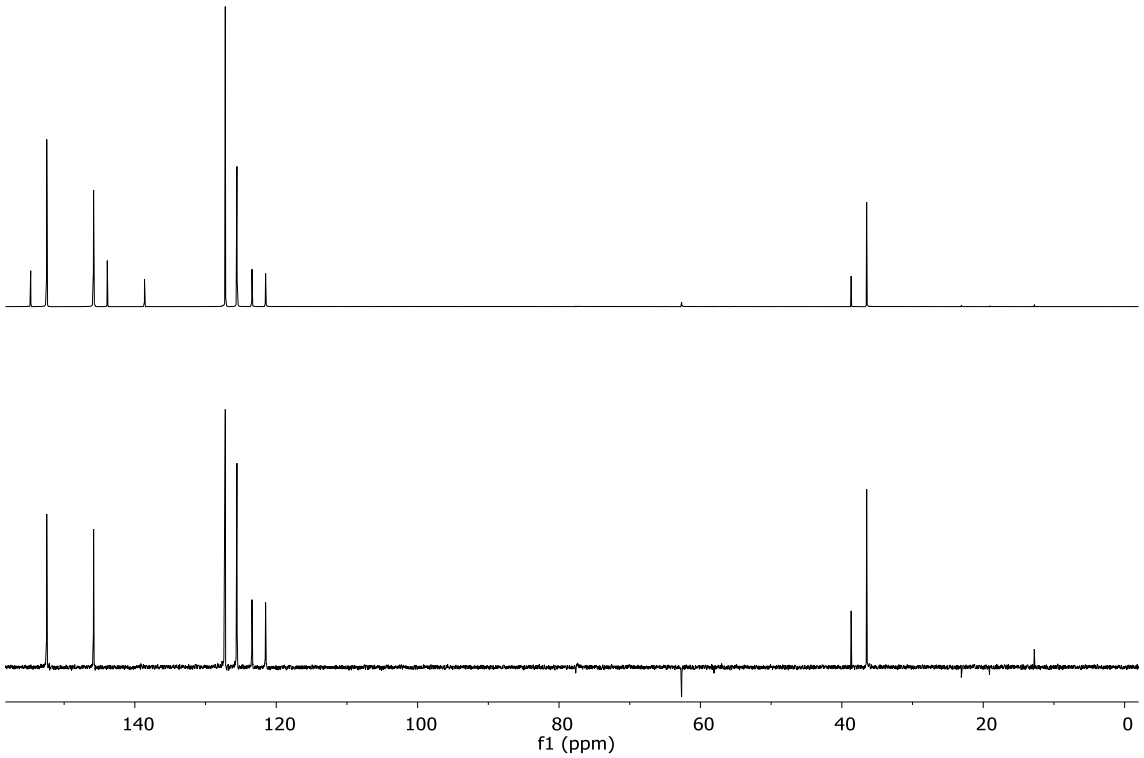

^{13}C NMR and DEPT (125 MHz, D_2O) full spectra of **R7**·8NO_3.

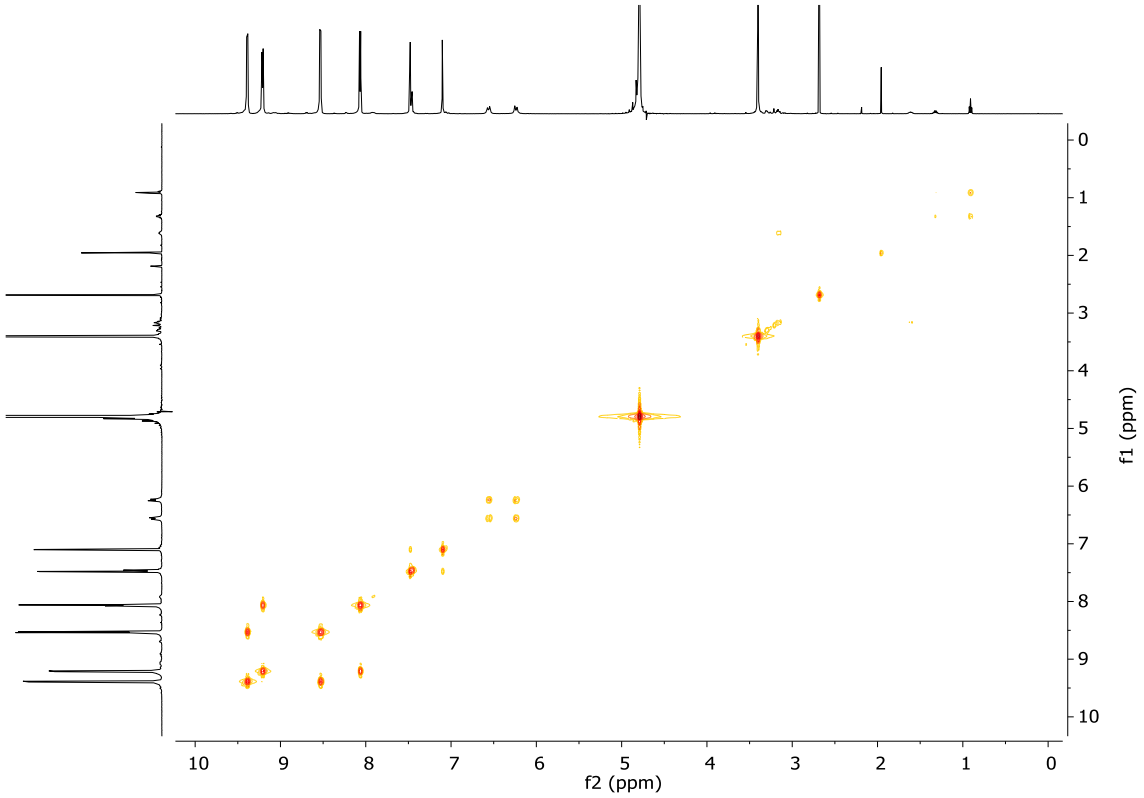

COSY (500 MHz, D_2O) full spectra of **R7**·$8NO_3$.

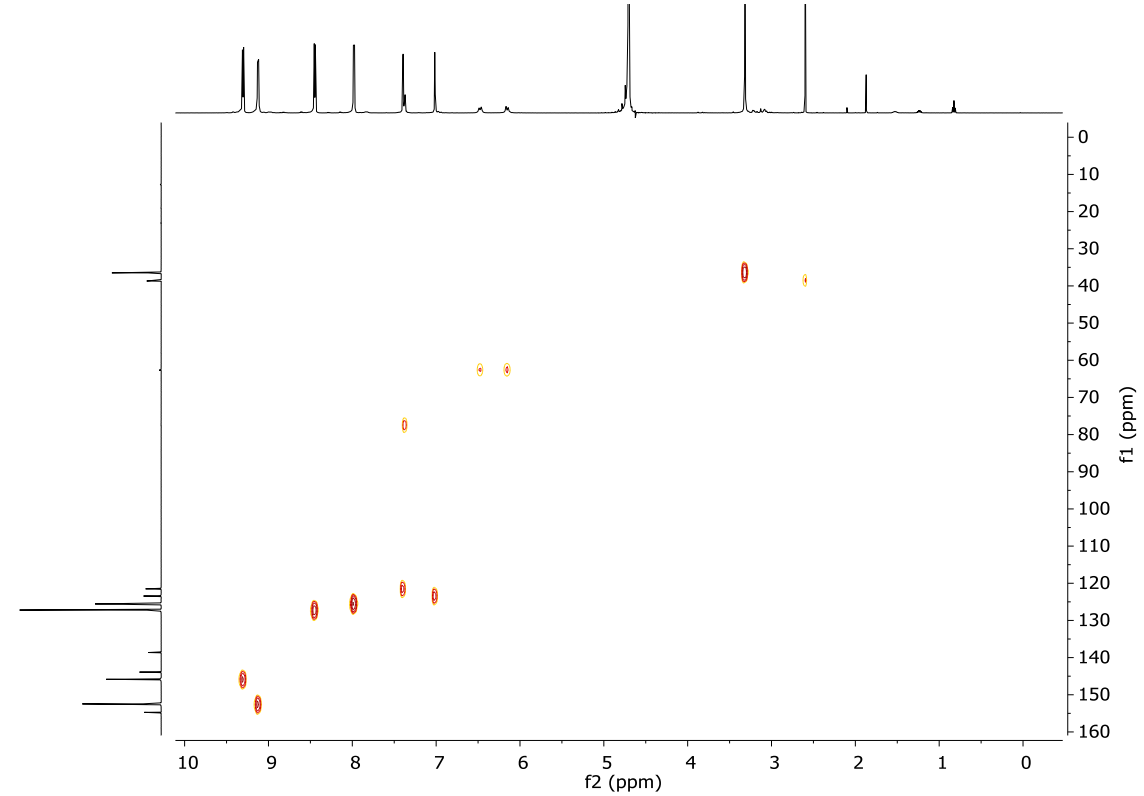

HSQC (125 and 500 MHz, D_2O) full spectra of **R7**·$8NO_3$.

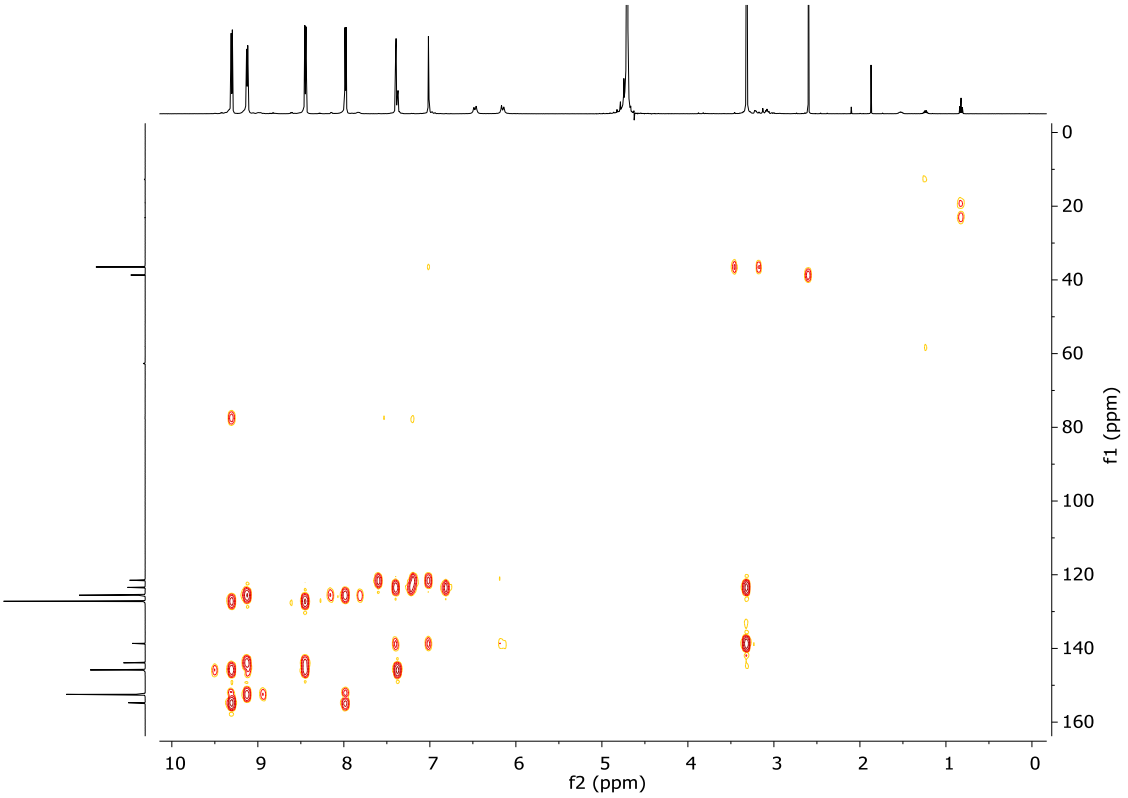

HMBC (125 and 500 MHz, D_2O) full spectra of **R7**·$8NO_3$.

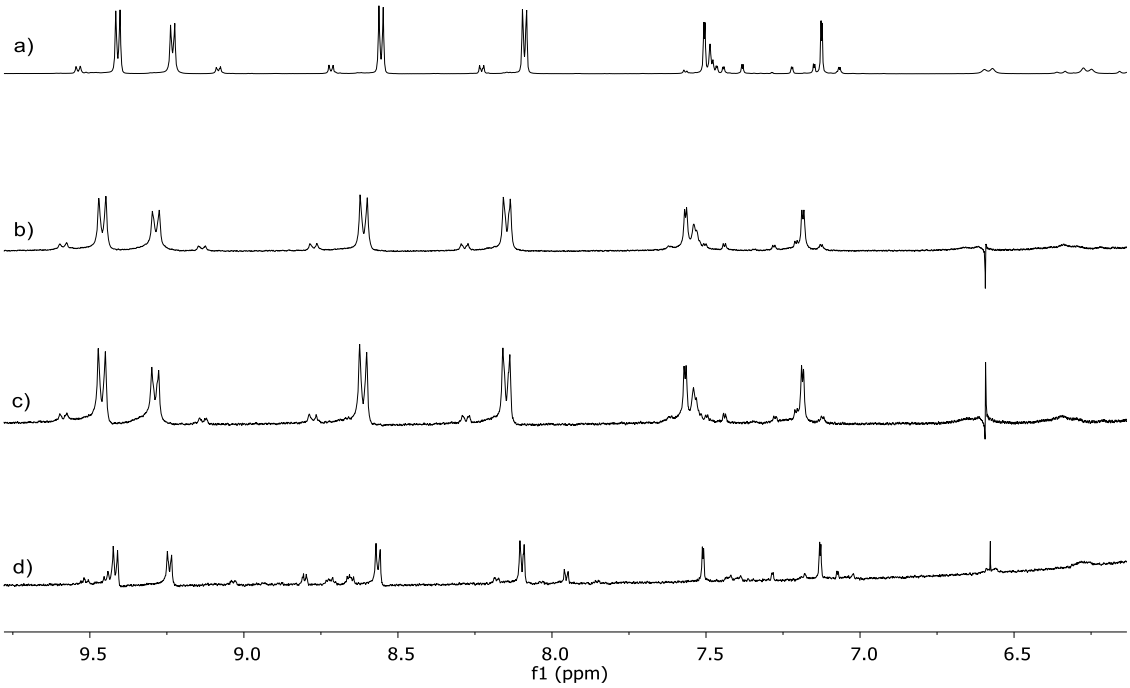

^1H NMR (300 MHz, D_2O) partial espectra of **R7**·$8NO_3$ at a) 5mM; b) 2.5 mM, c) 1.25 mM and d) 0.1 mM.

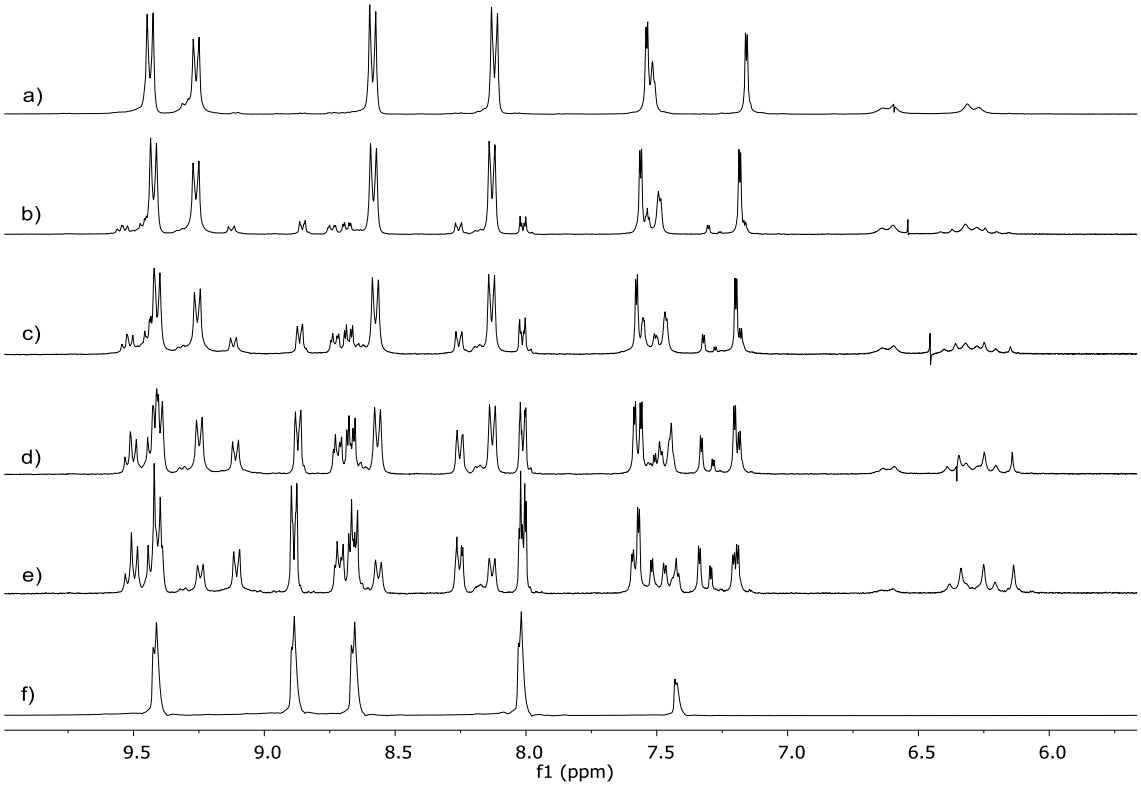

^{1}H NMR (300 MHz, D_2O) partial spectra of a) **R7**·8NO_3 (5mM), **R7**·8NO_3 in the presence of b) 10 %, c) 20%, d) 30%, and e) 50% of CD_3CN in media, and f) ligand **3** (5 mM, D_2O/CD_3CN 1:1).

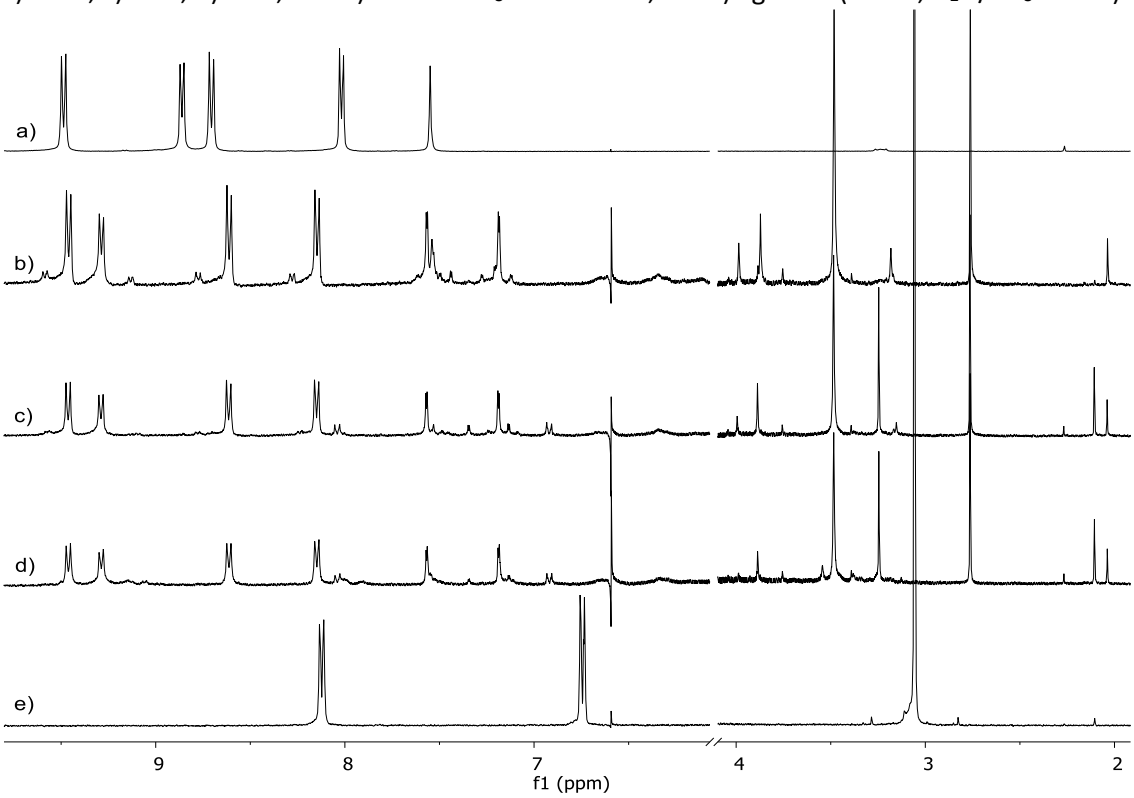

^{1}H NMR (300 MHz, D_2O) partial spectra of a) **3**, b) **R7**·8NO_3 (1.25mM), **R7**·8NO_3 in the presence of 2 equiv. of dimethylaminopyridine 48h, c) **R7**·8NO_3 in the presence of 4 equiv. of dimethylaminopyridine and d) t=48h and e) dimethylaminopyridine.

1.10. Metallacycle **R8**·8NO_3.

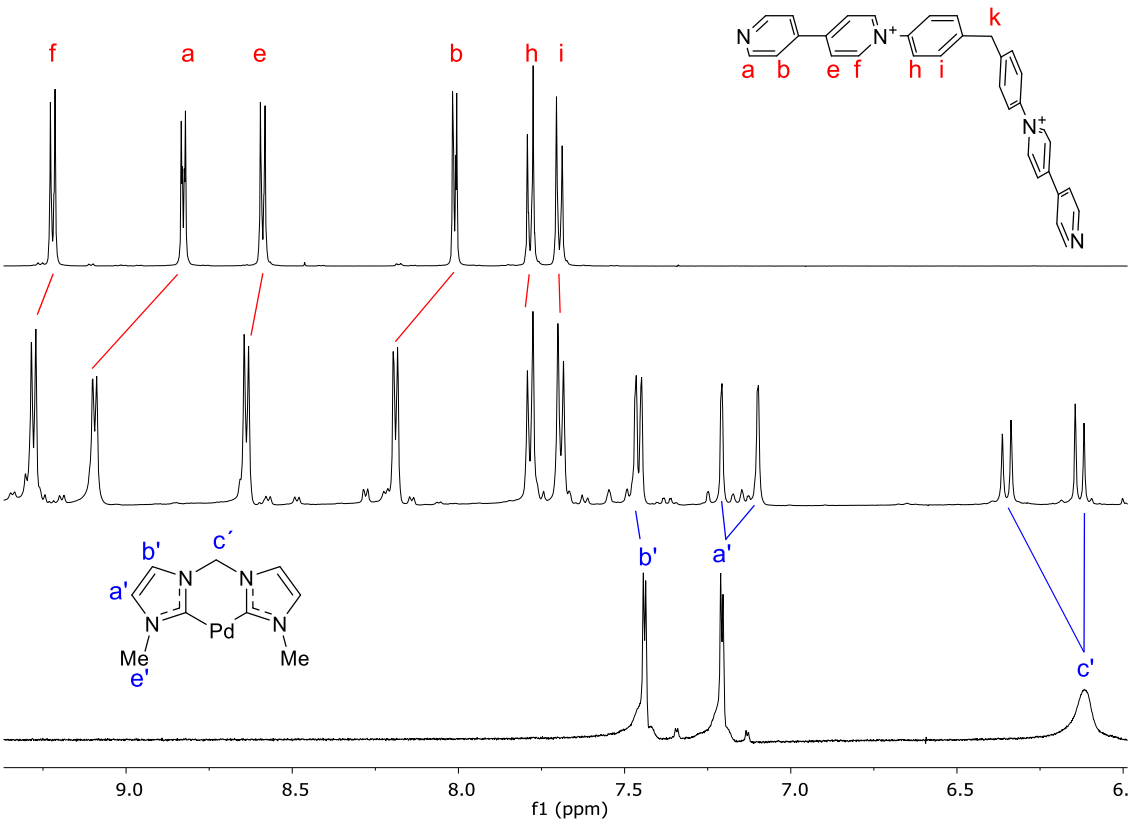

^{1}H NMR (500 MHz, D_2O) spectra of **4** (top), **R8**·8NO_3 (middle) and **6(Pt)**·2NO_3 (bottom).

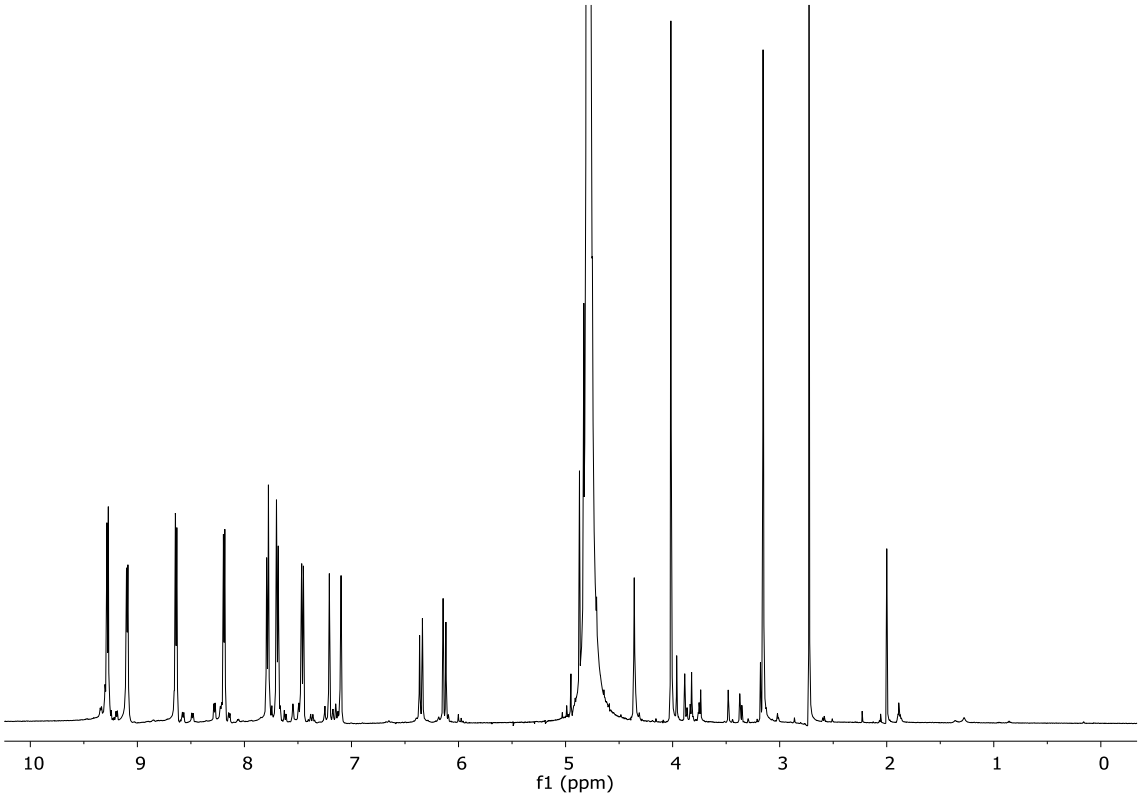

^{1}H NMR (500 MHz, D_2O) full spectra of **R8**·8NO_3

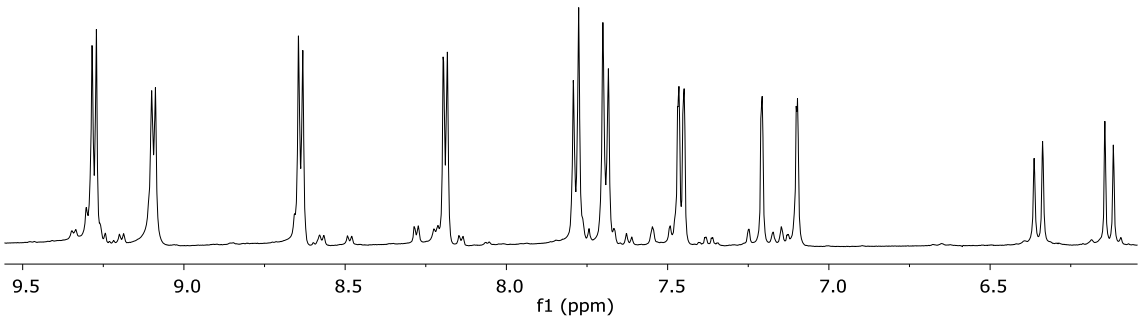

^{1}H NMR (500 MHz, D_2O) partial spectra of **R8**·8NO_3

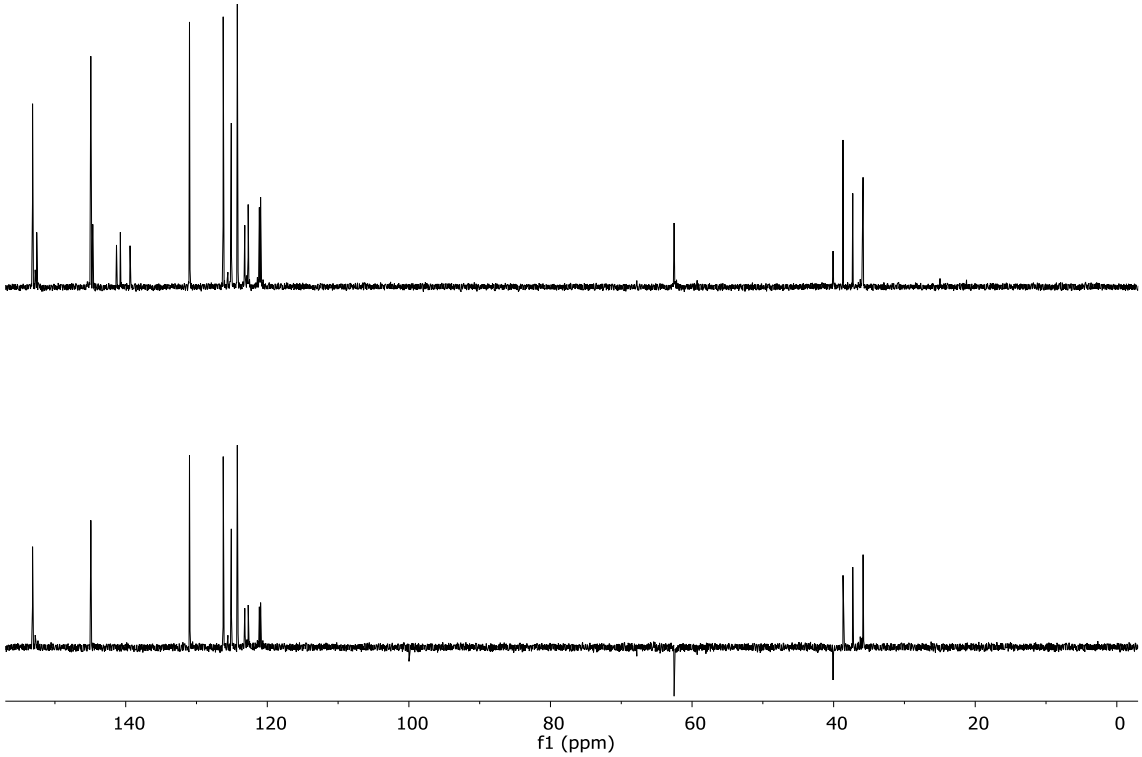

^{13}C NMR and DEPT (125 MHz, D_2O) full spectra of **R8**·8NO_3

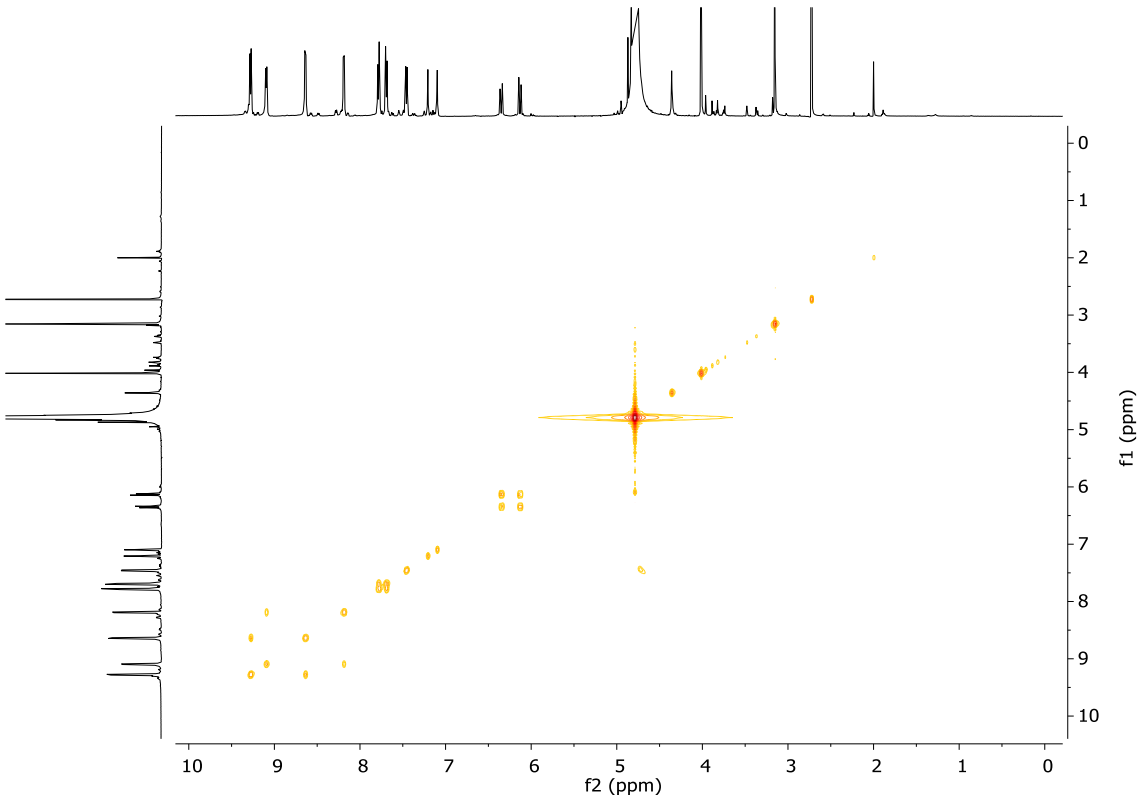

COSY (500 MHz, D_2O) full spectra of **R8**·8NO_3

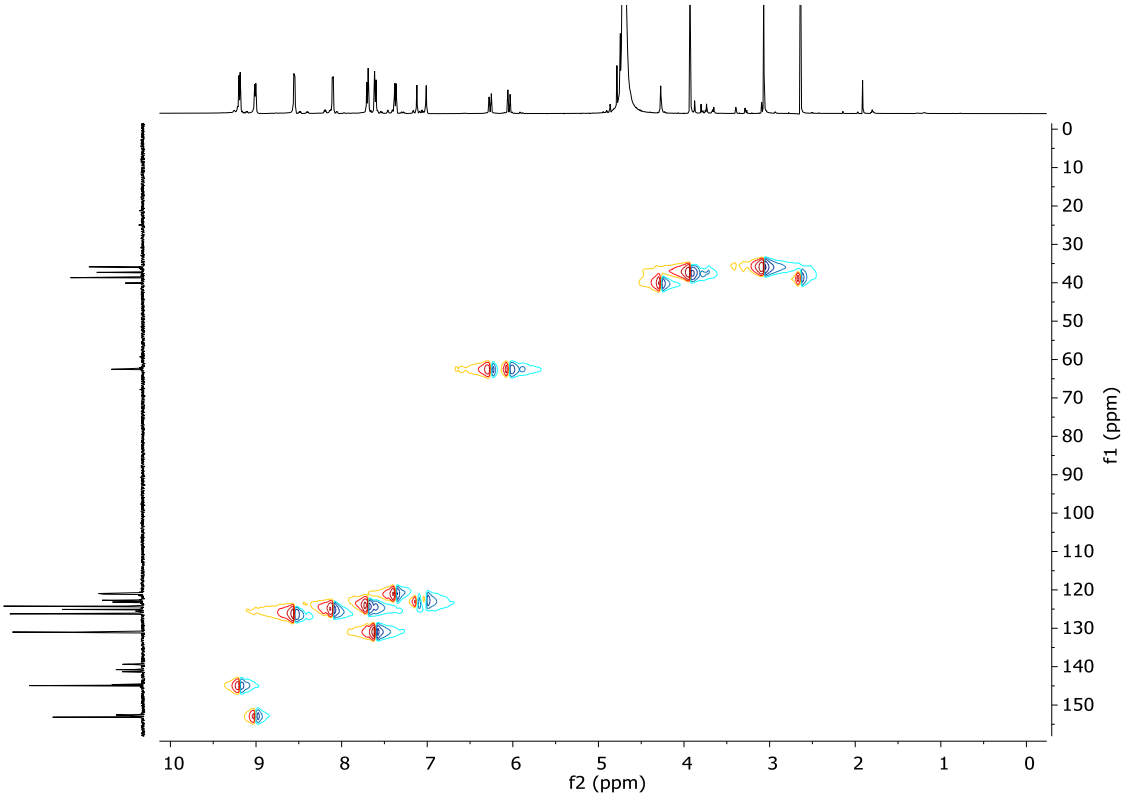

HSQC (125 and 500 MHz, D_2O) full spectra of **R8**·8NO_3

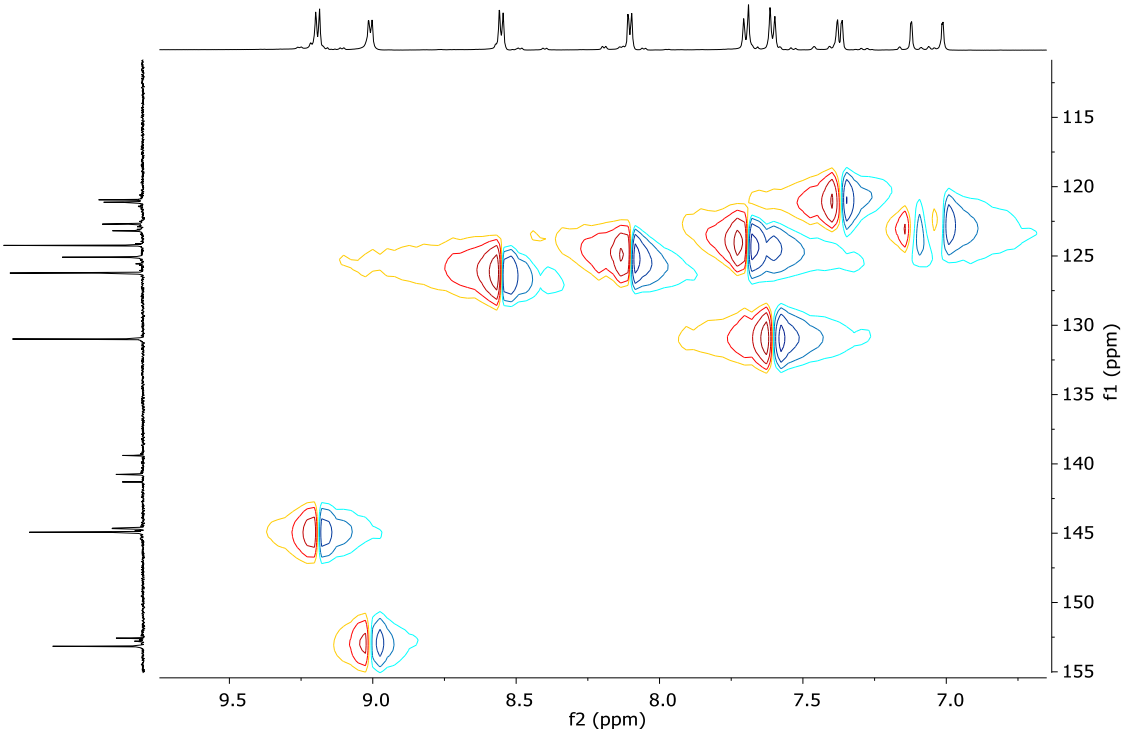

HSQC (125 and 500 MHz, D_2O) partial spectra of **R8**·8NO_3

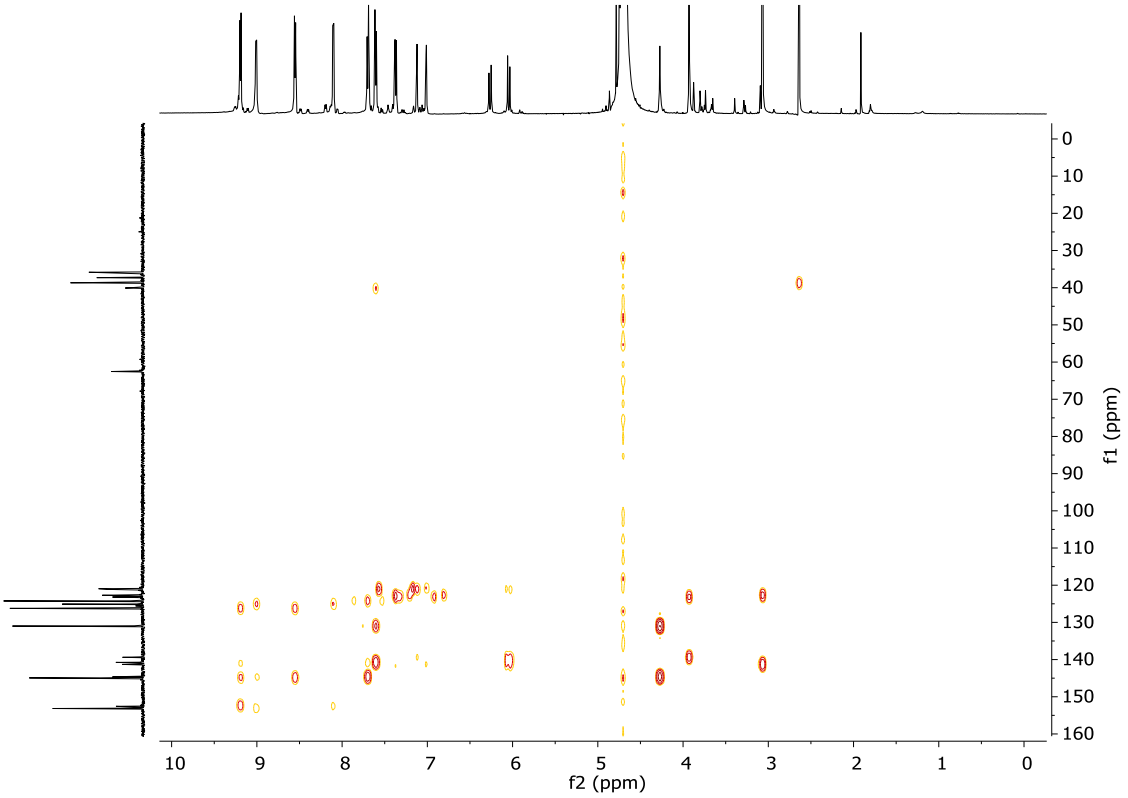

HMBC (125 and 500 MHz, D_2O) full spectra of **R8**·$8NO_3$

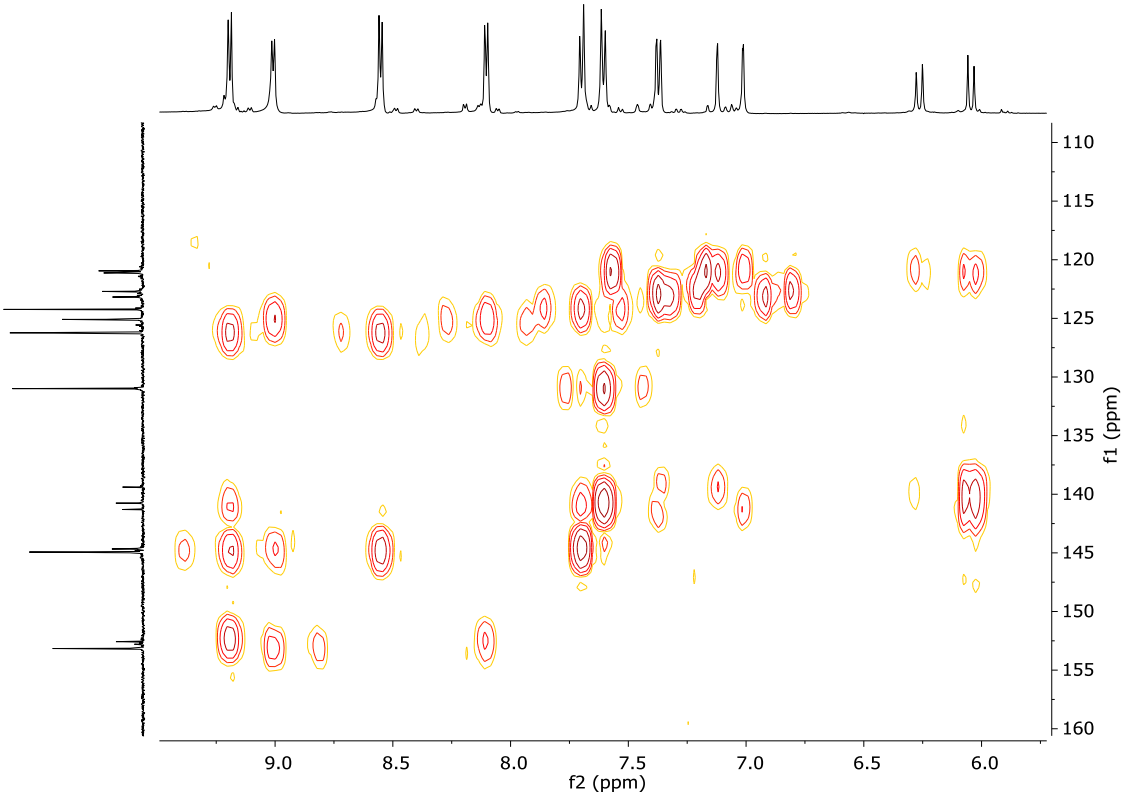

HMBC (125 and 500 MHz, D_2O) partial spectra of **R8**·$8NO_3$

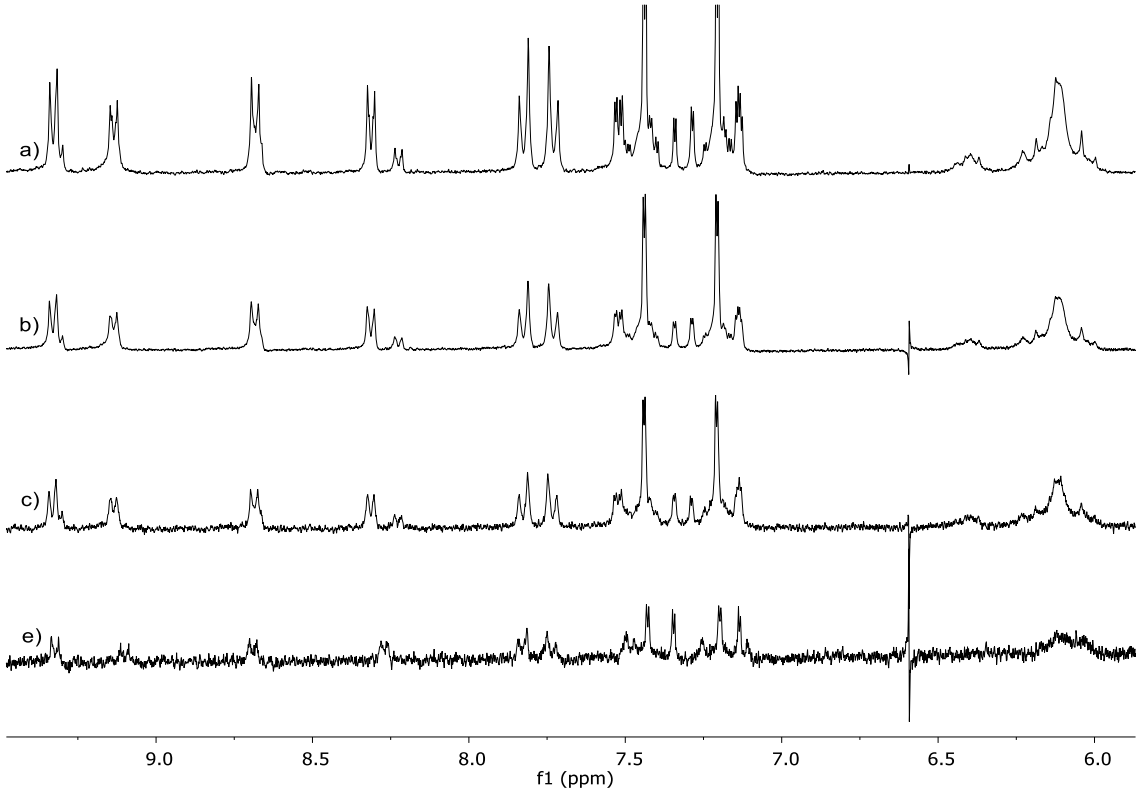

^{1}H NMR (300 MHz, D_2O) partial espectra of **R8**·8NO_3 at a) 5mM; b) 2.5 mM, c) 1.25 mM and d) 0.1 mM.

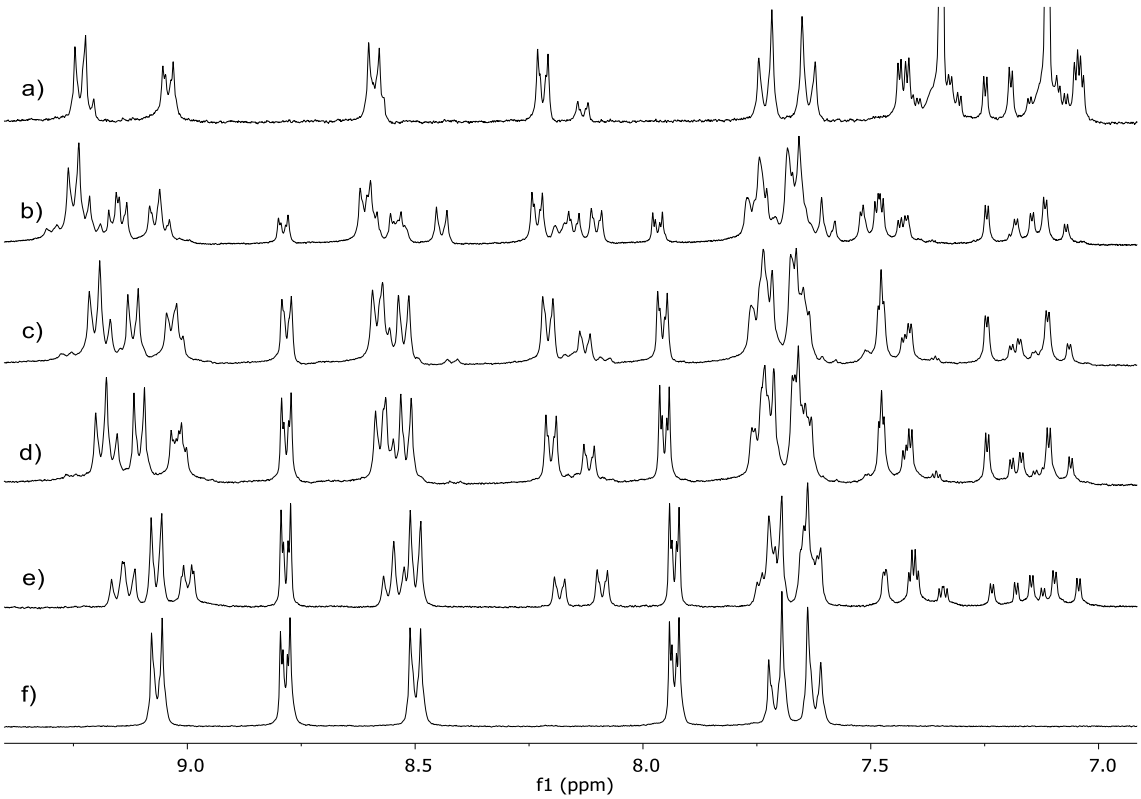

^{1}H NMR (300 MHz, D_2O) partial spectra of a) **R8**·8NO_3 (5mM), **R8**·8NO_3 in the presence of b) 10 %, c) 20%, d) 30%, and e) 50% of CD_3CN in media, and f) ligand **4** (5 mM, D_2O/CD_3CN 1:1).

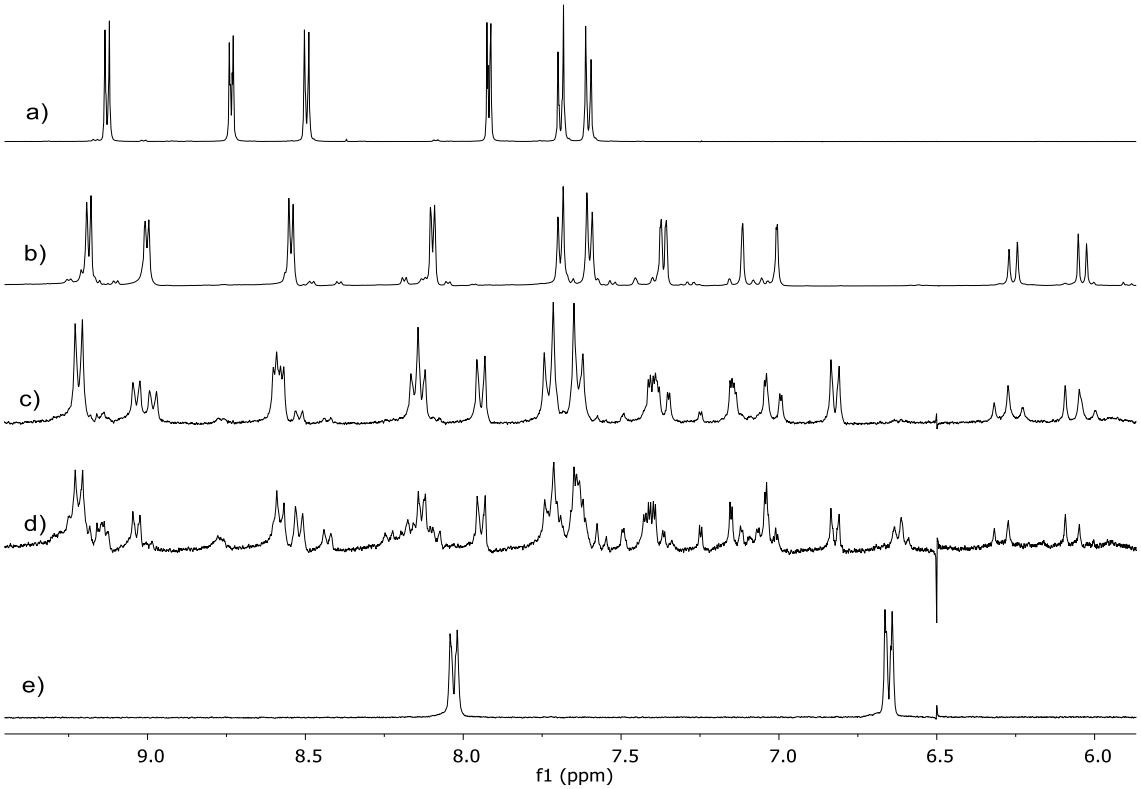

^{1}H NMR (300 MHz, D_2O) partial spectra of a) **4**, b) **R8**·8NO_3 (1.25mM), c) **R8**·8NO_3 in the presence of 2 equiv. of dimethylaminopyridine 24h, d) **R7**·8NO_3 in the presence of 4 equiv. of dimethylaminopyridine 24h and e) dimethylaminopyridine

1.11. Inclusion complex **R1⊂12**·6NO_3.

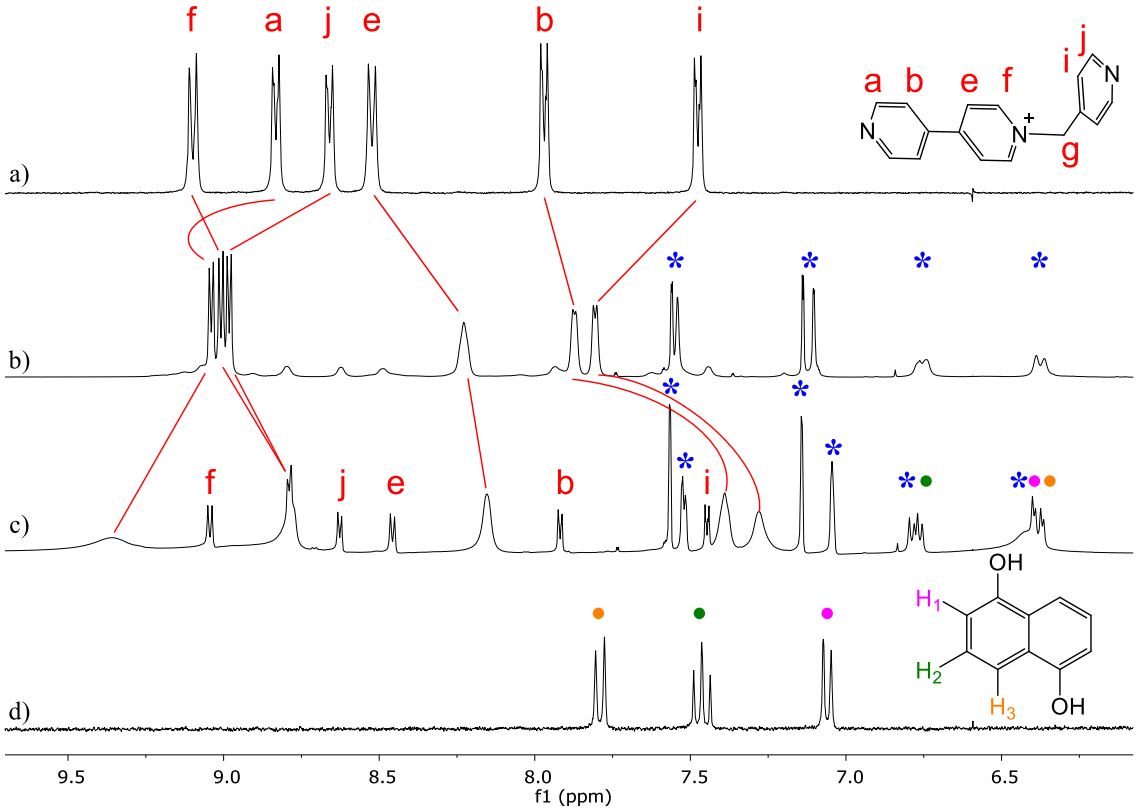

^{1}H NMR (500 MHz, D_2O) partial spectra of a) ligand **1**, b) **R1**·6NO_3, c) **R1⊂12**·6NO_3 and d) **12**. Carbene **6(Pd)**·2NO_3 signals are indicated with blue stars.

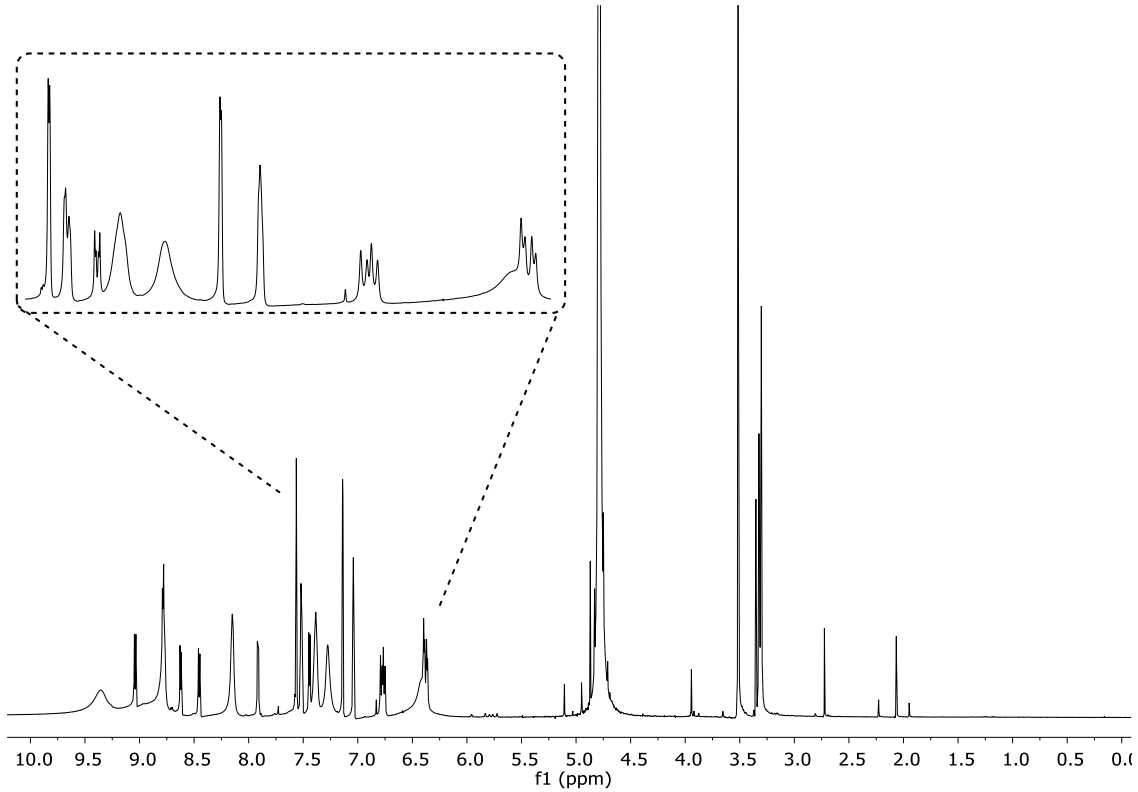

^{1}H NMR (500 MHz, D_2O) full spectra of **R1⊂12**·6NO_3.

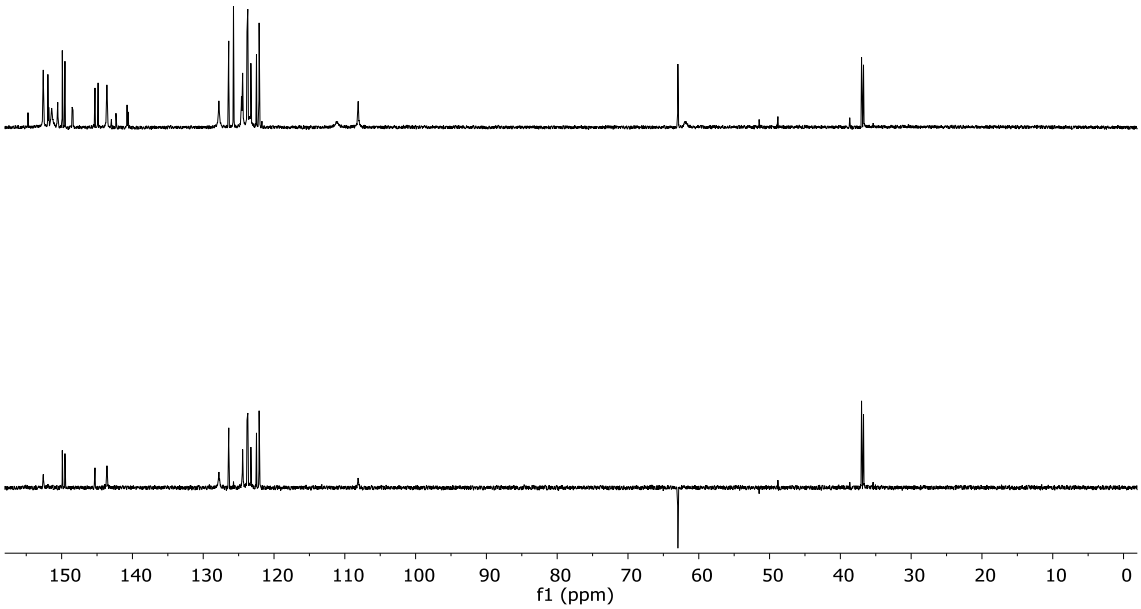

^{13}C NMR and DEPT (125 MHz, D_2O) full spectra of **R1**⊂**12**·6NO_3.

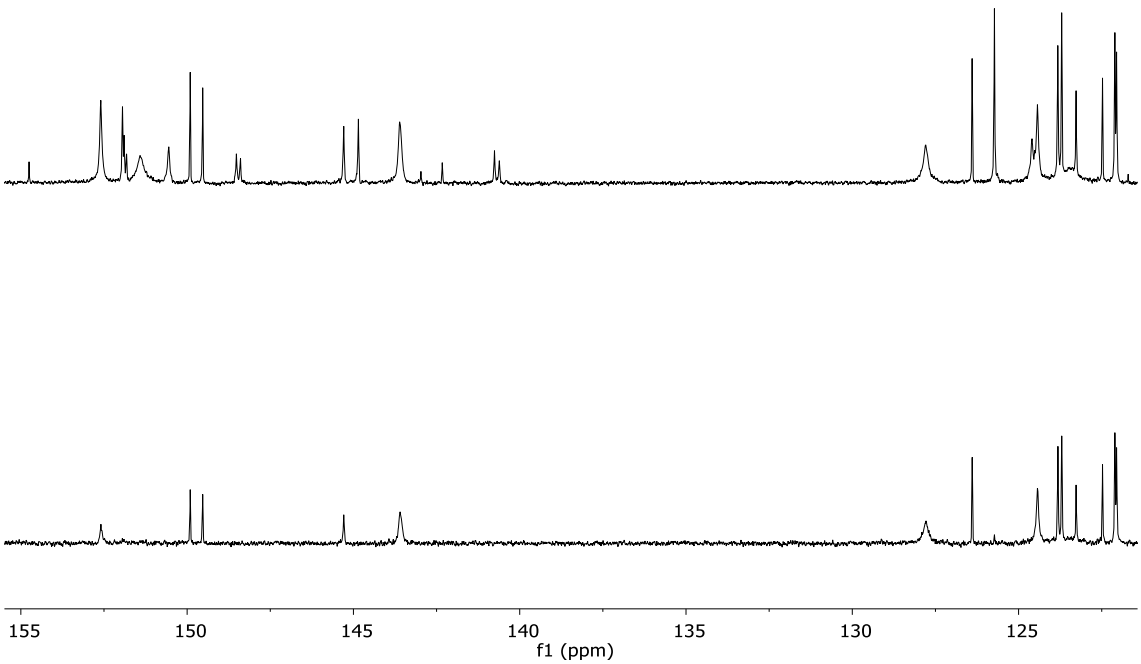

^{13}C NMR and DEPT (125 MHz, D_2O) partial spectra of **R1**⊂**12**·6NO_3.

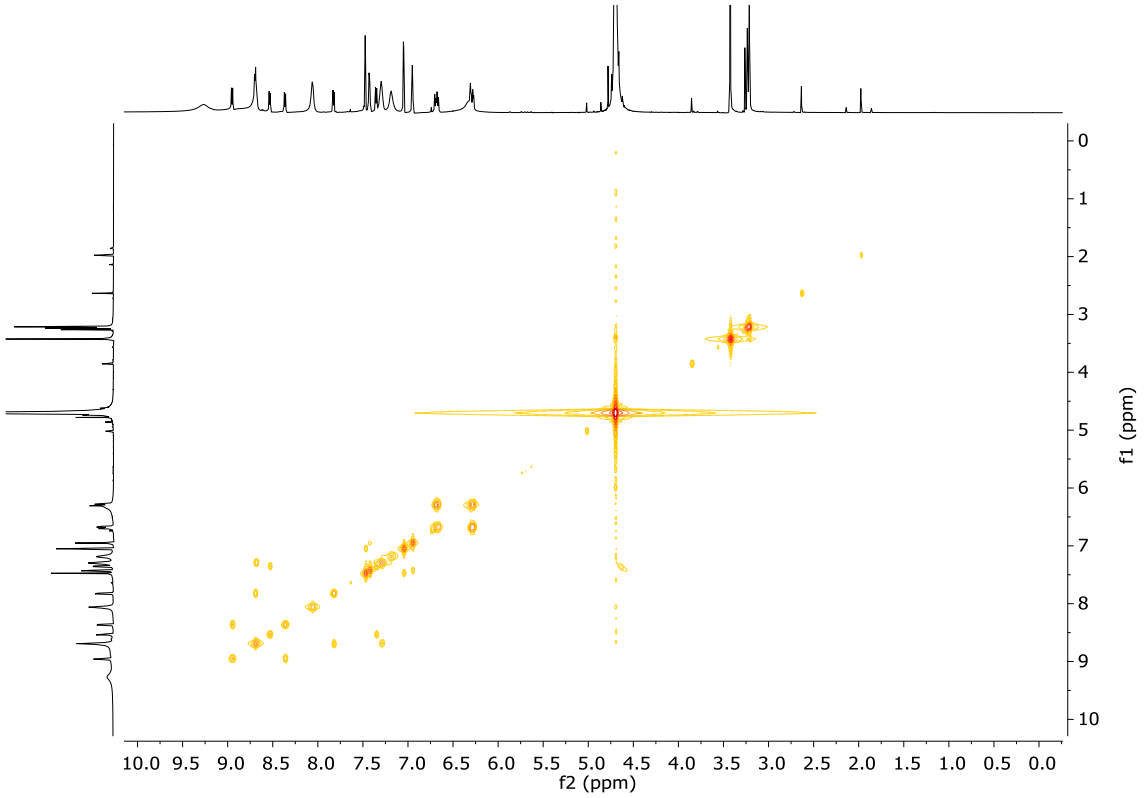

COSY (500 MHz, D_2O) full spectra of **R1**⊂**12**·6NO_3.

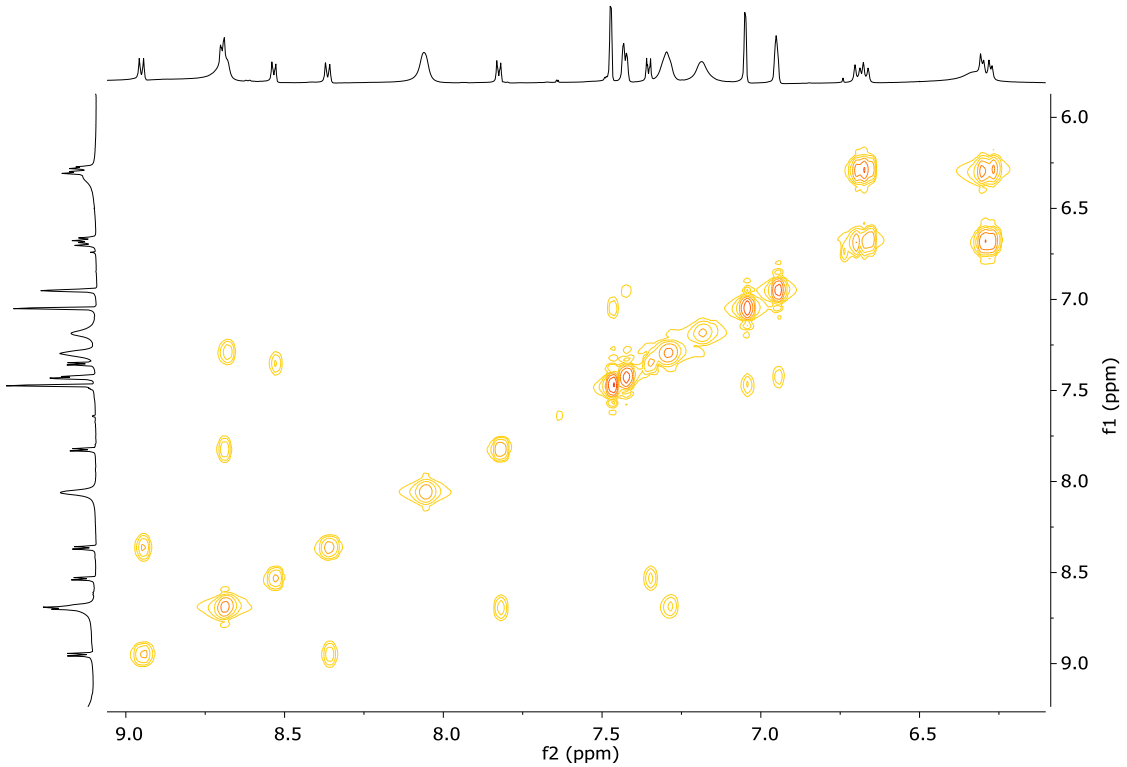

COSY (500 MHz, D_2O) partial spectra of of **R1**⊂**12**·6NO_3.

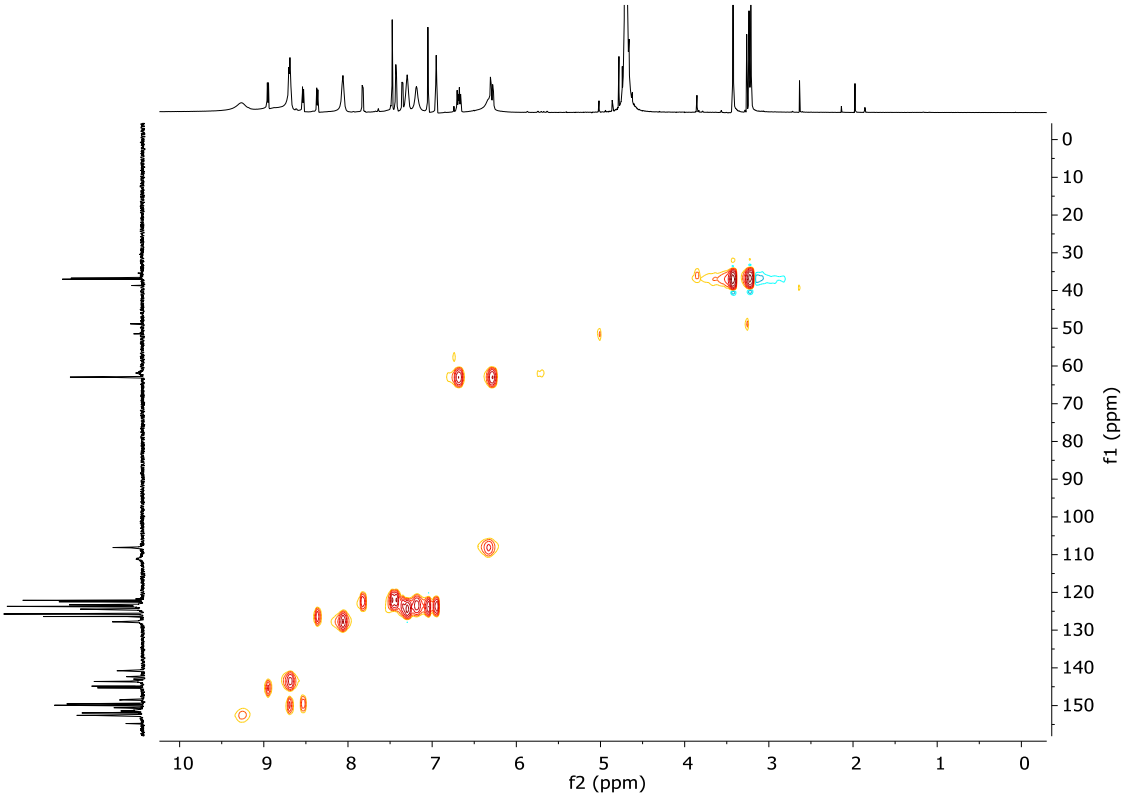

HSQC (125 and 500 MHz, D_2O) full spectra of of **R1**⊂**12**·6NO_3.

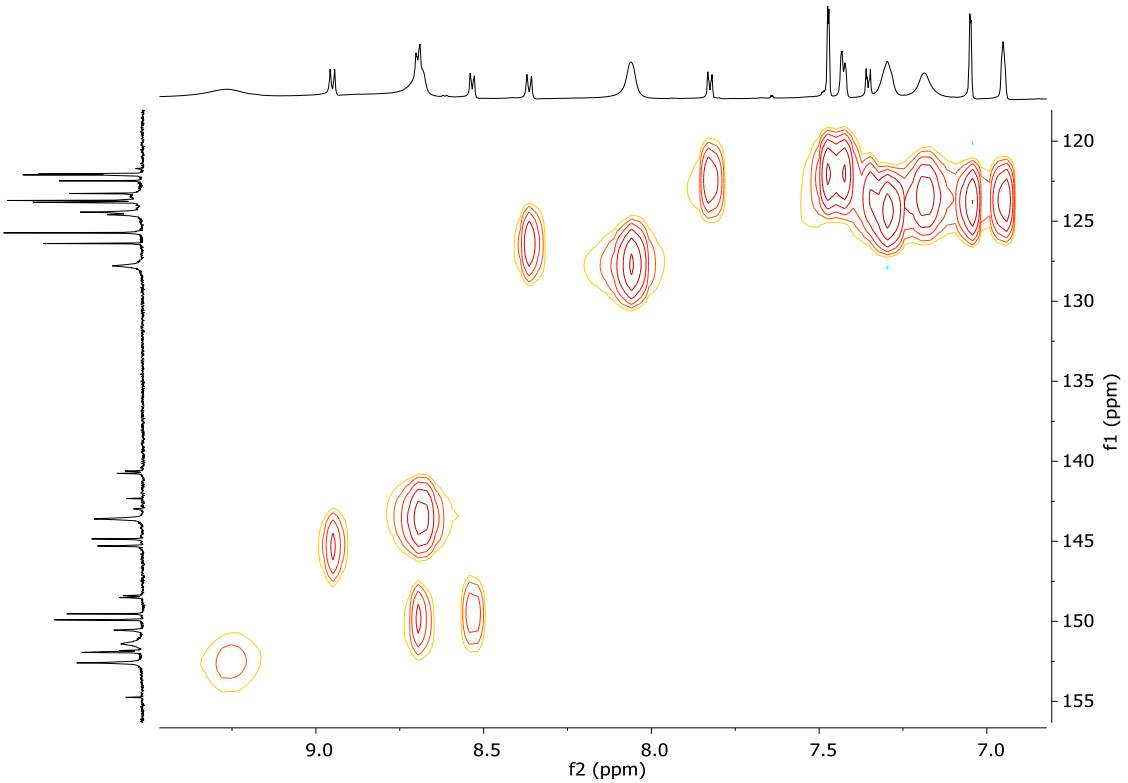

HSQC (125 and 500 MHz, D_2O) partial spectra of of **R1**⊂**12**·6NO_3.

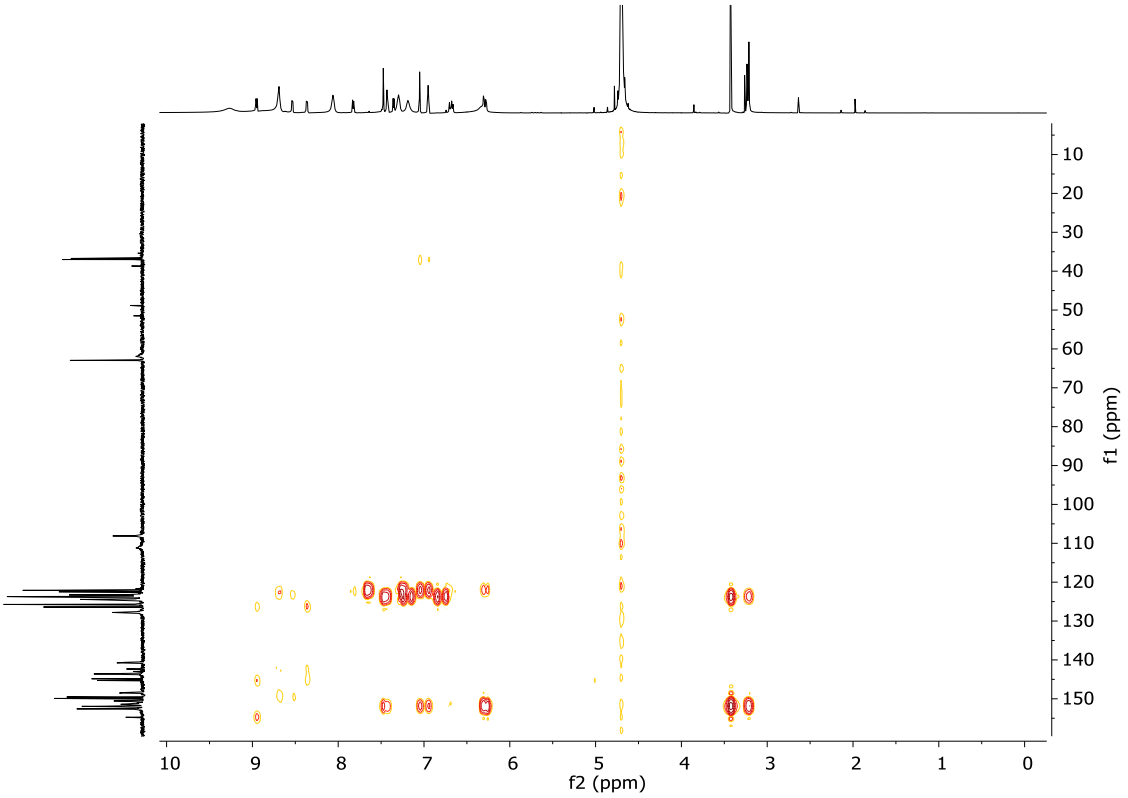

HMBC (125 and 500 MHz, D_2O) full spectra of of **R1**⊂**12**·6NO_3.

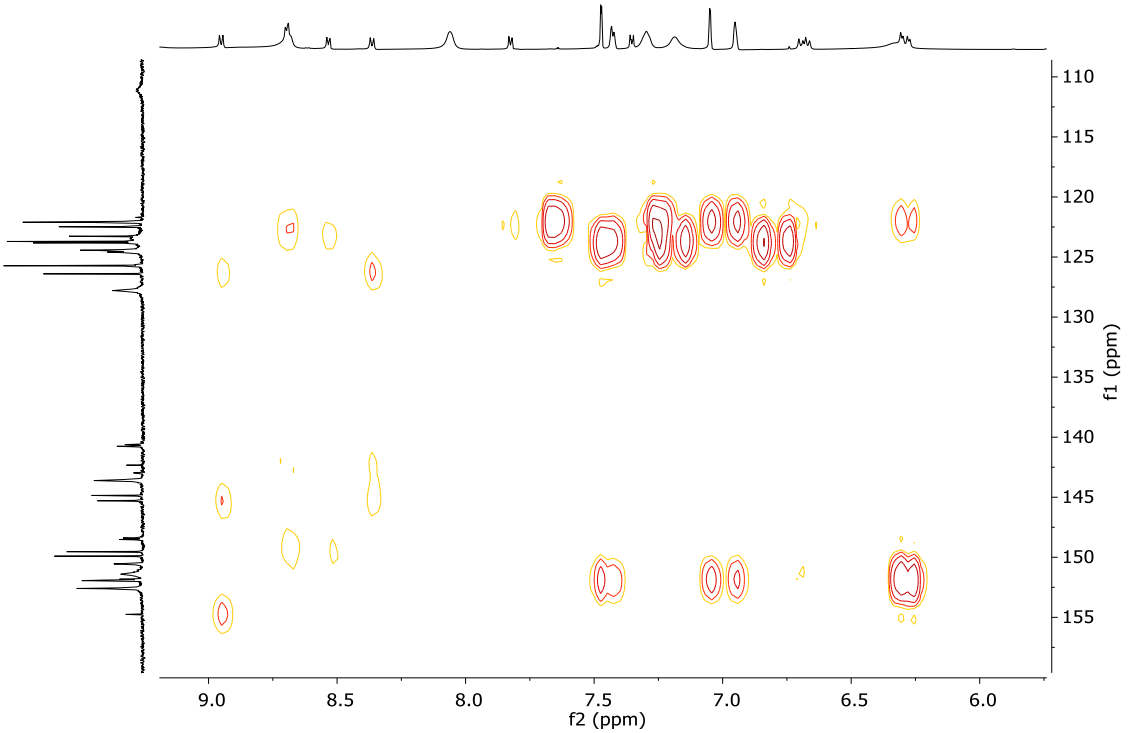

HMBC (125 and 500 MHz, D_2O) partial spectra of of **R1**⊂**12**·6NO_3.

1.12. Inclusion complex **R2⊂12**·6NO_3.

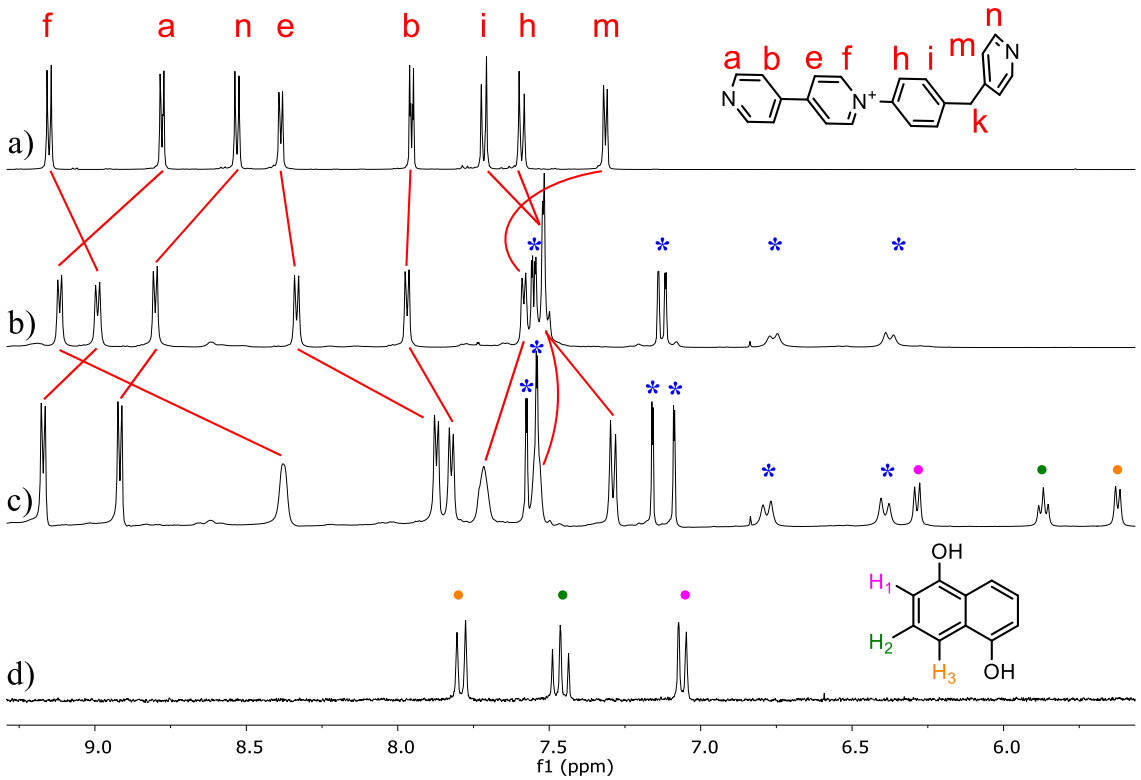

^{1}H NMR (500 MHz, D_2O) partial spectra of a) ligand **2**,b) **R2**·6NO_3,c) **R2⊂12**·6NO_3 and d) **12**. Carbene **6(Pd)**·2NO_3 signals are indicated with blue stars.

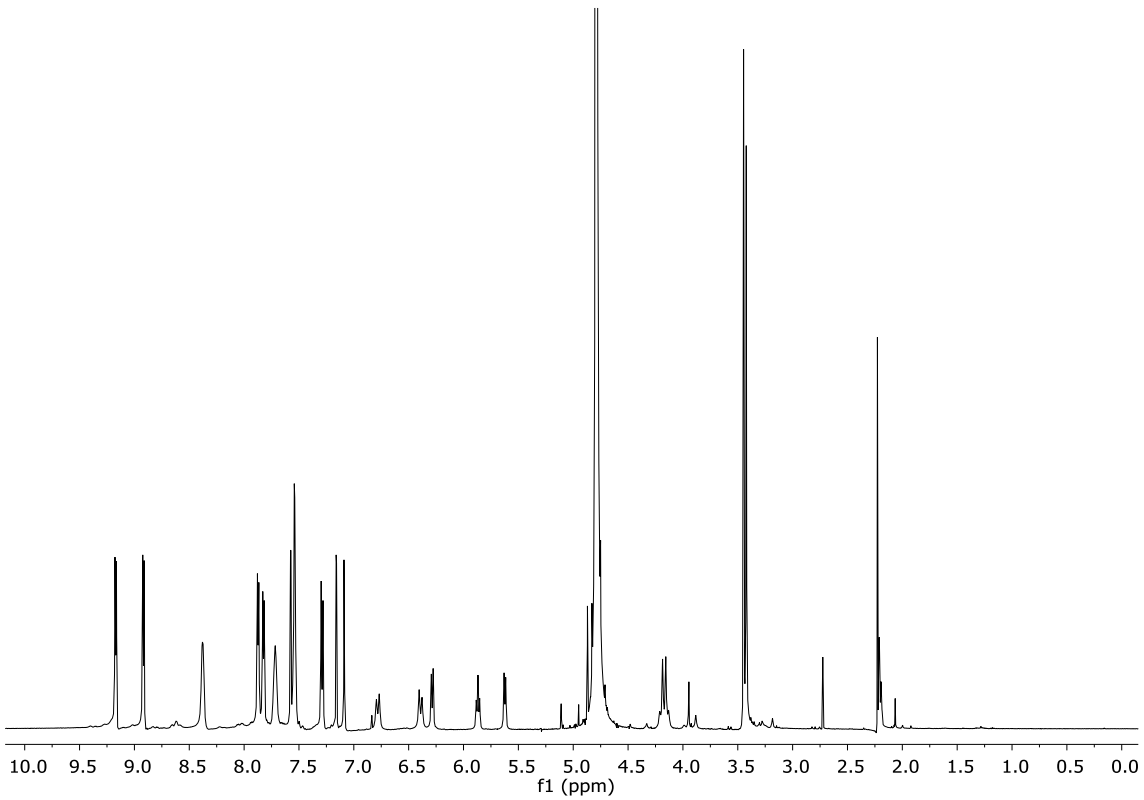

^{1}H NMR (500 MHz, D_2O) full spectra of **R2⊂12**·6NO_3.

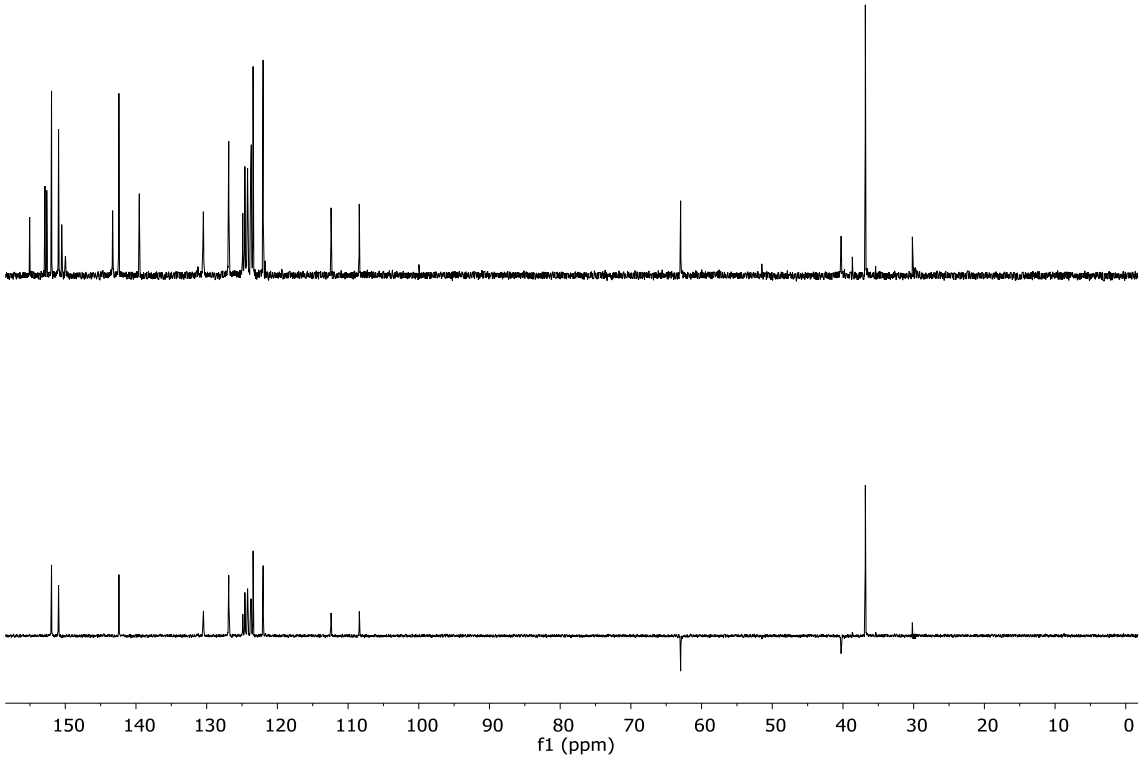

^{13}C NMR and DEPT (125 MHz, D_2O) full espectra of **R2**⊂**12**·6NO_3.

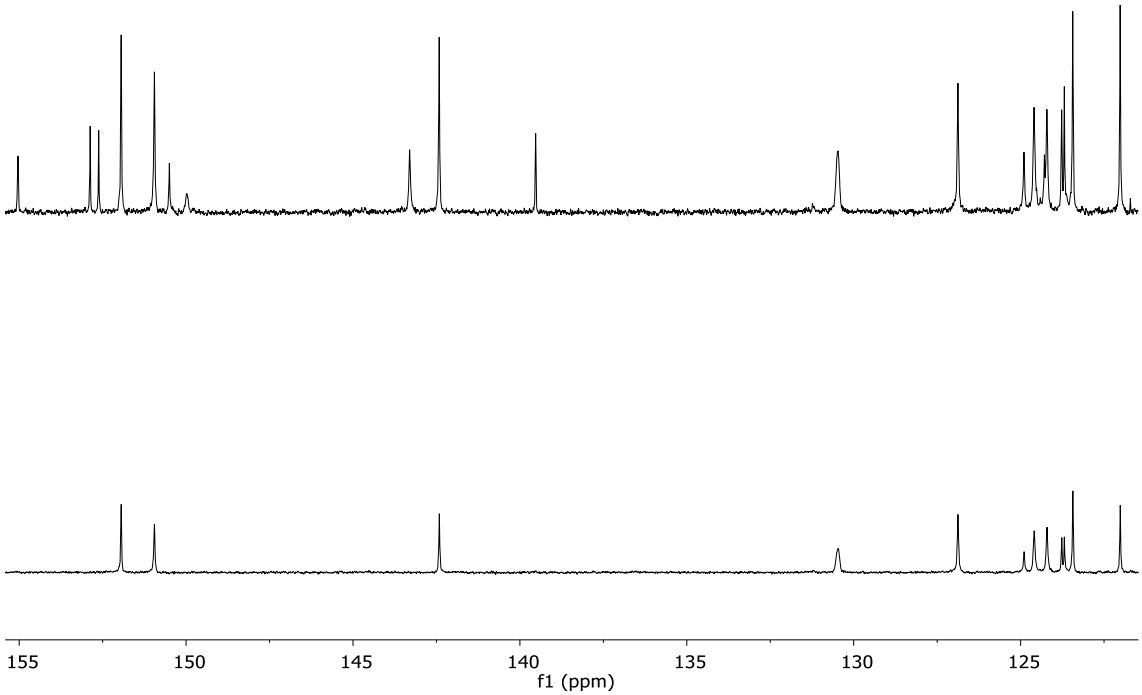

^{13}C NMR and DEPT (125 MHz, D_2O) detail spectra of **R2**⊂**12**·6NO_3.

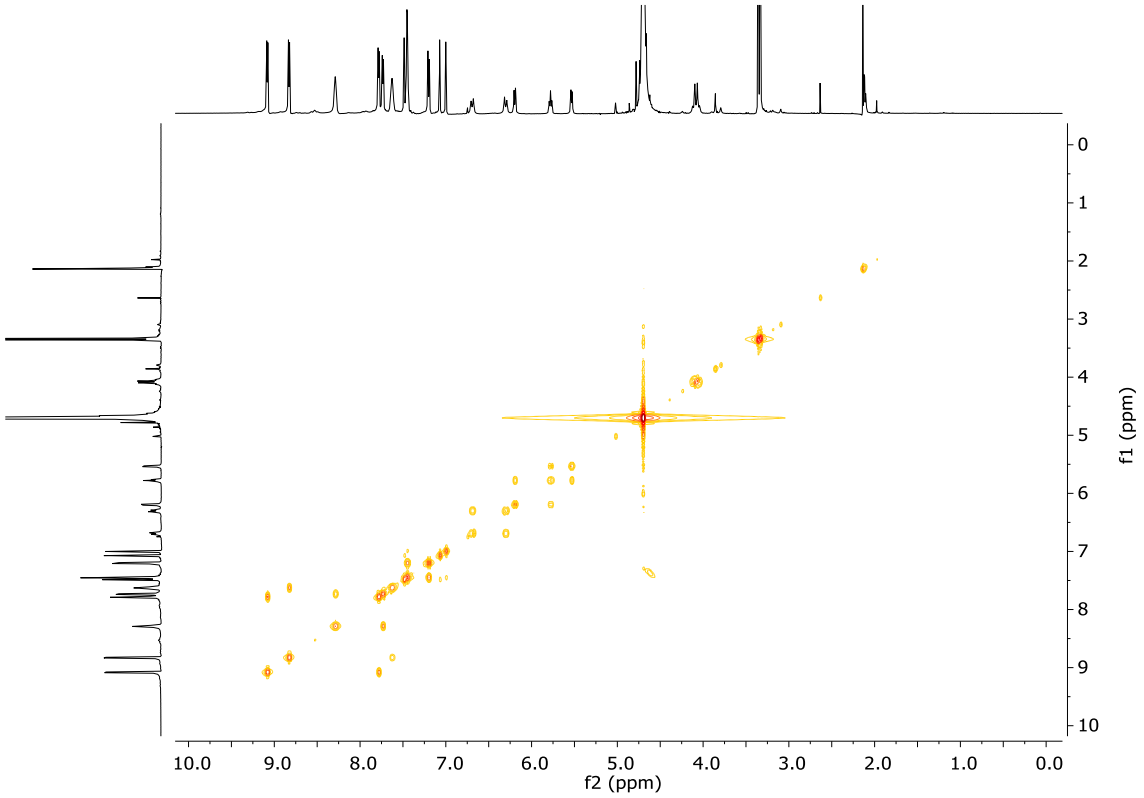

COSY (500 MHz, D_2O) full spectra of **R2**⊂**12**·6NO_3.

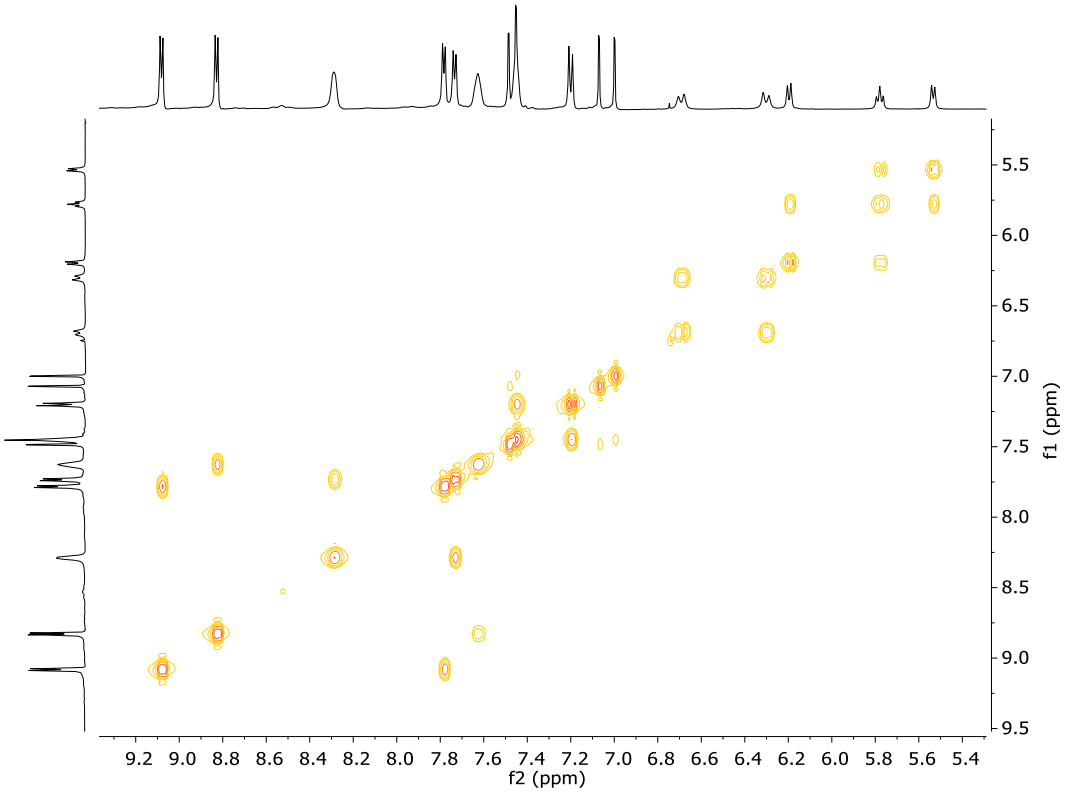

COSY (500 MHz, D_2O) partial spectra of of **R2**⊂**12**·6NO_3.

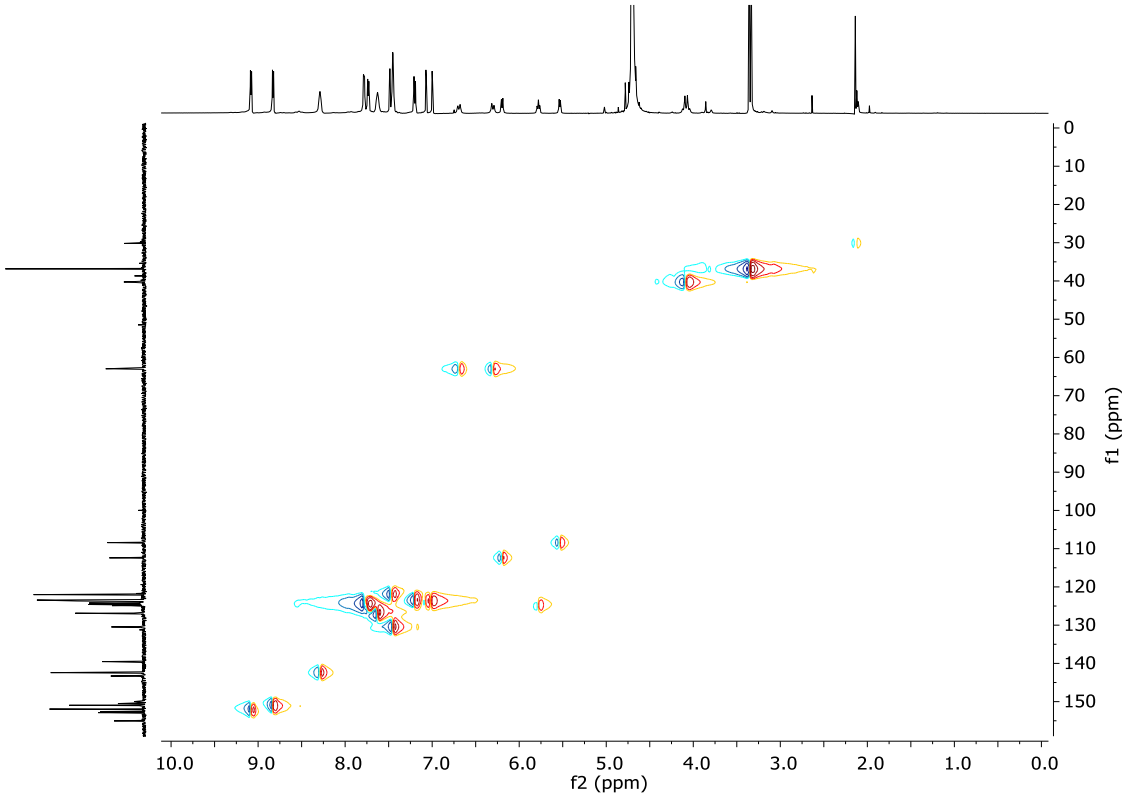

HSQC (125 and 500 MHz, D_2O) full spectra of of **R2**⊂**12**·6NO_3.

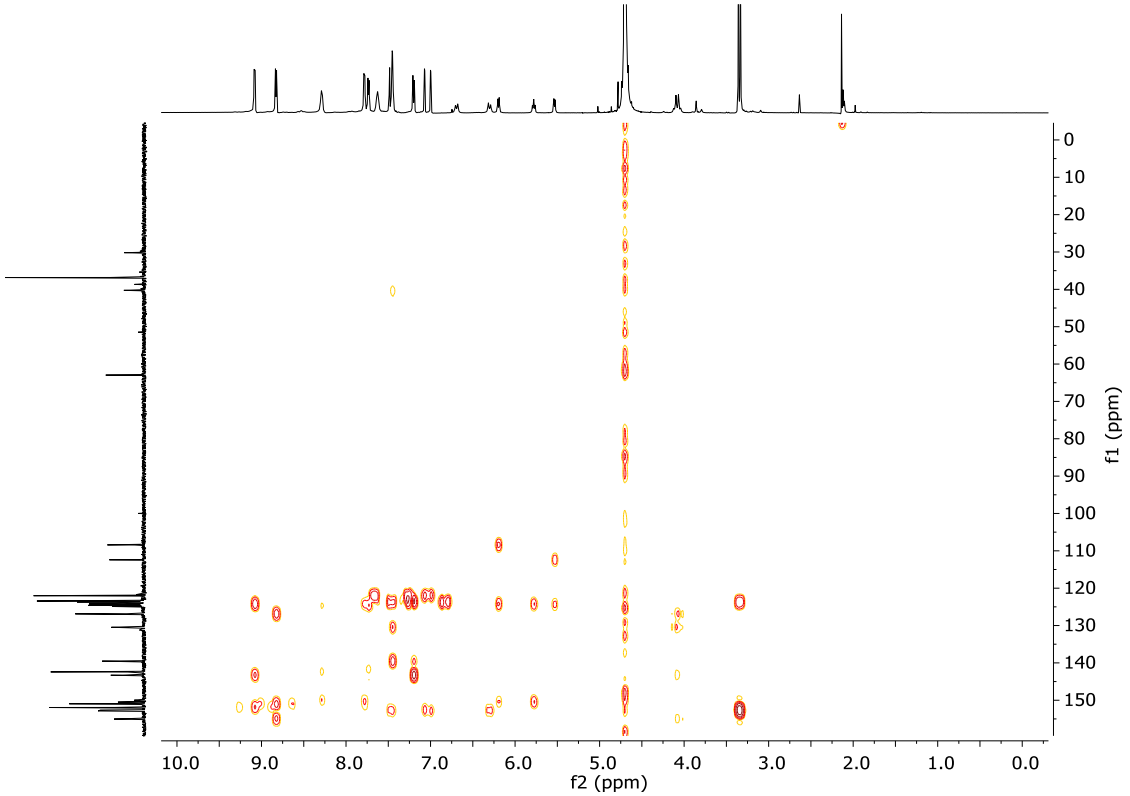

HMBC (125 and 500 MHz, D_2O) full spectra of of **R2**⊂**12**·6NO_3.

1.13. Inclusion complex **R3**⊂(**12**)$_2$8NO_3.

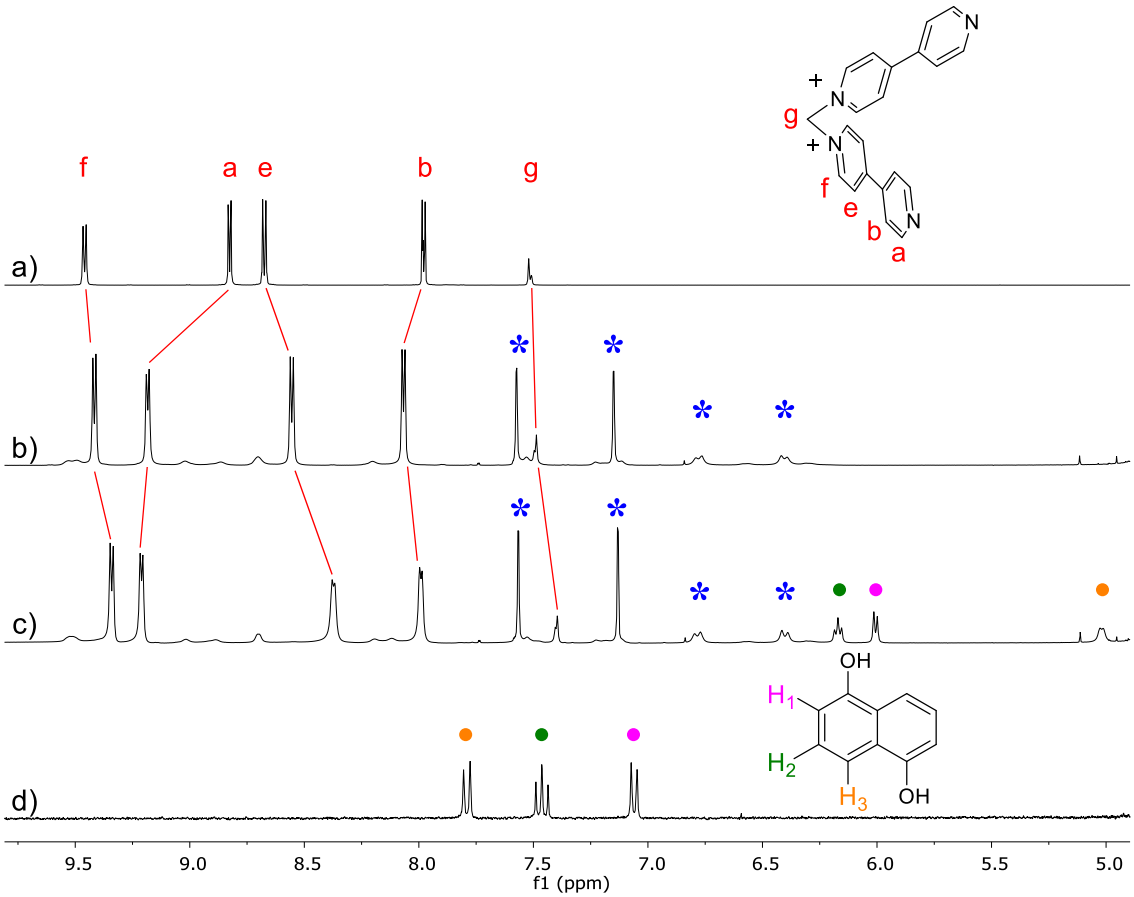

^{1}H NMR (500 MHz, D_2O) partial spectra of a) **3**, b) **R3**·8NO_3, c) **R3**⊂(**12**)$_2$·8NO_3 and d) **12**. Carbene **6(Pd)**·2NO_3 signals are indicated with blue stars.

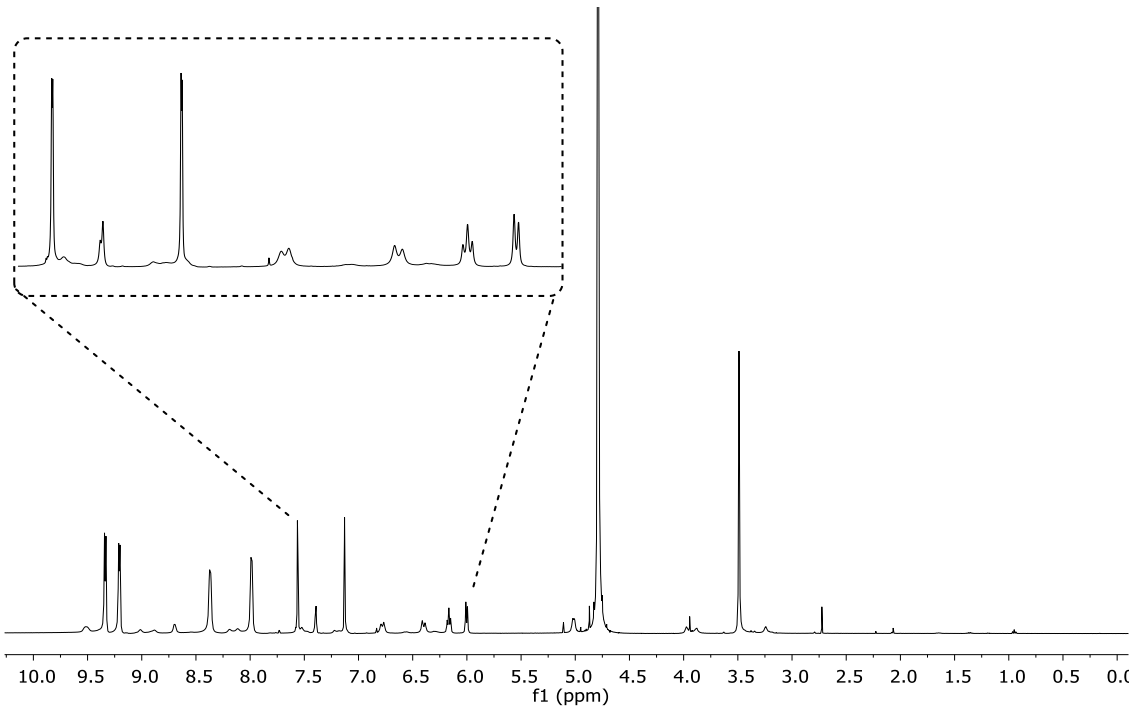

^{1}H NMR (500 MHz, D_2O) full spectra of **R3**⊂(**12**)$_2$·8NO_3.

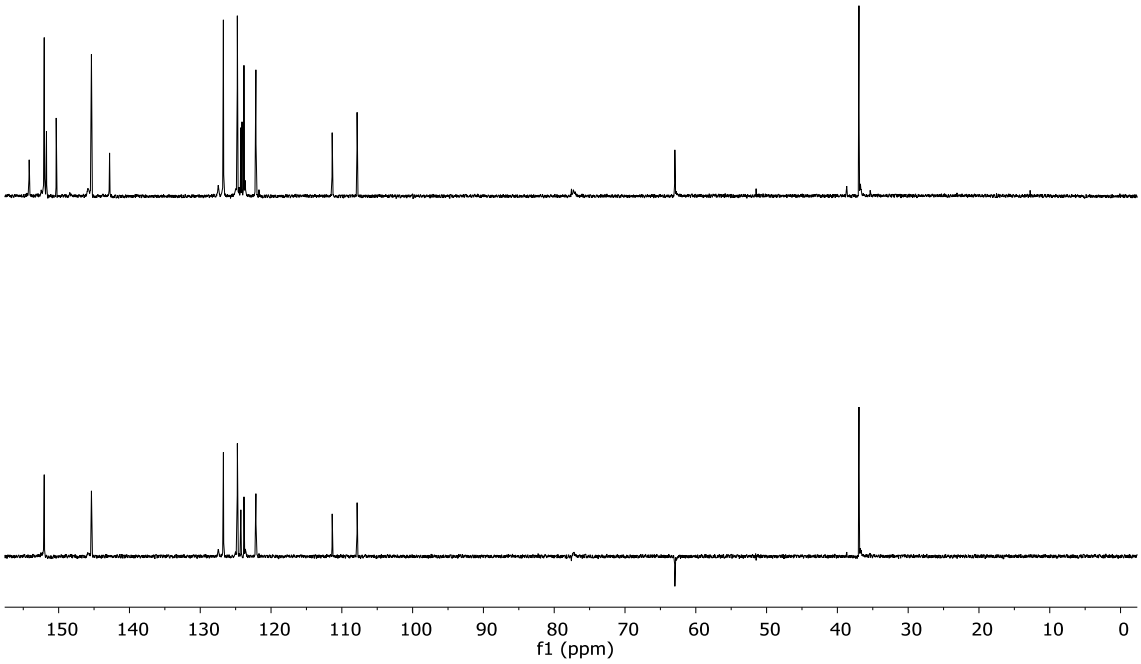

^{13}C NMR and DEPT (125 MHz, D_2O) full spectra of **R3**⊂(**12**)$_2$·8NO_3.

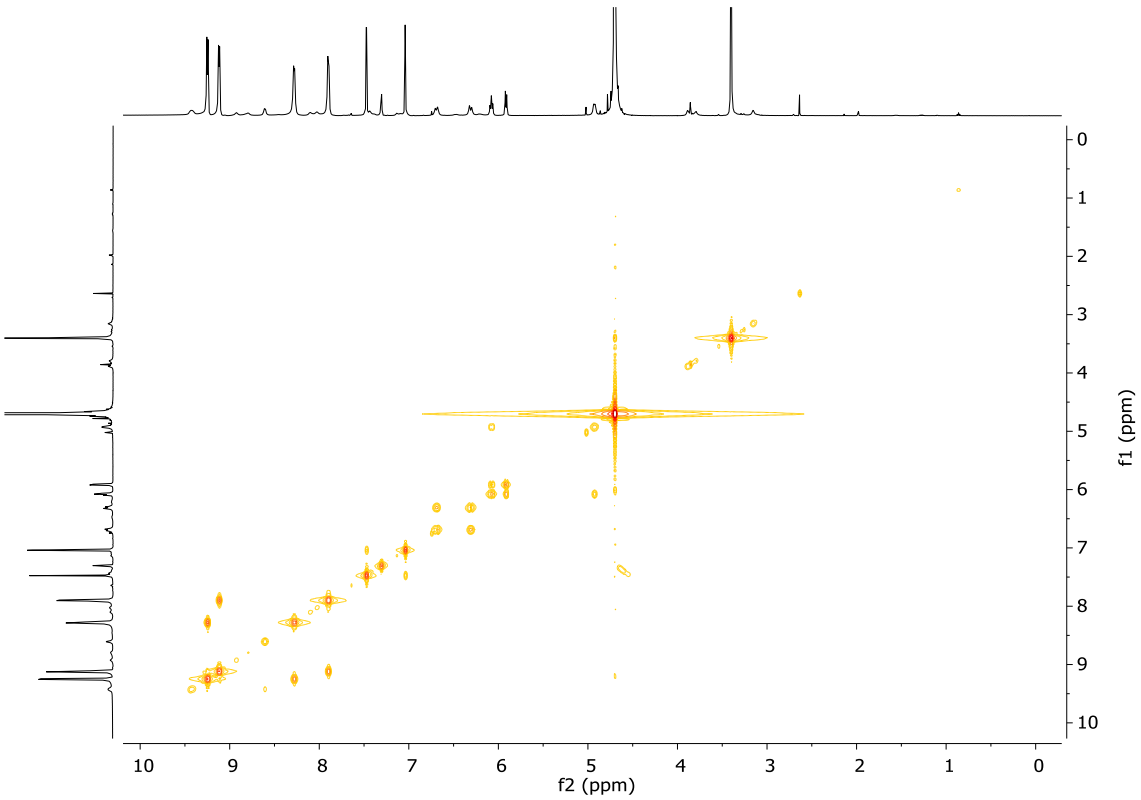

COSY (500 MHz, D_2O) full spectra of **R3**⊂(**12**)$_2$·8NO_3.

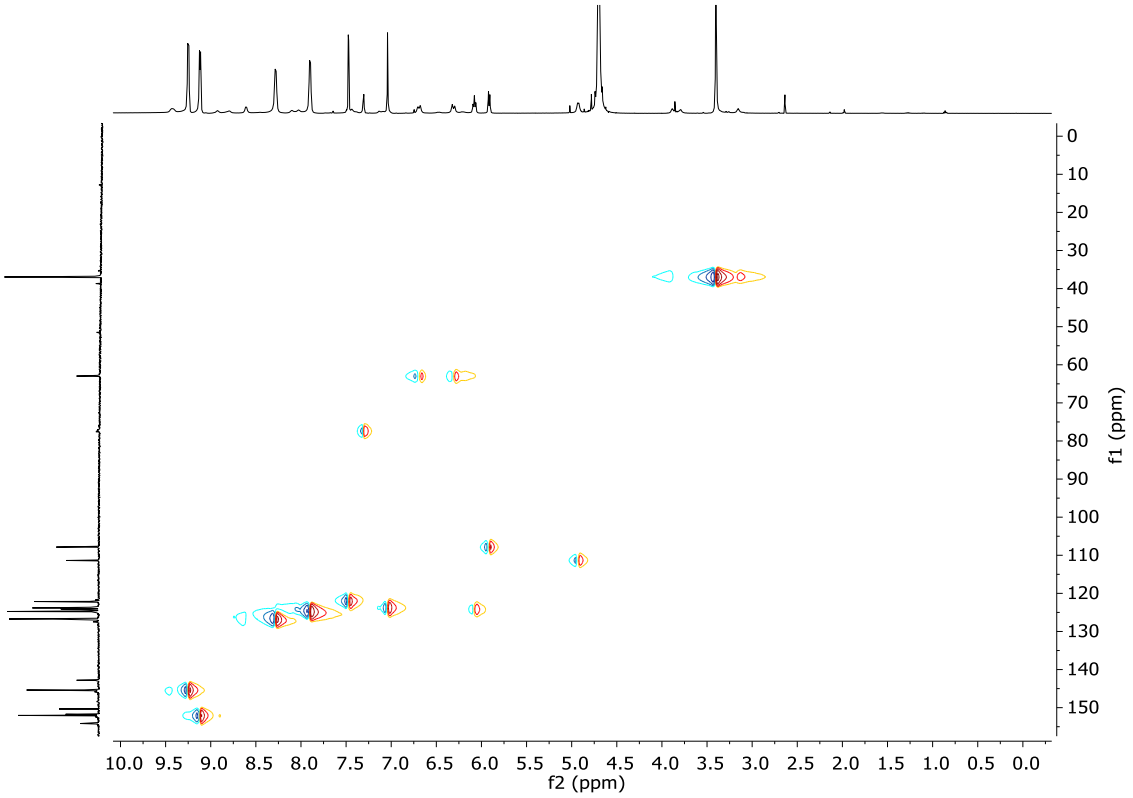

HSQC (125 and 500 MHz, D_2O) full spectra of **R3**⊂(**12**)$_2$·8NO_3.

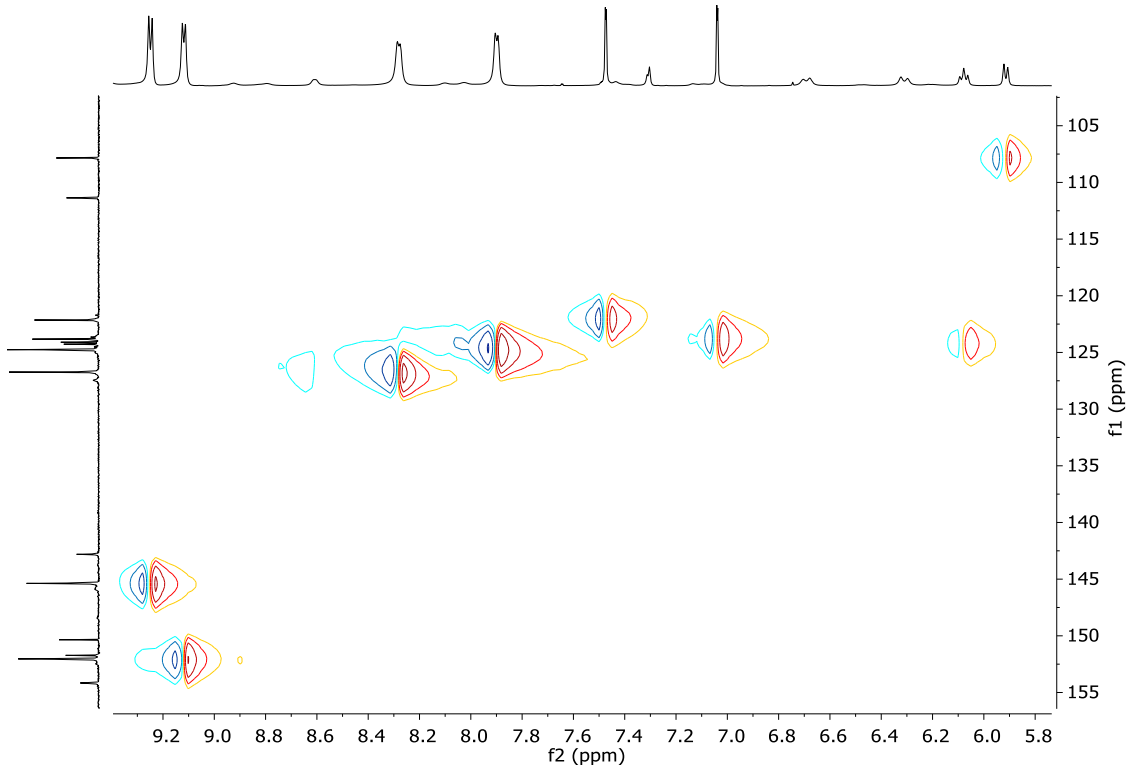

HSQC (125 and 500 MHz, D_2O) partial spectra of **R3**⊂(**12**)$_2$·8NO_3.

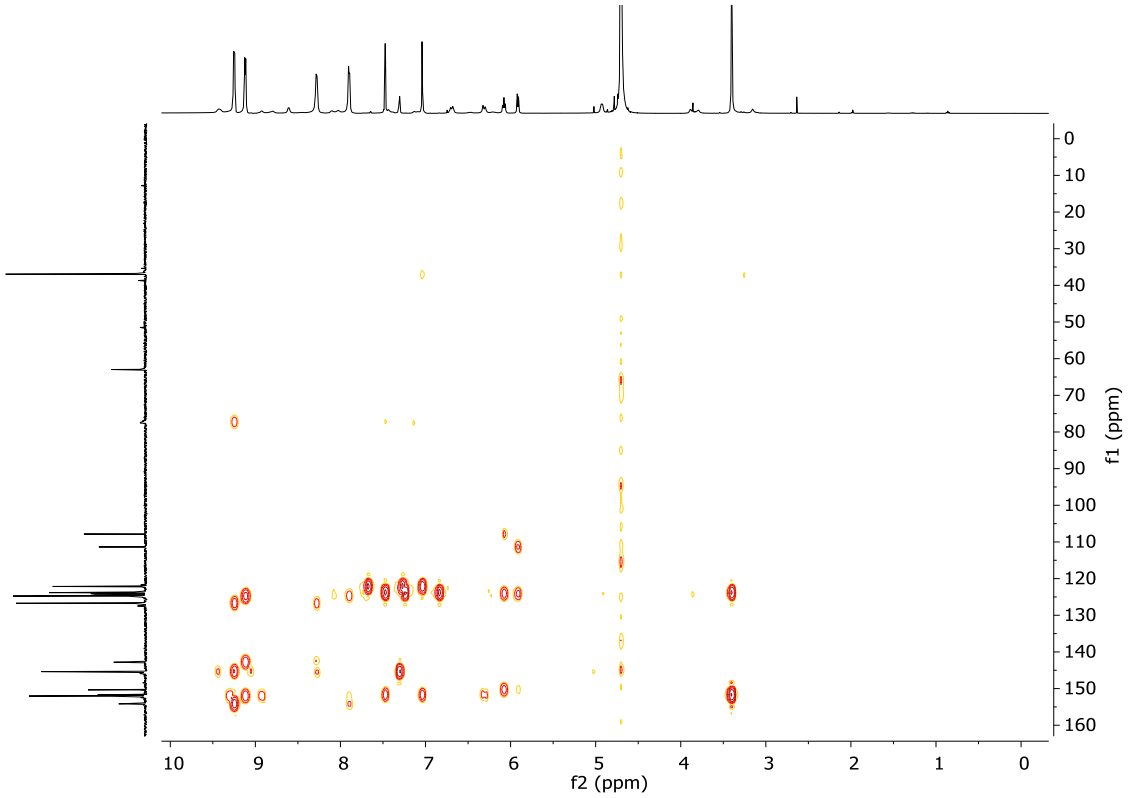

HMBC (125 and 500 MHz, D_2O) full spectra of **R3**⊂(**12**)$_2$·8NO_3.

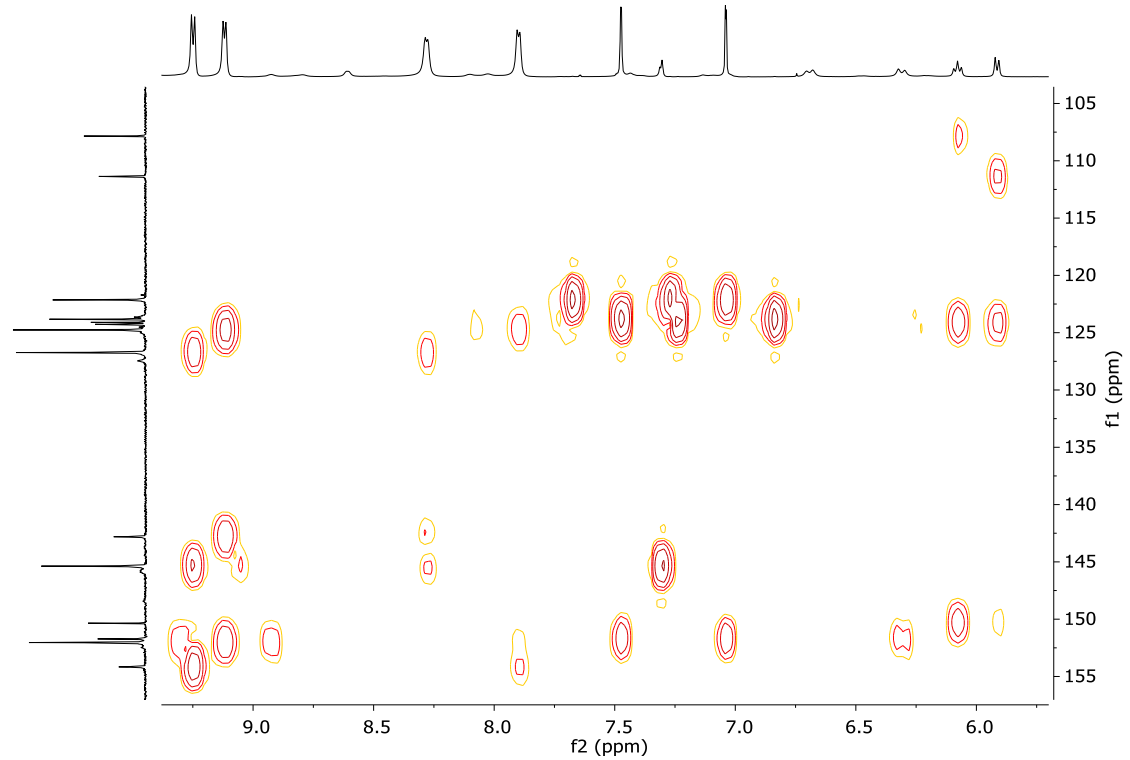

HMBC (125 and 500 MHz, D_2O) partial spectra of**R3**⊂(**12**)$_2$·8NO_3.

1.14. Inclusion complex **R5⊂12**·6NO_3.

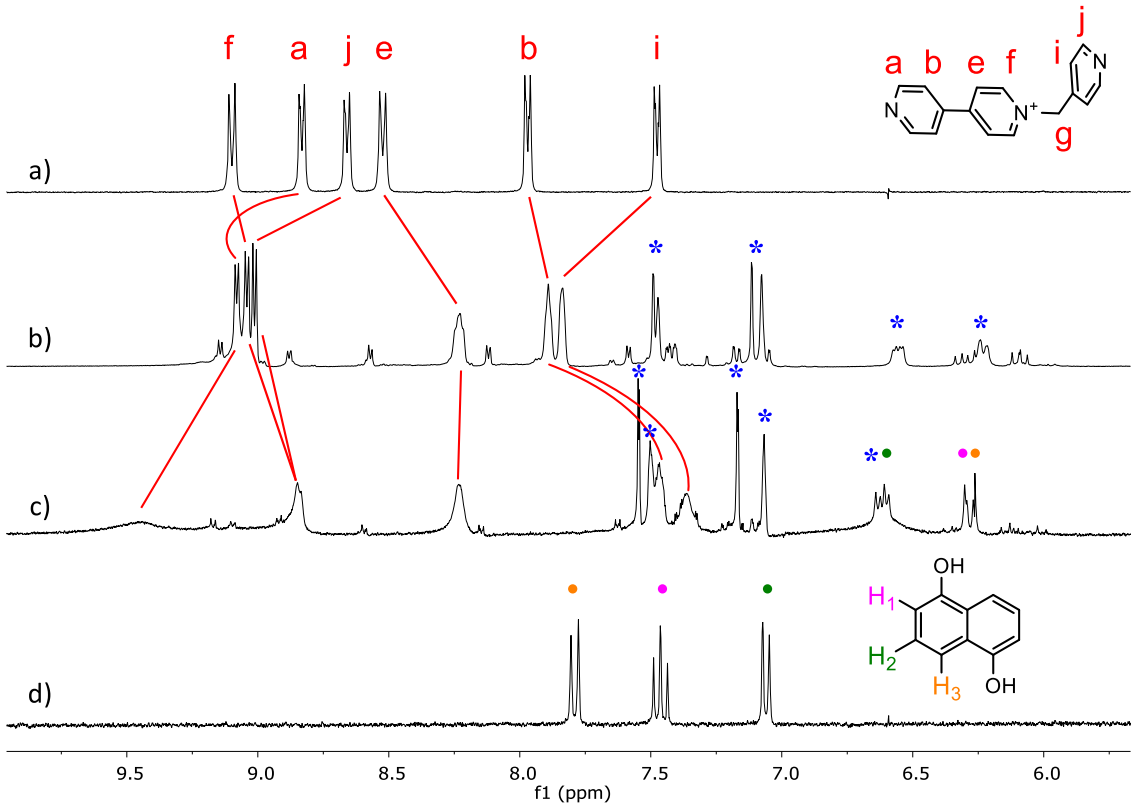

^{1}H NMR (300 MHz, D_2O) partial spectra of a) **1**, b) **R5**·6NO_3, c) **R5⊂12**·6NO_3 and d) **12**. Carbene **6(Pt)**·2NO_3 signals are indicated with blue stars.

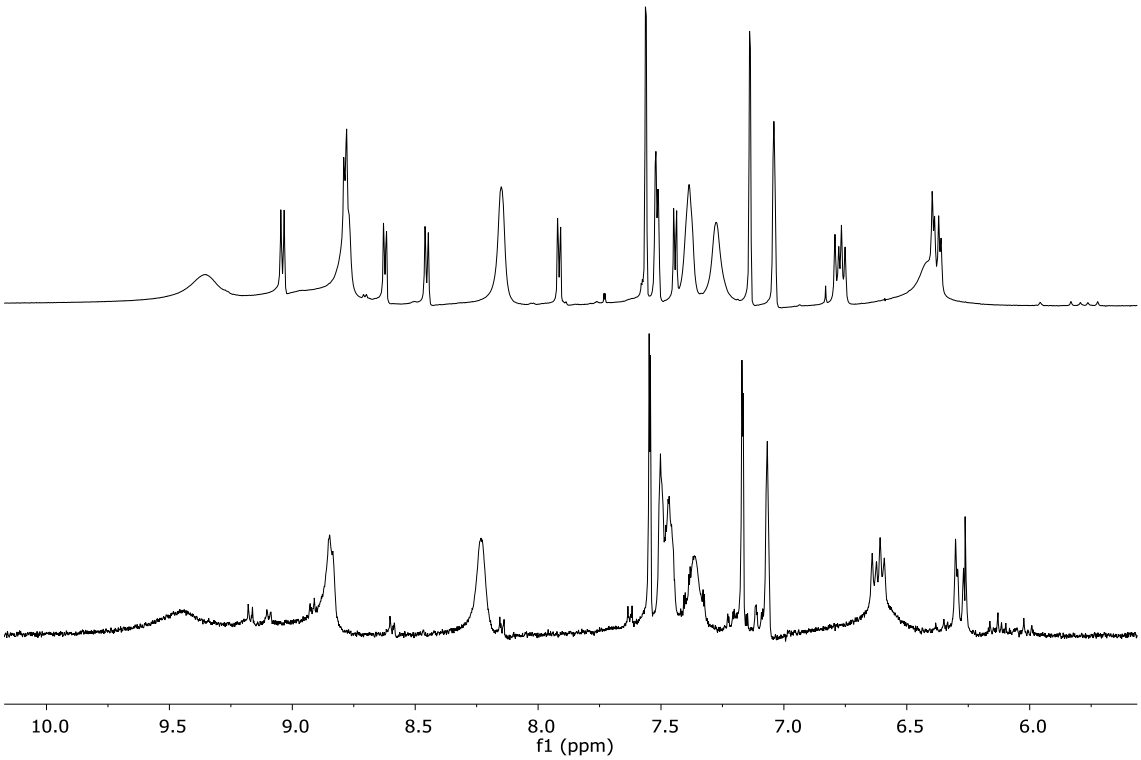

^{1}H NMR (500 MHz and 300 MHz, D_2O) partial spectra of **R1⊂12**·6NO_3 (top) and **R5⊂12**·6NO_3 (bottom).

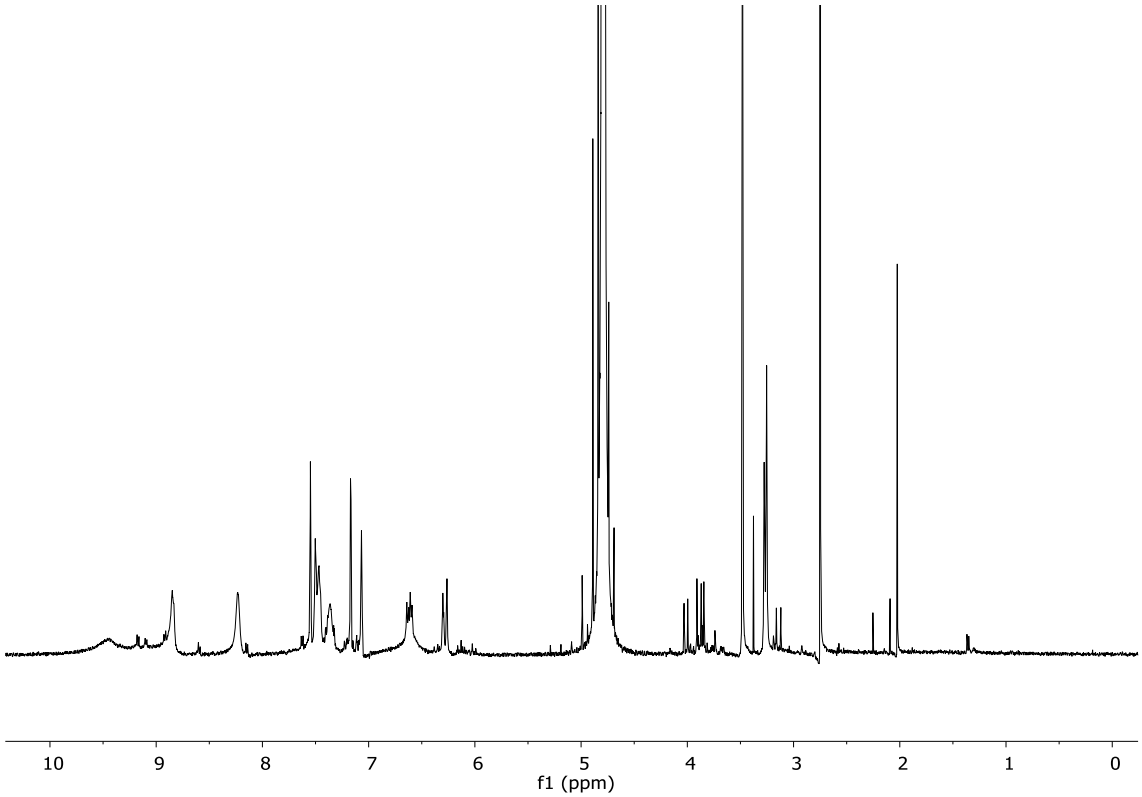

^{1}H NMR (300 MHz and 300 MHz, D_2O) full spectra of **R5**⊂**12**·6NO_3.

1.15. Inclusion complex **R6⊂12**·6NO_3.

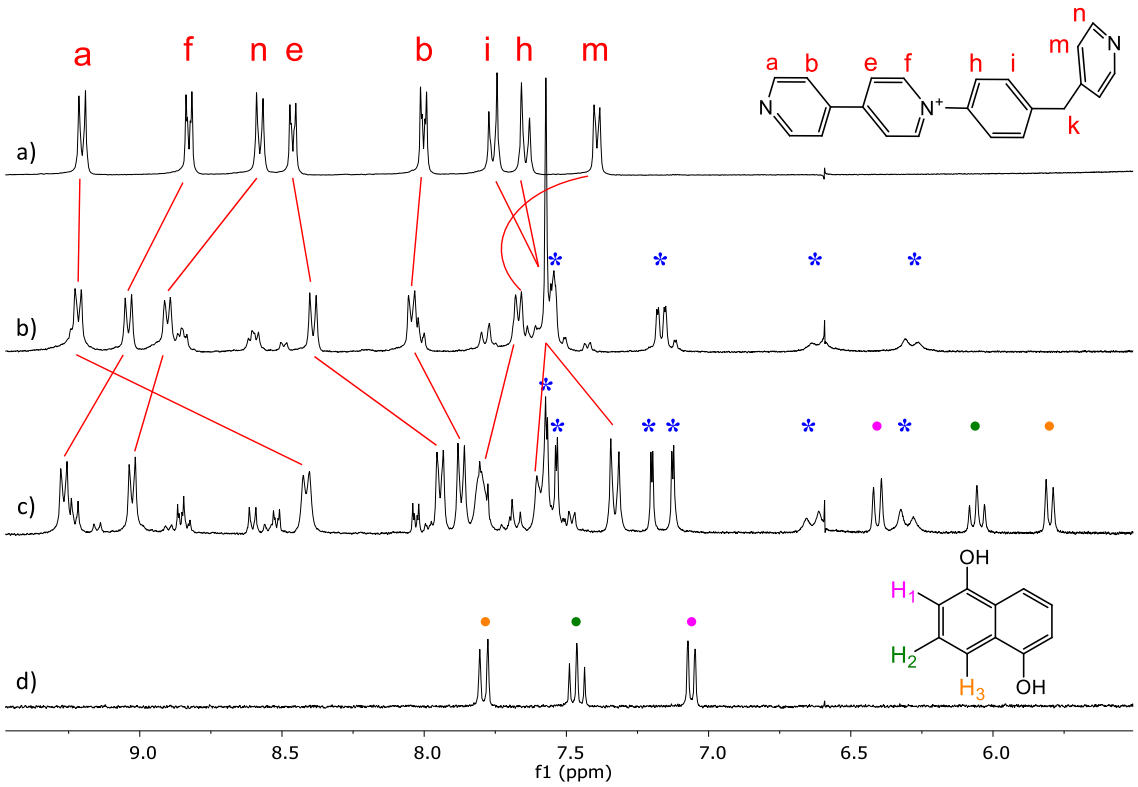

^{1}H NMR (300 MHz, D_2O) partial spectra of ligand **2** (top), **R6**·6NO_3 (middle) and **R6⊂12**·6NO_3 (bottom). Carbene **6(Pt)**·2NO_3 signals are indicated with blue stars.

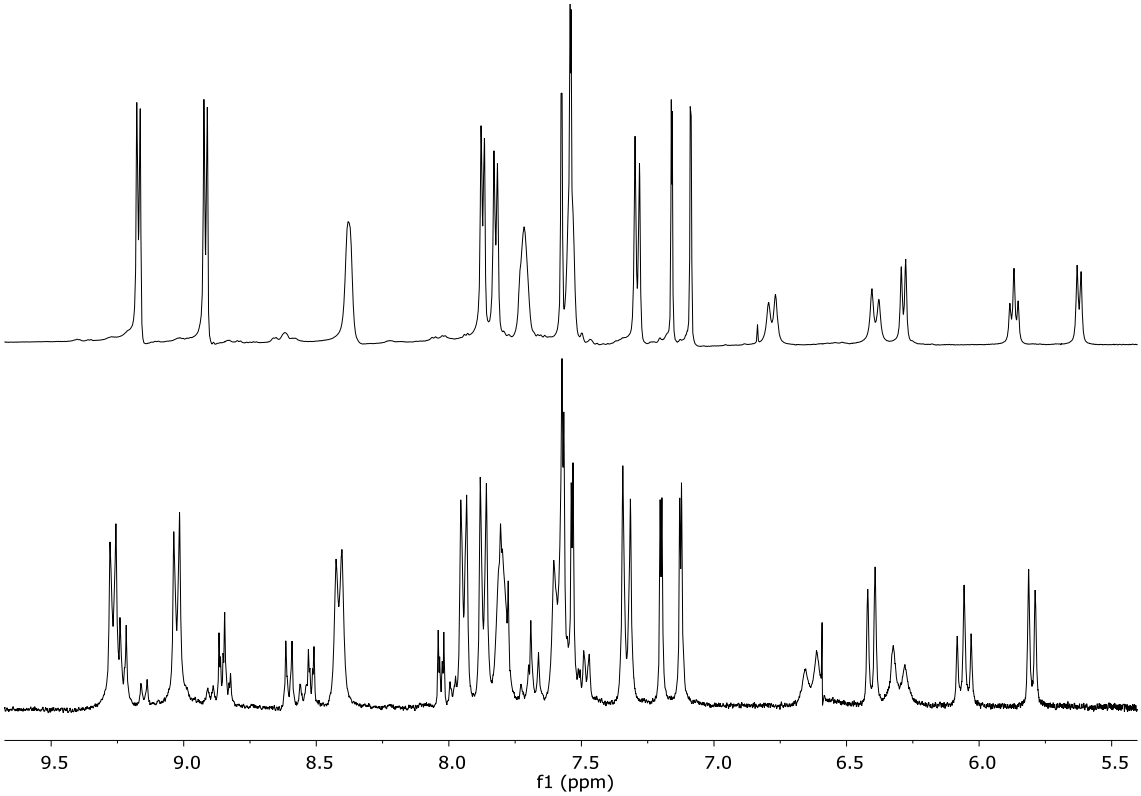

^{1}H NMR (500 and 300 MHz, D_2O) partial spectra of **R2⊂12**·6NO_3 (top) and **R6⊂12**·6NO_3 (bottom)

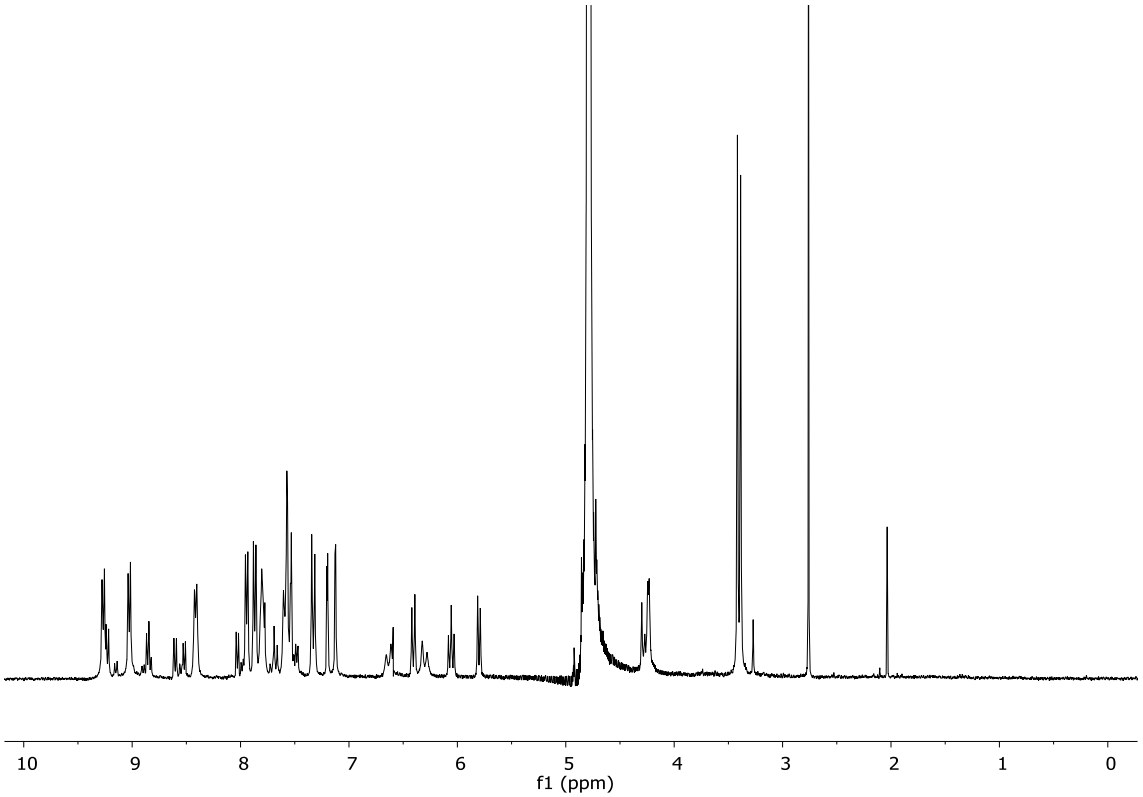

^{1}H NMR (300 MHz, D_2O) full spectra of **R6**⊂**12**·6NO_3..

1.16. Inclusion complex R7⊂(12)$_2$·8NO$_3$.

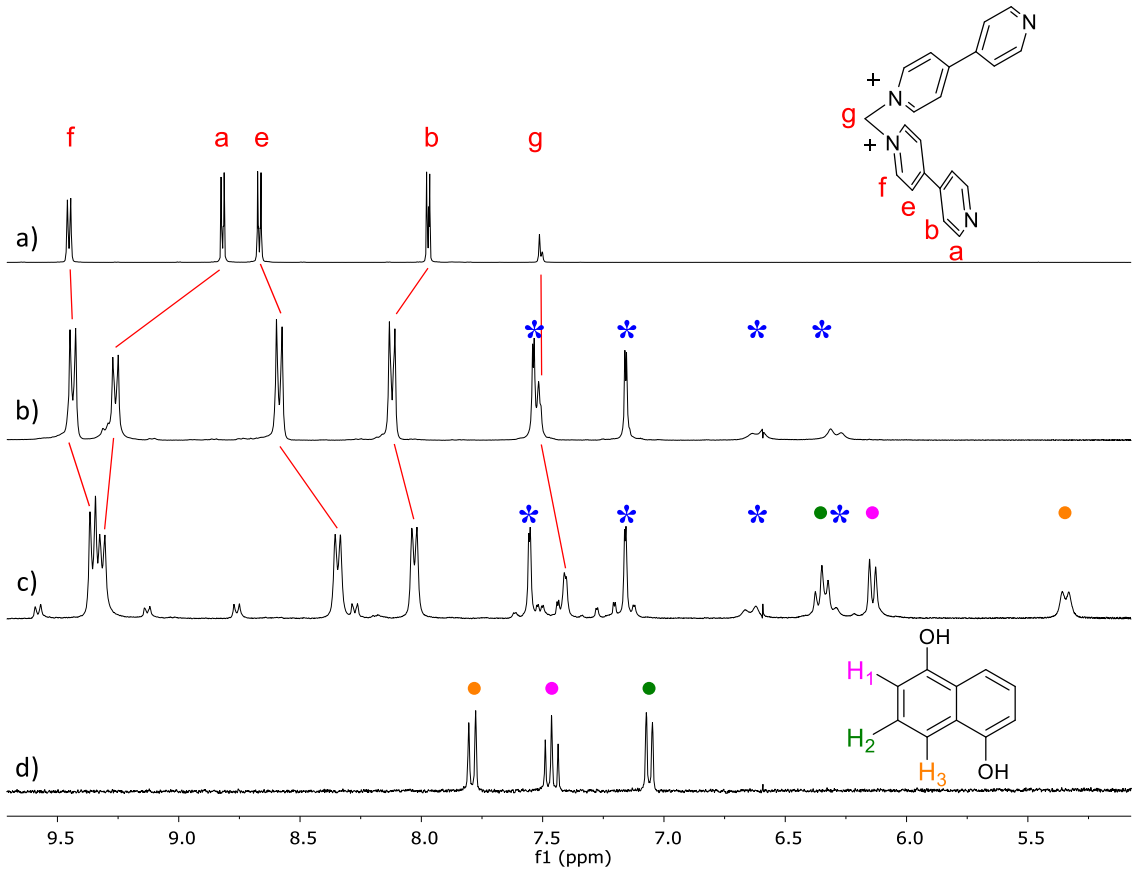

^{1}H NMR (500 MHz, D_2O) partial espectra of ligand **2** (top), **R7**·6NO$_3$ (middle) and **R7**⊂(**12**)$_2$·8NO$_3$ (bottom). Carbene **6(Pt)**·2NO$_3$ signals are indicated with blue stars.

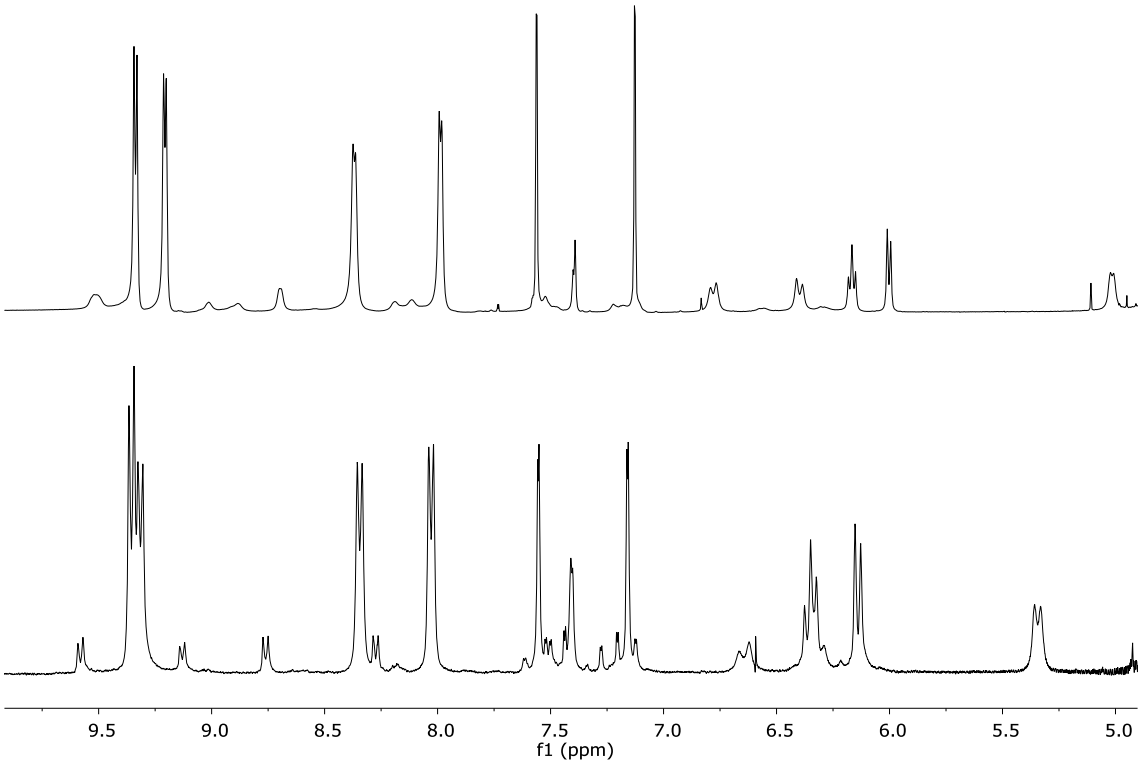

^{1}H NMR (500 and 300 MHz, D_2O) partial spectra of **R3**⊂(**12**)$_2$·8NO$_3$ (top) and **R7**⊂(**12**)$_2$·8NO$_3$ (bottom).

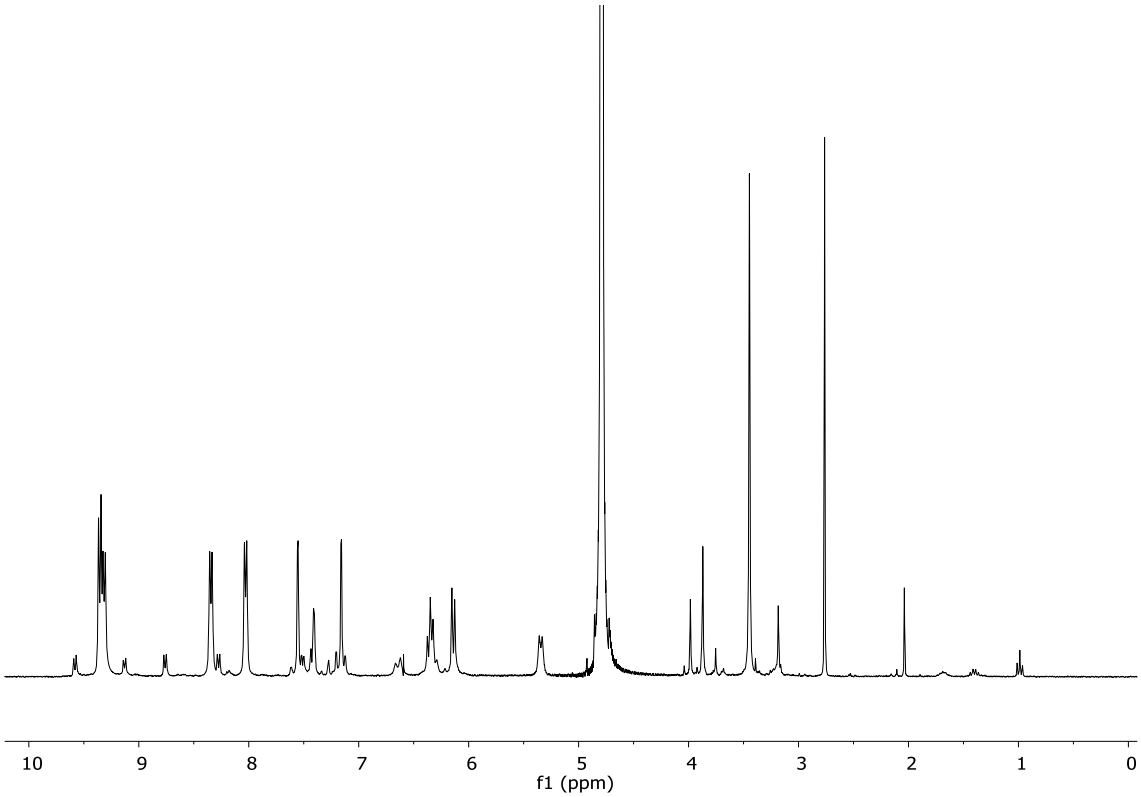

^{1}H NMR (300 MHz, D_2O) full spectra of **R7**⊂(**12**)$_2$8NO_3.

2. Mass espectra

2.1. Carbene **6(Pd)**·$2NO_3$.

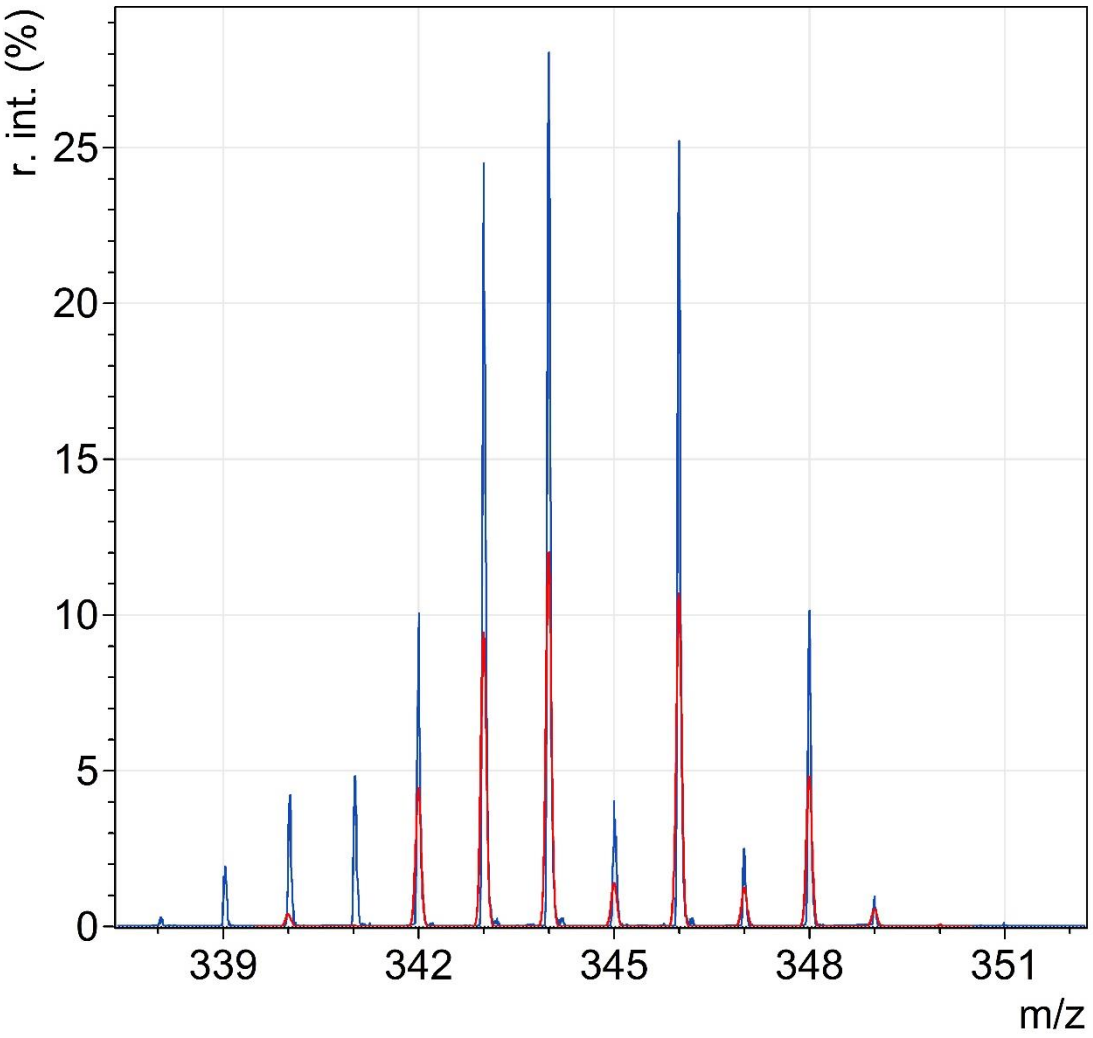

HR-MS +ESI (TOF) theorical (red) and observed (blue) for the fragment $C_9H_{12}N_5O_3Pd$ $[M\text{-}NO_3]^+$ (exp. m/z= 343.9969, theoretical m/z= 343.9969), error, -0.1 ppm.

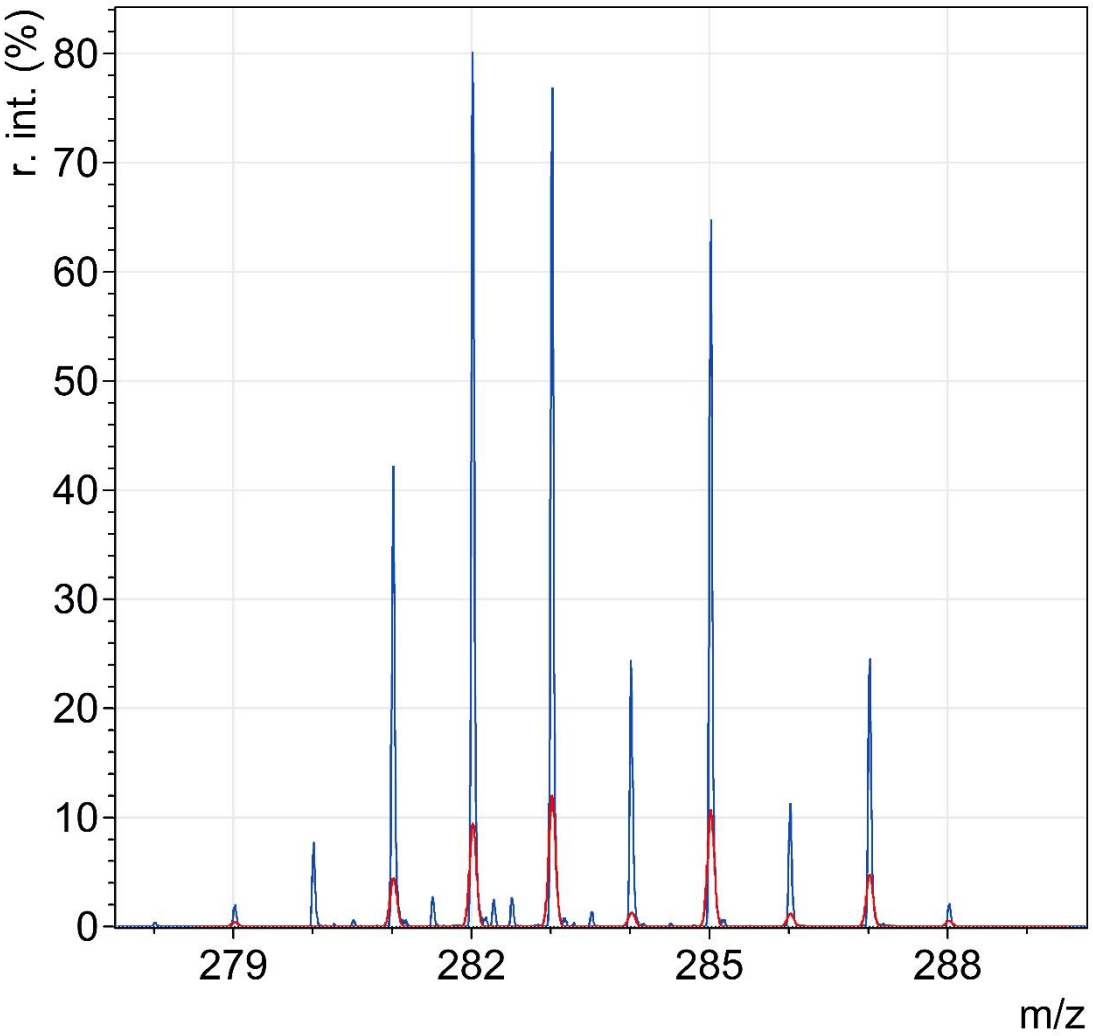

HR-MS +ESI (TOF) theorical (red) and observed (blue) for the fragment $C_9H_{13}N_4Pd$ $[MH-2NO_3]^+$ (exp. m/z= 283.0170, theoretical m/z= 283.0174), error, -1.7 ppm.

2.2. Carbene **6(Pt)**·$2NO_3$.

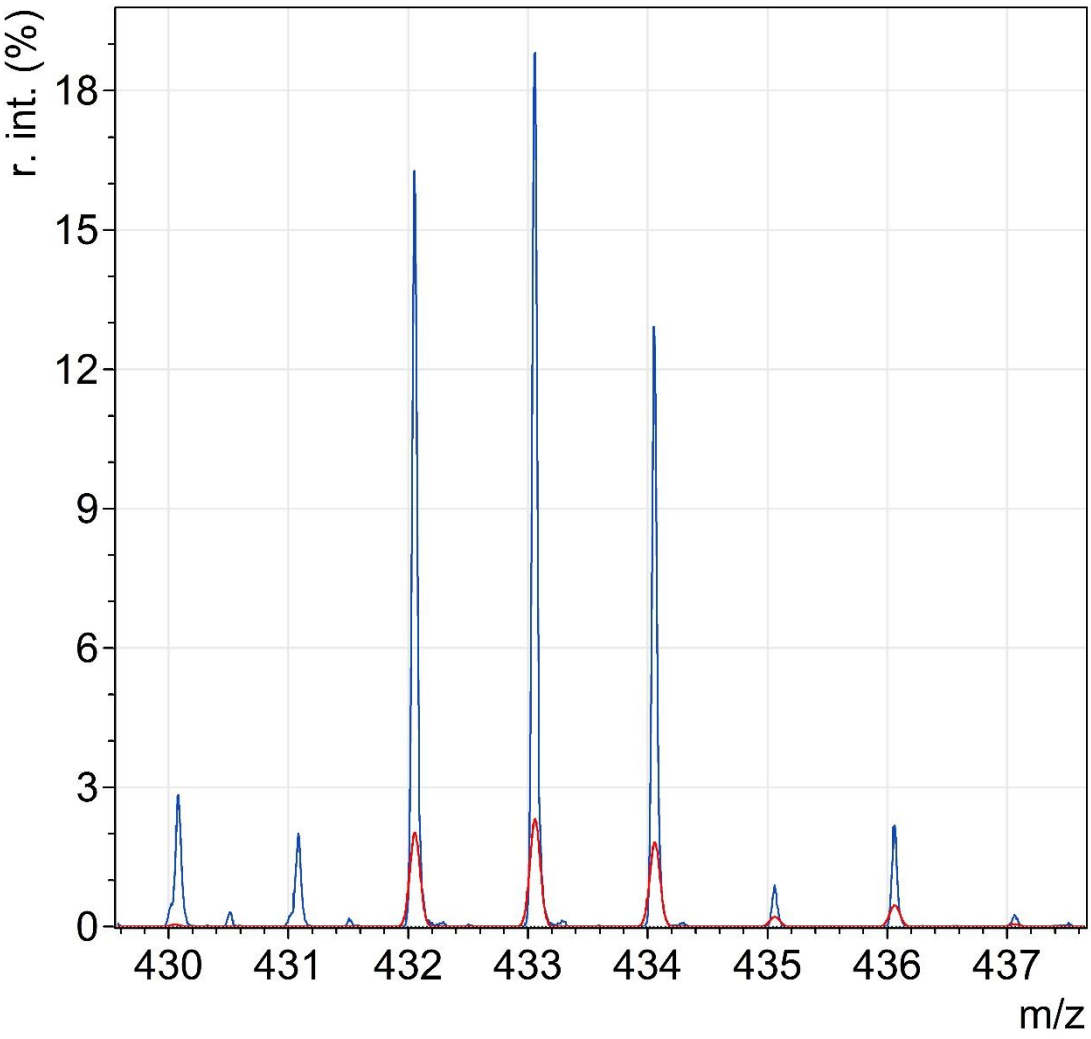

HR-MS +ESI (TOF) theorical (red) and observed (blue) for the fragment $C_9H_{12}N_5O_3Pt$ $[M\text{-}NO_3]^+$ (exp. m/z= 433.0554, theoretical m/z= 433.0582), error, 0.3 ppm.

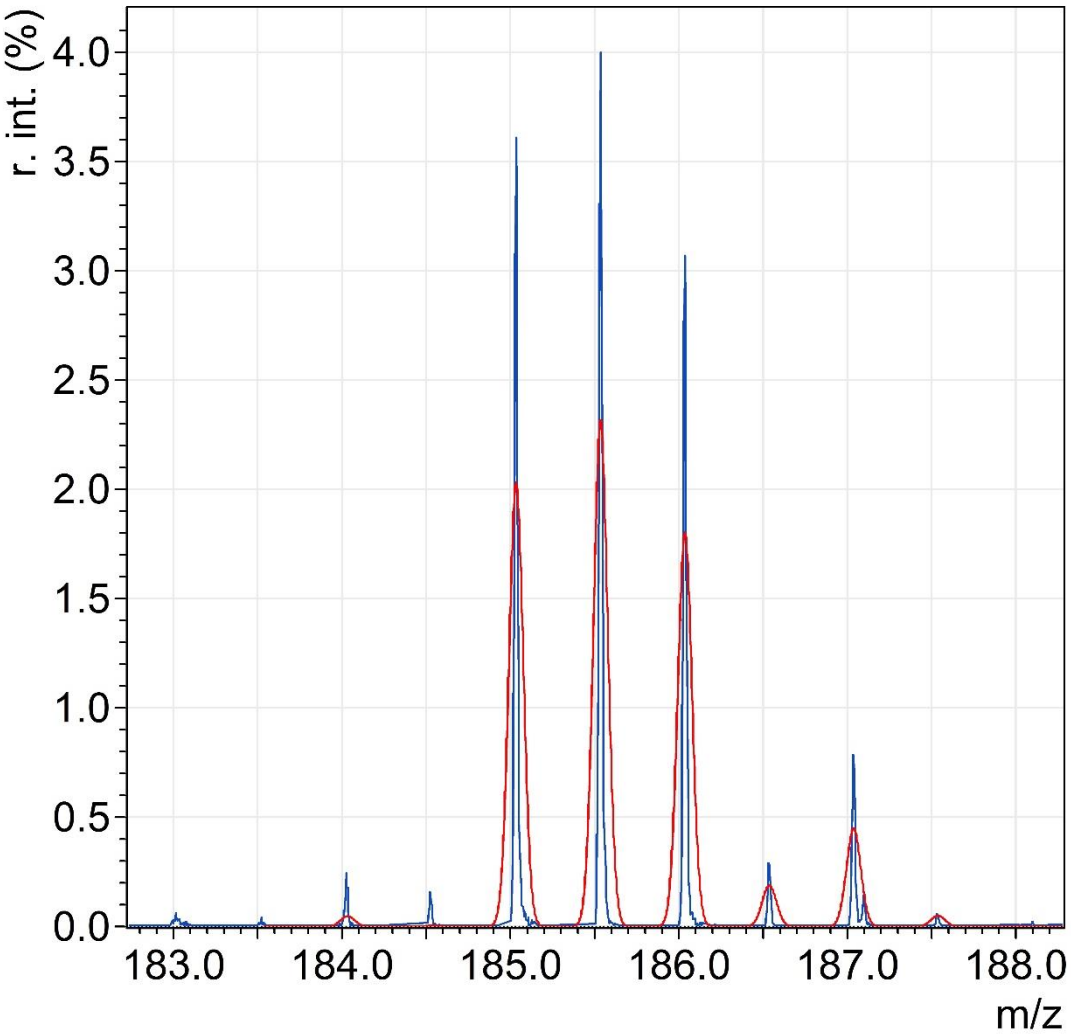

HR-MS +ESI (TOF) theorical (red) and observed (blue) for the fragment $C_9H_{12}N_4P$ $[M\text{-}2NO_3]^{+2}$ (exp. m/z= 185.5370, theoretical m/z= 185.5360); error 0.1 ppm.

3. Crystallographic data

Colorless and orange prismatic crystals of **R3**·8PF_6 and **R6**·2Br·4NO_3 (crystal size 0.148 x 0.138 x 0.090 for **R3**·8PF_6 and 0.156 x 0.115 x 0.044 mm^3 for **R6**·2Br·4NO_3) were obtained by vapor diffusion of diisopropyl ether into an acetonitrile solution of (**R3**·8PF_6) or by recrystallization from a water solution of complex (**R6**·6NO_3) containing KBr (**R6**·2Br·4NO_3) and used in X-ray analysis.

Three-dimensional, room temperature X-ray data were collected on a Bruker X8 Apex diffractometer using graphite-monochromated Mo K_α radiation. The structures were solved by direct methods and refined by full matrix least squares on F^2. Hydrogen atoms were included in calculated positions and refined in riding mode.

The fluorine atoms of the two hexafluorophosphate anions found in the asymmetric unit of complex **9** were found to be disordered over two positions and were refined with complementary occupancies.

The four hexafluorophosphate anions found in the asymmetric unit of **R3**·8PF_6 showed less than ideal geometries and, consequently, were refined with the necessary restrains. No restrain was applied to the molecular cation. A number of molecules of disordered solvent were present in the crystal, and the best approach to handling this electron density was found to be the SQUEEZE routine of PLATON.[i] The squeezed void volume was 5866.0 $Å^3$, equivalent to 27.5% of the unit cell. After the use of SQUEEZE the *R* index showed a slight improvement; (0.166 to 0.1396).

Crystals of **R6**·2Br·4NO_3 formed in clumplike aggregates. The diffraction pattern from the sample selected for data collection was indexed on the basis of two orientation matrices. The relationship between these matrices (the 'twin law') could be expressed with the matrix

$$\begin{pmatrix} -0.63154 & -0.43567 & 0.12420 \\ 0.26655 & -0.54100 & 0.50659 \\ -1.88342 & 1.29130 & 0.55699 \end{pmatrix}$$

The data set used for structure elucidation was taken from the more strongly diffracting of the two domains.

The C16, C17, C18 and C19 carbon atoms of one the phenyl rings belonging to the ligand were disordered in two positions and refined in complementary positions, with occupancies of approximately 50%. Restrictions were also applied in order to keep the ring planar.

After the final stages of refinement, a potential void of 323.1 $Å^3$ (15% of unit cell volume) was found in the unit cell. The void probably corresponds to additional nitrate counterions that could not be modelled adequately. The residuals improved slightly after the use of SQEEZE.

Refinement converged at a final *R* of 0.1396 and 0.0939 (for complexes **R3**·8PF_6 and **R6**·2Br·4NO_3, respectively; reflections with $I > 2\sigma(I)$, *F*) and wR_2 = 0.3967 and 0.2707 (for **R3**·8PF_6 and **R6**·2Br·4NO_3, respectively; unique data, F^2), with allowance for thermal anisotropy of all non-hydrogen atoms (except for the nitrate counterions of **R6**·2Br·4NO_3, that were refined isotropically). The structure solution and refinement were carried out using the program package SHELX-97.[ii]

CCDC 1518376 and 1518377 contains the supplementary crystallographic data for the complexes. These data can be obtained free of charge from The Cambridge Crystallographic Data Centre via http://www.ccdc.cam.ac.uk/data_request/cif.

[1] A. Spek, *J. Appl. Cryst*., 2003, **36**, 7-13.

[2] G. M. Sheldrick, *Acta Crystallogr*. 2008, *A64*, 112.

3.1. Metallacycle **R3**·8PF_6.

Identification code	**R3**·8PF_6
Empirical formula	$C_{66}H_{66}F_{48}N_{19}P_8Pd_2$
Formula weight	2497.93
Temperature	100(2) K
Wavelength	0.71073 Å
Crystal system	Orthorhombic
Space group	Fmmm
Unit cell dimensions	*a* = 19.316(1) Å
	b = 33.160(3) Å.
	c = 35.500(2) Å.
Volume	22738(3) $Å^3$
Z	8
Density (calculated)	1.459 Mg/m^3
Absorption coefficient	0.550 mm^{-1}
F(000)	9912
Crystal size	0.148 x 0.138 x 0.090 mm^3
Theta range for data collection	1.147 to 26.036°.
Index ranges	-22<=h<=23, -38<=k<=38, -38<=l<=40
Reflections collected	73947
Independent reflections	5423 [R(int) = 0.1276]
Completeness to theta = 25.242°	95.8 %
Max. and min. transmission	0.7825 and 0.6223
Data / restraints / parameters	5423 / 147 / 358
Goodness-of-fit on F^2	1.385
Final R indices [*I*>2sigma(*I*)]	R_1 = 0.1396, wR_2 = 0.3672
R indices (all data)	R_1 = 0.2314, wR_2 = 0.3967
Largest diff. peak and hole	0.992 and -0.762 $e.Å^{-3}$

Table 1. Crystal data and structure refinement for **R3**·8PF_6.

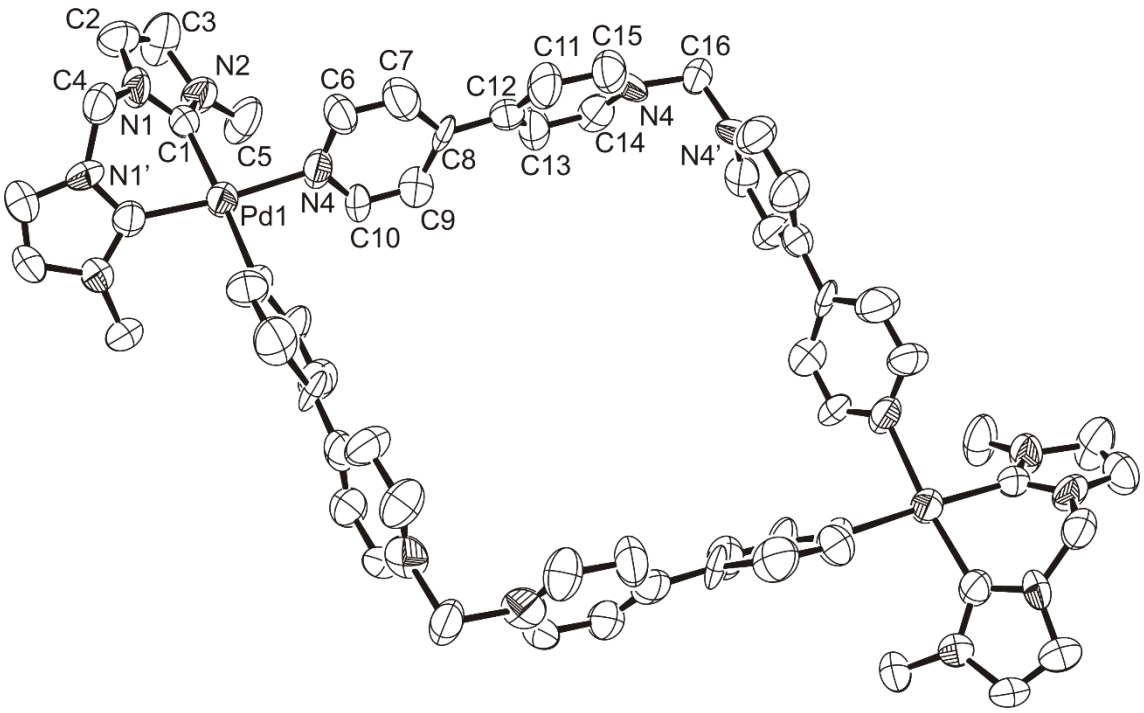

Figure 1. Structural view of **R3**·cation showing 30% thermal ellipsoids. All hydrogen atoms, PF_6^- counterions and solvent molecules were omitted for clarity**.**

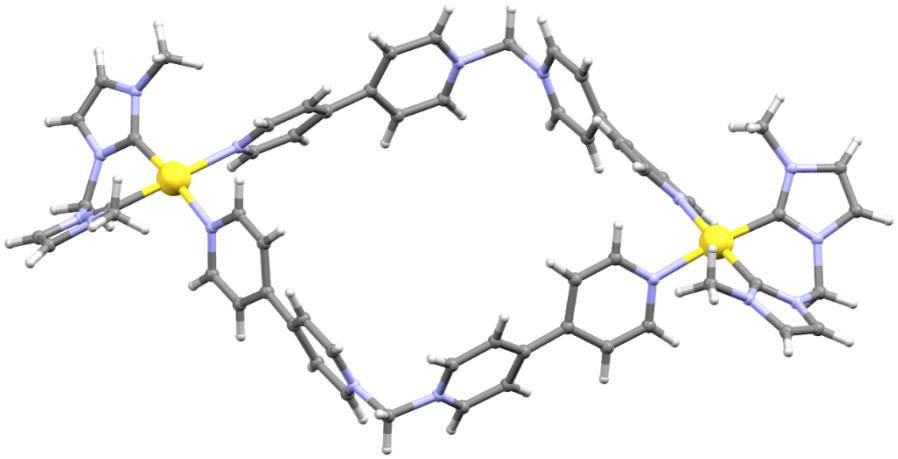

Figure 2. Ball and Stick representation of cation $\mathbf{R3}^{8+}$ within the C2/*m* crystal structure of **R3**·8PF_6. Colour code: Pd, yellow; C, dark grey; H, light grey; N, blue.

3.2. Metallacycle **R6**·2Br·4NO_3.

Identification code	**R6**·2Br·4NO_3	
Empirical formula	$C_{62}H_{56}Br_2N_{18}O_{12}Pt_2$	
Formula weight	1795.24	
Temperature	100(2) K	
Wavelength	0.71073 Å	
Crystal system	Triclinic	
Space group	P-1	
Unit cell dimensions	a = 8.963(2) Å	α= 92.670(7)°.
	b = 12.025(1) Å	β= 98.160(5)°.
	c = 21.868(2) Å	γ = 111.839(4)°.
Volume	2152.9(3) $Å^3$	
Z	1	
Density (calculated)	1.385 Mg/m^3	
Absorption coefficient	4.231 mm^{-1}	
F(000)	876	
Crystal size	0.156 x 0.115 x 0.044 mm^3	
Theta range for data collection	0.946 to 26.688°.	
Index ranges	-11<=h<=11, -15<=k<=15, 27<=l<=0	
Reflections collected	8888	
Independent reflections	8888 [R(int) = 0.1366]	
Completeness to theta = 25.242°	99.9 %	
Max. and min. transmission	0.7453 and 0.6027	
Data / restraints / parameters	8888 / 150 / 450	
Goodness-of-fit on F^2	0.995	
Final R indices [I>2sigma(I)]	R_1 = 0.0939, wR_2 = 0.2516	
R indices (all data)	R_1 = 0.1288, wR_2 = 0.2707	
Largest diff. peak and hole	2.705 and -2.552 e.$Å^{-3}$	

Table 2. Crystal data and structure refinement for **R6**·2Br·**4**NO_3.

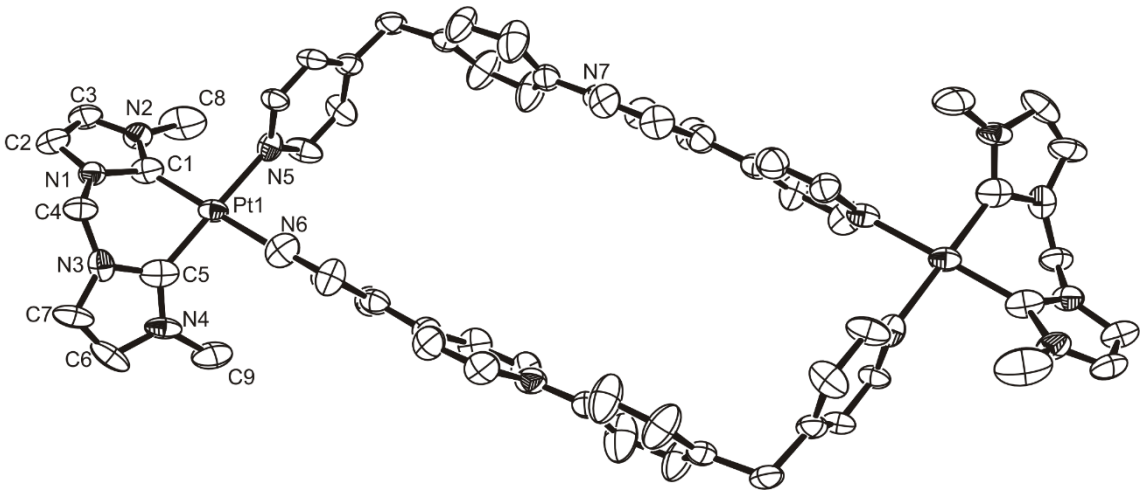

Figure 3. Structural view of **R6**·cation showing 30% thermal ellipsoids. All hydrogen atoms and NO_3^- counterions were omitted for clarity.

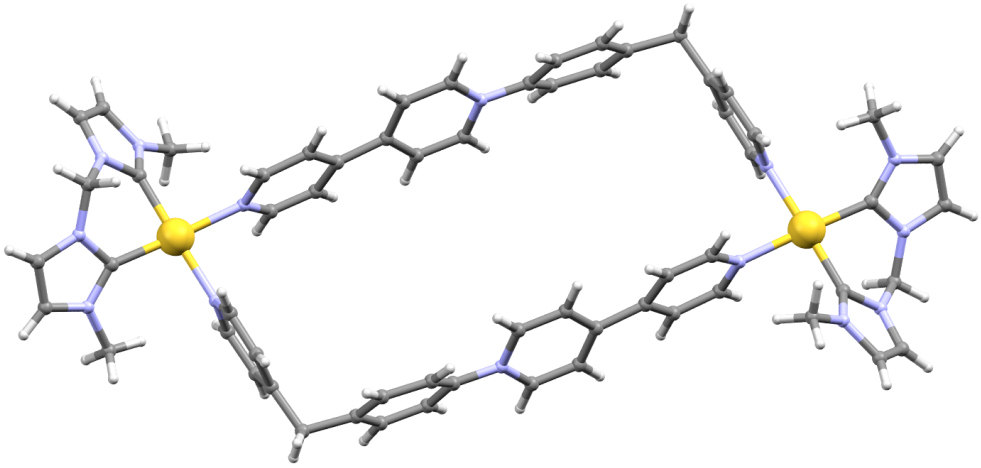

Figure 4. Ball and Stick representation of cation **R6**$^{6+}$ within the P-1 crystal structure. Colour code: Pt, yellow; C, dark grey; H, light grey; N, blue.

4. Job Plot experiments

4.1 Inclusion complex R5⊂12·6NO3.

The stoichiometry of the inclusion complex between **R5** and **12** was determined by the continuous variation (Job's Plot) method. In the figure, the plot shows maximum value at χ=0.5, corroborating the existence of a complex with 1:1 stoichiometry.

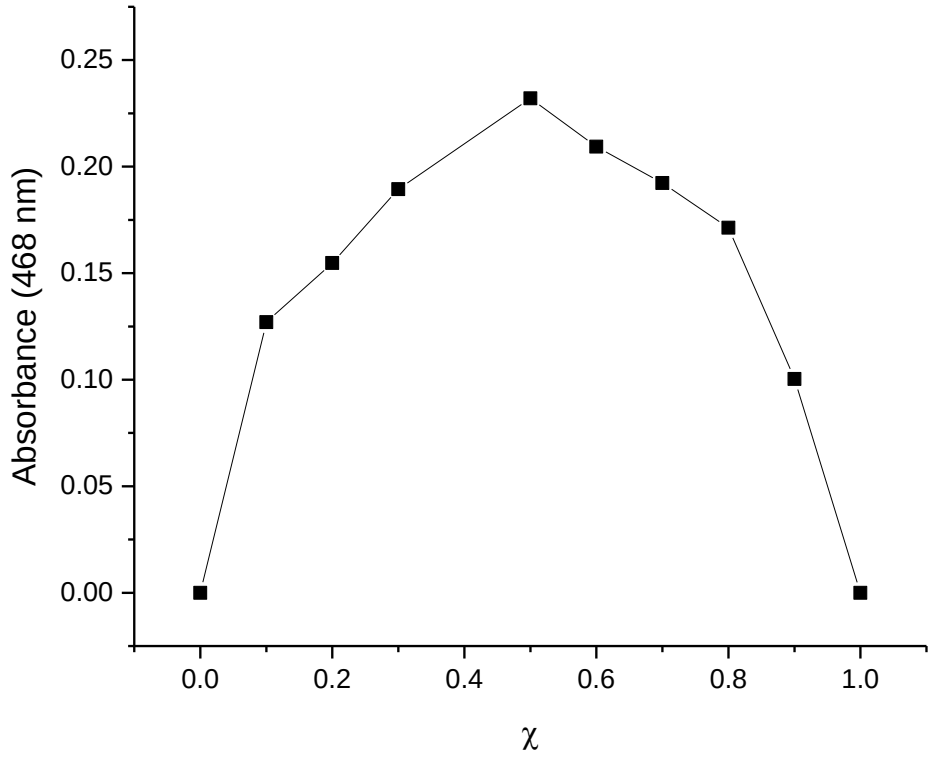

Job's Plot diagram (λ=468 nm) showing the 1:1 stoichiometry of **R5⊂(12)$_2$·**6NO_3.

4.2 Inclusion complex **R6⊂(12)$_2$**·6NO3.

The stoichiometry for the inclusion complex between **R6** and **12** was determined by the Job's Plot method. In the figure, the plot shows maximum value at χ = 0.5, signifying the existence of a complex with 1:1 stoichiometry.

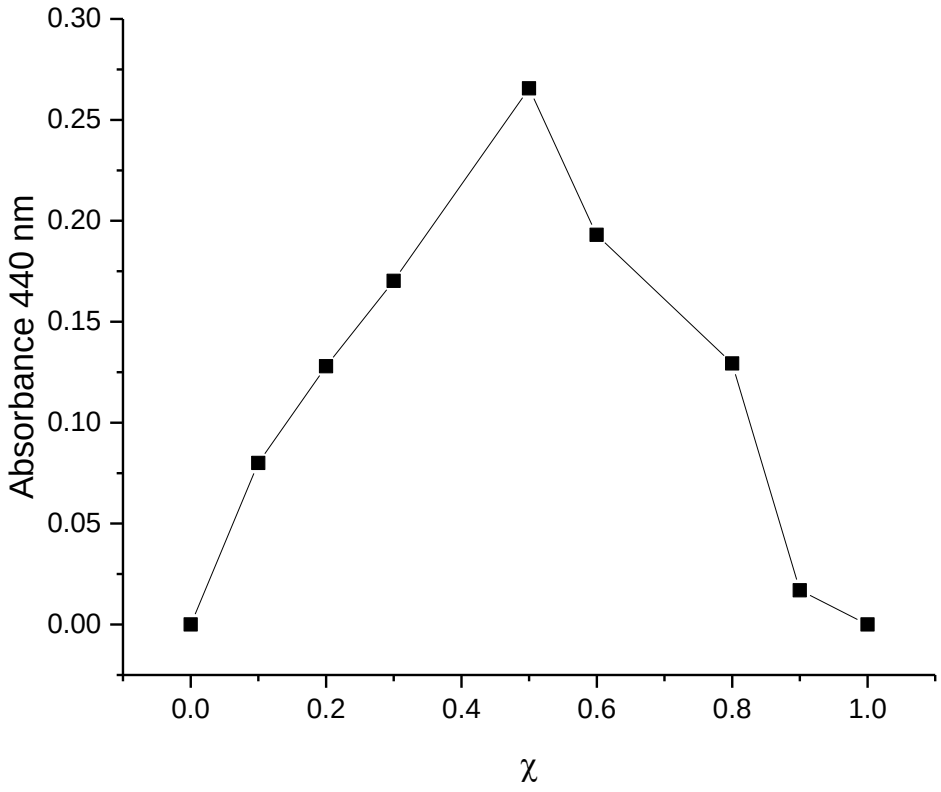

Job's Plot diagram (λ=440 nm) showing the 1:1 stoichiometry of **R6⊂12**·6NO_3

4.3 Inclusion complex R7⊂12·8NO3.

The Job Plot's diagram for the inclusion complex between **R7** and **12** shows a maximum value at χ = 0.3, corroborating the existence of a complex with 1:2 stoichiometry.

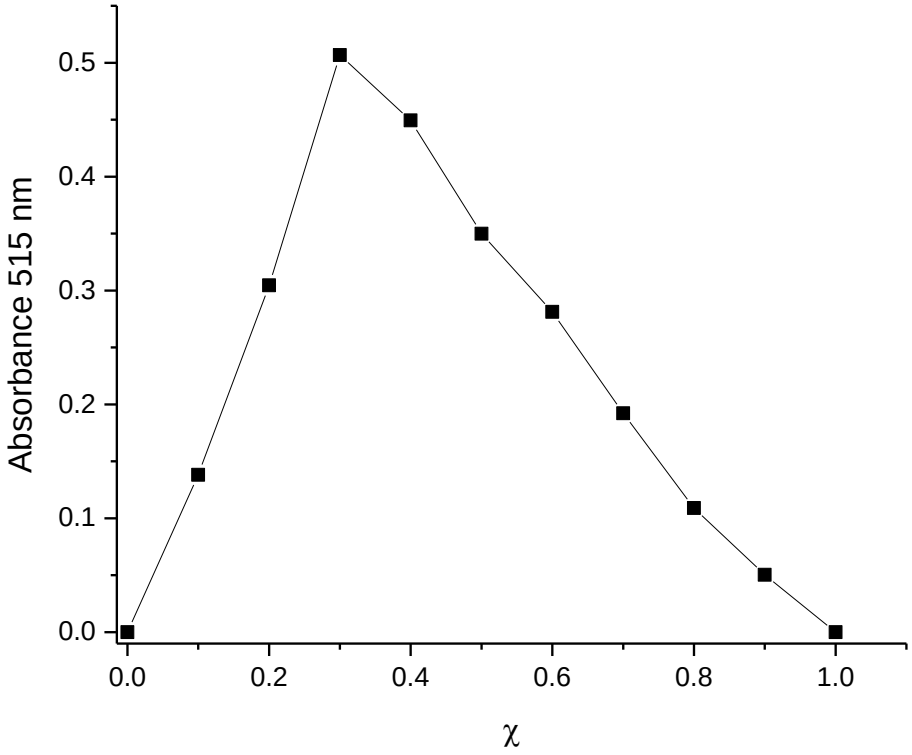

Job's Plot diagram (λ=515 nm) showing the 1:2 stoichiometry of **R7⊂(12)$_2$·**8NO_3.

5. Determination of binding constant (ka) using the UV/Vis dilution method

Typically, a 1 mM solution of guest (**12**) in water, and a solution of guest (1mM) and host (**R5**·6NO_3, **R6**·6NO_3 and **R7**·8NO_3, 7.5 mM) in water, were separately prepared. Aliquots of the host/guest solution (10µL initially, then 20, 50, 100, and finally 200 µL) were added to the guest solution (2 mL).Then, the corresponding UV-vis spectra were recorded after each addition. The titration curves were well fitted to 1:1 or 1:2 models by using the Nelder-Mead method implemented on the *bindfit* webapp (www.supramolecular.org) provided by Pall Thordarson *et al.* The absorbances at five different wavelengths centered on the host-guest complex charge-transfer band were plotted against the concentration of the corresponding host and then fitted. For **R5**·6NO_3 and **R6**·6NO_3, the curves were well fitted to a 1:1 binding isotherm and, conversely, to a 2:1 binding isotherm for **R7**·8NO_3.

5.1. Inclusion complex R5⊂12·6NO3.

T= 298 K, λ= 458, 463, 468, 473, 478 nm

Ka= 238,27 ± 1.24 M^{-1}

K error= ± 0,52 % M^{-1}

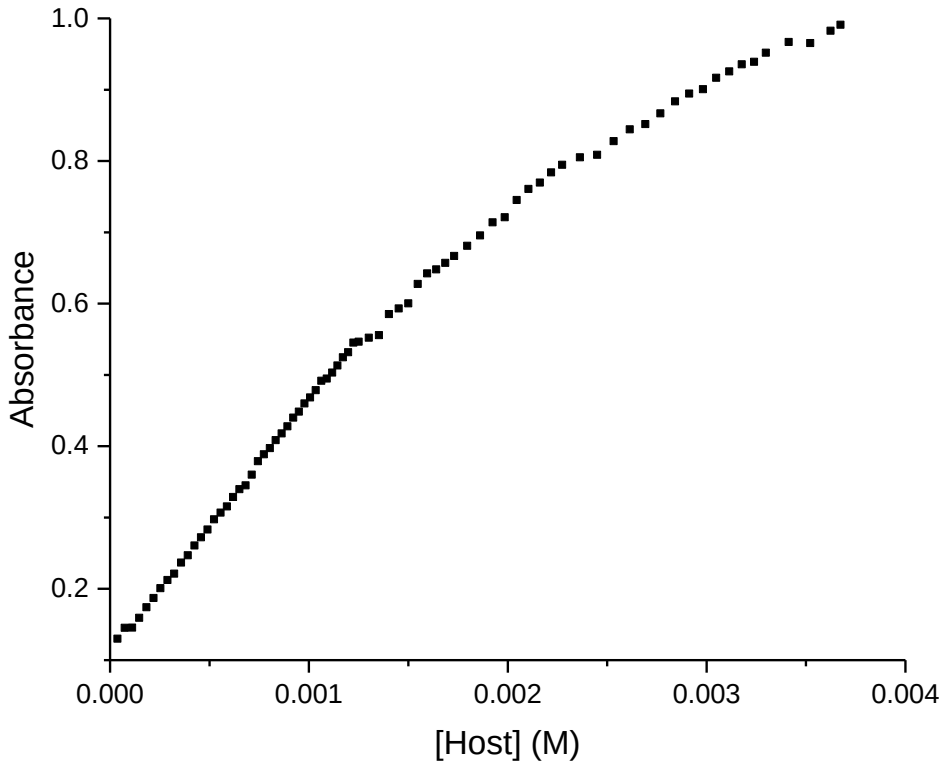

Representation of the titration of the complex **R5⊂12**·6NO_3

V added (10^{-6} L)	[Host] (10^{-3} M)	Absorbance (458 nm)	Absorbance (463 nm)	Absorbance (468 nm)	Absorbance (473 nm)	Absorbance (478 nm)
10	0.037	0.137	0.133	0.130	0.126	0.123
20	0.074	0.152	0.149	0.145	0.142	0.138
30	0.111	0.152	0.149	0.146	0.142	0.139
40	0.147	0.166	0.163	0.159	0.156	0.152
50	0.183	0.180	0.177	0.174	0.170	0.166
60	0.218	0.194	0.191	0.187	0.184	0.179
70	0.254	0.207	0.204	0.201	0.197	0.193
80	0.288	0.220	0.216	0.212	0.209	0.204
90	0.323	0.228	0.225	0.221	0.218	0.213
100	0.357	0.243	0.240	0.237	0.233	0.228
110	0.391	0.253	0.251	0.247	0.243	0.238
120	0.425	0.268	0.265	0.261	0.257	0.252
130	0.458	0.279	0.276	0.272	0.268	0.263
140	0.491	0.290	0.287	0.283	0.279	0.274
150	0.523	0.305	0.301	0.297	0.293	0.287
160	0.556	0.314	0.311	0.307	0.303	0.298
170	0.588	0.323	0.319	0.315	0.311	0.305
180	0.619	0.335	0.332	0.329	0.325	0.319
190	0.651	0.347	0.344	0.340	0.335	0.329
200	0.682	0.353	0.350	0.345	0.340	0.335
210	0.713	0.368	0.364	0.360	0.355	0.349
220	0.743	0.386	0.383	0.379	0.374	0.368
230	0.774	0.396	0.393	0.389	0.383	0.377
240	0.804	0.406	0.402	0.397	0.392	0.385
250	0.833	0.416	0.413	0.408	0.403	0.397
260	0.863	0.426	0.423	0.418	0.413	0.406
270	0.892	0.436	0.433	0.428	0.422	0.416
280	0.921	0.448	0.445	0.440	0.434	0.427
290	0.950	0.455	0.453	0.448	0.443	0.437
300	0.978	0.467	0.464	0.460	0.454	0.447
310	1.006	0.476	0.473	0.468	0.463	0.456
320	1.034	0.485	0.483	0.479	0.473	0.466
330	1.062	0.497	0.495	0.492	0.487	0.480
340	1.090	0.501	0.499	0.495	0.490	0.483
350	1.117	0.511	0.508	0.503	0.497	0.490
360	1.144	0.521	0.518	0.513	0.506	0.498
370	1.171	0.531	0.529	0.525	0.519	0.512
380	1.197	0.538	0.536	0.532	0.526	0.519
390	1.224	0.551	0.549	0.545	0.540	0.533
400	1.250	0.552	0.550	0.547	0.542	0.535
420	1.302	0.558	0.556	0.552	0.547	0.539
440	1.352	0.562	0.560	0.556	0.550	0.543
460	1.402	0.589	0.588	0.585	0.580	0.573
480	1.452	0.599	0.598	0.593	0.588	0.580

500	1.500	0.605	0.604	0.600	0.596	0.588
520	1.548	0.631	0.630	0.628	0.622	0.615
540	1.594	0.646	0.645	0.642	0.637	0.630
560	1.641	0.651	0.651	0.648	0.643	0.635
580	1.686	0.661	0.661	0.657	0.651	0.644
600	1.731	0.669	0.670	0.667	0.662	0.657
630	1.797	0.683	0.683	0.681	0.676	0.668
660	1.861	0.697	0.698	0.696	0.691	0.684
690	1.924	0.715	0.716	0.714	0.711	0.705
720	1.985	0.723	0.724	0.721	0.717	0.710
750	2.045	0.748	0.747	0.745	0.741	0.734
780	2.104	0.761	0.762	0.761	0.756	0.750
810	2.162	0.769	0.771	0.770	0.766	0.759
840	2.218	0.784	0.786	0.784	0.781	0.773
870	2.274	0.794	0.796	0.795	0.792	0.785
920	2.363	0.804	0.806	0.805	0.802	0.795
970	2.449	0.808	0.810	0.809	0.806	0.800
1020	2.533	0.827	0.829	0.828	0.824	0.816
1070	2.614	0.840	0.844	0.844	0.841	0.834
1120	2.692	0.849	0.852	0.852	0.849	0.843
1170	2.768	0.862	0.866	0.867	0.864	0.859
1220	2.842	0.878	0.882	0.884	0.883	0.878
1270	2.913	0.888	0.892	0.895	0.893	0.888
1320	2.982	0.895	0.900	0.901	0.899	0.894
1370	3.049	0.911	0.915	0.917	0.915	0.911
1420	3.114	0.918	0.923	0.926	0.924	0.920
1470	3.177	0.931	0.935	0.936	0.934	0.928
1520	3.239	0.932	0.937	0.939	0.938	0.934
1570	3.298	0.945	0.950	0.952	0.950	0.945
1670	3.413	0.960	0.965	0.967	0.966	0.962
1770	3.521	0.957	0.963	0.965	0.965	0.961
1870	3.624	0.976	0.980	0.983	0.981	0.977
1920	3.673	0.982	0.988	0.991	0.991	0.987

Table 3. Data of the titration for the estimation of the Ka of the complex **R5⊂12**·6NO_3

5.2. Inclusion complex **R6⊂12**·6NO3.

T= 298 K, λ= 451, 455, 459, 462 nm

Ka= 170.91 ± 1.16 M^{-1}

Ka error= ± 0.68 % M^{-1}

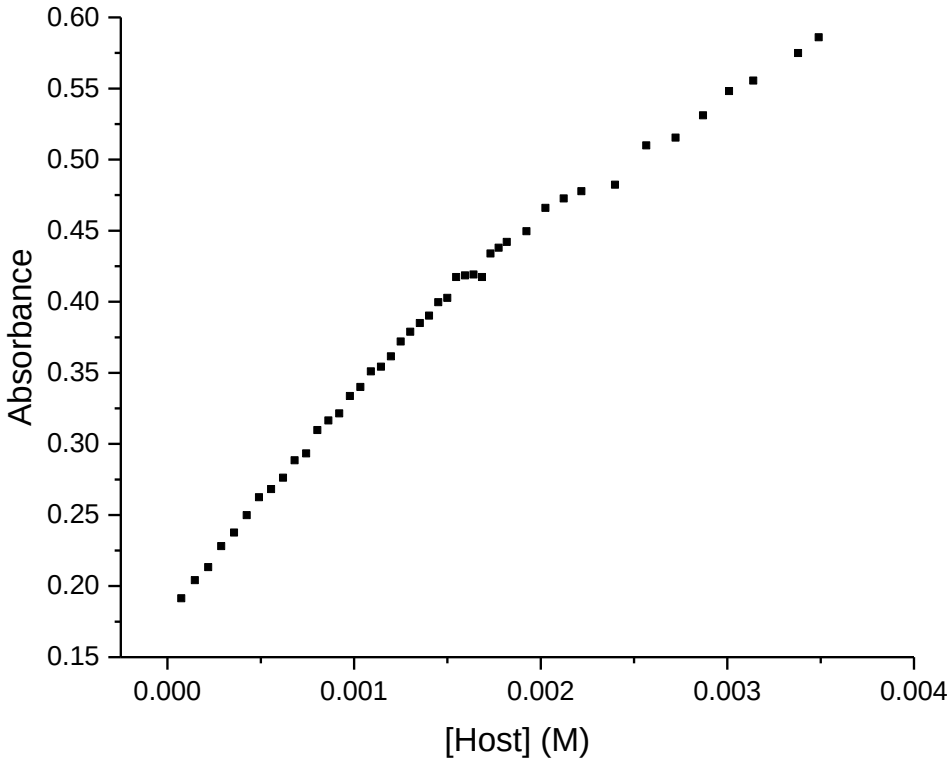

Representation of the titration of the complex **R6⊂12**·$6NO_3$

V_{added} (10^{-6} L)	[Host] (10^{-3} M)	Absorbance (451 nm)	Absorbance (455 nm)	Absorbance (459 nm)	Absorbance (462 nm)
20	0.074	0.195	0.191	0.188	0.184
40	0.147	0.208	0.204	0.200	0.196
60	0.218	0.218	0.213	0.209	0.205
80	0.288	0.233	0.228	0.224	0.220
100	0.357	0.242	0.238	0.233	0.229
120	0.425	0.255	0.250	0.246	0.242
140	0.491	0.267	0.262	0.258	0.253
160	0.556	0.274	0.268	0.263	0.259
180	0.619	0.281	0.276	0.271	0.266
200	0.682	0.294	0.288	0.283	0.279
220	0.743	0.299	0.293	0.289	0.284
240	0.804	0.315	0.310	0.305	0.300
260	0.863	0.322	0.316	0.311	0.306
280	0.921	0.327	0.322	0.316	0.312
300	0.978	0.339	0.334	0.328	0.322
320	1.030	0.346	0.340	0.335	0.329
340	1.090	0.357	0.351	0.345	0.340
360	1.140	0.360	0.354	0.349	0.344
380	1.200	0.368	0.362	0.356	0.350
400	1.250	0.379	0.372	0.365	0.359
420	1.300	0.384	0.379	0.373	0.368
440	1.350	0.391	0.385	0.379	0.373
460	1.400	0.396	0.390	0.384	0.378
480	1.450	0.406	0.400	0.394	0.388
500	1.500	0.409	0.403	0.397	0.392
520	1.550	0.423	0.417	0.411	0.406
540	1.590	0.425	0.418	0.413	0.407
560	1.640	0.425	0.419	0.412	0.407
580	1.690	0.423	0.417	0.411	0.406
600	1.730	0.440	0.434	0.427	0.422
620	1.770	0.444	0.438	0.431	0.425
640	1.820	0.448	0.442	0.436	0.430
690	1.920	0.456	0.450	0.443	0.437
740	2.030	0.473	0.466	0.459	0.453
790	2.120	0.479	0.473	0.466	0.460
840	2.220	0.484	0.478	0.472	0.466
940	2.400	0.489	0.482	0.476	0.470
1040	2.570	0.517	0.510	0.503	0.496
1140	2.720	0.522	0.515	0.508	0.501
1240	2.870	0.538	0.531	0.524	0.517
1340	3.010	0.554	0.548	0.541	0.535
1440	3.140	0.562	0.556	0.549	0.543
1640	3.380	0.582	0.575	0.568	0.561

Table 4. Data of the titration for the estimation of the Ka of the complex **R6⊂12**·6NO_3

5.3. Inclusion complex **R7⊂12**·8NO3.

T= 298 K, λ= 510, 515, 520, 525 nm

Ka = $K_{11}*K_{12}$ = $2.32*10^6 \pm 5.1*10^3$; K_{11}= 541.21 ± 23.76 M^{-1}; K_{21}= 4292.56 ± 214.63 M^{-1}

K_{11} error= ± 4.39 % M^{-1}; K_{21} error= ± 5.00 % M^{-1}

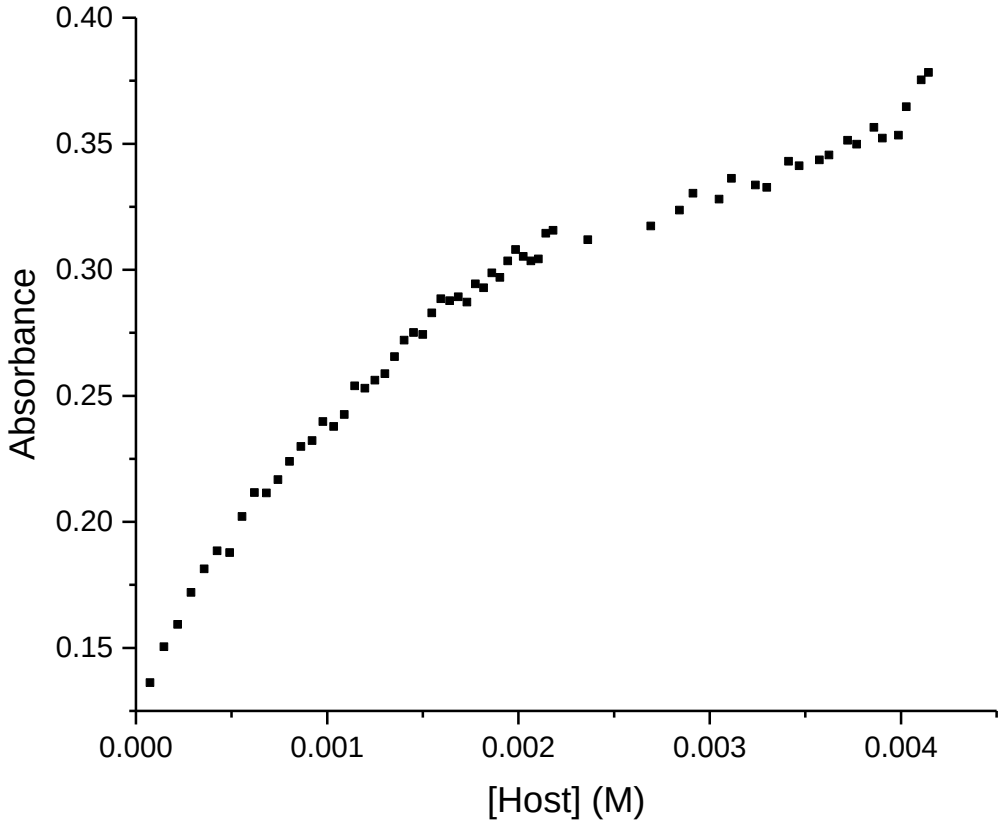

Representation of the titration of the complex **R7⊂12**·8NO_3

V_{added} (10^{-6} L)	[Host] (10^{-3} M)	Absorbance (510 nm)	Absorbance (515 nm)	Absorbance (520 nm)	Absorbance (525 nm)
20	0.074	0.139	0.136	0.134	0.132
40	0.147	0.153	0.150	0.148	0.145
60	0.218	0.162	0.159	0.158	0.156
80	0.288	0.174	0.172	0.171	0.169
100	0.357	0.183	0.181	0.181	0.178
120	0.425	0.190	0.188	0.188	0.185
140	0.491	0.189	0.188	0.187	0.185
160	0.556	0.204	0.202	0.202	0.200
180	0.619	0.213	0.212	0.212	0.209
200	0.682	0.213	0.211	0.212	0.210
220	0.743	0.218	0.217	0.217	0.215
240	0.804	0.225	0.224	0.223	0.221
260	0.863	0.230	0.230	0.229	0.227
280	0.921	0.233	0.232	0.232	0.230
300	0.978	0.240	0.240	0.239	0.237
320	1.034	0.239	0.238	0.237	0.236
340	1.090	0.243	0.243	0.242	0.241
360	1.144	0.255	0.254	0.253	0.252
380	1.197	0.253	0.253	0.252	0.251
400	1.250	0.257	0.256	0.256	0.254
420	1.302	0.260	0.259	0.258	0.256
440	1.352	0.266	0.266	0.266	0.263
460	1.402	0.273	0.272	0.272	0.270
480	1.452	0.276	0.275	0.275	0.273
500	1.500	0.275	0.274	0.274	0.272
520	1.548	0.284	0.283	0.283	0.281
540	1.594	0.289	0.288	0.288	0.286
560	1.641	0.288	0.288	0.288	0.286
580	1.686	0.289	0.289	0.288	0.288
600	1.731	0.287	0.287	0.287	0.285
620	1.775	0.294	0.294	0.294	0.292
640	1.818	0.293	0.293	0.293	0.291
660	1.861	0.299	0.299	0.299	0.297
680	1.903	0.297	0.297	0.297	0.296
700	1.944	0.305	0.304	0.303	0.302
720	1.985	0.308	0.308	0.308	0.306
740	2.026	0.306	0.305	0.305	0.302
760	2.065	0.304	0.304	0.303	0.302
780	2.104	0.305	0.304	0.304	0.302
800	2.143	0.315	0.314	0.314	0.313
820	2.181	0.316	0.316	0.315	0.313
920	2.363	0.312	0.312	0.312	0.311
1120	2.692	0.318	0.317	0.317	0.315
1220	2.842	0.324	0.324	0.323	0.321

1270	2.913	0.331	0.330	0.330	0.328
1370	3.049	0.328	0.328	0.327	0.326
1420	3.114	0.337	0.336	0.335	0.333
1520	3.239	0.334	0.334	0.333	0.331
1570	3.298	0.333	0.333	0.332	0.330
1670	3.413	0.345	0.343	0.342	0.339
1720	3.468	0.342	0.341	0.341	0.339
1820	3.573	0.345	0.344	0.343	0.341
1870	3.624	0.347	0.346	0.346	0.344
1970	3.722	0.352	0.351	0.350	0.350
2020	3.769	0.350	0.350	0.349	0.347
2120	3.859	0.356	0.356	0.356	0.354
2170	3.903	0.352	0.352	0.352	0.350
2270	3.987	0.354	0.353	0.353	0.351
2320	4.028	0.365	0.365	0.365	0.362
2420	4.106	0.376	0.375	0.376	0.374
2470	4.144	0.379	0.378	0.377	0.375

Table 5. Data of the titration for the estimation of the Ka of the complex **R7⊂12**·8NO_3